



Minke Rab

**Novel biomarkers
for sickle cell disease and other
hereditary hemolytic anemias**

**Novel biomarkers
for sickle cell disease and other
hereditary hemolytic anemias**

Minke Rab

Novel biomarkers for sickle cell disease and other hereditary hemolytic anemias

© Minke Rab, 2021

All rights reserved. No part of this thesis may be reproduced, stored or transmitted in any form or by any means without prior permission of the author, or the copyright-owning journals for previously published chapters.

ISBN: 9789039374009

Cover design & lay-out: Wendy Schoneveld || www.wenziD.nl

Printed by: ProefschriftMaken.nl || Proefschriftmaken.nl

The research described in this thesis was supported by an Eurostars grant and an unrestricted research grant of RR Mechatronics

Financial support by RR Mechatronics and Global Blood Therapeutics for printing of this thesis is gratefully acknowledged.

Novel biomarkers for sickle cell disease and other hereditary hemolytic anemias

Nieuwe biomarkers voor sikkelcelziekte en andere erfelijke hemolytische anemieën

(met een samenvatting in het Nederlands)

Proefschrift

ter verkrijging van de graad van doctor aan de
Universiteit Utrecht
op gezag van de
rector magnificus, prof.dr. H.R.B.M. Kummeling,
ingevolge het besluit van het college voor promoties
in het openbaar te verdedigen op

woensdag 29 september 2021 des middags te 4.15 uur

door

Minke Ariena Elisabeth Rab

geboren op 25 februari 1982
te 's-Gravenhage

Promotoren:

Prof. dr. G. Pasterkamp

Prof. dr. R.E.G Schutgens

Copromotoren:

Dr. R. van Wijk

Dr. E.J. van Beers

Voor mijn zus

Table of content

Chapter 1	General introduction	9
------------------	----------------------	---

Part I

Development and standardization of oxygen gradient ektacytometry

Chapter 2	Rapid and reproducible characterization of sickling during automated deoxygenation in sickle cell disease patients	23
Chapter 3	Characterization of sickling during controlled automated deoxygenation with oxygen gradient ektacytometry: the oxygenscan	53
Chapter 4	Methodological aspects of the oxygenscan in sickle cell disease: a need for standardization	73

Part II

Applications of oxygen gradient ektacytometry

Chapter 5	Oxygen gradient ektacytometry derived-biomarkers are associated with vaso-occlusive crises and correlate with treatment response in sickle cell disease	83
Chapter 6	Oxygen gradient ektacytometry-derived biomarkers are associated with the occurrence of cerebral infarction, acute chest syndrome and vaso-occlusive crisis in sickle cell disease	107
Chapter 7	Use of oxygen gradient ektacytometry in the titration of hydroxyurea dosing in children with sickle cell disease	129
Chapter 8	Decreased activity and stability of pyruvate kinase in sickle cell disease: a novel target for mitapivat therapy	139
Chapter 9	Identification of biomarkers that are associated with clinical complications of hemoglobin SC disease and sickle cell anemia	151

Part III

Ektacytometry in other hereditary hemolytic anemias

- Chapter 10** AG-348 (Mitapivat), an allosteric activator of red cell pyruvate kinase, increases enzymatic activity, protein stability and ATP levels over a broad range of PKLR genotypes 175
- Chapter 11** Ektacytometry analysis of post-splenectomy red blood cell properties identifies cell membrane stability test as a novel biomarker of membrane health in hereditary spherocytosis 203
- Chapter 12** Red cell dehydration is associated with distinctive alterations of red cell metabolism in hereditary xerocytosis caused by PIEZO1 and KCNN4 defects 223

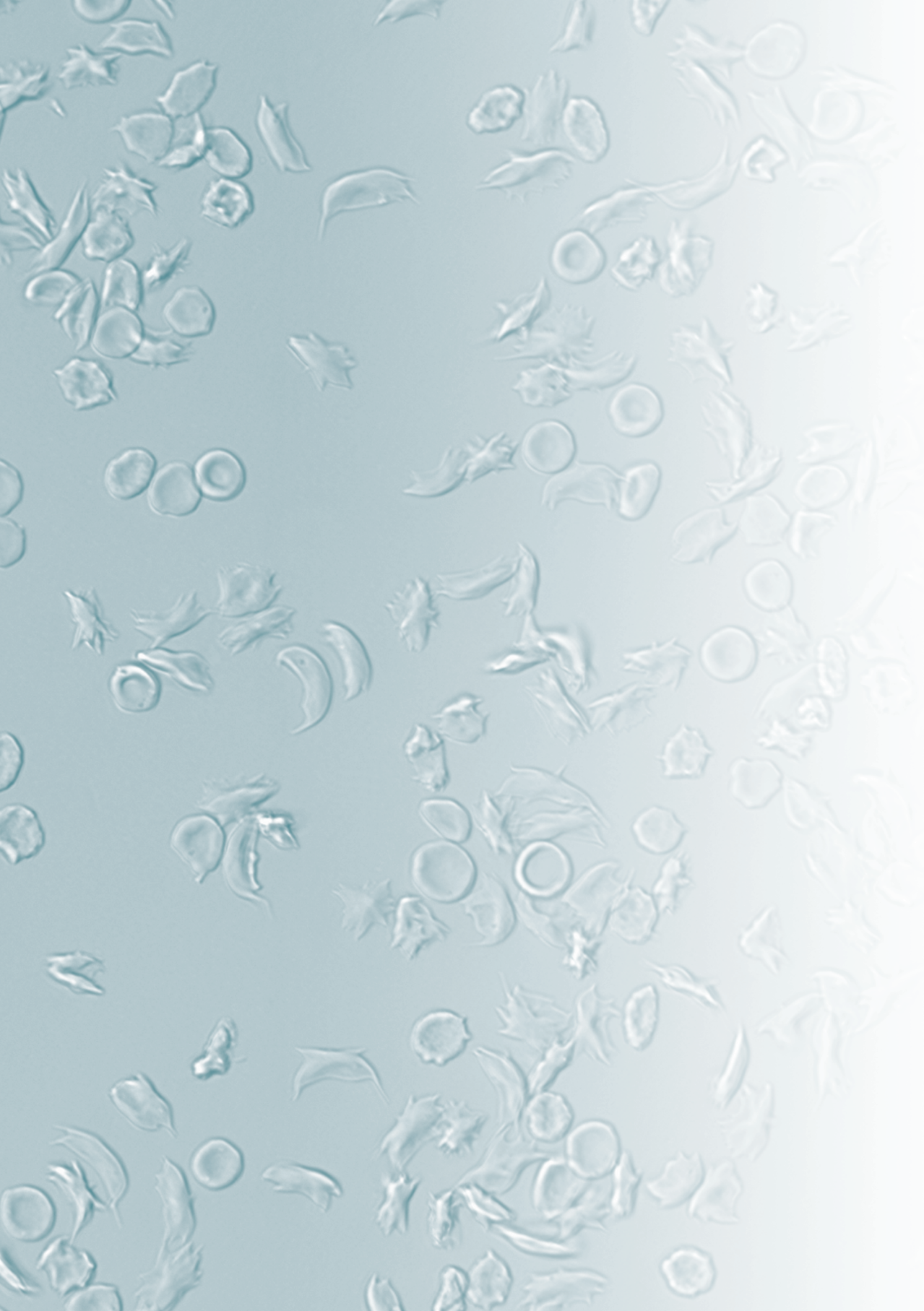
Part IV

Summary and general discussion

- Chapter 13** Summary and general discussion 247

Appendices

- Nederlandse samenvatting (Dutch summary) 267
- List of publications 273
- Dankwoord (acknowledgements) 279
- Curriculum Vitae 289



Chapter 1

General introduction

General introduction

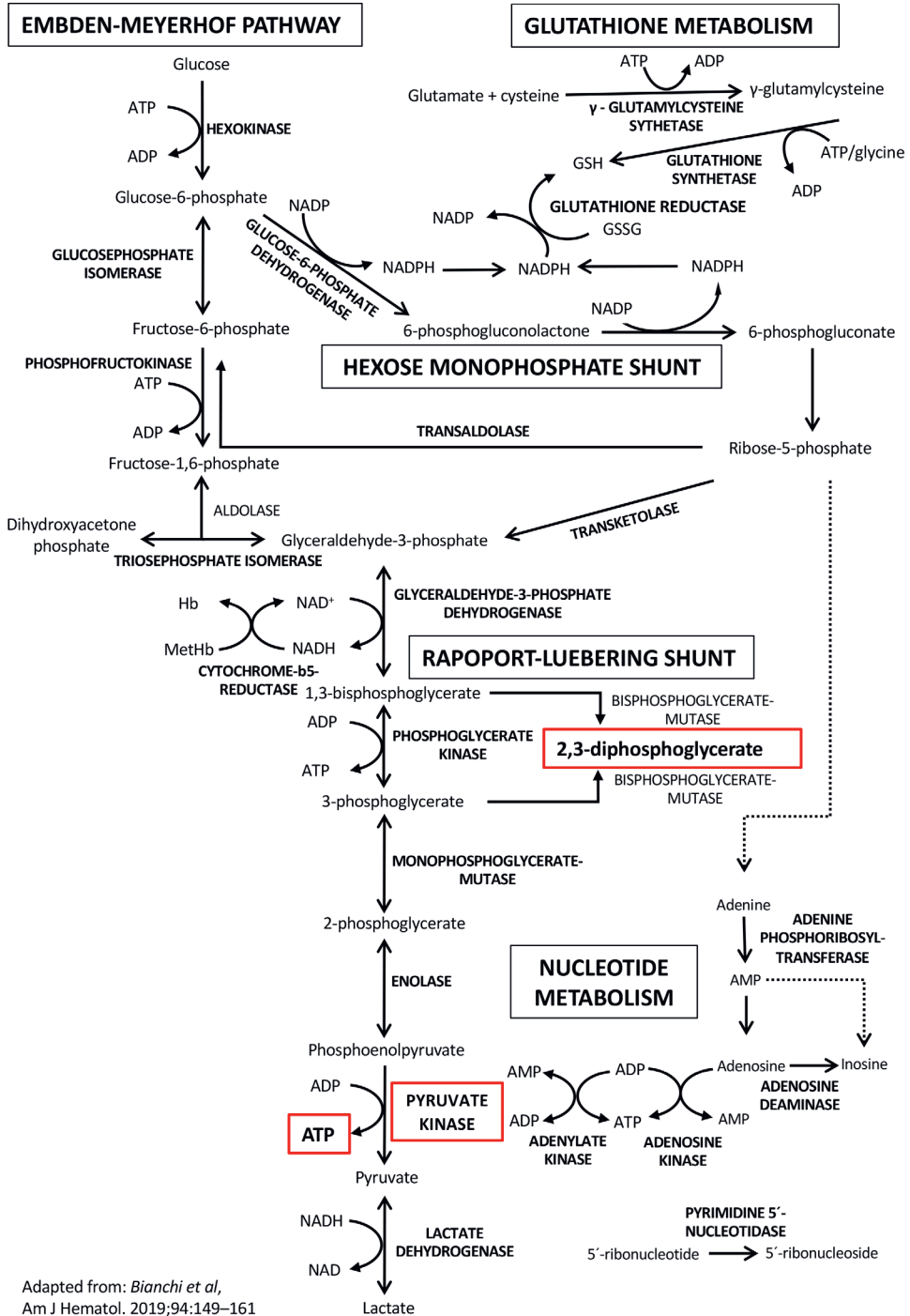
Red blood cell physiology and deformability

Red blood cells (RBC) have a crucial role in the delivery of oxygen to all vital tissues and to do so they must be highly deformable to pass through narrow capillaries and traverse through endothelial slits present in the red pulp of the spleen.¹ When an RBC fails to pass through these narrow endothelial slits it will be taken up by a macrophage which will break it down. Besides impaired deformability, other factors result in the removal of RBCs from the bloodstream, which include phosphatidyl serine (PS) exposure², altered CD47 on the RBC membrane³, binding of autologous IgG to the transmembrane protein band 3 or binding of activated RBC adhesion molecules to laminin in the spleen.⁴ In contrast, extravascular hemolysis seems to be directly triggered by reduced RBC deformability.^{5,6} The ability of RBCs to deform is a result of different RBC properties including the interaction of transmembrane and cytoskeletal proteins.^{7,8} Besides these structural properties, the metabolic processes within RBCs that generate ATP are of importance in maintaining shape and the capacity to deform. Mature RBCs lack mitochondria and are therefore totally dependent on anaerobic glycolysis. The Embden Mayerhof pathway generates ATP, with pyruvate kinase (PK) in the final step accounting for at least 50% of ATP production (Figure 1).^{9,10} ATP is suggested to be crucial in the activity of ion transport mechanism such as the Na/K/ATPase¹¹⁻¹³ and Ca²⁺ pumps¹⁴, that regulate ion homeostasis and RBC hydration.

Deformability of RBCs can be measured by several techniques that measure active deformation, i.e. microfluidic approaches or filtration techniques, or more passive deformation, i.e. ektacytometry or atomic force microscopy for single cell assays. Ektacytometry is defined by applying shear stress on RBCs resulting in elongation of the cells. The Laser Optical Rotational Red Cell Analyzer (Lorrrca) is a next generation ektacytometer that quantifies RBC deformability by means of a laser beam shining through a sample solution containing a small amount of whole blood in polyvinylpyrrolidone (PVP). This generates a diffraction pattern, which is determined by the total population of RBCs present in the solution. By means of the height and width of this pattern the elongation index (EI) is calculated. Deformability can be measured as a function of changing osmolality (osmotic gradient ektacytometry or osmoscan) or different levels of shear stress. With the Cell Membrane Stability Test (CMST), deformability can also be measured before, during and after applying a certain shear stress during a defined amount of time.¹⁵ This test, could be an effective way to investigate how the RBC membrane responds to continuously applied (supraphysiological) shear stress, or intermittent episodes of shear stress¹⁶ and is indicative of membrane health.

Sickle cell disease

Sickle cell disease (SCD) is the major cause of anemia and accounts for the majority of years lost to disability by anemia in northern America and Western Europe.¹⁷ Although this disease is classified as rare in The Netherlands, due to migration the incidence is rising throughout Europe. SCD is a monogenetic disorder in which a single mutation in the β -globin gene results in the formation of the abnormal hemoglobin S (HbS). Upon deoxygenation HbS



Adapted from: Bianchi et al, Am J Hematol. 2019;94:149–161

Figure 1. Red blood cell metabolism

polymerizes which eventually leads to formation of polymers that subsequently drive the red cell into the characteristic sickle shape. There are several factors that influence the sickling process including 2,3-diphosphoglycerate (2,3-DPG), which is produced in the Rapoport-Luebering shunt, a bypass of the Embden-Mayerhof pathway that is unique for the RBC (Figure 1).¹⁸ The increased 2,3-DPG levels found in SCD result in lowered oxygen affinity of HbS, which subsequently leads to an increase in the p50 (the oxygen tension at which 50% of hemoglobin is saturated with oxygen due to a right shift of the hemoglobin oxygen dissociation curve). This change in affinity for oxygen makes HbS more prone to polymerization and subsequently sickling¹⁹ which negatively affects RBC deformability. Deformability of sickle RBCs is thought to be compromised due to increased density of the cell and intracellular polymer formation and subsequently sickling. These poorly deformable cells can occlude blood vessels leading to (painful) vaso-occlusive crises (VOC). The pathophysiology of VOC is highly complex with other factors next to RBC sickling that add to the development of a crisis.²⁰ Hemolysis, increased red cell adhesion, endothelial dysfunction, inflammation, oxidative stress, and hemostatic activation, also contribute to the development of VOC, although their relative contribution remains subject to debate.²⁰⁻²² The non-RBC factors are also found in other disease conditions, yet no other disease is associated with VOC, highlighting the key contribution of the sickle RBC to SCD pathophysiology.²⁰

SCD comprises several different genotypes, which contributes to the heterogeneity and variable severity of the disease, and even individuals with the same genotype demonstrate variable clinical expression. To date there are no laboratory test available that can accurately assess clinical severity and predict complications. There is a clinical need for the development of biomarkers since several new treatments with different points of action are currently in clinical trial. However, development of a clinically relevant biomarker is difficult due to the various factors that influence the occurrence of complications. Moreover, biomarkers are generally representing just one aspect of the pathophysiology of SCD. As such, the routinely obtained laboratory parameters fetal hemoglobin (HbF), hemoglobin, mean corpuscular volume (MCV), and hemolysis parameters lactate dehydrogenase (LDH), bilirubin and reticulocyte count are generally used to monitor patients with SCD.

Pyruvate kinase deficiency

Pyruvate kinase (PK) deficiency is a rare hereditary hemolytic red cell disorder that affects RBC glycolysis resulting in life long chronic hemolytic anemia.²³ This autosomal recessive disorder is the most common cause of chronic hereditary nonspherocytic hemolytic anemia and occurs worldwide, although its exact prevalence is unknown.²⁴⁻²⁶ It is caused by mutations in *PKLR*, the gene encoding for RBC and liver specific isoforms PK-R and PK-L, respectively.^{27,28} PK-deficient RBCs are characterized by changes in metabolism associated with impaired glycolysis, including an increase of the upstream metabolite 2,3-DPG and decreased ATP. Since RBCs rely totally on glycolysis for ATP production it is hypothesized that insufficient energy production affects red cell homeostasis, promoting premature removal of PK-deficient RBCs from the circulation by the spleen. Increased activity of the Gardos channel and consequent potassium efflux results in dehydrated RBC²⁹⁻³¹; as well as ATP depletion-mediated changes in RBC membrane integrity have been proposed as mechanisms that trigger this premature clearance.^{11,32}

Deformability of PK deficient RBCs has not been described as a pathognomic sign of the disease. Osmotic gradient ektacytometry of non-splenectomized PKD patients showed a modest decrease in O_{hyper} , one of the parameter reflecting RBC hydration.³³ However, PKD patients generally present with marked reticulocytosis, and reticulocytes generally have an increased deformability compared to mature and old RBCs. Moreover, deformability measured by ektacytometry represents the overall deformability of the RBC population, and is therefore likely to be decreased when corrected for reticulocyte count.

Hereditary spherocytosis

Hereditary spherocytosis (HS) is a disorder of the cell membrane of the RBC and in Caucasians the most common hereditary hemolytic anemia. The overall incidence of HS is estimated to be 200-300/million in northern European countries. HS represents a heterogeneous group of mutations in genes that code for RBC membrane and cytoskeletal proteins that are important for integrity and function of the RBC membrane. Molecular defects in the genes coding for these proteins result in defective cytoskeleton or defective anchoring of the lipid bilayer to the cytoskeletal network, subsequently leading to destabilization of the RBC membrane. Decreased stability causes progressive membrane loss through vesiculation of essentially hemoglobin free vesicles, which leads to the formation of spherocytes instead of oval biconcave disks.^{34,35} Deformability and flexibility of these spherocytes with high density are compromised.³⁶ As a result, spherocytes are recognized and removed by the spleen⁶, which clinically leads to (episodes of) hemolytic anemia, jaundice and splenomegaly. Splenectomy is an established treatment in cases of (severe) HS, as it removes the primary site of RBC destruction.^{35,37-39} Nevertheless, a careful evaluation of the risks and benefits should be made, as splenectomy results in a permanently increased risk of encapsulated bacterial infections and delayed adverse cardiovascular events including thrombosis.^{38,40}

Diagnosis of HS can be made by specific tests that assesses specific RBC characteristics. These tests include RBC morphology, i.e. presence of spherocytes in peripheral blood cells, flow cytometry measurements to determine eosin-5-maleimide (EMA) binding, osmotic gradient ektacytometry and next generation sequencing.⁴¹ Although ektacytometry is not mentioned in the guidelines of 2011, for HS it is a useful method to assess deformability, surface-area to volume ratio and hydration of RBCs in patients with RBC membrane disorders.^{33,42,43} Besides its additional value in diagnosing HS it can provide more insight into the pathophysiology of HS.

Hereditary xerocytosis

Hereditary xerocytosis (HX) is a rare hemolytic red cell disorder that is caused by mutations in *PIEZO1*, the gene coding for the mechanosensitive cation channel PIEZO1, or *KCNN4*, the gene encoding for the Gardos channel, a calcium-dependent potassium channel. In both cases, inappropriate Gardos channel activation leads to loss of potassium and water, thereby causing dehydration of the red cell. While patients with a *KCNN4* mutation present with hemolytic anemia⁴⁴, *PIEZO1* patients show fully compensated hemolysis with marked reticulocytosis and iron overload.⁴⁵ The mechanism by which HX RBCs in both disorders are cleared from the circulation is unknown. However, in contrast to other hereditary hemolytic

anemias, such as HS, splenectomy is contraindicated in PIEZO1-HX patients due to the increased risk of thromboembolic complications post-splenectomy.⁴⁶⁻⁴⁸ The exact mechanism that causes post-splenectomy thrombosis remains to be elucidated.

RBC deformability measured with osmotic gradient ektacytometry shows a left shift of the curve indicating dehydrated RBCs in patients with PIEZO1 mutations. In contrast, this typical left shift is generally absent in RBCs of patients with a KCNN4 mutation. The common denominator of both PIEZO1 HX and KCNN4 HX is the occurrence of stomatocytes on peripheral blood film.^{45,49} If these 2 subtypes should be considered part of the same disease is still under debate.⁴⁵

Outline of the thesis

The aim of this thesis was to develop and validate new biomarkers in hereditary hemolytic anemia. A new application of ektacytometry, so called oxygen gradient ektacytometry, that characterizes red cell sickling, is described in *Part I* of this thesis. In **Chapter 2** the potential and methodological aspects of oxygen gradient ektacytometry are evaluated. **Chapter 3**, a video article, provides the scientific community with the exact protocol and knowledge to correctly perform oxygen gradient ektacytometry measurements. Additional factors, such as timing of the measurement, technical settings and amount of RBCs, that can influence results of this technique are reported in **Chapter 4**.

Part II of this thesis gives insight in how oxygen gradient ektacytometry relates to the occurrence of complications in individuals with SCD. In **Chapter 5** the association of oxygen gradient ektacytometry-derived biomarkers with VOC is described, next to the response of those biomarkers to standard of care therapy. Further clinical validation of oxygen gradient ektacytometry is described in **Chapter 6** in which the association with acute chest syndrome, cerebral infarction and VOC is assessed.

Besides clinical validation other applications of oxygen gradient ektacytometry in SCD are explored. **Chapter 7**, describes a case of twins with SCD in which optimal hydroxyurea dosing is achieved with oxygen gradient ektacytometry. In **Chapter 8**, a new therapeutic agent mitapivat, an allosteric PK activator, is tested *ex vivo* in RBCs from SCD patients with oxygen gradient ektacytometry as a functional read out for efficacy. As a part of an in depth characterization of RBCs of both homozygous HbS (HbSS) and compound heterozygous for HbS and hemoglobin C (HbSC) patients, oxygen gradient ektacytometry can aid in further unraveling the pathophysiology of sickle cell disease, which is evaluated in **Chapter 9**.

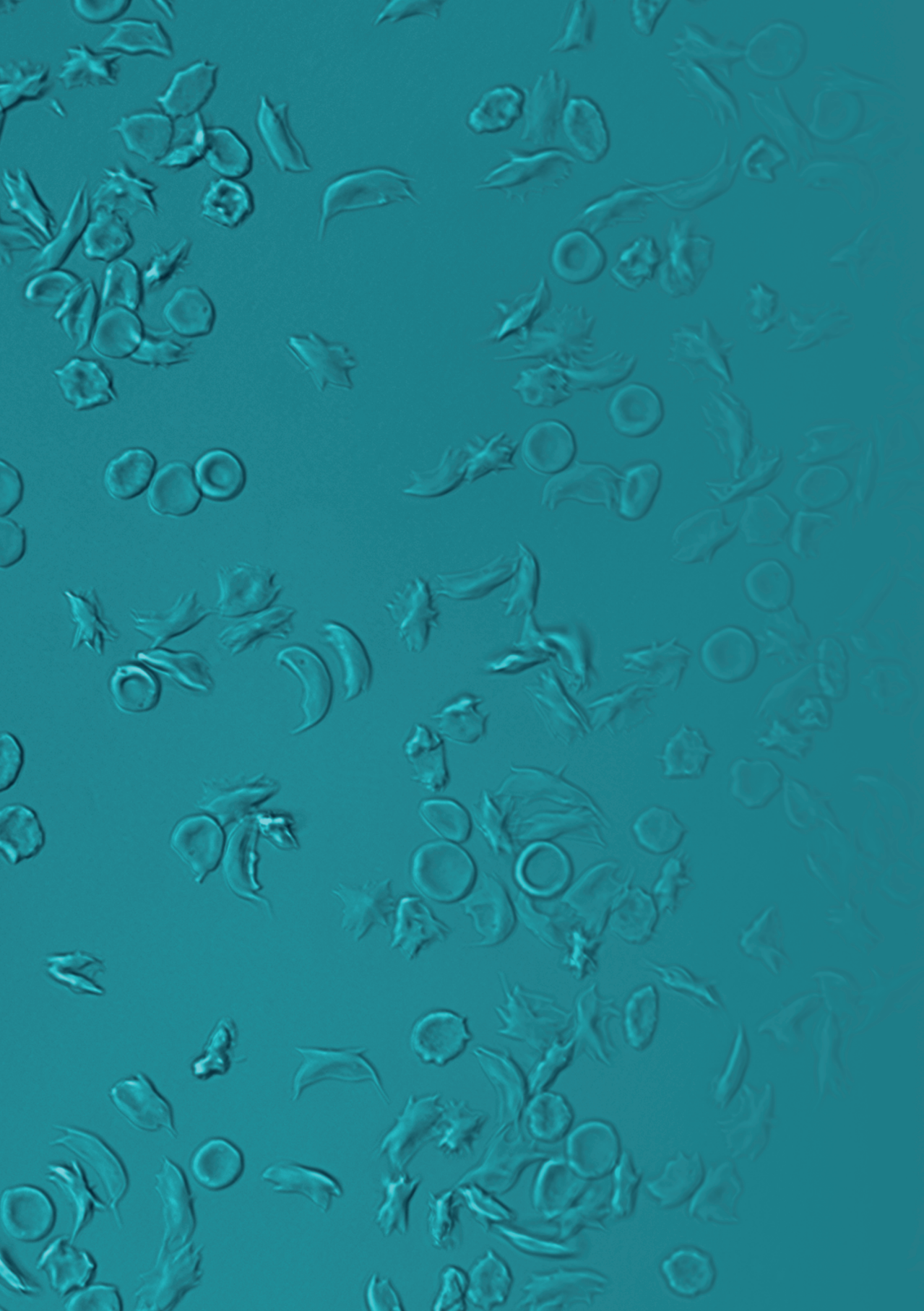
Part III of this thesis describes additional ektacytometry methods in other hereditary hemolytic anemia's. In **Chapter 10** the effects of mitapivat are evaluated in an *ex vivo* study of RBCs from patients with PK deficiency. Osmotic gradient ektacytometry, amongst other outcome parameters such as PK activity and stability, was used to show efficacy of this new treatment. **Chapter 11** shows the effects of splenectomy, an established treatment in hereditary spherocytosis, on RBC morphology, density and deformability. The latter was assessed with osmotic gradient ektacytometry as well as the cell membrane stability test (CMST), thereby providing the first clinical validation of this technique. These 2 ektacytometry based tests are also described in **Chapter 12** which shows similarities and differences between PIEZO1 and KCNN4 mutations both resulting in hereditary xerocytosis. The findings of this thesis are summarized and put into a broader perspective in **Chapter 13**.

References

- Danielczok JG, Terriac E, Hertz L, et al. Red blood cell passage of small capillaries is associated with transient Ca²⁺-mediated adaptations. *Front Physiol.* 2017;8(Dec 5):979. doi:10.3389/fphys.2017.00979
- Boas FE, Forman L, Beutler E. Phosphatidylserine exposure and red cell viability in red cell aging and in hemolytic anemia. *Proc Natl Acad Sci U S A.* 1998;95(6):3077-3081. doi:10.1073/pnas.95.6.3077
- Burger P, Hilarius-Stokman P, De Korte D, Van Den Berg TK, Van Bruggen R. CD47 functions as a molecular switch for erythrocyte phagocytosis. *Blood.* 2012;119(23):5512-5521. doi:10.1182/blood-2011-10-386805
- Klei TRL, Dalimot J, Nota B, et al. Hemolysis in the spleen drives erythrocyte turnover. *Blood.* 2020;136(14):1579-1589. doi:10.1182/blood.2020005351
- Deplaine G, Safeukui I, Jeddi F, et al. The sensing of poorly deformable red blood cells by the human spleen can be mimicked in vitro. *Blood.* 2011;117(8):1-3. doi:10.1182/blood-2010-10-312801
- Mebius RE, Kraal G. Structure and function of the spleen. *Nat Rev Immunol.* 2005;5(8):606-616. doi:10.1038/nri1669
- Nans A, Mohandas N, Stokes DL. Native ultrastructure of the red cell cytoskeleton by cryo-electron tomography. *Biophys J.* 2011;101(10):2341-2350. doi:10.1016/j.bpj.2011.09.050
- Burton NM, Bruce LJ. Modelling the structure of the red cell membrane. *Biochem Cell Biol.* 2011;89(2):200-215. doi:10.1139/O10-154
- Van Wijk R, Van Solinge WW. The energy-less red blood cell is lost: Erythrocyte enzyme abnormalities of glycolysis. *Blood.* 2005;106(13):4034-4042. doi:10.1182/blood-2005-04-1622
- Zanella A, Bianchi P, Fermo E. Pyruvate kinase deficiency. *Haematologica.* 2007;92(6):721-723. doi:10.3324/haematol.11469
- Weed RI, LaCelle PL, Merrill EW. Metabolic dependence of red cell deformability. *J Clin Invest.* 1969;48(5):795-809. doi:10.1172/JCI106038
- Fischer DJ, Torrence NJ, Sprung RJ, Spence DM. Determination of erythrocyte deformability and its correlation to cellular ATP release using microbore tubing with diameters that approximate resistance vessels in vivo. *Analyt.* 2003;128(9):1163-1168. doi:10.1039/b308225n
- Tuvia S, Levin S, Bitler A, Korenstein R. Mechanical fluctuations of the membrane-skeleton are dependent on F-actin ATPase in human erythrocytes. *J Cell Biol.* 1998;141(7):1551-1561. doi:10.1083/jcb.141.7.1551
- Glader BE, Sullivan DW. Erythrocyte disorders leading to potassium loss and cellular dehydration. *Prog Clin Biol Res.* 1979;30:503-513.
- Baskurt OK, Meiselman HJ. Red blood cell mechanical stability test. *Clin Hemorheol Microcirc.* 2013;55(1):55-62. doi:10.3233/CH-131689
- Horobin JT, Sabapathy S, Simmonds MJ. Repetitive Supra-Physiological Shear Stress Impairs Red Blood Cell Deformability and Induces Hemolysis. *Artif Organs.* 2017;00(00):1-9. doi:10.1111/aor.12890
- Kassebaum NJ, Jasrasaria R, Naghavi M, et al. A systematic analysis of global anemia burden from 1990 to 2010. *Blood J.* 2015;123(5):615-625. doi:10.1182/blood-2013-06-508325.
- MacDonald R. Red cell 2,3-diphosphoglycerate and oxygen affinity. *Anaesthesia.* 1977;32(6):544-553. doi:10.1111/j.1365-2044.1977.tb10002.x
- Charache S, Grisolia S, Fiedler AJ, Hellegers AE. Effect of 2,3-diphosphoglycerate on oxygen affinity of blood in sickle cell anemia. *J Clin Invest.* 1970;49(4):806-812. doi:10.1172/JCI106294
- Kalpatthi R, Novelli EM. Measuring success: Utility of biomarkers in sickle cell disease clinical trials and care. *Hematology.* 2018;2018(1):482-492. doi:10.1182/asheducation-2018.1.482
- Liu Y, Zhong H, Bao W, et al. Patrolling monocytes scavenge endothelial-adherent sickle RBCs: A novel mechanism of inhibition of vaso-occlusion in SCD. *Blood.* 2019;134(7):579-590. doi:10.1182/blood.2019000172
- Manwani D, Frenette PS. Vaso-occlusion in sickle cell disease: pathophysiology and novel targeted therapies. *Blood.* 2013;122(24):3892-3898. doi:10.1182/asheducation-2013.1.362

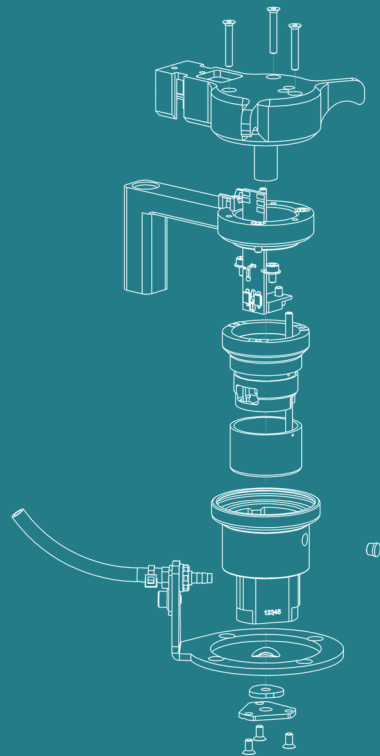
23. Koralkova P, Van Solinge WW, Van Wijk R. Rare hereditary red blood cell enzymopathies associated with hemolytic anemia - pathophysiology, clinical aspects, and laboratory diagnosis. *Int J Lab Hematol*. 2014;36(3):388-397. doi:10.1111/ijlh.12223
24. Beutler E, Gelbart T. Estimating the prevalence of pyruvate kinase deficiency from the gene frequency in the general white population. *Blood*. 2000;95(11):3585-3588. <http://www.ncbi.nlm.nih.gov/pubmed/10828047>
25. Carey PJ, Chandler J, Hendrick A, et al. To the editor: Prevalence of pyruvate kinase deficiency in a northern European population in the north of England. *Blood*. 2000;96(12):4005-4007.
26. de Medicis E, Ross P, Friedman R, et al. Hereditary nonspherocytic hemolytic anemia due to pyruvate kinase deficiency: a prevalence study in Quebec (Canada). *Hum Hered*. 1992;42(3):179-183.
27. Kanno H, Fujii H, Miwa S. Structural Analysis of Human Pyruvate Kinase L-Gene and Identification of the Promoter Activity in Erythroid Cells ' Hitoshi KANNO ', Hisaichi FUJII ' and Shiro MIWA '. *Biochem Biophys Res Commun*. 1992;188(2):516-523.
28. Kanno H, Fujii H, Hirono A, Miwa S. cDNA cloning of human R-type pyruvate kinase and identification of a single amino acid substitution (Thr384 --> Met) affecting enzymatic stability in a pyruvate kinase variant (PK Tokyo) associated with hereditary hemolytic anemia. *Proc Natl Acad Sci*. 1991;88(September):8218-8221.
29. Glader B. Salicylate-induced injury of pyruvate-kinase-deficient erythrocytes. *N Engl J Med*. 1976;294(17):916-918.
30. Mentzer WC, Baehner RL, Schmidt-Schönbein H, Robinson SH, Nathan DG. Selective reticulocyte destruction in erythrocyte pyruvate kinase deficiency. *J Clin Invest*. 1971;50(3):688-699. doi:10.1172/JCI106539
31. Koller CA, Orringer EP, Parker JC. Quinine protects pyruvate-kinase deficient red cells from dehydration. *Am J Hematol*. 1979;7(3):193-199. doi:10.1002/ajh.2830070302
32. Park Y, Best CA, Badizadegan K, et al. Measurement of red blood cell mechanics during morphological changes. *Proc Natl Acad Sci*. 2010;107(15):6731-6736. doi:10.1073/pnas.0909533107
33. Zaninoni A, Fermo E, Vercellati C, et al. Use of laser assisted optical rotational cell analyzer (LoRRca MaxSis) in the diagnosis of RBC membrane disorders, enzyme defects, and congenital dyserythropoietic anemias: A monocentric study on 202 patients. *Front Physiol*. 2018;9(APR):1-12. doi:10.3389/fphys.2018.00451
34. Chasis JA, Agre P, Mohandas N. Decreased membrane mechanical stability and in vivo loss of surface area reflect spectrin deficiencies in hereditary spherocytosis. *J Clin Invest*. 1988;82(2):617-623. doi:10.1172/JCI113640
35. Eber SW, Lux SE. Hereditary spherocytosis-defects in proteins that connect the membrane skeleton to the lipid bilayer. *Semin Hematol*. 2004;41(2):118-141.
36. Nakashima K. Erythrocyte and Membrane deformability in Hereditary Spherocytosis. *Blood*. 1979;53(3):481-486.
37. Musser G, Lazar G, Hocking W, Busuttill W. Splenectomy for hematologic disease. The UCLA experience with 306 patients. *Ann Surg*. 1984;200(1):40-45. doi:10.1097/0000658-198407000-00006
38. Perrotta S, Gallagher PG, Mohandas N. Hereditary spherocytosis. *Lancet*. 2008;372(9647):1411-1426. doi:10.1016/S0140-6736(08)61588-3
39. Reliene R, Mariani M, Zanella A, et al. Splenectomy prolongs in vivo survival of erythrocytes differently in spectrin/ankyrin- and band 3-deficient hereditary spherocytosis. *Blood*. 2002;100(6):2208-2215. doi:10.1182/blood.v100.6.2208.h81802002208_2208_2215
40. Schilling RF, Gangnon RE, Traver MI. Delayed adverse vascular events after splenectomy in hereditary spherocytosis. *J Thromb Haemost*. 2008;6(8):1289-1295. doi:10.1111/j.1538-7836.2008.03024.x
41. Girodon, Francois Garcon, Loic, Bergoin, Emilie Largier, Marie Delaunay, Jean Feneant-Thibault, Madeleine Maynadie, Marc Couillaud, Gerard Moreira, Sophie Cynober T. Usefulness of the eosin-5'-maleimide cytometric method as a first-line screening test for the diagnosis of hereditary spherocytosis: comparison with ektacytometry and protein electrophoresis. *Br J Haematol*. 2007;140(4):464-468. doi:10.1111/j.1365-2141.2007.06940.x

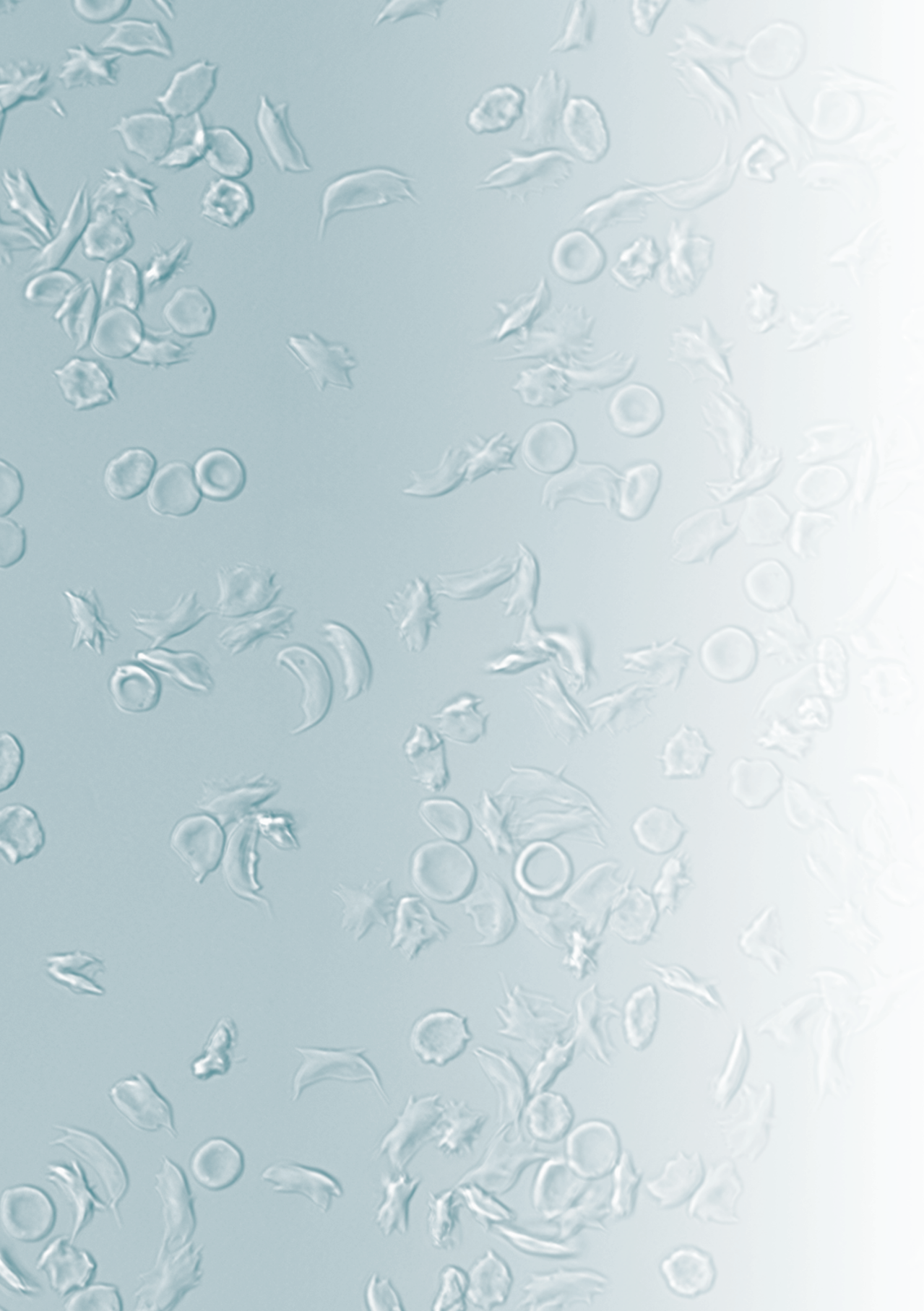
42. DaCosta L, Suner L, Galimand J, et al. Diagnostic tool for red blood cell membrane disorders : Assessment of a new generation ektacytometer. *Blood Cells, Mol Dis.* 2016;56(1):9-22. doi:10.1016/j.bcmd.2015.09.001
43. Lazarova E, Gulbis B, Oirschot B Van, Van Wijk R. Next-generation osmotic gradient ektacytometry for the diagnosis of hereditary spherocytosis: Interlaboratory method validation and experience. *Clin Chem Lab Med.* 2017;55(3):394-402. doi:10.1515/cclm-2016-0290
44. Fermo E, Bogdanova A, Petkova-Kirova P, et al. "Gardos Channelopathy": A variant of hereditary Stomatocytosis with complex molecular regulation. *Sci Rep.* 2017;7(1):1-13. doi:10.1038/s41598-017-01591-w
45. Picard V, Guitton C, Thuret I, et al. Clinical and biological features in PIEZO1-hereditary xerocytosis and gardos channelopathy: A retrospective series of 126 patients. *Haematologica.* 2019;104(8):1554-1564. doi:10.3324/haematol.2018.205328
46. Iolascon A, Andolfo I, Barcellini W, et al. Recommendations regarding splenectomy in hereditary hemolytic anemias. *Haematologica.* 2017;102(8):1304-1313. doi:10.3324/haematol.2016.161166
47. Stewart GW, Amess JAL, Eber SW, et al. Thrombo-embolic disease after splenectomy for hereditary stomatocytosis. *Br J Haematol.* 1996;93(2):303-310. doi:10.1046/j.1365-2141.1996.4881033.x
48. Jaïs X, Till SJ, Cynober T, et al. An extreme consequence of splenectomy in dehydrated hereditary stomatocytosis: Gradual thrombo-embolic pulmonary hypertension and lung-heart transplantation. *Hemoglobin.* 2003;27(3):139-147. doi:10.1081/HEM-120023377
49. Andolfo I, Russo R, Rosato BE, et al. Genotype-phenotype correlation and risk stratification in a cohort of 123 hereditary stomatocytosis patients. *Am J Hematol.* 2018;93(12):1509-1517. doi:10.1002/ajh.25276



Part I

Development and standardization of oxygen gradient ektacytometry





Chapter 2

Rapid and reproducible characterization of sickling during automated deoxygenation in sickle cell disease patients

American Journal of Hematology 2019; May;94(5):575-584

Minke A.E. Rab^{1,2}, Brigitte A. van Oirschot¹, Jennifer Bos¹, Tesy H. Merckx¹, Annet C.W. van Wesel¹, Osheiza Abdulmalik³, Martin K. Safo⁴, A. Birgitta Versluijs⁵, Maite E. Houwing⁶, Marjon H. Cnossen⁶, Jurgen Riedl⁷, Roger E.G. Schutgens², Gerard Pasterkamp¹, Marije Bartels⁵, Eduard J. van Beers² and Richard van Wijk¹

¹ Laboratory of Clinical Chemistry & Hematology, University Medical Center Utrecht, Utrecht University, Utrecht, The Netherlands

² Van Creveldkliniek, University Medical Center Utrecht, Utrecht University, Utrecht, The Netherlands

³ Division of Hematology, The Children's Hospital of Philadelphia, Philadelphia, Pennsylvania

⁴ Department of Medicinal Chemistry, Institute for Structural Biology, Drug Discovery and Development, School of Pharmacy, Virginia Commonwealth University, Richmond, Virginia

⁵ Department of Pediatric Hematology, University Medical Center Utrecht, Utrecht University, Utrecht, The Netherlands

⁶ Department of Pediatric Hematology, Erasmus University Medical Center– Sophia Children's Hospital, Rotterdam, The Netherlands

⁷ Result Laboratory, Albert Schweitzer Hospital, Dordrecht, The Netherlands

Abstract

In sickle cell disease (SCD), sickle hemoglobin (HbS) polymerizes upon deoxygenation, resulting in sickling of red blood cells (RBCs). These sickled RBCs have strongly reduced deformability, leading to vaso-occlusive crises and chronic hemolytic anemia. To date, there are no reliable laboratory parameters or assays capable of predicting disease severity or monitoring treatment effects. We here report on the oxygenscan: a newly developed method to measure RBC deformability (expressed as Elongation Index – EI) as a function of pO_2 . Upon a standardized, 22 minute, automated cycle of deoxygenation (pO_2 median 16mmHg \pm 0.17) and reoxygenation, a number of clinically relevant parameters are produced in a highly reproducible manner (coefficients of variation <5%). In particular, physiological modulators of oxygen affinity, i.e. pH and 2,3-diphosphoglycerate showed a significant correlation (respectively $R=-0.993$ and $R=0.980$) with Point of Sickling ($PoS_{5\%}$), which is defined as the pO_2 where a 5% decrease in EI is observed during deoxygenation. Furthermore, *in vitro* treatment with anti-sickling agents, including GBT440, which alter the oxygen affinity of hemoglobin, caused a reproducible left-shift of the PoS, indicating improved deformability at lower oxygen tensions. When RBCs from 21 SCD patients were analyzed, we observed a significantly higher PoS in untreated homozygous SCD patients compared to treated patients and other genotypes. We conclude that the oxygenscan is a state-of-the-art technique that allows for rapid analysis of sickling behavior in SCD patients. The method is promising for personalized treatment, development of new treatment strategies and could have potential in prediction of complications.

Introduction

In sickle cell disease (SCD) a single point mutation in the gene encoding for β -globin chain underlies the production of the abnormal hemoglobin S (HbS). HbS polymerizes upon deoxygenation which results in the formation of hemoglobin polymers and eventually gives the red blood cell (RBC) its characteristic sickled shape. Exacerbating the hypoxia-induced polymerization is the inherent low-affinity of HbS, presumably due to high levels of 2,3-diphosphoglycerate (2,3-DPG) present in sickle RBCs.¹ These sickled RBCs have strongly reduced deformability and show increased adherence to vascular endothelium, leading to vaso-occlusive crises.²⁻⁴ Hydroxyurea (HU), regular blood transfusion and L-glutamine are the main treatment options in SCD, with allogeneic hematopoietic stem cell transplantation being the only curative therapy currently available.⁵ Remarkably, clinical severity varies considerably despite the fact that all SCD patients carry the same homozygous point mutation in the β -globin gene. To date there is no reliable laboratory or clinical parameter available to predict severity and/or complications.

An individual patient's tendency to "sickle" can be tested *in vitro* using a so-called sickling assay: RBCs are incubated under hypoxic conditions and manually or digitally counted using a light microscope. This assay is still widely applied in research, and many preclinical and early phase pharmacologic and gene therapy trials use this assay as outcome variable to predict clinical effect.⁶⁻¹¹ However, there are many disadvantages: it is time consuming, it has low sensitivity and high variability, and the process is not automated. More importantly, morphological characteristics of sickle cells may not correlate well with physiologic characteristics, such as deformability.¹²

RBC deformability at normoxic conditions is compromised in patients with SCD due to irreversibly sickled cells, as well as altered hydration causing a decrease in surface/volume ratio.¹²⁻¹⁴ Osmotic gradient ektacytometry, in which deformability is measured as a function of a continuous change in osmolarity, is a well-established method, in particular in hereditary disorders of the red cell membrane.¹⁵⁻¹⁸ In SCD, osmotic gradient ektacytometry showed that increasing HbF induces a better surface-to-volume ratio thereby improving deformability in untransfused patients with SCD.¹⁹ RBC deformability during normoxic conditions as a marker for complications has also been investigated in the past, and a negative correlation was found between an increase in RBC deformability and osteonecrosis or painful sickle cell crises.²⁰⁻²² In contrast to these findings, RBC deformability was found to be decreased during an acute vaso-occlusive crises when compared to steady state values.²³ Thus, in itself, RBC deformability during normoxic conditions gives inconsistent results which makes it unsuitable to be used as predictive biomarker.

Therefore, an assay that investigates sickling during deoxygenation is required to monitor treatment and disease state in patients with SCD. Importantly, this assay could identify individuals who are at increased risk for certain complications, and potentially predict response to therapy. Finally, it contributes to a better understanding of the clinical effect of new anti-sickling agents. In this study, we evaluate the oxygenscan, which investigates RBC deformability as a function of continuously changing pO_2 , allowing us to characterize individual sickling behavior in SCD patients.

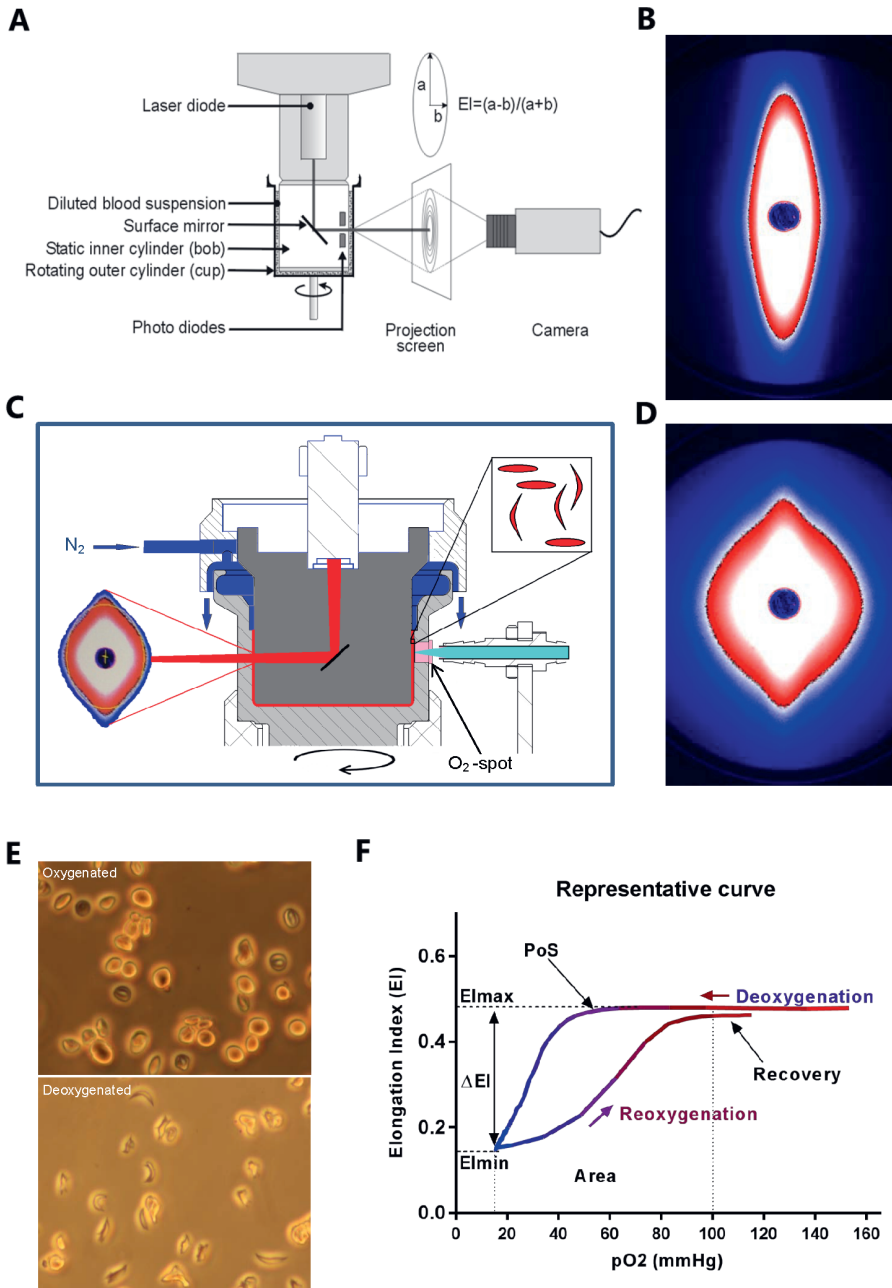


Figure 1. Experimental setup of the Lorrca with the oxygenscan module and representative oxygenscan curve. (A) Experimental setup of the Lorrca. (B) The diffraction pattern of healthy RBCs is elliptical when shear stress of 30 Pa is applied. (C) Schematic graph of the oxygenscan add-on which shows deoxygenation with nitrogen gas (N_2), the O_2 -spot and LED-fiber, a device to measure oxygen tension. (D) Upon deoxygenation and shear stress (30 Pa) the diffraction pattern changes from an ellipse to a rhomboid shape. ▶

(E) Sickle RBCs fixated after a similar round of deoxygenation show change in shape, control sickle RBCs, without nitrogen gas, show no change in shape. (F) A representative curve of the oxygenscan. Maximum Elongation Index (Elmax) represents baseline position, and shows overall deformability of the total RBC population. Minimum EI (Elmin) represents minimal deformability which is caused by change in shape and orientation of RBCs upon deoxygenation. DeltaEI (difference in EI between Elmax and Elmin) shows how many cells can sickle during one round of deoxygenation. Point of sickling (PoS5%, pO_2 at 5% EI decrease) embodies the oxygen tension when the first RBCs start to sickle. The area under the curve (from minimum pO_2 -100 mmHg) is calculated in the parameter Area and this summarizes Elmax, Elmin, and PoS. The capacity of sickled cells to unsickle during reoxygenation is represented in the parameter Recovery (percentage of Elmax reached during reoxygenation). To aid interpretation, we connected all data points in every individual experiment by a line in the graphical presentation of the results.

Methods

Blood Specimens

University Medical Center Utrecht (UMCU): Whole blood of patients with SCD who were included in 2 different clinical studies (Netherlands Trial Register [NTR] identifier, NTR 6779 and NTR 6462) was used. Additional samples were collected from discarded anonymized EDTA blood of patients with SCD who visited outpatient clinic. Whole blood from healthy controls was collected through the Mini Donor Service, which is approved by the ethical committee of the UMCU and in accordance to the declaration of Helsinki.

The Children's Hospital of Philadelphia (CHOP): Leftover EDTA blood samples from individuals with SCD after routine clinical visits were utilized for the traditional anti-sickling studies. The use of such samples, with informed consent, is in accordance to an approved IRB protocol.

Oxygen gradient ektacytometry: the oxygenscan

The Laser Optical Rotational Red Cell Analyzer (Lorrca, RR Mechatronics) is a next generation ektacytometer which measures different qualitative aspects of RBC deformability expressed as Elongation Index (EI). The pO_2 scan is a new add-on of the Lorrca, allowing the measurement of red cell deformability as a function of a continuously changing gradient of O_2 tension. In brief, a couette system is used to apply shear stress on the RBCs, which are diluted in a viscous solution (Iso Oxy), consisting of polyvinylpyrrolidone (PVP) with characteristics of whole blood (i.e. osmolarity and pH). Between a static cylinder (bob) and rotating cylinder (cup), there is a small gap in which the blood suspension is injected (Figure 1A). Light from the laser beam is scattered by the presence of RBCs and this diffraction pattern is projected and analyzed. In healthy controls, the diffraction pattern is circular at rest and elliptical shaped at higher shear stress (Figure 1B).¹⁵

To carry out the oxygenscan, 50 μ L of whole blood, standardized to a fixed RBC count of 200×10^6 is suspended into 5ml Iso Oxy (osmolarity 282-286mOsm/kg, pH 7.35-7.45) at room temperature ($\pm 22^\circ\text{C}$). Approximately 2 ml of the sample solution is slowly injected into the gap between the cup and bob until a fixed level is attained (Figure 1C). The bob is maintained at a constant temperature of 37°C . Inlet of nitrogen gas from above facilitates deoxygenation (Figure 1C). O_2 tension is measured every 20 seconds by means of a small oxygen (O_2)-spot which is covered with luminophore that is present in the wall of the cup. The pO_2 is calculated

from the amount of quenching of the signal that is sent from the fiber to the O₂-spot. One oxygenscan consists of approximately 80 measurements of EI, during one round of deoxygenation (1300 seconds), and followed by reoxygenation (280 seconds). Shear stress is fixed at 30 pascal (Pa). Ambient air pO₂ in the cup was about 160mmHg and is gradually lowered to below 20mmHg (2.7kPa, 2,9%) O₂. Reoxygenation occurs due to passive diffusion of ambient air.

Oxygenscan parameters

When considering a typical oxygenscan curve (Figure 1F) six parameters are considered to reflect various features of the process of HbS polymerization or sickling: **Elmax**: maximum EI before deoxygenation that represents baseline position and shows overall deformability of the total RBC population. **Elmin**: minimum EI, representing minimal deformability resulting from changes in shape and orientation of (sickle) RBCs upon deoxygenation (Figure 1D). **DeltaEI**: difference between Elmax and Elmin, indicating sickling capacity during one round of deoxygenation. **Point of Sickling_{5%} (PoS_{5%})**: pO₂ (mmHg) at which 5% decrease of Elmax during deoxygenation is observed. This indicates the pO₂ where sickling starts. **Area**: area under the curve which is defined by an integral calculation of the EI and pO₂ measurements between minimum pO₂ and 100mmHg. This is the result of Elmax, Elmin and PoS. **Recovery**: percentage of EI after reoxygenation compared to EI just before deoxygenation measured at the pO₂ between 100-120mmHg. This represents the capacity of sickled cells to unsickle during reoxygenation.

Digital Microscopy

Smears of peripheral blood of patients were analyzed using the CellaVision digital microscope DM96 (software 5.0.1build11), the traditional neural network of which classifies sickle cells based on manually designed features, such as shape, color and texture features. Sickle cell counts were expressed as percentage of absolute cell count analyzed by digital microscopy.²⁴

In vitro addition of HbAA blood to HbSS blood, mimicking red cell transfusions

To investigate the effect of adding RBCs of healthy donors, ABO and rhesus matched RBCs of a healthy donor was mixed with whole blood of a patient with SCD to reach the following percentages of HbS blood: 100%, 75%, 50%, 25% and 0%.

Influence of 2,3-DPG levels, pH and temperature

To assess the influence of 2,3-DPG levels on oxygenscan parameters, complete blood count and oxygenscans were performed within 10 minutes after blood collection, and after 24 hours. Whole blood was kept either at 4°C, room temperature (\pm 22°C) and 37°C for 24 hours. 2,3-DPG was measured by spectrophotometry (SpectraMax M2e, Molecular Devices) using the 2,3-DPG assay kit (Roche). 2,3-DPG levels were normalized to hemoglobin levels. To assess the influence of temperature, oxygenscans were carried out with bob temperatures of 35, 37, 39, 41 and or 43°C.

To investigate the influence of pH, the pH of the Iso Oxy was set to 6.9, 7.1, 7.3, 7.7 and 7.9 before being used in the oxygenscan.

***In vitro* incubation with anti-sickling agents GBT440, 5-PMFC, and INN312**

GBT440, 5-PMFC and INN312 are a class of anti-sickling aromatic aldehyde agents that modulate hemoglobin oxygen affinity by stabilizing the higher oxygen affinity relaxed state (R-state) of hemoglobin and/or destabilizing the low oxygen affinity tense state (T-state) of hemoglobin. GBT440 (2-hydroxy-6 ((2-(1-isopropyl-1H-pyrazol-5-yl) pyridin-3-yl)-methoxy) benzaldehyde, MedChemExpress) is a novel, orally bioavailable agent currently in clinical trials for SCD.^{9,25} 5-PMFC (5-(Phenoxymethyl)-2-furan carbaldehyde) is an aryl ether derivative of 5-(hydroxymethyl)furfural (5-HMF), with a potent anti-sickling effect.¹⁰ Designated International Nonproprietary Name-312 (INN312) is a designed and synthesized derivative of vanillin.^{8,26}

Whole blood (20% hematocrit) was added to N-[Tris(hydroxymethyl)methyl]-2-aminoethanesulfonic acid (TES)-buffer (pH 7.4), which contained 30mM TES-sodium salt and 30mM TES-free acid (both Merck KGaA), supplemented with 130mM NaCl, 5mM KCl, 10mM glucose and 0.2% bovine serum albumin. These suspensions were incubated with the agents for 1 hour at 37°C at normoxia. Concentrations used for incubation were 1mM and 2mM of GBT440, and 1 and 5mM of 5-PMFC and INN-312.^{7,10} Anti-sickling agents were dissolved in dimethyl sulfoxide (DMSO), while incubation with DMSO alone was used as a negative control.

Morphological analysis after *in vitro* incubation with anti-sickling agents

To compare the outcome of the effect of the agents mentioned above, sickling was also measured using previously reported methodology with slight modifications.^{7,10,27} Briefly, whole blood was suspended (20% hematocrit) in isotonic Hemox buffer (TCS Scientific Corp), pH 7.4, supplemented with 10mM glucose and 0.2% bovine serum albumin and incubated at normoxia in varying concentrations of GBT440 (1, 2 and 5mM), 5-PMFC (1 and 5mM) and INN312 (1 and 5mM) at 37°C for 1 hour. Next, suspensions were incubated under hypoxic condition (2.5% Oxygen gas/97.5% Nitrogen gas) at 37°C for 1 hour. Cells were fixed and analyzed by light microscopy.

Statistical Analysis

Experiments were mainly carried out in duplicates, mean, standard deviation (SD) and coefficient of variation (CV) were calculated. Statistical analysis was performed using IBM Statistics SPSS (v21) and Graphpad Prism. One-way ANOVA (Post-hoc Tukey's test or Dunnett's test) or a Kruskal-Wallis test (Post-hoc Dunn's test) was used when appropriate. We normalized results in the experiments with 2,3-DPG because of known individual differences in 2,3-DPG levels. Results of incubation with anti-sickling agents was normalized to enable the comparison of DeltaEI at 18mmHg with the classical, microscopy based sickling assay. Pearson's correlation was used to determine correlations of oxygenscan parameters with laboratory and clinical parameters. A *p*-value of <0.05 was considered statistical significant.

Results

The Oxygenscan reproducibly characterizes red blood cell sickling

To validate the technique whole blood samples of 21 individuals with SCD, 5 individuals with sickle cell trait, and 8 healthy donors were used. A representative oxygenscan and its derived parameters is shown in Figure 1F. Importantly, parameters from duplicate measurements generally had a coefficient of variation (CV) <5% (median 1.83%). In case a CV >5% was obtained, a third measurement was performed. The parameters Elmax and Recovery appeared to be the most robust with median CVs <1%. Measurements of pO₂ and EI are not performed at the same position in the cup. This ensures a better discrimination between the deoxygenation and reoxygenation curves and, hence, a better interpretation of them.

In order to confirm that the change in diffraction pattern during deoxygenation reflects sickling, cells were deoxygenated outside the Lorrca, under comparable conditions, fixed and analyzed by light microscopy as described. Compared to oxygenated conditions sickling is clearly induced upon deoxygenation (Figure 1E and Supplemental Methods).

Upon storage of whole blood at 4°C oxygenscan curves shifted slightly upwards. When stored for 24 hours at 4°C curves remained stable, with minor increases in Elmax (1.7%), PoS (2.7%), DeltaEI (9.2%) and Area (6.7%). Minor decreases of 6.7% in Elmin and 0.6% in Recovery were observed under these conditions. Upon longer storage oxygenscans shifted upwards. (Supplemental Table 1).

The oxygenscan can adequately assess the effect of blood transfusion

In order to investigate the direct effects of blood transfusions on sickling behavior RBCs of a healthy control (HC) was mixed with whole blood of a SCD patient in different amounts (Supplemental Figure 2A). Supplemental Figure 2B and 2G shows that Elmax and Elmin shifted towards normal upon increasing percentages of HbAA blood. At the same time the PoS shifted to the left (Supplemental Figure 2D), whereas DeltaEI decreased and Area increased (Supplemental Figure 2C and E). Recovery also increased to 100% (Supplemental Figure 2F).

All oxygenscan parameters correlated significantly with the percentage of whole blood. Elmin showed a striking linear correlate of $r=0.998$, $p<0.0001$ (pooled data of 3 patients, individual correlations were above $r=0.987$ and $p<0.01$, Supplemental Figure 2G- L).

Oxygenscan parameters reflect the influence of physiologic modulators of the Hb-dissociation curve

Temperature, pH and 2,3-DPG are important cellular modulators of the O₂ affinity of hemoglobin and thereby of sickling. These parameters are therefore expected to exert effect on the oxygenscan. Oxygenscans and 2,3-DPG were essentially unchanged after 24 hours at 4°C (Supplemental Figure 2A-G). When kept at room temperature or 37°C, 2,3-DPG had decreased after 24 hours (normalized and pooled data is shown in Supplemental Figure 2B). 2,3-DPG showed a strong correlation with PoS ($r=0.980$, $p=0.020$, Supplemental Figure 2F and K) and Elmin (Supplemental Figure 2D and I).

Upon lowering the pH of Iso Oxy, an increase of Elmax, DeltaEI and PoS was observed, and

Elmin, Area and Recovery decreased (Supplemental Figure 3A-G). Upon increasing the pH the opposite effect was observed (Supplemental Figure 3A-G). PoS appeared to correlate best with pH change ($r=-0.993$, $p<0.001$ (pooled data, Supplemental Figure 3K), indicating that lowering pH results in sickling that starts at higher pO_2 .

Next, we performed series of oxygenscans of a single sample at different cup and bob temperatures. Results were similar as those found with pH adjustments (Supplemental Figure 4). Elmax decreased upon increased temperature and correlated best (linear correlate $r=0.996$, $p<0.001$), indicating RBC deformability at normoxic conditions is temperature dependent (Supplemental Figure 4G).

The oxygenscan provides a means to evaluate the efficacy of anti-sickling agents

Currently several new drugs for SCD are being tested in clinical trials. With blood of 6 SCD patients we investigated 3 of those drugs (GBT440, 5-PMFC and INN312) for their efficacy on directly preventing hypoxia-induced sickling using the oxygenscan as readout. GBT440, showed a large improvement in oxygenscan parameters at a concentration of 1mM and an even larger effect at 2mM (Figure 2A). After incubation with GBT440, Elmax slightly decreased. In contrast, Elmin increased with increasing doses of GBT440, which was significant for 2 and 5mM ($p=0.005$ and 0.001 , Figure 2B). Similar to these findings, DeltaEI and PoS significantly improved with increasing GBT440 concentration ($p<0.001$, Figure 2C and D). Area significantly improved as well ($p<0.001$). The same pattern was observed with 5-PMFC and INN312, with the latter showing the higher efficacy of the two (Figure 2B-E). However, at dosages of 1mM the effect of these 2 compounds was lower compared to GBT440 (Figure 2B-E): Elmin increased with 1mM and significantly increased with 5mM ($p<0.001$), DeltaEI decreased significantly with 5-PMFC 5mM ($p<0.001$) and INN312 1 and 5mM ($p<0.01$). PoS decreased in both concentrations of 5-PMFC and INN312, with 5mM being significant in both ($p<0.001$).

Importantly, when oxygenscan parameters were compared with the conventional sickling assay (microscopy) the results showed similar patterns and were correlated ($r=0.934$ $p=0.002$, Figure 2F and G). However at a lower concentration of GBT440, and to lesser extent also 5-PMFC and INN312, a slightly larger anti-sickling effect was observed with the conventional sickling assay (Figure 2F).

The oxygenscan is able to discriminate between different genotypes and treatment regimens

In order to investigate if the oxygenscan can detect differences between genotypes and treatment regimens, oxygenscans were performed with whole blood of 21 individuals with SCD, 5 individuals with HbS trait, and 5 healthy controls (HC). Homozygous patients without treatment (HbSS untreated, $n=7$) were compared to HbSS patients treated with HU ($n=5$), HbSS patients treated with exchange transfusion ($n=3$), HbS/ β^0 thalassemia ($n=1$), HbSS patients with α -thalassemia ($n=2$), hemoglobin SC disease patients (HbSC, $n=3$), HbS traits ($n=5$) and HC ($n=5$). Representative curves of groups with 3 or more patients are shown in

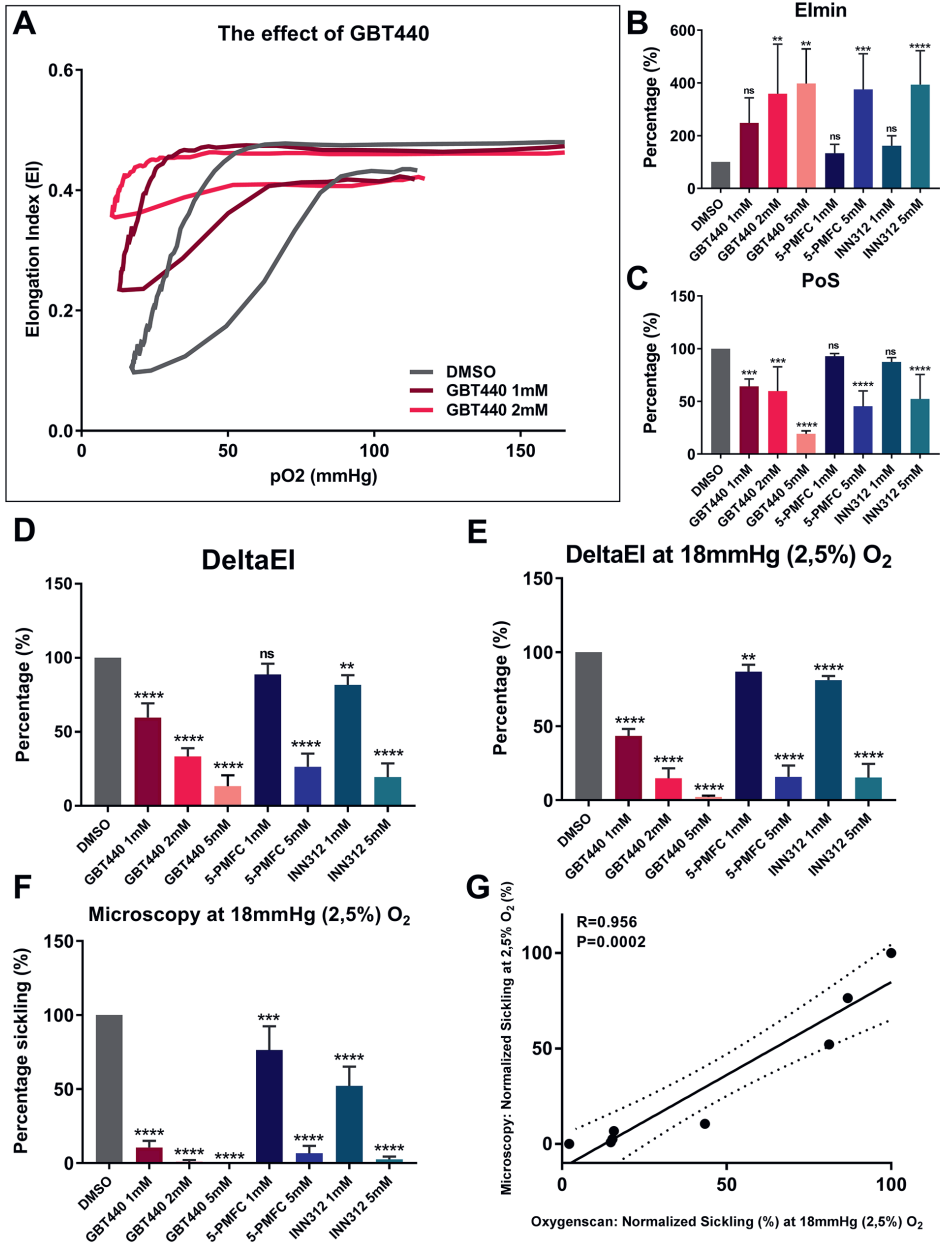


Figure 2. Effect of pharmacologic modulators of HbS polymerization on OxygenScan parameters. Incubations were carried out with n = 3 in case of 2 and 5 mM GBT440, n = 6 in other incubations. (A) Representative graph of effect of in vitro treatment of RBCs of patients with SCD with GBT440 1 and 2 mM. (B) Normalized means of minimum Elongation Index (Elmin) of RBCs incubated in absence or presence with different concentrations of antisickling agents. (C) Normalized means of Point of Sickling (PoS). (D) Normalized means of DeltaEI (difference between Elmax and Elmin) which represents sickling capacity. (E) Normalized means of DeltaEI at the specific pO₂ tension of 18 mmHg (2.5% O₂). ▶

(F) Normalized sickling after incubation in absence or presence of antisickling agents, measured by microscopy, after deoxygenation at 18 mmHg (2.5% O₂). G, Linear correlation between Oxygenscan measured sickling by DeltaEI and microscopy. Error bar represents SD. ****P < 0.0001, ***P < 0.001, **P < 0.01, *P < 0.05, ns, not significant. Dashed lines represent 95% confidence intervals

Figure 3A-D, with the mean of the different groups of Elmax, Elmin, PoS and Recovery shown in Figure 3E-H. Absolute values of all oxygenscan parameters are reported in Supplemental Table 2. A significant decrease of PoS was seen in all groups compared to untreated HbSS patients, except HbSS individuals who had been recently transfused. Recovery was significantly lower in HbSC patients compared to all the other groups. These results show that the oxygenscan is able to discriminate between different genotypes and treatment regimens.

When levels of HbF and HbS of patients with HbSS, HbSβ⁰, HbSS/α-thalassemia with/without HU, were correlated with oxygenscan parameters, Elmin showed the strongest correlations (r=0.833 and r=-0.852, both p<0.001, Figure 4A-B and Supplemental Figure 5). Digital microscopy findings of these patients were also correlated with oxygenscan parameters. Elmax showed the strongest correlation with sickled cells at normoxia (r=0.596, p=0.019, Figure 4C).

Discussion

The oxygenscan is a rapid and reproducible technique, that is developed to assess RBC sickling under automated continuous deoxygenation and re-oxygenation. We report for the first time on the potential of the oxygenscan to monitor clinical conditions and parameters that influence HbS polymerization. We found strikingly strong correlations of oxygenscan parameters with physiological and pharmacological modulators of HbS polymerization that are much stronger than in previously reported assays.¹¹ Importantly, diverse physiologic and pharmacologic conditions correlated best with particular oxygenscan parameters. This underlines the specificity of the various oxygenscan parameters: conditions mimicking exchange blood transfusion were found to specifically affect Elmin, similarly to HbF and HbS levels (Figure 4A-B). Physiological modulators of oxygen affinity predominantly affected PoS (Supplemental Figures 2 and 3). Regarding *in vivo* treatment of SCD, our findings show that RBCs of untreated HbSS patients start to sickle at higher oxygen tensions. Treatment with either HU or transfusion lowers the PoS indicating a lower pO₂ at which cells start to sickle. In case of HbSC patients, Recovery is significantly lower compared to the other groups indicating distinct processes of unsickling.²⁸ We speculate that this reduced capacity to recover could be involved in the distinct vaso-occlusive phenotype of HbSC patients.

Elmin is a reliable biomarker of the efficacy of blood transfusion

Our results show a strong correlation of Elmin with the distribution of HbS, HbF and HbA, and their effect on polymerization (Figure 2B, 3F and 4A-B). Elmin shows the deformability at the point of minimal pO₂ during an oxygenscan and reflects how many cells are sickled.

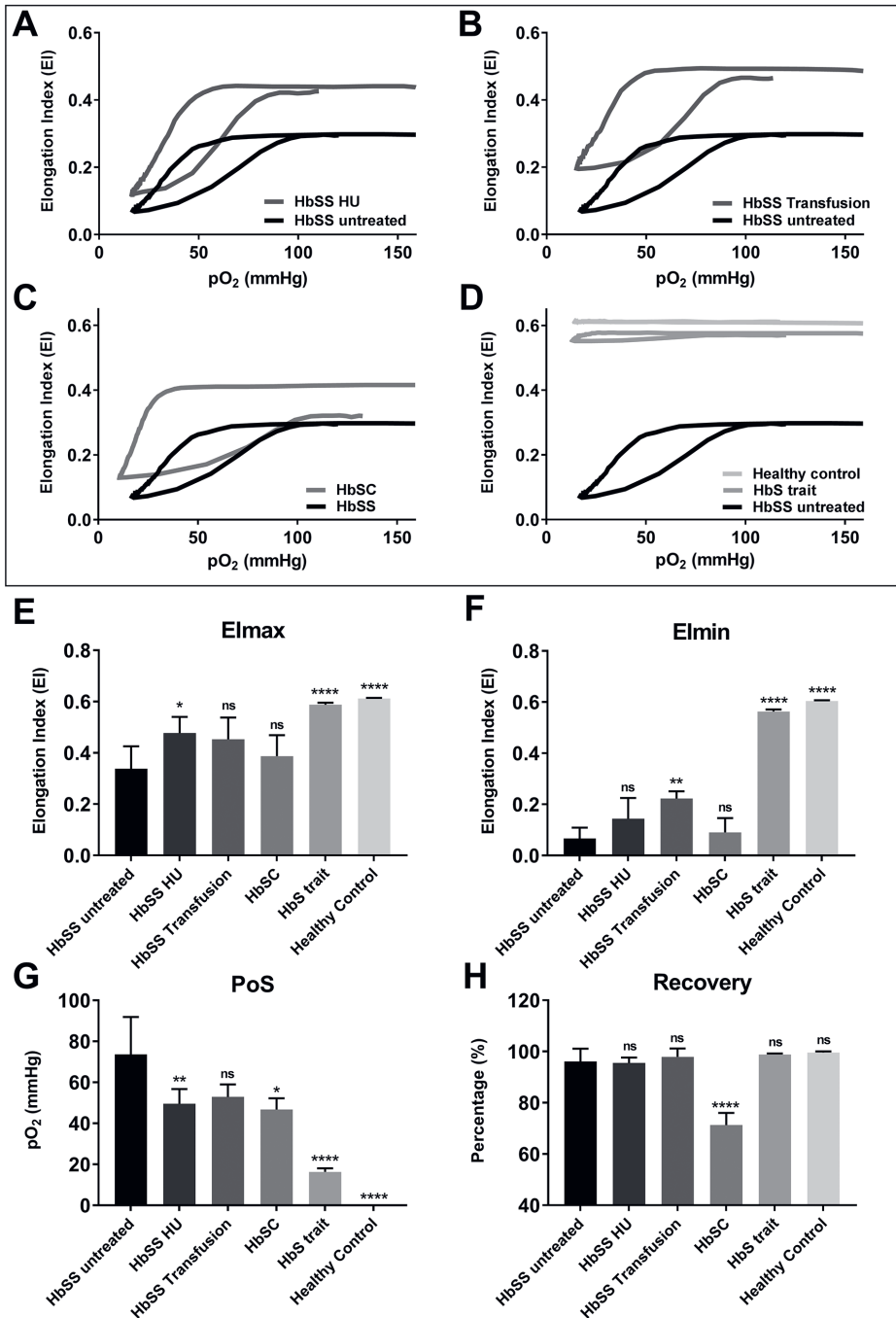


Figure 3. Oxygen scan parameters in relation to different genotypes and treatment of patients with SCD. (A) Representative graph of RBCs of Hydroxyurea treated homozygous SCD patients (HbSS HU) in relation to untreated HbSS patients. ▶

(B) Representative graph of RBCs of HbSS patients treated with blood transfusion (HbSS transfusion). (C) Representative graph of RBCs of patients with Hemoglobin SC Disease (HbSC). (D) Representative graph of RBCs of HbS carriers (HbS trait) and healthy controls. (E) Means of maximum Elongation Index (Elmax) in various conditions mentioned earlier. (F) Means of minimum EI (Elmin) in various conditions. (G) Means of Point of Sickling (PoS, pO_2 when 5% decrease in EI is reached) in various conditions. (H) Means of Recovery (% of start EI) in various conditions. Error bar represents SD. ****P < 0.0001, ***P < 0.001, ** P < 0.01, *P < 0.05, ns, not significant

The physiological ranges of intravascular pO_2 tension differ between tissues and blood vessel diameters, with the lowest values found in the bone marrow of live animals (i.e. 17.7mmHg).^{29,30} Oxygenscans curves reach at least 20mmHg in >95% of measurements, with a mean of 15.9mmHg (SEM 0.17). The minimal pO_2 during the oxygenscan is yet another relevant functional characteristic. In contrast to other sickling assays, in which a non-physiologically low pO_2 is used, often during several hours. Other assays use sodium metabisulfite, which depletes RBCs fully from oxygen. Both techniques result in full sickling of RBCs, even in sickle cell trait. The fact that oxygenscans of individuals with sickle cell trait do not show any significant sickling behavior compared to patients with SCD underlines the physiological applicability of the oxygenscan (Figure 3A-D and F).

Elmin therefore is a potent parameter for assessing the direct effects of blood transfusion and distribution of HbS, HbF and HbA. We suggest Elmin is mostly predicted by the percentage of cells that are not able to sickle at all and therefore is most influenced by blood transfusion and F-cells.

The potency of anti-sickling agents is captured by DeltaEI

DeltaEI can be used as outcome parameter in the assessment of the efficacy of new treatments that inhibit sickling. As shown by the experiments mimicking blood transfusion (Supplemental Figure 1), DeltaEI reflects the percentage of RBCs that sickle upon deoxygenation and as such is comparable with the conventional sickling assays (microscopy). In our experiments with the anti-sickling agents GBT440, 5-PMFC and INN312, data of the conventional assay was compared to DeltaEI and a similar pattern was observed (Figure 2E-F). Overall, the effects were more pronounced in the conventional assay, which could be due to a longer exposure to hypoxic conditions in the latter. This results in a higher amount of sickled cells at the start, and thus a more pronounced effect of anti-sickling agents. Importantly, cells that sickle instantly do not have the 'sickle' shape but a more irregularly shaped or 'star' shaped appearance, also called 'mosaic' cells.³¹ These cells have a different orientation in the flow in the Lorrca than fully sickled RBCs and, hence, behave differently in deformability measurements. Moreover, such cells are regarded as sickled cells but they likely are still able to deform to a certain extent. This could account for the less pronounced effect of anti-sickling agents as determined by the oxygenscan.

DeltaEI has a strong correlation with percentage HbSS blood (Supplemental Figure 1J) and can distinguish between a mixture of HbSS and HbAA RBCs and a population of HbAS RBCs (HbS trait, Supplemental Figure 1C, 3D and 4D-F). A feature that could be very helpful for upcoming gene-therapy trials in which an assay is needed that discriminates between mixed chimerism of fully corrected cells (50% HbAA and 50%HbSS) and fully engraftment of half

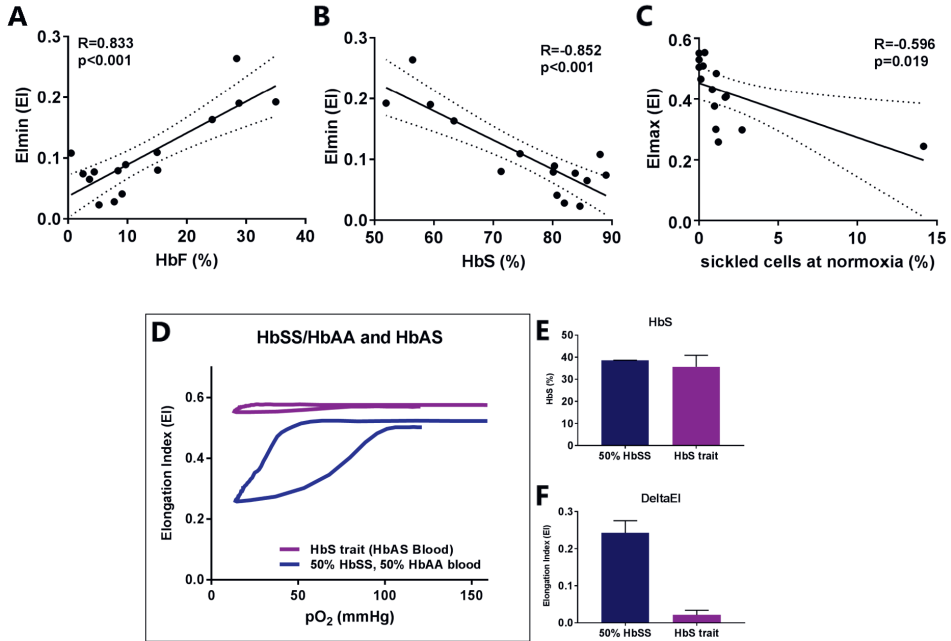


Figure 4. Oxygen scan parameters are associated with HbF, HbS, and sickled cells at normoxia. (A) Linear correlation of minimum Elongation Index (Elmin) and HbF. (B) Linear correlation of Elmin and %HbS. (C) Linear correlation of maximum EI (Elmax) and % sickled cells at normoxia measured with digital microscopy. (D) Representative curve of the effect of addition of 50% HBAA blood to 50% HbSS blood and a representative curve of HbS trait. (E) Percentage HbS in the mixture of 50% HbSS blood with 50% HbAA blood (n = 2) and HbS trait (n = 5). (F) DeltaEI in both groups mentioned earlier. Dashed lines represent 95% confidence intervals. Error bar represents SD.

corrected (100% HbAS) cells. Therefore DeltaEI is an useful parameter, in particular in the evaluation of individuals with HbS trait and the development of new treatment strategies.

PoS discriminates between genotypes and different treatment regimens

We show that PoS correlates with 2,3-DPG levels and other modulators that have an effect on the hemoglobin dissociation curve, such as pH and temperature (Supplemental Figure 2A, B, F and J). PoS is unique in its ability to determine the pO_2 at which RBCs start to sickle, and is therefore of high value in the development and clinical testing of new drugs, in particular anti-sickling agents. When considering individuals with HbS trait, PoS has a distinct value in this group compared to controls and SCD patients (Figure 3G). PoS also is the most informative parameter when considering different treatment in groups of SCD patients. Based on these observations we conclude that PoS likely reflects properties of an individual's hemoglobin dissociation curve.

Elmax reflects percentage of sickled cells at normoxia and RBC hydration

In whole blood, the percentage of sickled cells at normoxia compared to relatively healthy cells seem to have the most pronounced effect on Elmax. The number of sickled cells at

normoxia correlated to Elmax (Figure 4C), indicating that already sickled cells lower the overall deformability and thereby Elmax. We suggest that Elmax reflects the percentage of non-deformable cells at ambient air, which are the dense cells containing HbS polymer and sickled cells at normoxia.

Comparison with other hypoxic deformability assays

In the past several approaches to measure RBC deformability under hypoxic conditions have been developed. All but one were based on a deoxygenation step that took place outside the ektacytometer.³²⁻³⁵ In contrast to the oxygenscan, these approaches involved either a deoxygenation or reoxygenation step, or used hypoxia and normoxia as different conditions. A very recent study demonstrated a strong effect of GBT440 on RBC deformability, but no pO_2 could be determined and related to the measurements.³⁶ The oxygenscan allows now for the first time the study of sickling behavior during both automated deoxygenation and reoxygenation in a reproducible and fast manner.

One of the strengths of the oxygenscan is that deformability is measured at a whole range of different oxygen tensions. Furthermore, the technique has an excellent reproducibility, the time to perform an oxygenscan measurement is relatively short and it takes only a small amount of whole blood. More importantly, the oxygenscan is a functional assay that determines various aspects of the sickling process, each represented by different parameters.

A limitation of the technique is that measurements are performed on the total RBC population. Therefore, individual differences in cellular behavior or subpopulations of cells are not considered and, consequently, outcome parameters always reflect the mean behavior of all cells. Also, the minimal pO_2 during deoxygenation does not reach 0mmHg. Although this pO_2 is not a physiologically relevant value, it would be of interest to measure in order to see how much the EI would further decrease.

Our data show that apart from the influence of HbF, HbS and HbA, this assay also takes individual hemoglobin dissociation curves and percentage of sickled cells at normoxia into account. Therefore, the oxygenscan is an assay which simultaneously determines a number of clinically important factors involved in SCD pathophysiology. As such it may represent a better alternative for the conventional sickling assay and fill the clinical need for a reliable biomarker. Current studies are aimed at investigating the applicability of the oxygenscan in the determination of clinical severity and vaso-occlusive crisis, as well as a more comprehensive analysis of the effect of current and new treatment strategies.

Acknowledgments

This research has been funded in part by Eurostars grant estar18105 and by an unrestricted grant provided by RR Mechatronics. This work was supported in part by NIH/NIMHD grant MD009124 (MKS).

The authors would like to thank Jan de Zoeten and Sisto Hendriks of RR Mechatronics for the technical support of the oxygenscan.

Authorship

Contribution: M.A.E.R, B.A.O, E.J.B. and R.W. designed the experiments. M.A.E.R., B.A.O., J.B., T.H.M., A.C.W.W., O.A., A.B.V., M.E.H., and J.R. collected samples and/or performed experiments. M.S. and O.A. provided new drugs. M.A.E.R., E.J.B. and R.W. analyzed the data and wrote the manuscript with input and revisions of B.A.O., O.A., M.S., M.E.H., M.H.C., M.B., R.E.G.S., and G.P.

Conflict-of-interest disclosure

The authors declare no conflicts of interest

References

- Poillon WN, Kim BC, Labotka RJ, et al. Antisickling effects of 2,3-diphosphoglycerate depletion. *Blood*. 1995;85(11):3289-3296.
- Mohandas N, Evans E. Adherence of Sickle Erythrocytes to Vascular Endothelial Cells: Requirement for both Cell Membrane Changes and Plasma Factors. *Blood*. 1984;64(1):282-287.
- Mohandas N, Evans E. Sickle cell adherence to vascular endothelium: Morphologic correlates and the requirement for divalent cations and collagen-binding plasma proteins. *J Clin Invest*. 1985;76(4):1605-1612.
- Papageorgiou DP, Abidi SZ, Chang H-Y, et al. Simultaneous polymerization and adhesion under hypoxia in sickle cell disease. *Proc Natl Acad Sci*. 2018;(13):201807405.
- Kato GJ, Piel FB, Reid CD, et al. Sickle cell disease. *Nat Rev Dis Prim*. 2018;4:1-22.
- Antoniani C, Meneghini V, Lattanzi A, et al. Induction of fetal hemoglobin synthesis by CRISPR/Cas9-mediated editing of the human β -globin locus. *Blood*. 2018;131(17):1960-1973.
- Abdulmalik O, Ghatge MS, Musayev FN, et al. Crystallographic analysis of human hemoglobin elucidates the structural basis of the potent and dual antisickling activity of pyridyl derivatives of vanillin. *Acta Crystallogr Sect D Biol Crystallogr*. 2011;67(12):1076.
- Oder E, Safo MK, Abdulmalik O, Kato GJ, Discovery D. New Developments in Anti-Sickling Agents: Can Drugs Directly Prevent the Polymerization of Sickle Haemoglobin In Vivo? *Br J Haematol*. 2016;175(1):24-30.
- Oksenberg D, Dufu K, Patel MP, et al. GBT440 increases haemoglobin oxygen affinity, reduces sickling and prolongs RBC half-life in a murine model of sickle cell disease. *Br J Haematol*. 2016;175(1):141-153.
- Xu GG, Pagare PP, Ghatge MS, et al. Design, Synthesis, and Biological Evaluation of Ester and Ether Derivatives of Antisickling Agent 5-HMF for the Treatment of Sickle Cell Disease. *Mol Pharm*. 2017;14(10):3499-3511.
- van Beers EJ, Samsel L, Mendelsohn L, et al. Imaging flow cytometry for automated detection of hypoxia-induced erythrocyte shape change in sickle cell disease. *Am J Hematol*. 2014;89(6):598-603.
- Smith C, Kuettner J, Tukey D, White J. Variable Deformability of Irreversibly Sickled Erythrocytes. *Blood*. 1981;58(1):71-78.
- Clark MR, Mohandas N, Shohet SB. Deformability of oxygenated irreversibly sickled cells. *J Clin Invest*. 1980;65(1):189-196.
- Clark M, Mohandas N, Embury S, Lubin B. A simple laboratory alternative to irreversibly sickled (ISC) counts. *Blood*. 1982;60(3):659-663.
- DaCosta L, Suner L, Galimand J, et al. Blood Cells, Molecules and Diseases Diagnostic tool for red blood cell membrane disorders: Assessment of a new generation ektacytometer. *Blood Cells, Mol Dis*. 2016;56(1):9-22.
- Lazarova E, Gulbis B, Oirschot B Van, Van Wijk R. Next-generation osmotic gradient ektacytometry for the diagnosis of hereditary spherocytosis: Interlaboratory method validation and experience. *Clin Chem Lab Med*. 2017;55(3):394-402.
- Llaudet-Planas E, Vives-Corróns JL, Rizzuto V, et al. Osmotic gradient ektacytometry: A valuable screening test for hereditary spherocytosis and other red blood cell membrane disorders. *Int J Lab Hematol*. 2018;40(1):94-102.
- Zaninoni A, Fermo E, Vercellati C, et al. Use of laser assisted optical rotational cell analyzer (LoRRca MaxSis) in the diagnosis of RBC membrane disorders, enzyme defects, and congenital dyserythropoietic anemias: A monocentric study on 202 patients. *Front Physiol*. 2018;9(APR):1-12.
- Parrow NL, Tu H, Nichols J, et al. Measurements of red cell deformability and hydration reflect HbF and HbA2in blood from patients with sickle cell anemia. *Blood Cells, Mol Dis*. 2017;65:41-50.
- Lemonne N, Lamarre Y, Romana M, Mukisimukaza, Martin; Hardy-Dessources, M.-D; Tarer, V; Mouguel, D; Waltz, Xavier; Tressieres, B; Lalanne-Mistrih, M.-L; Etienne-Julan, M; Connes P. Does increased red blood cell deformability raise the risk for osteonecrosis in sickle cell anemia? *Blood*. 2013;121(15):3054-3057.
- Ballas, S K Larner, J Smith ED, Surrey S, Schwartz, E Rappaport EF. Rheologic predictors of the severity of the painful sickle cell crisis. *Blood*. 1988;72(4):1216-1223.
- Lande WM, Andrews DL, Clark MR, et al. The Incidence of Painful Crisis in Homozygous Sickle Cell Disease: Correlation with Red Cell Deformability. *Blood*. 1988;72(6):2056-2059.

23. Ballas SK, Smith ED. Red blood cell changes during the evolution of the sickle cell painful crisis. *Blood*. 1992;79(8):2154-2163.
24. Huisjes R, Solinge WW, Levin MD, Wijk R, Riedl JA. Digital microscopy as a screening tool for the diagnosis of hereditary hemolytic anemia. *Int J Lab Hematol*. 2017;40(2):159-168.
25. Metcalf B, Chuang C, Dufu K, et al. Discovery of GBT440, an Orally Bioavailable R-State Stabilizer of Sickle Cell Hemoglobin. *ACS Med Chem Lett*. 2017;8(3):321-326.
26. Pagare PP, Ghatge MS, Musayev FN, et al. Rational design of pyridyl derivatives of vanillin for the treatment of sickle cell disease. *Bioorganic Med Chem*. 2018;26(9):2530-2538.
27. Abdulmalik O, Safo MK, Chen Q, et al. 5-Hydroxymethyl-2-furfural modifies intracellular sickle haemoglobin and inhibits sickling of red blood cells. *Br J Haematol*. 2005;128(4):552-561.
28. Nagel RL, Fabry ME, Steinberg MH. The paradox of hemoglobin SC disease. *Blood Rev*. 2003;17(3):167-178.
29. Spencer JA, Ferraro F, Roussakis E, et al. Direct measurement of local oxygen concentration in the bone marrow of live animals. *Nature*. 2014;508(7495):269-273.
30. Intaglietta M, Johnson PC, Winslow RM. Microvascular and tissue oxygen distribution. *Cardiovasc Res*. 1996;32(4):632-643.
31. Asakura, T; Mayberry J. Relationship between morphologic characteristics of sickle cells and method of deoxygenation. *J Lab Clin Med*. 1984;104(6):987-994.
32. Bessis, M; Feo, C; Jones E. Quantitation of red cell deformability during progressive deoxygenation and oxygenation in sickling disorders (the use of an automated Ektacytometer). *Blood Cells*. 1982;8(1):17-28.
33. Sorette, M P Lavenant, M G Clark MR. Ektacytometric measurement of sickle cell deformability as a continuous function of oxygen tension. *Blood*. 1987;67(6):1600-1606.
34. Huang Z, Hearne L, Irby CE, King SB, Ballas SK, Kim-Shapiro DB. Kinetics of increased deformability of deoxygenated sickle cells upon oxygenation. *Biophys J*. 2003;85(4):2374-2383.
35. Lu X, Chaudhury A, Higgins JM, Wood DK. Oxygen-dependent flow of sickle trait blood as an in vitro therapeutic benchmark for sickle cell disease treatments. *Am J Hematol*. 2018;93(10):1227-1235.
36. Dufu K, Patel M, Oksenberg D, Cabrales P. GBT440 improves red blood cell deformability and reduces viscosity of sickle cell blood under deoxygenated conditions. *Clin Hemorheol Microcirc*. 2018;70(1):95-105.

Supplemental Methods

Hematological laboratory parameters

Routine hematological parameters were measured using the Abbott Cell-Dyne Sapphire (Abbott Diagnostics, Santa Clara, CA, USA) and included complete blood counts and absolute reticulocyte count. Hemoglobin characterization was carried out with high-performance liquid chromatography (HPLC, Tosoh Europe, Tessenderlo, Belgium).

Light microscopy of deoxygenated RBCs

To visualize red blood cell shape and/or the presence of sickle RBCs during deoxygenation, whole blood was mixed with Iso Oxy and injected into 2 tubes (Falcon) and placed on a roller bench. One tube was deoxygenated using nitrogen gas for 15 minutes during rotation, whilst the other tube remained oxygenated during rotation. Cells were fixated with 1% paraformaldehyde and 0.2% glutaraldehyde. Fixed cells were examined by light microscopy (Axiovert 40C, Zeiss).

Effect of storage of whole blood on oxygenscan measurements

Whole blood was stored for 8 days at 4 degrees Celsius. From day 0 to day 7 an oxygenscan was carried out every consecutive day. In addition, at day 0, 3 and 7 free hemoglobin levels, indicating RBC lysis, was measured by absorbance measurements at 542nm using spectrophotometry (SpectraMax M2e (Molecular Devices, Sunnyvale, CA, USA). On the same days blood smears were made and analyzed by digital microscopy as described above.

2,3-DPG levels, pH and temperature

To assess the influence of 2,3-diphosphoglycerate (2,3-DPG) levels on the oxygenscan parameters, complete blood count and oxygenscans were performed within 10 minutes after blood collection, and after 3, 6 and 24 hours. Whole blood was kept either at 4°C, room temperature ($\pm 22^\circ\text{C}$) and 37°C for 24 hours. 2,3-DPG was measured using the 2,3-DPG assay kit (Roche, Mannheim, Germany). To measure 2,3-DPG, blood was collected in heparin tubes and immediately deproteinized with perchloric acid (0.6 M). Following centrifugation the solution was stabilized with potassium carbonate (2.5M) and centrifuged again. Method of 2,3-DPG measurement is based on the enzymatic conversion of 2,3-DPG to nicotinamide adenine dinucleotide (NAD⁺) in several steps. NAD⁺ concentration was measured with spectrophotometry (SpectraMax M2e, Molecular Devices, Sunnyvale, CA, USA). 2,3-DPG levels were normalized to hemoglobin levels.

To assess the influence of temperature, oxygenscan measurements were carried out with a Bob temperature set to either 35, 37, 39, 41 and 43°C.

To investigate the influence of pH, the pH of the PVP (Iso Oxy) was set to 6.9, 7.1, 7.3, 7.7 and 7.9 before being used in the oxygenscan.

Morphological analysis after *in vitro* incubation with anti-sickling agents

To compare the outcome of the effect of these agents sickling was also measured using previously reported methodology with slight modifications.¹⁻³ Briefly, whole blood was suspended (20%hematocrit) in isotonic Hemox buffer (TCS Scientific Corp, Southampton,

PA, USA), pH 7.4, supplemented with 10 mM glucose and 0.2% bovine serum albumin, in individual wells of a Costar polystyrene 96-well microplate (№ 9017; Corning, Corning, NY), then incubated under air in the absence (control, DMSO) or presence of varying concentrations of 5-PMFC, INN312, and GBT440 at 37°C for 1 hour to ensure that binding has attained equilibrium. Next, the suspensions were incubated under hypoxic condition (2.5% Oxygen gas/97.5% Nitrogen gas) at 37°C for 1 hour. Aliquots (10 µL) of each sample were obtained and fixed with 150 µL 2% glutaraldehyde solution without exposure to air. The fixed cell suspensions were introduced into glass microslides (Dawn Scientific, Inc., Newark, NJ, USA)¹ and subjected to microscopic morphological analysis of bright field images (at 40x magnification) of single layer cells on an Olympus BX40 microscope fitted with an Infinity Lite B camera (Olympus), and the coupled Image Capture software. The percentage of sickled cells was determined with a computer-assisted image analysis system as described elsewhere.⁴ Normalized sickling, reported as mean values from 3 replicates, was calculated by normalizing to untreated control (DMSO) samples.

Statistical Analysis

Experiments were carried out in duplicates, except for experiments consisting of series of oxygenescans (pH and temperature experiments). Mean, standard deviation (SD) and coefficient of variation (CV) were calculated. GraphPad Prism (v7.02) was used to plot individual oxygenescan curves and readout parameters. We normalized results in the experiments with 2,3-DPG because 2,3-DPG was heterogeneous among patients, and in experiments with anti-sickling agents to compare oxygenescans with microscopy, the conventional sickling assay.

Statistical analysis was performed using IBM Statistics SPSS (v21) and Graphpad Prism. One-way ANOVA (Post-hoc Tukey's test or Dunnett's test) was carried out. When groups were not normally distributed a Kruskal-Wallis test, followed by Dunn's tests for post-hoc analysis was used. Pearson's correlation was used to determine correlations of oxygenescan parameters with laboratory and clinical parameters. A *p*-value of <0.05 was considered statistical significant.

Supplemental Results

Effect of storage of whole blood on the oxygenscan

To identify the time-window after blood collection to perform an oxygenscan the effect of time was investigated. Oxygenscan curves shifted slightly upwards during storage of whole blood at 4 °C. When stored for 24 hours at 4°C curves remained stable, showing minor increases in Elmax (1,7%), PoS (2,7%), DeltaEI (9,2%) and Area (6,7%). Minor decreases of 6,7% in Elmin and 0,6% in Recovery were observed under these conditions (normalized and pooled data of 10 patients, Supplemental Table 1).

Elmax increased considerably upon longer storage with a mean increase of 8,1% after 3 days and 14,1% after 7 days. Initially Elmin slowly decreased, but after day 3, when a decrease of 4,4% was measured, Elmin increased with 25,3% after seven days. Looking at DeltaEI, an increase of 15,4% was observed after 3 days, however at day 7 there was a decrease of 4,3%. PoS was shifted towards the left as it decreased with 1,2% and 17,1%. Area and Recovery increased over time with 14,5% and 1,0% at day 3, and 20,9% and 2,1% at day 7 (normalized and pooled data of 3 patients). When percentage of lysis was measured it increased from 10.4% at day 3 until 12.8% at day 7. When peripheral blood smears were analyzed with digital microscopy a decrease in sickled cells was seen after 3 and 7 days, from 11.1% at day 0, 2.7% at day 3 and 1.1% at day 7 (measured in 1 patient, data not shown).

In vitro addition of HbAA blood to HbSS blood

To mimic blood transfusion and to investigate the effect of addition of HbAA blood, ABO and Rhesus compatible RBCs of a healthy control (HC) was mixed with whole blood of a patient with SCD in different amounts and oxygenscans were performed. Supplemental Figure 1A, B, E and G show that Elmax, Elmin and Area shifted towards normal upon increasing percentages of HbAA blood. At the same time the PoS and DeltaEI decreased (Supplemental Figure 1C,D). Recovery increased to 100% upon addition of HbAA blood (Supplemental Figure 1F).

All Oxygenscan parameters correlated significantly with the percentage of whole blood of HbSS patients but with a striking linear correlate of $r=0.998$, $p>0.0001$ (pooled data of 3 patients, individual correlations were above $r=0.987$ and $p<0.002$), Elmin was the strongest one (Supplemental Figure 1H). Elmax correlated second best with a linear correlate of $r=0.988$ ($p=0.002$, pooled data of 3 patients, individual correlations were above $r=0.982$ with $p<0.003$, Supplemental Figure 1G). Correlation of PoS with %HbSS blood was lower compared to Elmin and Elmax, with $r=0.946$, $p=0.015$ (pooled data, individual correlations were above $r=0.933$ with $p<0.021$, Supplemental Figure 1K). Linear correlations of DeltaEI, and Area are shown in (Supplemental Figure 1J and L).

Physiologic Hb-dissociation curve modulators (2,3-DPG, temperature and pH)

Temperature, pH and 2,3-DPG are important cellular modulators of the O₂ affinity of hemoglobin and thereby of sickling. They are therefore expected to exert an effect on the oxygenscan curve. For studying the effect of 2,3-DPG levels whole blood was stored under 3 different conditions for 24 hours. Oxygenscan curves and 2,3-DPG were essentially unchanged after 24 hours at 4 °C (Supplemental Figure 2A-G). When kept at room

temperature or 37 °C 2,3-DPG had decreased after 24 hours (normalized and pooled data is shown in Supplemental Figure 2B). 2,3-DPG showed the strongest correlation with PoS (Supplemental Figure 2J, individual correlations were $r=0.994$ $p=0.006$, $r=0.958$ $p=0.042$ and $r=0.978$ $p=0.022$) and Elmin (Supplemental Figure 2I, individual correlations were $r=0.991$ $p=0.009$, $r=0.749$ $p=0.251$, and $r=0.949$ $p=0.051$). Elmax showed a lower correlation which wasn't significant (Supplemental Figure 2H, individual correlations $r=0.920$ $p=0.080$, $r=-0.850$ $p=0.150$ and $r=0.637$ $p=0.363$). Linear correlation of DeltaEI and Area with 2,3-DPG are shown in Supplemental Figure 2K and L.

Upon lowering the pH of the PVP an increase of Elmax, DeltaEI and PoS was seen (Supplemental Figure 3A, B, D and E). Elmin, Area and Recovery decreased (Supplemental Figure 3C, F and G). Upon increasing the pH the opposite effect was observed (Supplemental Figure 3A-G). The 2 parameters with the strongest correlation were Elmax ($r=0.989$, $p<0.001$ pooled data, Figure 3H, individual values were above $r=0.972$, $p=0.001$), and PoS ($r=0.993$, $p<0.001$ (pooled data), Supplemental Figure 3K, individual correlations were all 3 above $r=0.980$, $p=0.002$). Linear correlations of pooled data of Elmin, DeltaEI, and Area are shown in Supplemental Figure 3I, J and L.

Next, we performed oxygenscans of a single sample at different Cup and Bob temperatures. When temperature was set to higher temperatures (39, 41 and 43 °), the PoS increased, with a linear correlate of 0.974 $p=0.005$ (pooled data, individual values were above $r=0.921$, $p=0.026$, Supplemental Figure 4D and J), indicating sickling starts already at higher pO_2 tension. Accordingly, the DeltaEI also increased (Supplemental Figure 4C, linear correlation overall $r=0.972$, $p=0.006$ Supplemental Figure 4I). A decrease in Elmax (overall $r=0.996$, $p<0.001$, individual values were above $r=0.965$ $p=0.008$ Supplemental Figure 4A and G), Elmin (overall $r=0.989$ $p=0.001$, individual correlations were above $r=0.927$ $p=0.024$ Supplemental Figure 4B and H) and the Area (overall $r=0.951$ $p=0.013$ Supplemental Figure 4E and K) was observed. Recovery was lower in high temperatures compared to 37 °C (overall $r=0.976$ $p=0.004$, Supplemental Figure 4F and L). When temperature was lowered to 35 °C an opposite effect was observed (Supplemental Figure 4A-F).

Supplemental Table 1. Effect of storage of whole blood at 4°C on oxygenscan parameters during 8 days. Data of 10 patients with SCD are shown looking at a storage duration of 24hours (day 1), data of 3 patients is shown considering storage duration of 8 days (day 0-day 7).

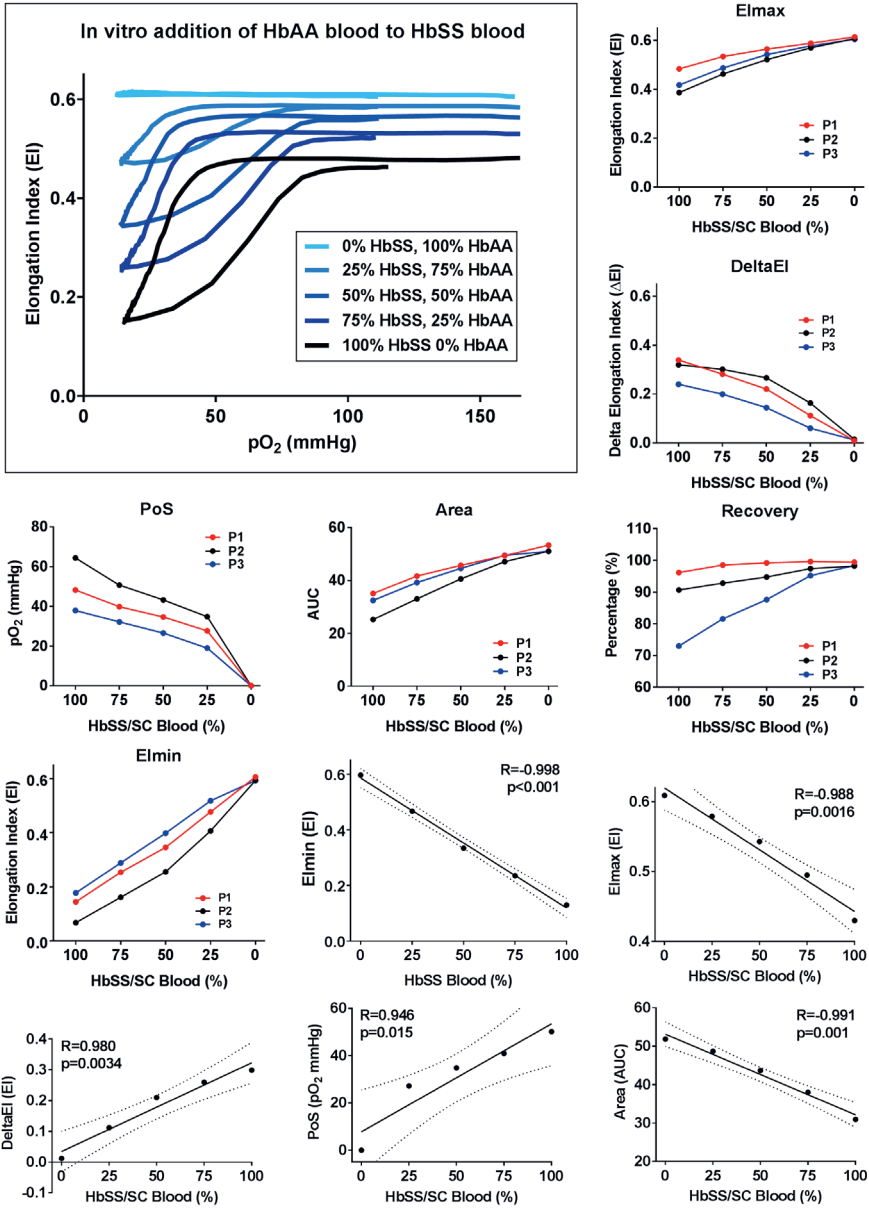
Increase due to storage	Day 1 (n=10)		Day 3 (n=3)	Day 7 (n=3)
	Mean (%)	SD	Mean (%)	Mean (%)
Elmax (EI)	1.7	2.6	8.1	14.1
Elmin (EI)	-6.7	10.0	-4.4	25.3
DeltaEI (EI)	9.2	8.3	15.4	-4.3
PoS (mmHg)	2.7	8.8	-1.2	-17.1
Area (AUC)	6.7	6.5	14.5	20.9
Recovery (%)	0.6	4.2	1.0	2.1

SD, standard deviation. PoS, point of sickling.

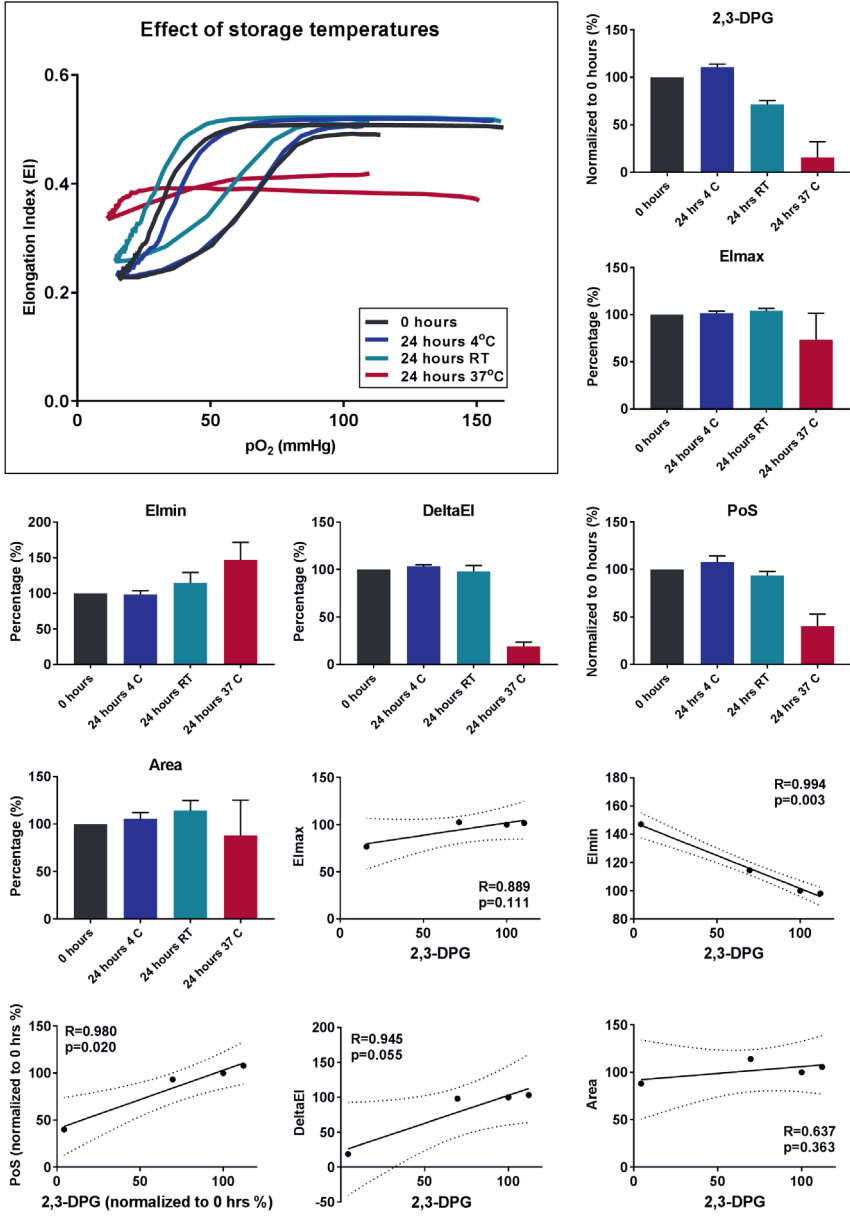
Supplemental Table 2. Discrimination between different genotypes and treatment regimens with oxygenscan parameters

	HbSS untreated (n=7)	HbSS HU (n=5)	HbSS transfusion (n=3)	HbSC (n=3)	HbS trait (n=5)	Healthy control (n=5)
Elmax (EI)	0.34 ± 0.01	0.48 ± 0.06*	0.45 ± 0.09	0.38 ± 0.06	0.59 ± 0.01****	0.61 ± 0.0****
Elmin (EI)	0.07 ± 0.04	0.14 ± 0.08	0.22 ± 0.03**	0.13 ± 0.09	0.56 ± 0.01****	0.60 ± 0.0****
DeltaEI (ΔEI)	0.28 ± 0.07	0.33 ± 0.05	0.23 ± 0.09	0.25 ± 0.06	0.02 ± 0.01****	0.01 ± 0.0****
PoS (mmHg)	73.6 ± 18.3	49.6 ± 7.2**	52.9 ± 6.1	41.3 ± 8.4**	16.3 ± 1.7****	-
Area (AUC)	22.4 ± 6.4	34.6 ± 7.1**	33.2 ± 6.6	28.9 ± 6.3**	48.9 ± 0.3****	49.7 ± 1.0****
Recovery (%)	96.1 ± 5.0	95.5 ± 3.2	97.9 ± 2.1	77.8 ± 12.0***	98.9 ± 0.4	99.6 ± 0.4

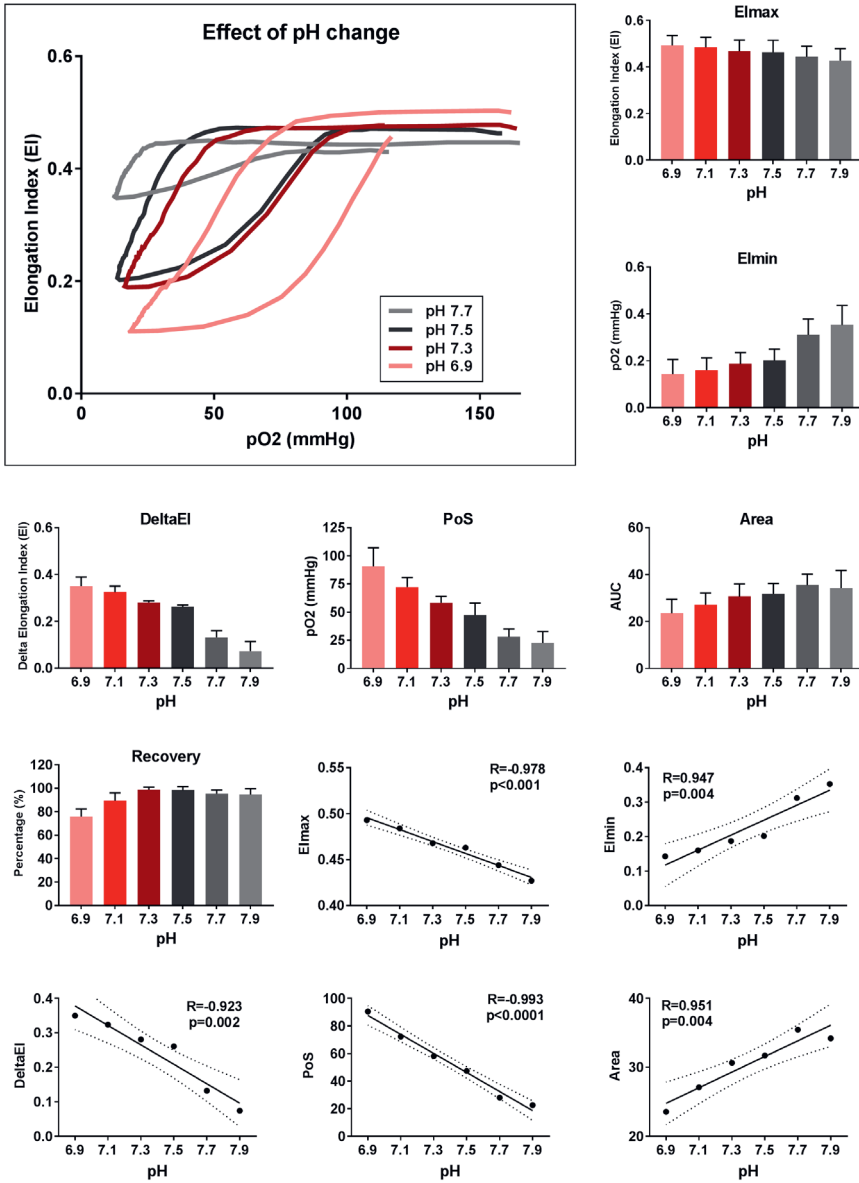
****p<0.0001, ***p<0.001, ** p<0.01, *p<0.05., PoS, point of sickling.



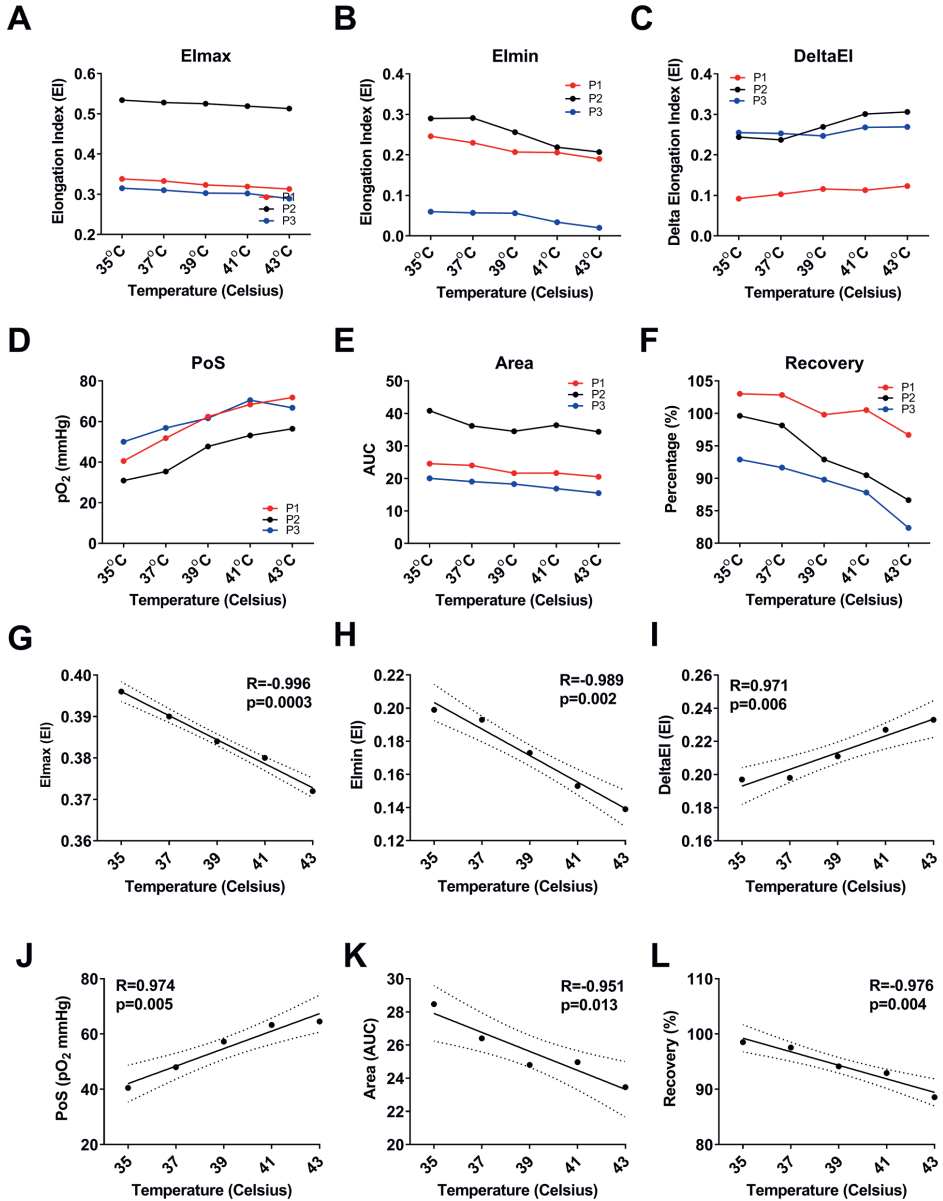
Supplemental Figure 1. Whole blood from SCD patients (n=3, P1, P2 (HbSS) and P3 (HbSC)) was mixed in various proportions with an ABO and Rhesus compatible healthy control blood. (A) Representative curve of the effect of addition of HbAA blood to HbSS blood. **(B)** Maximum Elongation Index (Elmax) in relation to different percentages of HbSS/SC and HbAA blood. **(C)** DeltaEI (Difference between Elmax and Elmin) in relation to % HbSS/SC blood. **(D)** Point of Sickling (PoS, pO_2 when 5% decrease in EI is observed) in relation to % HbSS/SC blood. **(E)** Area (area under curve between 10 and 100mmHg) in relation to %HbSS/SC blood. **(F)** Recovery (% of start EI reached during reoxygenation) in relation to % HbSS/SC blood. **(G)** Minimum EI (Elmin) in relation to % HbSS/SC blood. **(H)** Linear correlation of Elmin and % HbSS/SC blood. **(I)** Linear correlation of Elmax and % HbSS blood. **(J)** Linear correlation of DeltaEI and % HbSS blood. **(K)** Linear correlation of PoS and % HbSS blood. **(L)** Linear correlation of Area and % HbSS blood. AUC, area under the curve. HbSS, homozygous HbS. HbSC, Hemoglobin SC, HbAA, healthy control.



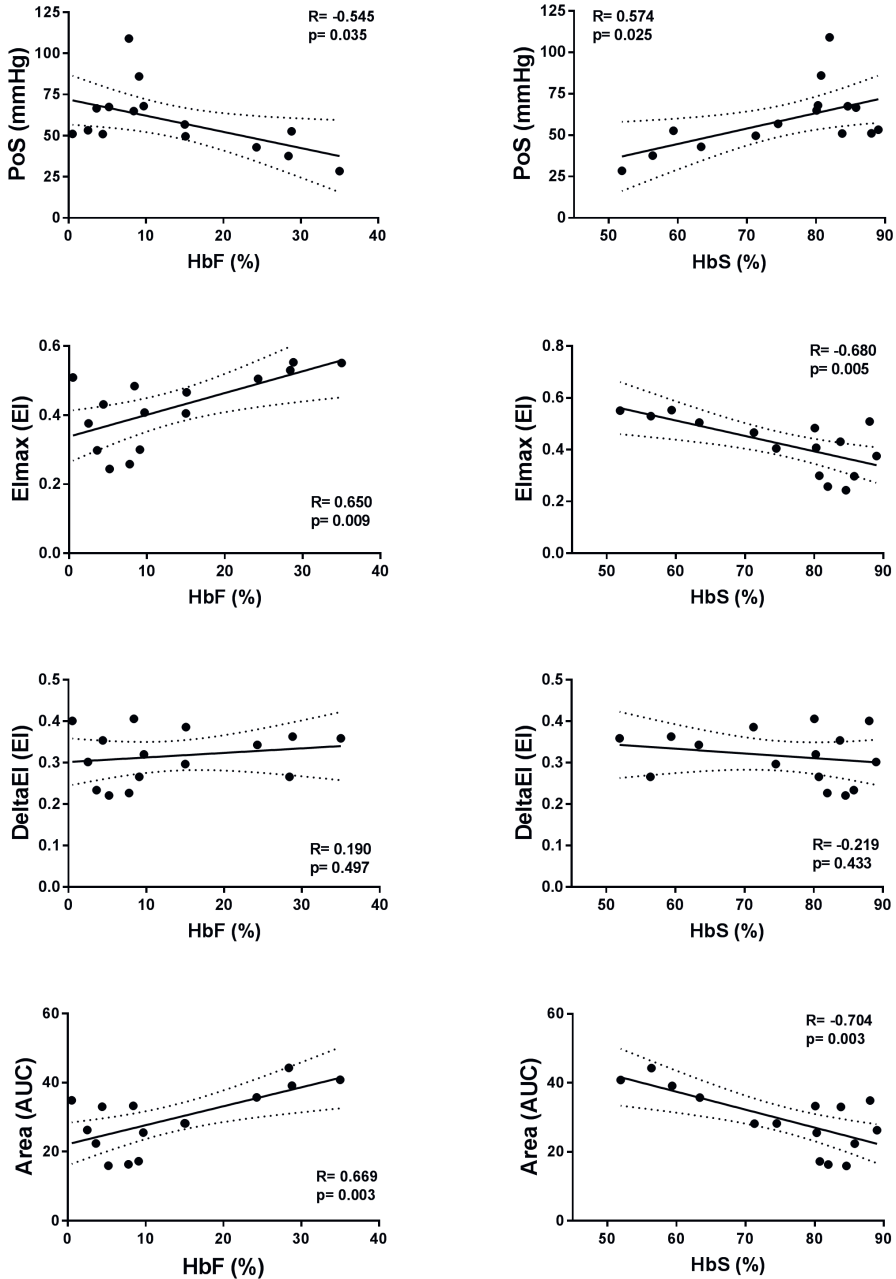
Supplemental Figure 2. Effect of different storage conditions on 2,3-DPG and oxygen scan parameters (n=3). (A) Representative graph of effect of 2,3-DPG on Oxygenscan curves in relation to storage of RBC of SCD patients (n=3) at different temperatures. (B) Normalized 2,3-DPG at baseline (0 hours) and after 24 hours storage at 4°C, room temperature (RT) and 37°C. (C) Normalized maximum elongation index (Elmax) at baseline (0 hours) and after 24 hours storage at 4°C, room temperature (RT) and 37°C. (D) Normalized minimum elongation index (Elmin) at baseline (0 hours) and after 24 hours storage at 4°C, room temperature (RT) and 37°C. (E) Normalized DeltaEI (difference between Elmax-Elmin) at baseline (0 hours) and after 24 hours storage at 4°C, room temperature (RT) and 37°C. (F) Normalized Point of Sickling (PoS) at baseline (0 hours) and after 24 hours storage at 4°C, room temperature (RT) and 37°C. (G) Normalized area at baseline (0 hours) and after 24 hours storage at 4°C, room temperature (RT) and 37°C. (H) Linear correlation of Elmax and 2,3-DPG. (I) Linear correlation of Elmin and 2,3-DPG. (J) Linear correlation of PoS and 2,3-DPG. (K) Linear correlation of DeltaEI and 2,3-DPG. (L) Linear correlation of Area and 2,3-DPG. Error bar represents SD. Dashed lines represent 95% confidence interval.



Supplemental Figure 3. Effect of pH changes on oxygen scan parameters (n=3). (A) Representative graph of the effect of pH change of Lorrca reagent (Iso Oxy) on oxygen scan curves. (B) Maximum elongation index (Elmax) at pH 6.9-7.9. (C) Minimum elongation index (Elmin) at pH 6.9-7.9. (D) DeltaEI (difference between Elmax-Elmin) at pH 6.9-7.9. (E) Area at pH 6.9-7.9. (F) Recovery at pH 6.9-7.9. (G) Point of Sickling (PoS) at pH 6.9-7.9. (H) Linear correlation of Elmax and pH. (I) Linear correlation of Elmin and pH. (J) Linear correlation of DeltaEI and pH. (K) Linear correlation of PoS and pH. (L) Linear correlation of Area and pH. (M) Linear correlation of Recovery and pH. Error bar represents SD. Dashed lines represent 95% confidence interval.



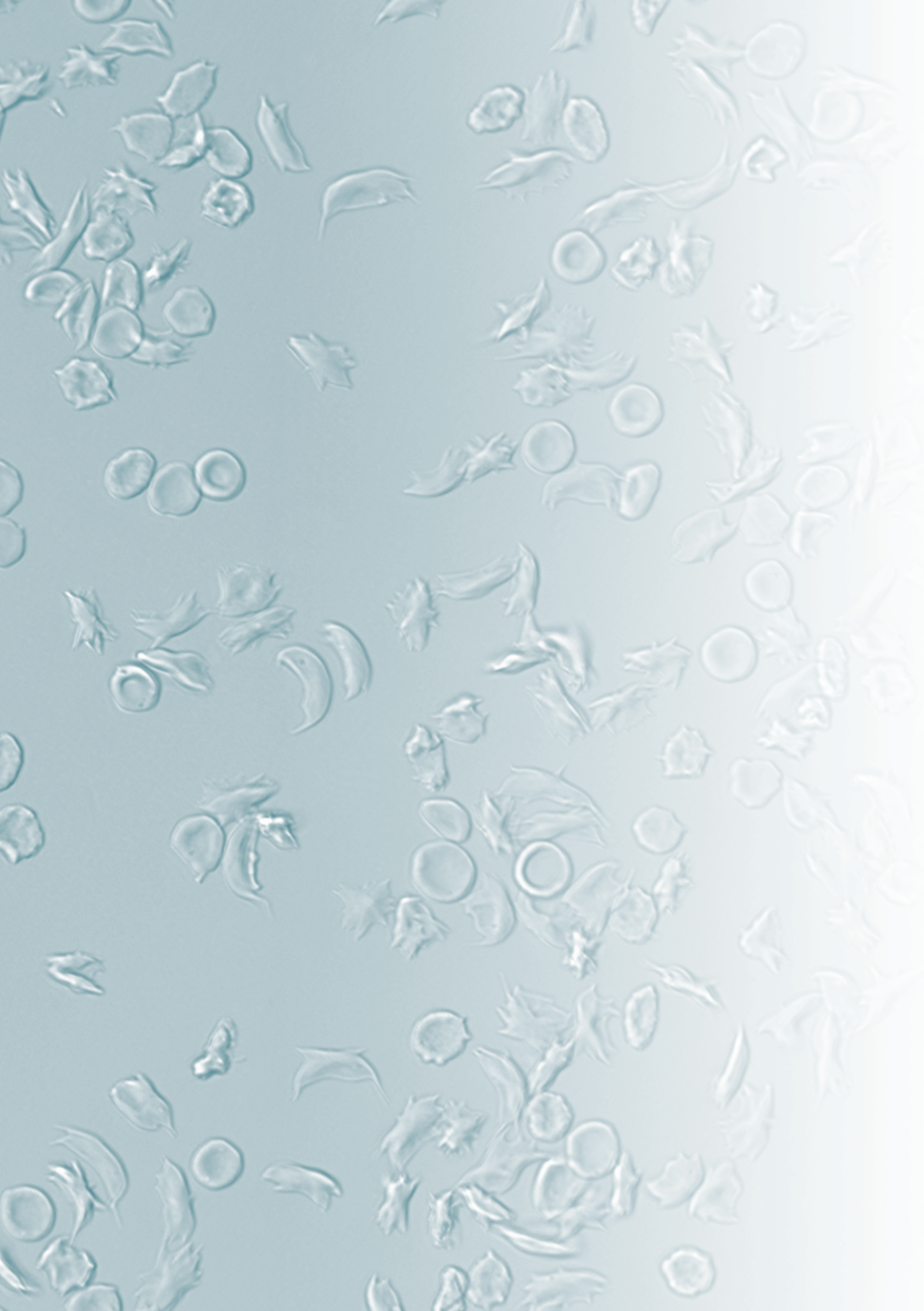
Supplemental Figure 4. Effect of temperature changes on Oxygenscan parameters (n=3). (A) Maximum elongation index (Elmax) at 35°C, 37°C, 39°C, 41°C and 43°C. (B) Minimum elongation index (Elmin) at temperatures 35°C-43°C. (C) DeltaEI (difference between Elmax-Elmin) at temperatures 35°C-43°C. (D) Point of Sickling (PoS) at temperatures 35°C-43°C. (E) Area at temperatures 35°C-43°C. (F) Recovery at temperatures 35°C-43°C. (G) Linear correlation of Elmax and temperature. (H) Linear correlation of Elmin and temperature. (I) Linear correlation of DeltaEI and temperature. (J) Linear correlation of PoS and temperature. (K) Linear correlation of Area and temperature. (L) Linear correlation of Recovery and temperature. Error bar represents SD. Dashed lines represent 95% confidence interval.



Supplemental Figure 5. Oxygenscan parameters in relation to HbS and HbF. (A) Linear correlation of Point of Sickling (PoS) and %HbF. (B) Linear correlation of PoS and %HbS. (C) Linear correlation of maximum EI (Elmax) and % HbF. (D) Linear correlation of Elmax and %HbS. (E) Linear correlation of DeltaEI (difference between Elmax and Elmin) and %HbF. (F) Linear correlation of DeltaEI and %HbS. (G) Linear correlation of Area and %HbF. (H) Linear correlation of Area and %HbS. Dashed lines represent 95% confidence intervals.

References

1. Abdulmalik O, Safo MK, Chen Q, et al. 5-Hydroxymethyl-2-furfural modifies intracellular sickle haemoglobin and inhibits sickling of red blood cells. *Br J Haematol.* 2005;128(4):552-561.
2. Abdulmalik O, Ghatge MS, Musayev FN, et al. Crystallographic analysis of human hemoglobin elucidates the structural basis of the potent and dual antisickling activity of pyridyl derivatives of vanillin. *Acta Crystallogr Sect D Biol Crystallogr.* 2011;67(12):1076.
3. Xu GG, Pagare PP, Ghatge MS, et al. Design, Synthesis, and Biological Evaluation of Ester and Ether Derivatives of Antisickling Agent 5-HMF for the Treatment of Sickle Cell Disease. *Mol Pharm.* 2017;14(10):3499-3511. doi:10.1021/acs.molpharmaceut.7b00553
4. Horiuchi, K; Ballas, S.K; Asaskura T. The Effect of Deoxygenation Rate on the Formation of Irreversibly Sickled Cells. *Blood.* 1988;71(1):46-51.



Chapter 3

Characterization of sickling during controlled automated deoxygenation with oxygen gradient ektacytometry

Journal of Visualized Experiments 2019; nov 5; (153)

Minke A.E. Rab^{1,2}, Brigitte A. van Oirschot¹, Jennifer Bos¹, Celeste K. Kanne³,
Vivien A. Sheehan³, Eduard J. van Beers², Richard van Wijk¹

¹ Laboratory of Clinical Chemistry and Hematology, University Medical Center Utrecht, Utrecht University, The Netherlands

² Van Creveldkliniek, University Medical Center Utrecht, Utrecht University, The Netherlands

³ Department of Pediatrics, Division of Hematology/Oncology, Baylor College of Medicine, Houston, Texas, USA

Abstract

In sickle cell disease (SCD), a single point mutation in the gene coding for beta-globin causes the production of abnormal hemoglobin S (HbS). When deoxygenated, HbS can polymerize, forming rigid rods of hemoglobin, resulting in the sickling of red blood cells (RBCs). These sickled RBCs have significantly reduced deformability, causing vaso-occlusion, which leads to numerous SCD-related clinical complications, including pain, stroke, and organ damage. RBC deformability is also reduced by RBC dehydration, resulting in dense red blood cells that are more likely to sickle. To date, there is not a single widely available, rapid, and reproducible laboratory assay capable of predicting the disease severity or directly monitoring the treatment effects for novel, non-fetal hemoglobin inducing therapies. In this study, we describe a protocol to measure RBC deformability as a function of pO_2 that allows for the quantitation of sickling behavior in SCD patients. Oxygen gradient ektacytometry measures RBC deformability, expressed as the elongation index (EI), as a function of pO_2 . RBCs are exposed to a fixed shear stress of 30 Pa during one round of deoxygenation and reoxygenation. Six readout parameters are produced. Of these, the point of sickling (PoS), defined as the pO_2 at which maximum EI (EI_{max}) shows a 5% decrease, and minimum EI during deoxygenation (EI_{min}) are the most informative, reflecting an individual patient's pO_2 at which sickling starts and the minimal deformability of a patient's red blood cells, respectively. PoS is associated with an individual patient's hemoglobin affinity for oxygen, whereas EI_{min} shows a strong correlation with fetal hemoglobin levels. We conclude that oxygen gradient ektacytometry is a promising technique to monitor the treatment of patients with SCD, as a biomarker for anti-sickling agents in clinical and preclinical trials, and an important tool to study sickling behavior of RBCs from individuals with SCD and sickle cell traits.

Video Link

<https://www.jove.com/video/60213/>

Introduction

In SCD, a single point mutation results in the production of HbS, which can polymerize upon deoxygenation. HbS polymerization causes sickling of RBCs and reduces RBC deformability. The combination of RBC sickling and RBC adherence to the endothelium leads to various SCD complications, including vaso-occlusive crises (VOC), stroke, organ damage, and chronic hemolytic anemia. Even at normoxic conditions, RBC deformability is compromised in patients with SCD. Deformability is further decreased at low oxygen concentrations. Key players that determine deformability at normoxia are dense cells, irreversibly sickled cells (ISC), and dehydrated cells, all of which have a decreased surface-to-volume ratio¹⁻³.

Ektacytometry is an established method to measure RBC deformability, widely used for the diagnosis of hereditary hemolytic anemias, particularly membranopathies⁴. It can also be used to study hemorheology⁵⁻⁹. Osmotic gradient ektacytometry, in which RBC deformability is measured during a continuous change in osmolality, has been used to study SCD for over a decade^{10,11}. The percentage of fetal hemoglobin (HbF) is one of the strongest inhibitors of HbS polymerization because neither HbF nor its mixed hybrid tetramer ($\alpha\beta\gamma\delta$) can enter the deoxyHbS polymer phase¹². Recent studies suggest that increasing HbF levels in SCD patients leads to a better surface-to-volume ratio, thereby improving the hydration state and thus the deformability in nontransfused patients¹¹.

RBC deformability has been studied in the past as a biomarker for SCD complications, but with conflicting results. In studies performed cross-sectionally and at a steady state, individuals with higher levels of RBC deformability were found to have a higher incidence of osteonecrosis and more pain crises¹³⁻¹⁵. In contrast to these findings, when compared to the steady state values during an acute VOC, RBC deformability was decreased in longitudinal studies within the same individuals¹⁶. This discrepancy may be the result of studying RBC deformability under different conditions (i.e., during the steady state versus VOC). The percentage of sickled cells is high at the start of a VOC and the cells are rapidly destroyed as the crisis progresses, which may explain the difference between the steady state cross-sectional incidence data and longitudinal data obtained during the VOC. However, other factors, such as adherence of RBC subpopulations to the endothelial surface, may also be important in the occurrence of VOC. In SCD, it is more clinically relevant to measure the deformability during the deoxygenation, because vaso-occlusion typically occurs in the hypoxic post capillary venules and not in the less hypoxic microcapillary network¹⁷. Additionally, the presence of ISCs may alter the ability of an ektacytometer to measure the deformability at normoxia. Distortion of the diffraction pattern is caused by ISCs, which results from the non-alignment during the flow¹⁻³.

Alternative approaches to study the pathophysiology of VOC include measurements of RBC adherence to an artificial surface¹⁸, single cell electrical impedance microflow cytometry¹⁹, microfluidic-based models combining quantitative measurements of the cell sickling and unsickling with single cell rheology²⁰, and laser-induced polymerization²¹. Although promising, these techniques are costly, labor intensive, and require extensive operator training.

In addition, the assays that are morphology-based lack the ability to study cellular behavior, such as deformability, as a function of an oxygen gradient.

In this study, we describe a rapid and reproducible functional assay performed with an ektacytometer. This is a next generation ektacytometry measurement that measures the different qualitative aspects of RBC deformability expressed as the EI during deoxygenation (1,300 s) and swift reoxygenation (280 s). These time intervals allow for HbS polymer formation, and thereby the occurrence of morphological changes and then recovery. Deoxygenation occurs by introducing nitrogen gas, which slowly decreases the oxygen tension in the blood sample in the gap between the bob and cup of the ektacytometer. RBC deformability is continuously measured while oxygen tension is measured every 20 s by means of a small O₂-spot present in the wall of the cup. During the test, approximately 80 pO₂ measurements are coupled to the EI measured at that moment. The oxygen pressure drops below 20 mmHg during the deoxygenation, and reoxygenation is facilitated by the passive diffusion of ambient air. The experimental setup of the ektacytometer and oxygen gradient ektacytometry module is described in **Figure 1** and **Figure 2**. The principle of ektacytometry is based on RBC-induced scattering of light from a laser beam. This results in an elliptical diffraction pattern when shear stress is applied at the same time (**Figure 1**).

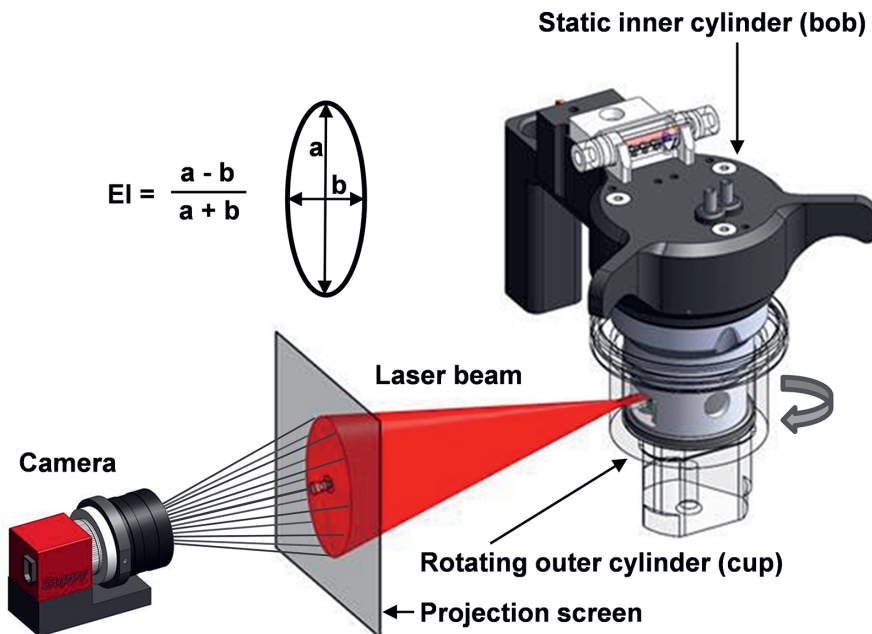


Figure 1. Schematic setup of the ektacytometer. The ektacytometer uses a Couette system to apply shear stress on the cells. A rotation outer cylinder (cup) and a static inner cylinder (bob) are used to induce shear stress by the creation of laminar flow at 37 °C. Between the bob and cup there is a small gap in which the blood suspension is injected. A laser beam shines from the bob through the blood suspension and is scattered by the presence of RBCs. The diffraction pattern is projected and analyzed by a camera. The elongation index (EI) is calculated with the height (a) and the width (b) of the diffraction pattern⁴.

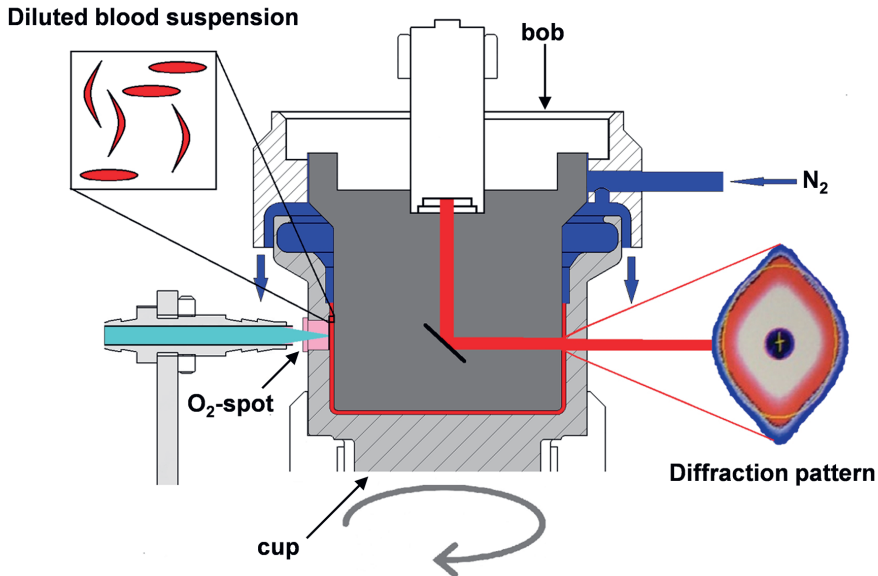


Figure 2. Schematic setup of the ektacytometer with oxygen gradient ektacytometry module. Schematic diagram of the module that shows deoxygenation of the blood suspension slowly with the infusion of nitrogen gas (N_2). Oxygen tension is measured by the amount of quenching of the luminophore signal sent from the LED-fiber to the O_2 -spot. Upon deoxygenation, sickle RBCs will start to sickle, their deformability will decrease, and they will no longer align with elliptical RBCs. The sickled RBCs will distort the diffraction pattern, changing its shape from an ellipse to a rhomboid or diamond-like shape. This change in the shape of the diffraction pattern results in a decrease of EI. Measurements of pO_2 and EI are not performed at the same height in the cup. This ensures better discrimination between the deoxygenation and reoxygenation curves and, hence, a better interpretation of the curve. This figure has been modified from Rab et al.²²

Protocol

All procedures were approved by the ethical committee of the University Medical Center Utrecht (UMCU) and in accordance to the Declaration of Helsinki. Patients enrolled at the Texas Children's Hematology Center (TCHC) were approved by the local IRB and in accordance with the Declaration of Helsinki.

1. General considerations

- 1.1. Begin by performing a test measurement to warm up the bob and cup. Ensure that the temperature of the bob and cup is 37 °C. This is important for good reproducibility.
- 1.2. Ensure that the viscous polyvinylpyrrolidone (PVP) solution falls within the strict limits for osmolarity (282–286 mOsm/kg), pH (7.35–7.45) and viscosity (27.5–32.5 MPa) at room temperature (22 °C).

NOTE: The PVP must be used at room temperature. If stored at a lower temperature, make sure it has warmed up to room temperature prior to taking any measurements.

2. Start-up of the ektacytometer

- 2.1. Switch on the computer and the ektacytometer from the back. Start the software program (**Table of Materials**) on the computer.
- 2.2. Make sure the nitrogen is available to deoxygenate the sample by opening the nitrogen cylinder.
- 2.3. Lower the bob in the cup and make sure the cup can turn freely. Clean the cup on the inside and outside with a soft cloth and distilled water, because debris can hamper the EI measurements.
- 2.4. When the software program is running, check for the following message on the screen: "**Make sure the gas valve is open**" and click **OK**.
- 2.5. Ensure that the ektacytometer starts the pO_2 self-check process that will appear on the screen. Select **Start (enter)**. If it fails, rerun the self-check by clicking **Hardware check | pO_2 | Self check**.

NOTE: If the self-check fails again, consider replacing the O_2 -spot. The O_2 -spot is replaced by gently pushing the spot out from the inside of the cup with a fingertip. A new spot is placed by gently pushing the spot from the outside into the cup.

- 2.5. Choose **pO_2 scan** from the different tests listed on the left. Choose **Settings** at the right of the screen and ensure they are set as per the parameters listed in **Table 1**. Keep the same settings for every measurement.
- 2.6. In order to save these settings, press **OK | OK**.

NOTE: Preferred settings are listed in **Table 1** but can be adjusted according to the user preferences and investigational purposes. For example, to study the sickling behavior more extensively, deoxygenation speed and duration can be altered.

3. Sample collection and preparation

NOTE: For the validation of the technique, ethylenediamine tetraacetic acid (EDTA)-treated blood from 38 SCD patients and 5 healthy controls included at the University Medical Center Utrecht or Texas Children's Hematology Center, in different clinical studies (Netherlands Trial Registry [NTR] identifier, NTR 6779 and NTR 6462), as well as anonymized leftover blood samples from patients who visited the outpatient clinic or were hospitalized were used.

- 3.1. Collect blood samples by venipuncture (a minimum of 300 μ L/sample) in a tube containing EDTA. Make sure the blood has been stored for at least 30 min at 4 °C, but no longer than 24 h.

NOTE: Citrate phosphate dextrose adenine (CPDA) or heparin can also be used, but the influence of these reagents on the sample preservation with respect to the oxygen gradient ektacytometry is not well-known.

- 3.2. Mix the sample gently by inversion to homogenize. Do not shake the sample. Let the sample warm up to room temperature on a roller bench before the measurement.

NOTE: A sample tube (9–10 mL) that is stored for more than 1 h at 4 °C must warm up for 15 min. When stored for less than 1 h at 4 °C, it must warm up for 10 min. A sample tube (2–6 mL) that is stored for more than 1 h at 4 °C must warm up for 10 min. When stored for less than 1 h at 4 °C, it must warm up for 5 min.

- 3.3. Measure the complete blood count on a hematology analyzer. To do so, take 20–200 µL of whole blood in a tube containing EDTA. Place the aspiration needle in the tube and press on the button behind the needle of the hematology analyzer to start the measurement.

NOTE: In the complete blood count, the RBC number is measured, which is an important factor for standardizing the oxygen gradient ektacytometry measurements. RBC count is calculated from forward and sideward scatter by flow cytometry. Normal RBC count in healthy controls is $3.7\text{--}5.0 \times 10^{12}/\text{L}$ for females and $4.2\text{--}5.5 \times 10^{12}/\text{L}$ for males. RBC count in patients with SCD is generally decreased. Some hematology analyzers will also measure percent dense red blood cells (% DRBC) which can be of additional value in the interpretation of individual oxygen gradient ektacytometry curves.

- 3.4. Standardize the whole blood sample to an RBC count of 200×10^6 RBCs in 5 mL PVP (200×10^6 RBCs/vial) by adjusting the volume of sample that will be added. If the total RBC count is less than 200×10^6 , the diffraction pattern and EI will be affected.

- 3.4.1. Use the equation below to perform the counting.

$$4.0/xx (x 10^{12}/\text{L}) \times 50 = yy \text{ } \mu\text{L whole blood/vial PVP}$$

where xx is the calculated RBC count obtained from step 3.3 and yy is the amount of whole blood that is required for the actual measurement. Depending on the grade of anemia and other factors influencing RBC counts, the amount of whole blood required is 40–90 µL.

4. Oxygen gradient ektacytometry measurement

- 4.1. Pipette the calculated sample volume (yy µL of blood) into PVP to obtain a total volume of 5 mL. Prewet the tip by gently resuspending the blood 3x. Use a pipette tip with a wide opening to avoid additional stress on the RBCs. Gently mix the sample manually by inversion until it is homogeneous.

NOTE: Open the PVP vial for as short a time as possible to avoid air contact.

- 4.2. Slowly draw 2.0 mL of the blood/PVP mixture into a 3 mL syringe without the needle. Push the plunger to remove any visible air bubbles and excessive sample solution until 1.5–1.8 mL is left in the syringe (depending on the cup volume).
- 4.3. Inject the total sample volume slowly and evenly in the bob through the connector. Make sure the level of the sample is above the oxygen sensor (pink spot) and above the small suction hole. Do not leave any sample solution in the syringe.
- 4.4. Click **New** and fill in the sample identifier, remarks, date of donation, and viscosity of PVP. Click **OK | Aspirate**. After 60 s, the cup will rotate and aspirate the sample for 15 s. Click **OK** when the rotation stops. Close the machine lid. Click **Continue | Start now**, as oxygen gradient ektacytometry is done with a fixed gain. The measurement will take about 28 min.
- 4.5. After the measurement, print the report that shows the curve and parameters that are automatically calculated by the software. Ensure that the raw data is automatically stored in the designated folder in **Settings**. Maximum EI (EI_{\max}), minimum EI (EI_{\min}), $pO_2@95\%EI$ (PoS), and area (area under the curve) are automatically calculated and added to the printed report and raw data.
- 4.6. Manually obtain ΔEI by calculating the difference between EI_{\max} and EI_{\min} . Calculate the percentage recovery by taking the difference in mean EI before deoxygenation (pO_2 100–120 mmHg) and mean EI values during reoxygenation at 100–120 mmHg.

5. Cleaning of the ektacytometer

- 5.1. Remove the sample syringe and replace it with a syringe filled with distilled water or deionized water.
- 5.2. Press **Clean**, slowly flushing the connector during rinsing. Make sure to flush in both directions.
- 5.3. Remove the syringe and lift the bob. Dry the bob, cup, and connector thoroughly with a soft cloth.
- 5.4. Use a large syringe (10–50 mL) to flush the connector in order to remove any water remaining in the tubes and bob. Block the lower inlet/outlet of the bob to get back pressure in the tubes, thereby removing remaining water.
- 5.5. Lower the bob in the cup. The machine is now ready for the next measurement.

6. Shutdown of the machine

- 6.1. Ensure the machine is properly rinsed after the last measurement, as described above. Ensure the proper tubes relate to the cleaning solution.
- 6.2. Close the software, press **Close**, and press **Start** to start end-of-day cleaning program.
- 6.3. After completing the whole cleaning program, remove the syringe and lift the bob. Flush the connector with a big syringe.
- 6.4. Empty the waste bottle and dry the bob and cup with a soft cloth. Flush the connector in order to remove the water remaining in the tubes and bob. Block the lower inlet/outlet of the bob to get back pressure in the tubes, thereby removing any remaining water.
- 6.5. Close the lid of the machine. Close the nitrogen cylinder. Turn off the computer and the machine.

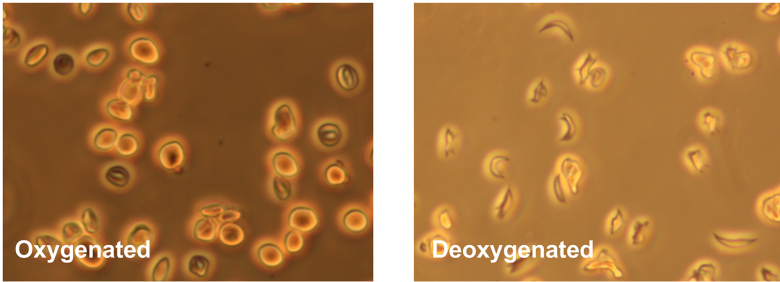
Representative results

Oxygen gradient ektacytometry can be used to characterize sickling behavior in patients with SCD. In this study, blood samples from a total of 38 SCD patients and five healthy controls were included. In healthy controls, the diffraction pattern is circular at rest and elliptical at higher shear stress⁴. From the elliptical diffraction pattern, the elongation index (EI) is calculated based on the height and width of the diffraction pattern. In oxygen gradient ektacytometry, slow and continuous deoxygenation of the sample by nitrogen gas is followed by swift reoxygenation by ambient air. Under these conditions, RBC sickling can be observed under deoxygenation. This will cause a distortion of the diffraction pattern because sickled red cells will not align properly under the applied shear stress. Hence, they appear to be less deformable as opposed to healthy RBCs (**Figure 2**).

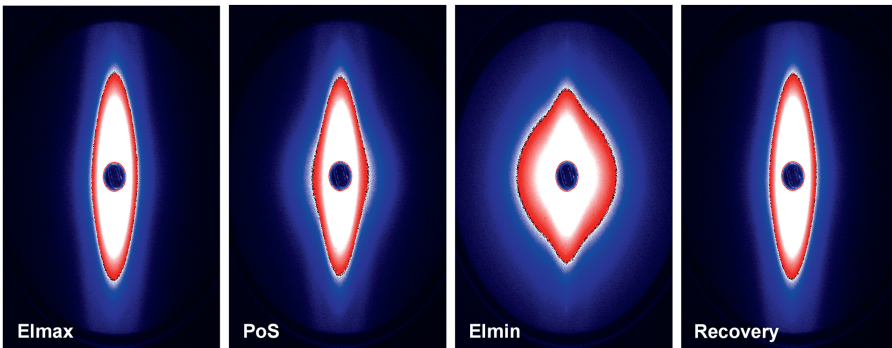
Figure 3A shows how sickle RBCs change in shape upon deoxygenation, which mimicked conditions during oxygen gradient ektacytometry, whereas control sickle RBCs without deoxygenation show no change in shape. This process results in distortion of the diffraction pattern during oxygen gradient ektacytometry, and thus in a decrease in EI. **Figure 3B** shows the different diffraction patterns from which different parameters are generated.

A representative curve obtained by the ektacytometer is shown in **Figure 3C**. Six parameters reflect different characteristics of sickling behavior of RBCs: EI_{\max} is the maximum EI at the start of the measurement before deoxygenation. This parameter represents the baseline position and reflects the overall deformability of the total RBC population at ambient air. EI_{\min} is the minimum EI, which represents minimal deformability after deoxygenation. This parameter reflects changes in the shape and orientation of (sickle) RBCs upon deoxygenation.

A



B



C

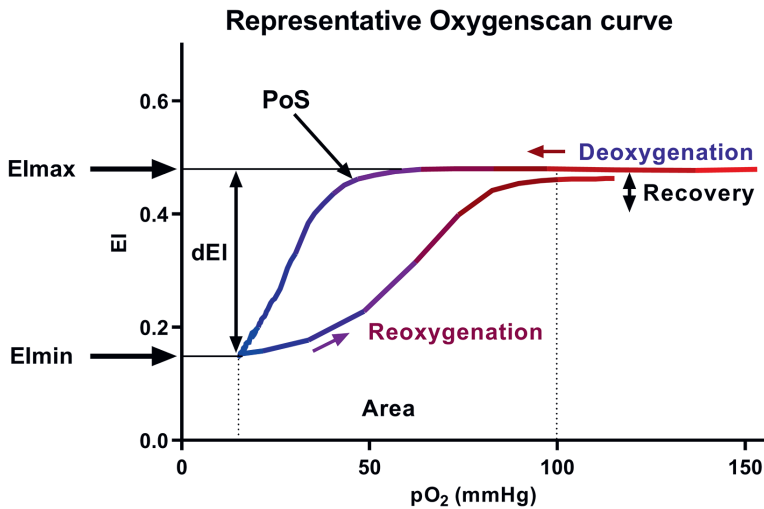


Figure 3. Representative oxygen gradient ektacytometry curve and diffraction patterns. (A) Upon deoxygenation under conditions similar to the oxygen gradient ektacytometry, sickle RBCs were fixed. ►

In control sickle RBCs, the same conditions were used, but without nitrogen gas. Deoxygenated sickle RBCs show a change in shape in contrast to control RBCs. **(B)** Upon deoxygenation and shear stress (30 Pa), the diffraction pattern changes from an ellipse to a rhomboid. **(C)** Representative curve of oxygen gradient ektacytometry. The maximum elongation index (El_{max}) represents the baseline position and shows an overall deformability of the total RBC population. Minimum EI (El_{min}) represents minimal deformability, which is caused by the change in shape and orientation of RBCs upon deoxygenation. ΔEI (dEI, the difference in EI between El_{max} and El_{min}) shows how many cells can sickle during one round of deoxygenation. Point of sickling (PoS , pO_2 at 5% EI decrease) shows the oxygen tension when the first RBCs start to sickle. The area under the curve (from $pO_{2min} = 100$ mmHg) is calculated in the parameter area. This summarizes El_{max} , El_{min} , and PoS . The capacity of sickled cells to unsickle during reoxygenation is represented in the parameter Recovery (percentage of El_{max} reached during reoxygenation). To aid in the interpretation, all data points were connected in every individual experiment by a line to graphically present the results. This figure has been modified from Rab et al.²²

ΔEI is the difference between El_{max} and El_{min} , which indicates how many cells can sickle during one round of deoxygenation. 5% Point of Sickling ($PoS_{5\%}$) is the pO_2 (mmHg) at which a 5% decrease of El_{max} during deoxygenation is measured. This represents the oxygen tension where the sickling process starts. Area reflects the area under the curve, which is determined by an integral calculation of EI and pO_2 measurements between 100 mmHg and pO_{2min} (mmHg). This is the result of previously described parameters El_{max} , El_{min} , and PoS . Recovery represents the difference of EI during the final part of reoxygenation compared to EI at baseline. Both EI values are measured at a pO_2 of 100–120 mmHg. This parameter reflects the capacity of RBCs that sickle during deoxygenation to reverse sickling during reoxygenation²². Parameters from duplicate measurements generally had a coefficient of variation (CV) <5% (median 1.83%). In case a CV > 5% was obtained, a third measurement was performed. The parameters El_{max} and Recovery are the most reproducible with median CVs <1%.

Representative curves of RBCs of healthy controls, patients with HbS traits (heterozygous HbS), and a homozygous SCD patient are shown in **Figure 4A**. The representative curve of the HbSC patient shows a lower recovery, which might indicate a different sickling process (**Figure 4B**). The representative curves of HbSS patients treated with hydroxyurea (HU) and transfusion are shown in **Figure 4C** and **Figure 4D**. Clearly, there is a big difference between the representative curves of HS traits (HbAS cells) and RBCs of HbSS patients treated with transfusion (consisting of a mixture of homozygous sickle (HbSS) and homozygous normal (HbAA) cells, **Figure 4A,D**). The clear differences in the curves of the untreated SCD patient and the HU and transfusion-treated patients highlights the usefulness of this assay (**Figure 4C,D**). Levels of HbF and HbS correlated significantly with El_{min} and, to a lesser extent, with PoS (**Figure 5A–D**). This indicates that those laboratory parameters that are important in the evaluation of the patient are also reflected in the oxygen gradient ektacytometry. The number of sickled cells at normoxia and percentage of dense RBCs (DRBCs) both influence El_{max} values, as they are significantly correlated (**Figure 5E–F**), which indicates that El_{max} reflects another important factor in the sickling process. These results show how different characteristics such as %HbS, %HbF, sickled cells at normoxia, and %DRBCs influence different parameters.

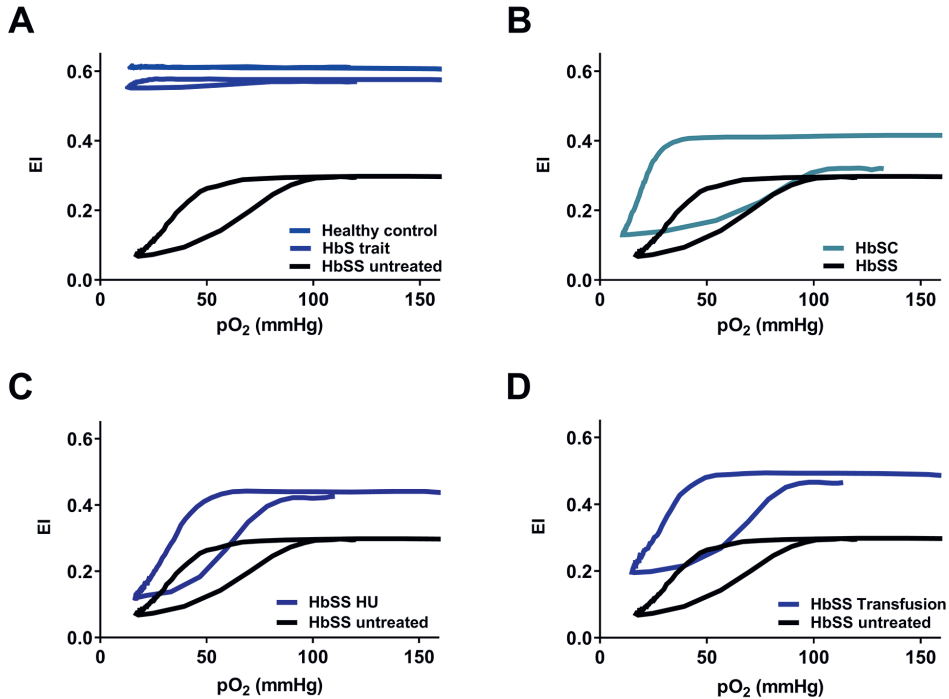


Figure 4. Oxygen gradient ektacytometry parameters correlate with genotype and treatment regimens of SCD patients with SCD. (A) Representative graph of RBCs of HbS carriers (HbS trait) and healthy controls in relation to untreated HbSS patients. (B) Representative graph of RBCs of patients with Hemoglobin SC Disease (HbSC) in relation to untreated HbSS patients. (C) Representative graph of RBCs of hydroxyurea treated homozygous SCD patients (HbSS HU) in relation to untreated HbSS patients. (D) Representative graph of RBCs of HbSS patients treated with blood transfusion (HbSS transfusion) in relation to untreated HbSS patients. This figure has been modified from Rab et al.²²

Discussion

Here we describe oxygen gradient ektacytometry, a method that can be used to study the sickling behavior of red blood cells from SCD patients under a range of oxygen concentrations (Figure 4 and Figure 5). In order to obtain reproducible results, it is important to identify the factors that influence the results. For instance, temperature has a large impact on RBC deformability, mostly due to its effects on the thickness of the viscous solution (PVP). We recommend performing a test measurement at the start of the day to thoroughly heat the machine to 37 °C. This will improve the reproducibility of the results. The osmolarity of the viscous solution should be within a narrow range (282–286 mOsm/kg for PVP), because osmolarity influences hydration status, which in turn affects RBC deformability. The pH and viscosity of PVP should also be tightly regulated. Differences in pH and temperature can influence curves dramatically²². Additionally, remaining water in the cup, bob, and tubes, may cause the lysis of RBCs, thereby resulting in incorrect data, because fewer intact RBCs present in the cup will be measured.

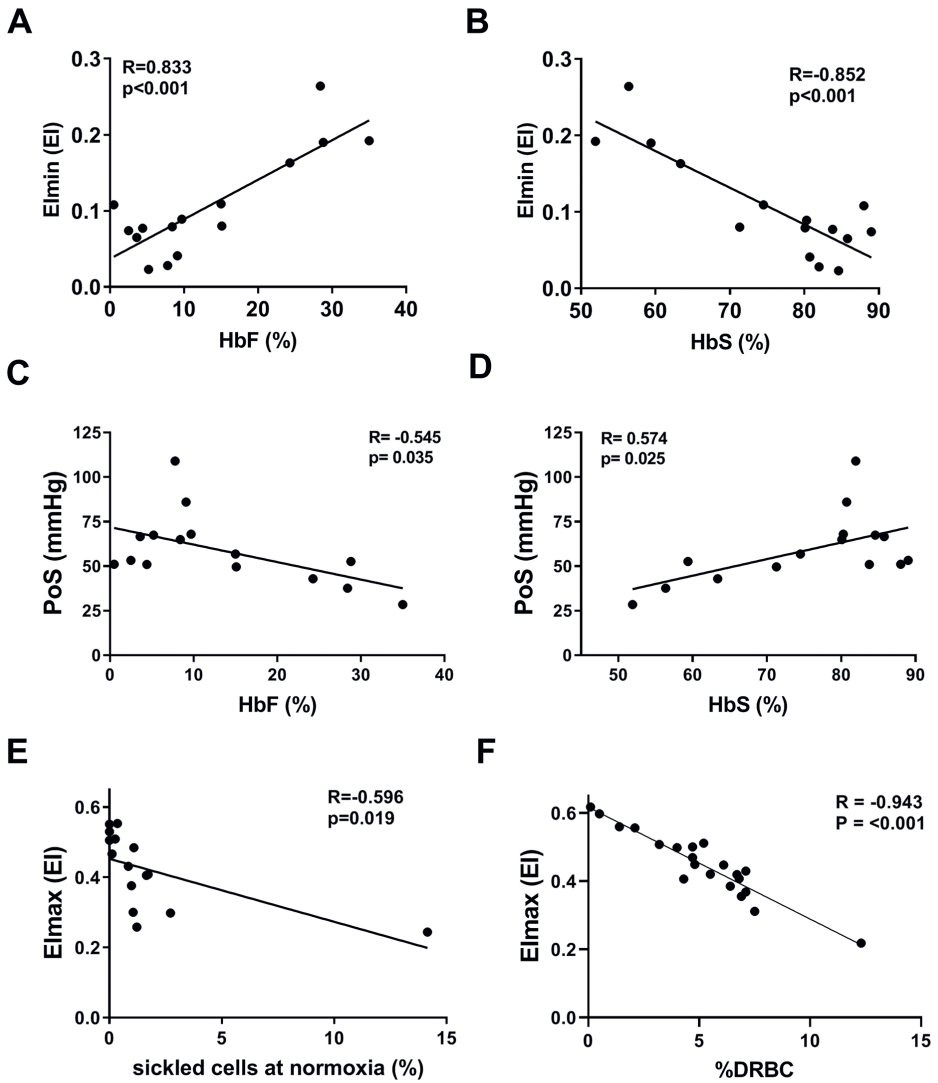


Figure 5. Oxygen gradient ektacytometry parameters are associated with %HbF, %HbS, %sickled cells at normoxia and %dense RBCs. (A) Linear correlation of minimum elongation index (EI_{min}) and %HbF of 15 HbSS or HbS/ β -thalassemia patients without transfusion. (B) Linear correlation of EI_{min} and %HbS. (C) Linear correlation of PoS and %HbF. (D) Linear correlation of PoS and %HbS. (E) Linear correlation of maximum EI (EI_{max}) and percent of sickled cells at normoxia measured with digital microscopy. (F) Linear correlation of EI_{max} and percentage dense RBCs (%DRBCs) of 21 patients with HbSS. This figure has been modified from Rab et al.²²

Settings to perform oxygen gradient ektacytometry can be adjusted to address specific investigational questions. Preferred settings are listed in **Table 1**. A deoxygenation time of 1,300 s was chosen based on observations showing that the extension of deoxygenation did not result in a lower El_{\min} for most patients. In contrast, shortening of the deoxygenation time would hamper the discriminative power of the oxygen gradient ektacytometry. The reoxygenation time was set to 280 s due to the rapidly resolving HbS polymers during reoxygenation, and concomitant restoration of EI towards values measured prior to the deoxygenation. Shear stress was set to 30 Pa, which is analogous to the osmotic gradient ektacytometry. Lowering this parameter could hamper the discriminative power. Deoxygenation control can be used if a set of deoxygenation speed is applied to every patient sample. In our preferred settings, this option was switched off because the rate of deoxygenation is patient-specific due to the unique hemoglobin dissociation curve. Hence, switching on the deoxygenation control would eliminate this characteristic from the assay. However, this feature of oxygen gradient ektacytometry is still under investigation.

Several well-known factors influence oxygen gradient ektacytometry parameters, namely pH, temperature, and osmolarity. Ektacytometry, especially PoS, is influenced by 2,3-diphosphoglycerate (2,3-DPG)²². Also, there is a clear correlation between %HbF and the El_{\min} , and to a lesser extent PoS (**Figure 5A-D**). El_{\min} is associated with sickle cells at normoxia, which can explain the observation that shortly after a VOC, RBC deformability at normoxia (El_{\max}), is higher. The latter is caused by the destruction of the most sickled cells, and hence less deformable RBCs during VOC¹⁶. As shown in **Figure 5F**, higher %dense RBCs (defined as RBCs with a hemoglobin concentration >1.11 mg/mL) correlate strongly with a lower El_{\max} . This indicates that dense cells are an important factor in RBC deformability at normoxia, similar to previously reported results¹.

Standardization of samples is very important for obtaining reproducible results and for distinguishing between different genotypes and treatments. Correcting for RBC count is important, as the number of RBCs influence the intensity of the diffraction pattern. If lower RBC numbers are present in the gap between the bob and cup, the curve will shift upward and to the left. Additionally, the curve will fluctuate, hampering accurate calculation of the parameters, especially the PoS.

A limitation of this technique is that the EI value represents an average of all cells, including different subpopulations. Heterogeneity of RBC populations in SCD patients and its influence on ektacytometry measurement has been intensively studied. This resulted in standardization wherein the size of the diffraction pattern is adjusted to a fixed value instead of corrected for the RBC count^{23,24}. Whether or not this way of standardization should also be applied to oxygen gradient ektacytometry measurements is currently under study.

Several techniques to measure RBC deformability under hypoxic conditions were developed based on a deoxygenation step that took place outside the ektacytometer²⁵⁻²⁷. Under these conditions, differences in cellular behavior were not observed between patients with HbS traits and healthy controls under physiological pH²⁵. Oxygen gradient ektacytometry,

Table 1. The preferred setting of the ektacytometer.

Settings		
Files	Storage directory	
General options	Default medium viscosity	Viscosity of PVP
pO ₂ scan	Minimum aspiration time (s)	60
	pO ₂ scan shear stress (Pa)	30
	Determine pO ₂ every (S)	20
	Moving average size	2
	pO ₂ scan step; Edit	0 -OFF; 60 -ON; 1360 -OFF; 1640 -OFF
	Cal. Area between (mmHg)	10 and 100
	pO ₂ control	Off (unchecked)

however, clearly shows a low but evident PoS in individuals with HbS traits (**Figure 4A**). To date, in routine clinical practice, the only alternative methods to measure the tendency of an individual patient's RBCs to sickle in vitro include a morphology-based sickling assay: RBCs are incubated under conditions that promote HbS polymerization, such as low oxygen tension or low pH. A fixative is added after incubation and the percentage of sickled cells is manually or digitally counted using light microscopy. Many preclinical and early phase pharmacologic trials use the sickling assay to generate a secondary outcome variable to be able to predict clinical efficacy in SCD²⁸⁻³². However, it is time consuming, variability is high and sensitivity is low, the technique is not automated and, therefore, labor intensive. Moreover, morphological changes due to sickling might not correlate well with physiological parameters, such as RBC deformability, because it is a 2-dimensional static assay².

Oxygen gradient ektacytometry provides a functional assay of sickling that is rapid and reproducible. This is an in vitro test that does not consider the endothelial surface. However, it does provide functional aspects of sickling behavior and RBC characteristics, making it a promising technique for sickle cell studies. Future applications of the technique include monitoring treatment efficacy in SCD patients, serving as a biomarker for new treatment strategies, studying sickling behavior, and monitoring chimerism after the stem cell transplantation in SCD.

Acknowledgments

This work was supported in part by a Eurostars grant estar18105 and by an unrestricted grant provided by RR Mechatronics. The authors thank Sisto Hendriks and Jan de Zoeten for their technical support.

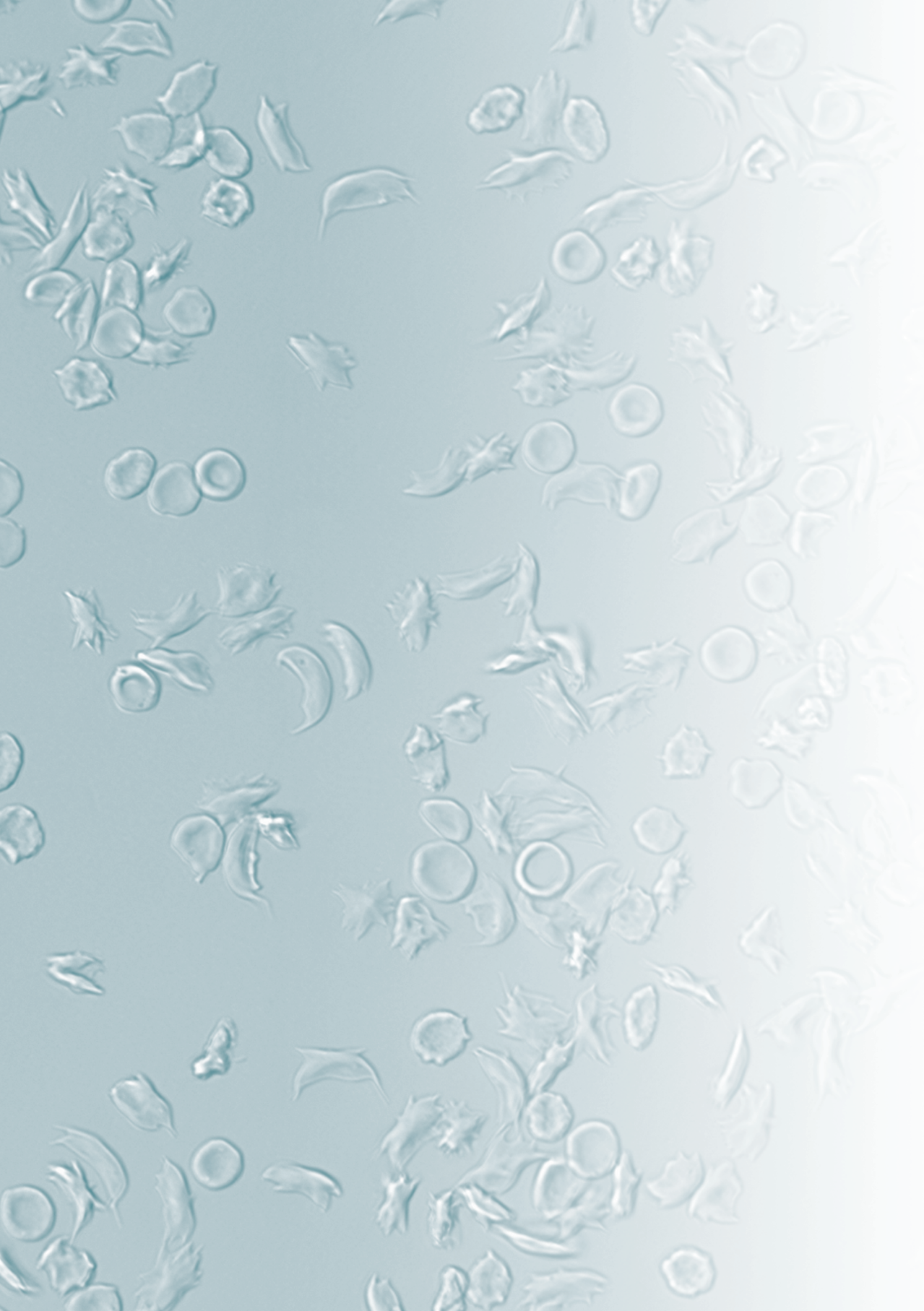
Disclosures

The authors declare no competing financial interests.

References

1. Clark, M. R., Mohandas, N., Shohet, S. B. Deformability of oxygenated irreversibly sickled cells. *Journal of Clinical Investigation*. 65 (1), 189–196 (1980).
2. Smith, C., Kuettner, J., Tukey, D., White, J. Variable Deformability of Irreversibly Sickled Erythrocytes. *Blood*. 58 (1), 71–78 (1981).
3. Clark, M., Mohandas, N., Embury, S., Lubin, B. A simple laboratory alternative to irreversibly sickled (ISC) counts. *Blood*. 60 (3), 659–663 (1982).
4. DaCosta, L. et al. Diagnostic tool for red blood cell membrane disorders : Assessment of a new generation ektacytometer. *Blood Cells, Molecules, and Diseases*. 56 (1), 9–22 (2016).
5. Rabai, M. et al. Deformability analysis of sickle blood using ektacytometry. *Biorheology*. 51 (2–3), 159–170 (2014).
6. Ballas, S. K., Mohandas, N. Sickle red cell microrheology and sickle blood rheology. *Microcirculation*. 11 (2), 209–225 (2004).
7. Connes, P., Alexy, T., Detterich, J., Romana, M., Hardy-Dessources, M. D., Ballas, S. K. The role of blood rheology in sickle cell disease. *Blood Reviews*. 30 (2), 111–118 (2015).
8. Hierso, R. et al. Effects of oxidative stress on red blood cell rheology in sickle cell patients. *British Journal of Haematology*. 166 (4), 601–606 (2014).
9. Mozar, A. et al. Red blood cell nitric oxide synthase modulates red blood cell deformability in sickle cell anemia. *Clinical Hemorheology and Microcirculation*. 64 (1), 47–53 (2016).
10. Clark, M. R., Mohandas, N., Shohet, S. B. Osmotic Gradient Ektacytometry: Comprehensive Characterization of Red Cell Volume and Surface Maintenance. *Blood*. 61 (5), 899–911 (1983).
11. Parrow, N. L. et al. Measurements of red cell deformability and hydration reflect HbF and HbA2in blood from patients with sickle cell anemia. *Blood Cells, Molecules, and Diseases*. 65, 41–50 (2017).
12. Steinberg, M. H., Chui, D. H. K., Dover, G. J., Sebastiani, P., Al Sultan, A. Fetal hemoglobin in sickle cell anemia: A glass half full? *Blood*. 123 (4), 481–485 (2014).
13. Ballas, S. K., Lerner, J., Smith, E. D., Surrey, S., Schwartz, E., Rappaport, E. F. Rheologic predictors of the severity of the painful sickle cell crisis. *Blood*. 72 (4), 1216–1223 (1988).
14. Lande, W. M. et al. The Incidence of Painful Crisis in Homozygous Sickle Cell Disease: Correlation with Red Cell Deformability. *Blood*. 72 (6), 2056–2059 (1988).
15. Lemonne, N. et al. Does increased red blood cell deformability raise the risk for osteonecrosis in sickle cell anemia? *Blood*. 121 (15), 3054–3057 (2013).
16. Ballas, S. K., Smith, E. D. Red blood cell changes during the evolution of the sickle cell painful crisis. *Blood*. 79 (8), 2154–2163 (1992).
17. Telen, M. Cellular adhesion and the endothelium: E-selectin, L-selectin, and pan-selectin inhibitors. *Hematology/Oncology Clinics of North America*. 28 (2), 341–354 (2014).
18. Papageorgiou, D. P. et al. Simultaneous polymerization and adhesion under hypoxia in sickle cell disease. *Proceedings of the National Academy of Sciences*. 115 (38), 201807405 (2018).
19. Liu, J., Qiang, Y., Alvarez, O., Du, E. Electrical impedance microflow cytometry with oxygen control for detection of sickle cells. *Sensors and Actuators, B: Chemical*. 255, 2392–2398 (2018).
20. Du, E., Diez-Silva, M., Kato, G. J., Dao, M., Suresh, S. Kinetics of sickle cell biorheology and implications for painful vasoocclusive crisis. *Proceedings of the National Academy of Sciences*. 112 (5), 1422–1427 (2015).
21. Li, Q. et al. Kinetic assay shows that increasing red cell volume could be a treatment for sickle cell disease. *Proceedings of the National Academy of Sciences*. 114 (5), E689–E696 (2017).
22. Rab, M. A. E. et al. Rapid and reproducible characterization of sickling during automated deoxygenation in sickle cell disease patients. *American Journal of Hematology*. 94 (February), 575–584 (2019).
23. Renoux, C. et al. Importance of methodological standardization of ektacytometric measures of red blood cell deformability in sickle cell anemia. *Clinical Hemorheology and Microcirculation*. 62 (2), 173–179 (2016).

24. Parrow, N. L. et al. Measuring Deformability and Red Cell Heterogeneity in Blood by Ektacytometry. *Journal of Visualized Experiments*. (131), 1–9 (2018).
25. Bessis, M., Feo, C., Jones, E. Quantitation of red cell deformability during progressive deoxygenation and oxygenation in sickling disorders (the use of an automated Ektacytometer). *Blood Cells*. 8 (1), 17–28 (1982).
26. Sorette, M. P., Lavenant, M. G., Clark, M. R. Ektacytometric measurement of sickle cell deformability as a continuous function of oxygen tension. *Blood*. 67 (6), 1600–1606 (1987).
27. Huang, Z., Hearne, L., Irby, C. E., King, S. B., Ballas, S. K., Kim-Shapiro, D. B. Kinetics of increased deformability of deoxygenated sickle cells upon oxygenation. *Biophysical journal*. 85 (4), 2374–2383 (2003).
28. Antoniani, C. et al. Induction of fetal hemoglobin synthesis by CRISPR/Cas9-mediated editing of the human β -globin locus. *Blood*. 131 (17), 1960–1973 (2018).
29. Abdulmalik, O. et al. Crystallographic analysis of human hemoglobin elucidates the structural basis of the potent and dual antisickling activity of pyridyl derivatives of vanillin. *Acta Crystallographica Section D: Biological Crystallography*. 67 (12), 1076 (2011).
30. Oder, E., Safo, M. K., Abdulmalik, O., Kato, G. J., Discovery, D. New Developments in Anti-Sickling Agents: Can Drugs Directly Prevent the Polymerization of Sickle Haemoglobin In Vivo? *British Journal of Haematology*. 175 (1), 24–30. (2016).
31. Oksenberg, D. et al. GBT440 increases haemoglobin oxygen affinity, reduces sickling and prolongs RBC half-life in a murine model of sickle cell disease. *British Journal of Haematology*. 175 (1), 141–153 (2016).
32. Xu, G. G. et al. Design, Synthesis, and Biological Evaluation of Ester and Ether Derivatives of Antisickling Agent 5-HMF for the Treatment of Sickle Cell Disease. *Molecular Pharmaceutics*. 14 (10), 3499–3511 (2017).



Chapter 4

Methodological aspects of the oxygen scan in sickle cell disease: a need for standardization

American Journal of Hematology 2020 Jan;95(1):E5-E8

Minke A.E. Rab^{1,2}, Celeste K. Kanne³, Jennifer Bos¹, Camille Boisson^{4,5},
Brigitte A. van Oirschot¹, Elie Nader^{4,5}, Céline Renoux^{4,5,6}, Philippe Joly^{4,5,6}, Romain Fort⁷,
Eduard J. van Beers², Vivien A. Sheehan^{3*}, Richard van Wijk^{1*} and Philippe Connes^{4,5*}

¹ Department of Clinical Chemistry & Haematology, University Medical Center Utrecht, Utrecht University, Utrecht, The Netherlands

² Van Creveldkliniek, University Medical Center Utrecht, Utrecht University, Utrecht, The Netherlands

³Department of Pediatrics, Division of Hematology/Oncology, Baylor College of Medicine, Houston Texas, USA

⁴ Laboratory LIBM EA7424, University of Lyon 1, "Vascular Biology and Red Blood Cell" team, Lyon, France

⁵ Laboratory of Excellence GR-Ex, Paris, France

⁶ Laboratory of Biochemistry and Molecular Biology, UF Biochemistry of Red Blood Cell diseases, Est Center of Biology and Pathology, Hospices Civils de Lyon, Lyon, France

⁷ Department of Internal Medicine, Hospices Civils de Lyon, Lyon, France

*equivalent position

To the Editor

Recently a method has been developed to assess red blood cell (RBC) deformability as a function of oxygen tension (pO_2)¹. This method, called oxygen gradient ektacytometry or the oxygenscan, is particularly useful for evaluating individuals affected by sickle cell disease (SCD). SCD is caused by a single point mutation in the β -globin gene (p.Glu7Val) leading to the production of an abnormal hemoglobin S (HbS). HbS polymerizes under deoxygenation, which causes RBC to take on a sickle shape. These sickled RBCs are poorly deformable and adhere to the endothelium, which contributes to painful vaso-occlusive crises and chronic anemia². The oxygenscan allows the determination of maximum RBC deformability under normoxic condition (Elmax), minimum RBC deformability under hypoxic condition (Elmin) and the specific pO_2 level at which RBC sickling occurs (i.e., the point of sickling; PoS)¹. Rab et al¹ recently demonstrated that hydroxyurea and blood transfusion increase Elmax and Elmin, and decrease PoS, indicating that these therapies are efficient in improving the rheological behavior of RBCs both in normoxic and hypoxic conditions. Moreover, the authors have shown that this technique has low inter sample variability (coefficient of variation <5%) and is very well suited to detect the effects of drugs that alter the affinity of hemoglobin for oxygen such as Voxelotor (GBT440), a promising drug recently tested in SCD^{1,3}. The joint experience of the authors of this study with the oxygenscan has prompted us to study methodological aspects and pre-analytical factors that could influence key oxygenscan parameters. A better understanding of these aspects and factors will strongly enhance reproducibility of results and will enable inter-laboratory comparison of results and collaboration.

The Laser Optical Rotational Red Cell Analyzer (Lorrca, RR Mechatronics, Zwaag, The Netherlands) with oxygenscan module was used. The ektacytometer measures RBC deformability (Elongation Index, EI) as a function of continuously changing oxygen concentrations. For this study, a standardized volume (50 μ L) of EDTA blood from SCD patients was mixed with 5mL of high viscous iso-osmolar polyvinylpyrrolidone (PVP) suspension (viscosity ~ 30cP). The sample solution was inserted into the couette system of the Lorrca, which exposes the cells to shear stress (30Pa, 37°C). At the same time, the pO_2 gradually decreases from 160mmHg to values below 20mmHg, after which pO_2 returns to normoxic values (for detailed description of the method see Rab et al¹). In this study, blood samples from 64 SCD patients were collected in three different centers to evaluate the effects of: 1) the time between blood sampling and measurement, 2) the amount of RBCs mixed with PVP, 3) the camera gain settings which controls the amount of light entering into the diaphragm of the camera, thereby changing the laser diffraction pattern, and 4) the speed of deoxygenation (Proportional integral control; PI control). The clinically most relevant parameters Elmax, Elmin and PoS were determined for each condition tested. Statistical analysis was done by Wilcoxon T test, a p-value <0.05 was considered significant. Details of the different conditions used are mentioned in the legend of the figure.

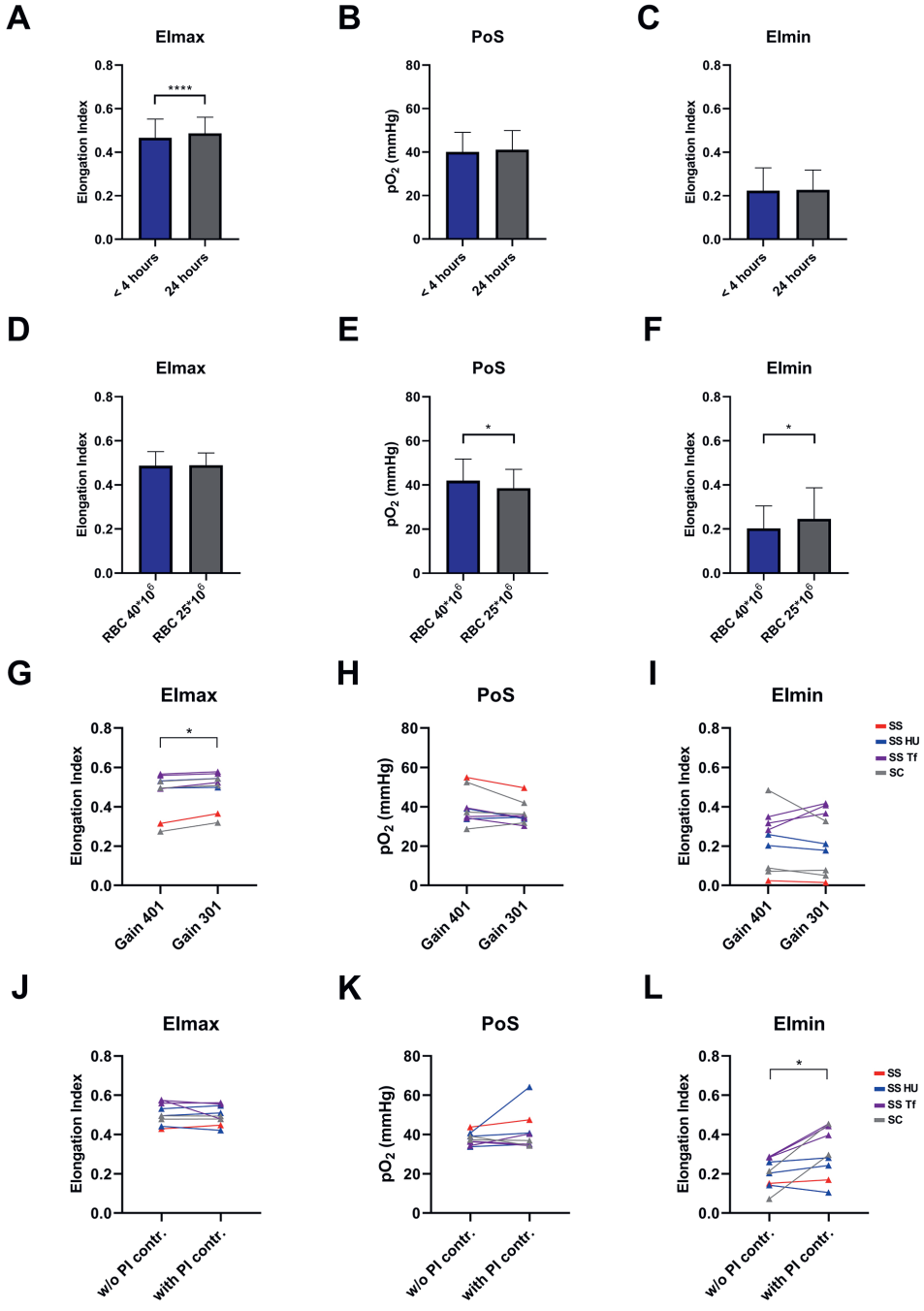


Figure 1. Lorca settings and sample handling influences key oxygen-scan measurements Elmax, PoS and Elmin. (A) RBCs of an untreated patient with HbSS (n=1), on hydroxyurea (n=7), on chronic transfusion therapy (n=9), on HU and transfusion (n=11) and 2 patients with hemoglobin SC, were measured within 4 hours after blood collection (stored at room temperature) and after 24 hours (stored at 4°C). Maximum deformability (Elmax) was significantly higher when measured after 24 hours; (B) Point of Sickling (PoS) showed no difference; (C) Deformability after deoxygenation (Elmin) did also not differ; ▶

(D) Different amounts of RBCs of untreated HbSS patients (n=4), on hydroxyurea (n=5), on chronic transfusion therapy (n=4), on HU and transfusion (n=3), and 1 HbSC patient and 1 HbS/ δ -thal patient were measured. Elmax did not vary; **(E)** PoS is significantly lower when the amount of RBCs used for the oxygenscan are low (25×10^6 RBCs/mL PVP) compared to reference RBC count (40×10^6 RBCs/mL PVP); **(F)** Elmin was significantly higher with low RBC count; **(G)** Adjusting the size of the diffraction pattern by changing the gain (401 increases the pattern, while 301 makes the pattern smaller) only significantly affects Elmax. This was investigated with RBCs of 6 HbSS patients (2 treated with HU, 3 with transfusion, and 1 untreated) and 3 HbSC patients; **(H)** PoS did not differ when the gain was changed, whilst individual values are different depending on genotype and treatment; **(I)** Elmin did not differ whilst individual values are different depending on genotype and treatment; **(J)** PI control permits slower deoxygenation, adjusting its speed to the individual patient RBCs. This was investigated in 7 HbSS patients (3 treated with HU, 3 with transfusion, and 1 untreated) and 2 HbSC patients. Elmax was not different; **(K)** PoS showed now difference; **(L)** Elmin, is higher when PI control is used, especially in SCD patients on transfusion therapy and HbSC patients. HU, hydroxyurea, Tf, transfusion, w/o, without. PI contr., proportional integral control. Bars represent means, error bars represent standard deviation. **** $p < 0.0001$, * $p < 0.05$

Our results show that 24 hours of blood storage (4°C) compared to 4 hours of storage (at room temperature) significantly increased the Elmax (Figure 1A). Elmax also increased significantly with a lower camera gain (Figure 1G). Although the effect was less pronounced, together, this indicates that deformability measured during normoxia is influenced by the age of the sample as well as the height of the diffraction pattern.

Elmin was significantly increased when less RBCs were used for the measurement (Figure 1F) and when PI control was switched on (Figure 1L). Together, this indicates that deformability under hypoxic conditions is dependent on the amount of RBCs used for measurements, and the speed at which deoxygenation occurs.

PoS was only significantly affected by the amount of RBCs used, in a sense that a lower number of RBCs was associated with a lower oxygen concentration at which RBCs start to sickle (i.e., PoS; Figure 1E). We also noted that methodological factors, i.e. the camera gain and deoxygenation speed, had different effects on variance caused by the genetic background or treatment. In particular RBCs from patients on chronic transfusion and patients with HbSC behaved differently at different machine settings (see details in the legends of the figure). There was greater influence of pre-analytical factors and run to run variability when blood from HbSC patients were used.

The present study clearly shows that key oxygenscan parameters (Elmax, PoS and Elmin) are dependent on methodological aspects and pre-analytical conditions. As a consequence, intra- and between-laboratories comparisons imply the need for standardization. Therefore, we believe that each laboratory using this technique should perform oxygenscan measurements in a standardized way.

The degree of anemia is highly variable in SCD: some patients having a hematocrit lower than 20% while others (Hemoglobin SC patients) have mild-to-moderate anemia. We recommend performing a RBC count prior to oxygenscan measurements to standardize the amount of RBCs used. A RBC count of 40×10^6 /mL, for example, ensures that a sufficient amount of RBCs will be present in the couette system of the Lorrca to render a reliable high quality diffraction pattern. Another pre-analytical aspect is the time between collecting a sample and performing the actual measurement. Several laboratories are not able to perform measurements within 4 hours due to shipping time. Since the time between blood

sampling and analysis affects Elmax, we recommend that each individual laboratory performs oxygenscan measurements at a standardized time point. From a practical point of view storing samples overnight before measurements would be the preferred option, allowing for the shipment of samples from other hospitals.

Our study also demonstrates that the speed of deoxygenation and the camera gain are important methodological parameters that influence outcome parameters of the oxygenscan module of the Lorrca. Regardless of the choice of settings we recommend that users control these methodological factors strictly in order to ensure correct interpretation of results.

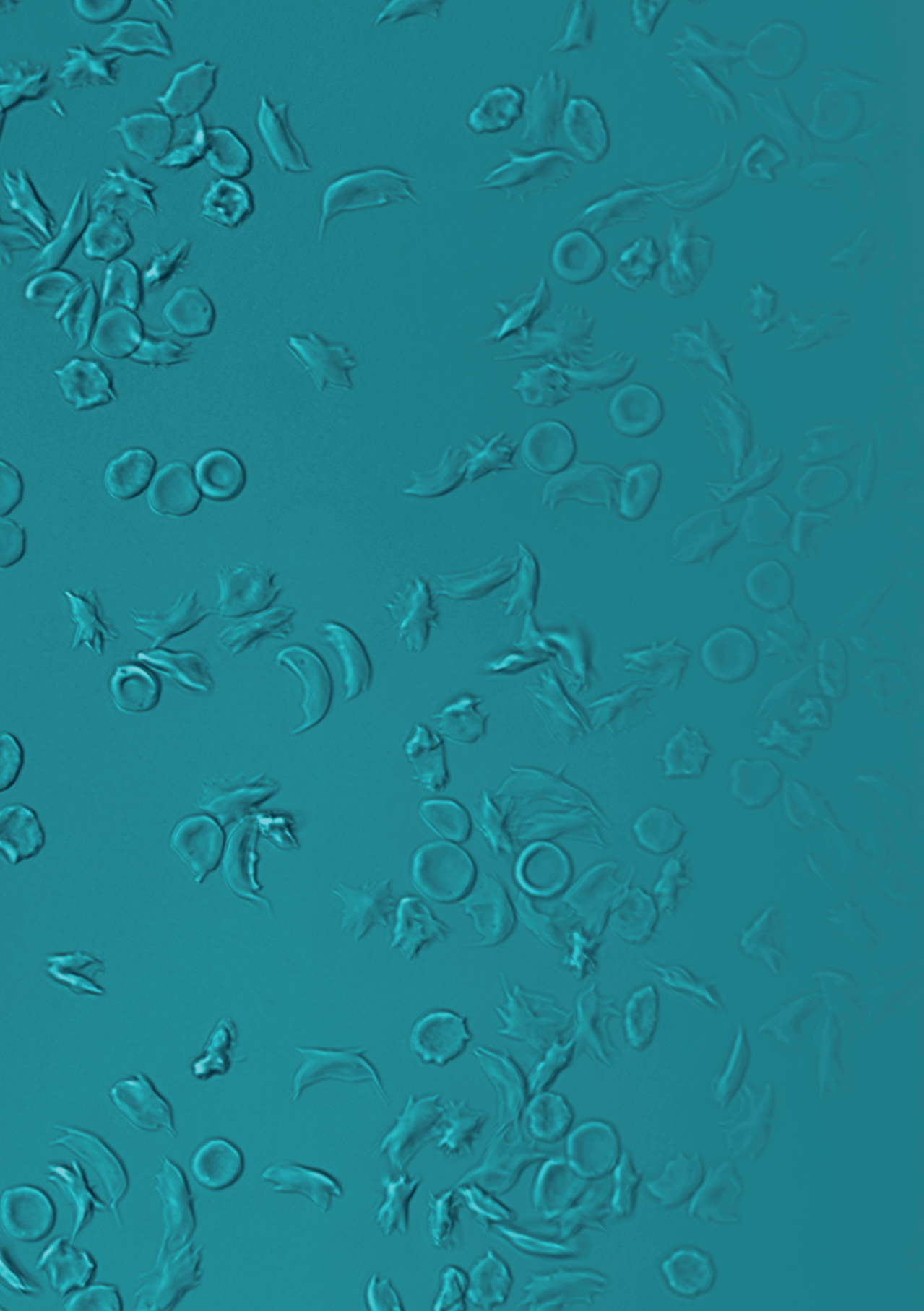
We strongly believe that standardization of oxygenscan measurements will enable comparisons as well as collaborations between the different laboratories studying RBC rheology in SCD. This is particularly important now given the high number of new therapies that are currently being developed for SCD. Thus, standardized oxygenscan measurements have the potential to become an important tool in the field of evaluation of new treatment strategies, personalized medicine and the prediction of complications in SCD.

Acknowledgments

This research has been funded in part by Eurostars grant estar18105 and by an unrestricted grant provided by RR Mechatronics.

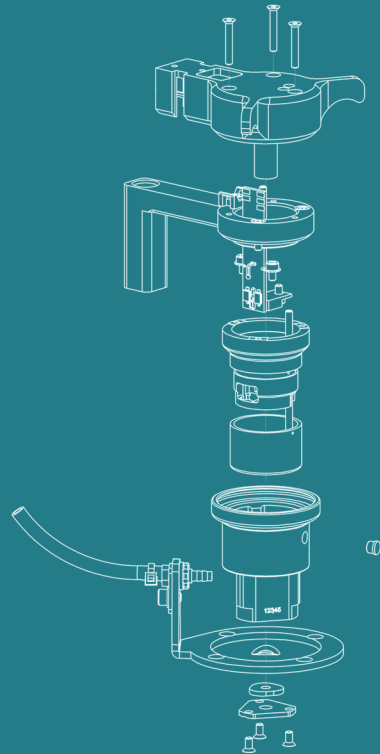
References

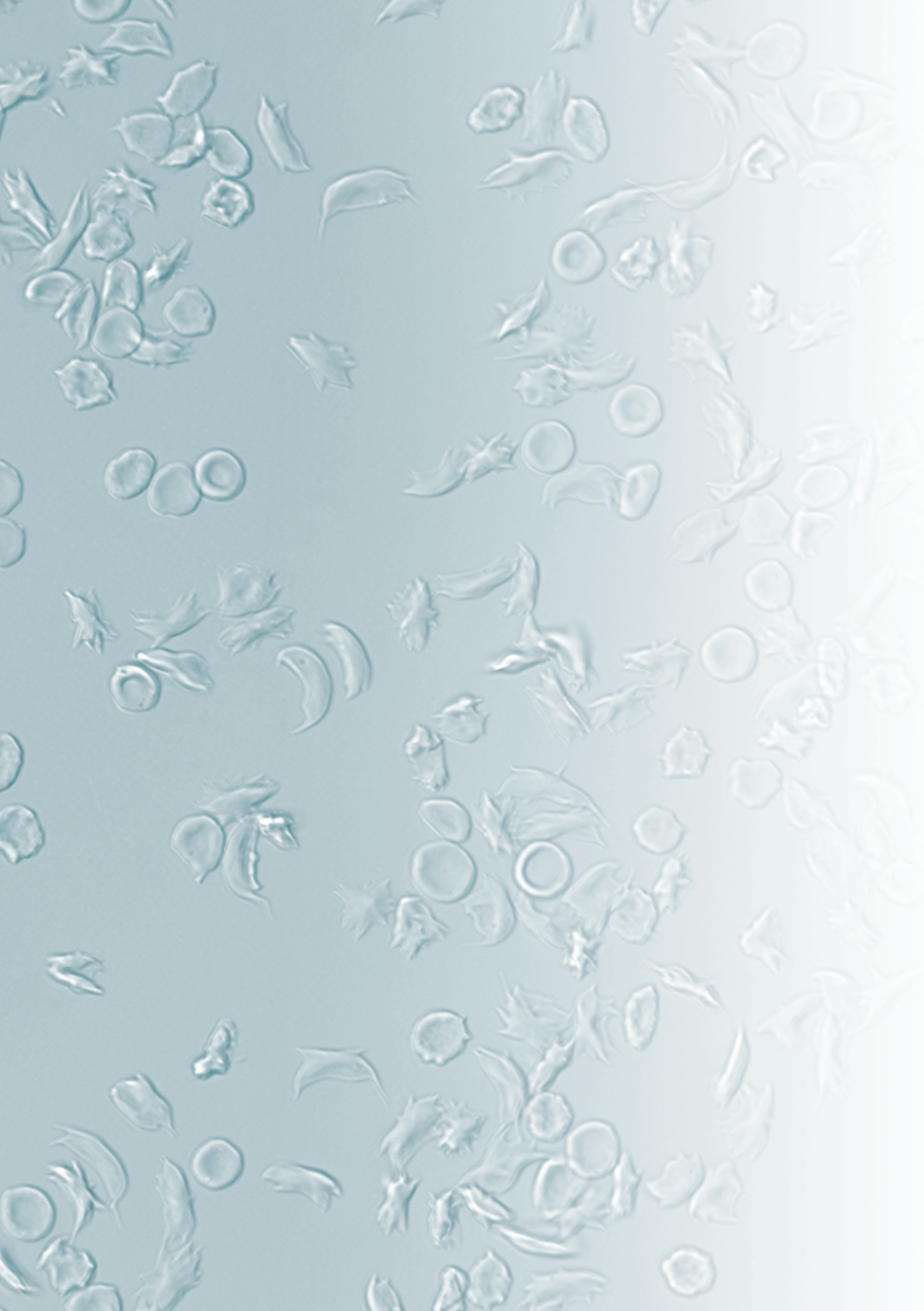
1. Rab MAE, van Oirschot BA, Bos J, et al. Rapid and reproducible characterization of sickling during automated deoxygenation in sickle cell disease patients. *Am J Hematol*. 2019;94:575-584.
2. Connes P, Alexy T, Detterich J, Romana M, Hardy-Dessources MD, Ballas SK. The role of blood rheology in sickle cell disease. *Blood Rev*. 2016;30:111-118.
3. Vichinsky E, Hoppe CC, Ataga KI, et al. A Phase 3 Randomized Trial of Voxelotor in Sickle Cell Disease. *N Engl J Med*. 2019;381(6):509-519.



Part II

Applications of oxygen gradient ektacytometry





Chapter 5

Oxygen gradient ektacytometry derived-biomarkers are associated with vaso-occlusive crises and correlate with treatment response in sickle cell disease

Published as Correspondence in American Journal of Hematology 2021 Jan;96(1):E29-E32

Minke A.E. Rab^{1,2}, Celeste K. Kanne³, Jennifer Bos¹, Brigitte A. van Oirschot¹, Camille Boisson^{4,5}, Maite E. Houwing⁶, Jorn Gerritsma⁷, Erik Teske⁸, Celine Renoux^{4,5,9}, Jurgen Riedl¹⁰, Roger E.G. Schutgens², Marije Bartels², Erfan Nur¹¹, Philippe Joly^{4,5,9}, Romain Fort¹², Marjon H. Cnossen⁶, Richard van Wijk¹, Philippe Connes^{4,5*}, Eduard J. van Beers^{2*} and Vivien A. Sheehan^{3*}

¹ Central Diagnostic Laboratory-Research, University Medical Center Utrecht, Utrecht University, Utrecht, The Netherlands

² Van Creveldkliniek, University Medical Center Utrecht, Utrecht University, Utrecht, The Netherlands

³ Department of Pediatrics Emory University School of Medicine, Atlanta, Georgia, USA

⁴ Laboratory LIBM EA7424, University of Lyon 1, "Vascular Biology and Red Blood Cell" team, Lyon, France

⁵ Laboratory of Excellence GR-Ex, Paris, France

⁶ Department of Pediatric Hematology, Erasmus Medical Center, Rotterdam, The Netherlands

⁷ Emma Children's Hospital, Pediatric Hematology, Amsterdam University Medical Centers, The Netherlands

⁸ Department of Clinical Sciences of Companion Animals, Faculty of Veterinary Medicine, Utrecht University, Utrecht, The Netherlands

⁹ Laboratory of Biochemistry and Molecular Biology, UF Biochemistry of Red Blood Cell diseases, Est Center of Biology and Pathology, Hospices Civils de Lyon, Lyon, France

¹⁰ Result Laboratory, Albert Schweitzer Hospital, Dordrecht, The Netherlands

¹¹ Department of Hematology, Amsterdam University Medical Centers, The Netherlands

¹² Department of Internal Medicine, Hospices Civils de Lyon, Lyon, France

**These authors contributed equally*

Abstract

Several new therapies are currently under development or in clinical trials to treat individuals with sickle cell disease (SCD). Many of these trials have subjective, time consuming clinical endpoints as their primary outcome measure; biomarkers assessing sickle red blood cells (RBC) function are therefore urgently needed. Oxygen gradient ektacytometry measures deformability of sickle RBCs over a range of oxygen tensions, producing key parameters: 1) EI_{max} , deformability at normoxia; 2) EI_{min} , deformability upon deoxygenation; and 3) Point-of-sickling (PoS), the patient-specific pO_2 at which sickling begins. Hence, this technique provides biomarkers that reflect RBC function and sickling potential. To begin clinical validation, we investigated correlations between these biomarkers and known effective disease modifying therapies, hydroxyurea and transfusion. Moreover, we investigated the possible association between these biomarkers and frequency of vaso-occlusive crises (VOC). We evaluated 126 individuals using oxygen gradient ektacytometry from an international multi-center SCD cohort (46 adults, 80 children). In both cohorts, PoS was significantly higher in patients with VOC compared to patients without VOC (adult; $p=0.0008$; pediatric, $p=0.0495$), indicating that RBCs of patients without VOC could tolerate lower pO_2 . PoS and EI_{min} significantly improved with all standard of care SCD therapies. This study is an early stage clinical validation of oxygen gradient ektacytometry-derived biomarkers, showing their correlation with response to disease modifying therapies of proven efficacy, and frequency of VOC in SCD. With further validation, modification of these biomarkers by novel therapies may serve as surrogate endpoints for VOC reduction in clinical trials and may compare and evaluate gene-based therapies.

Introduction

Sickle cell disease (SCD) is an inherited hemoglobinopathy caused by a single nucleotide mutation in the β -globin gene leading to the production of an abnormal hemoglobin S (HbS). When HbS becomes deoxygenated it polymerizes, deforming the red blood cells (RBCs) into a curved or sickle shape. Sickle RBCs are rigid and poorly deformable, and together with other abnormalities¹, block the microvasculature, causing painful vaso-occlusive crises (VOC), the hallmark complication of SCD. Hemolysis, increased red cell adhesion, endothelial dysfunction, inflammation, oxidative stress, and hemostatic activation, also contribute to the development of VOC², although their relative contribution remains subject to debate.^{3,4} The non-RBC factors are found in other disease conditions, yet no other disease is associated with VOC, highlighting the key contribution of the sickle RBC to SCD pathophysiology.² Oxygen gradient ektacytometry is a newly developed method that characterizes the sickling behavior of RBCs⁵. This functional assay measures RBC deformability of the total population of RBCs over a range of oxygen concentrations, providing a number of parameters that reflect features of sickling behavior and RBC function. The most important parameters are: 1) EI_{max} , RBC deformability when RBCs are fully oxygenated; 2) EI_{min} , lowest RBC deformability when HbS polymerization is at its peak value due to deoxygenation; 3) the Point of Sickling (PoS): the oxygen tension at which a 5% decrease in oxygenated EI_{max} is observed during the first minutes of deoxygenation, reflecting the patient-specific oxygen tensions at which HbS polymers are increasing and sickling of RBCs that are able to deform under normoxic conditions begins; 4) ΔEI , the difference between EI_{max} and EI_{min} , reflecting the sickling capacity of an individual's RBC population (Figure 1).⁵

Clinically relevant biomarkers are needed to serve as surrogate endpoints to evaluate new US Food and Drug Administration (FDA) approved therapies for SCD in subsequent clinical trials. Two such agents were approved based on subjective clinical endpoints of number of VOC or time to next VOC. L-glutamine reduced VOC per year in a randomized controlled trial (RCT), possibly by reducing RBC oxidative stress.⁶ Crizanlizumab is a monoclonal anti-P-selectin antibody that blocks P-selectin, an adhesion molecule that is expressed on activated endothelial cells and platelets. P-selectin mediated adhesion has been shown to play an important role in the pathophysiology of VOC.⁷ Crizanlizumab increased the time to next VOC. L-glutamine and crizanlizumab do not alter conventional clinical laboratory values, and the clinical endpoints used in their phase 3 clinical trials, reduction in VOC, are subjective and unwieldy. No functional (sickling) assay was included in the trial design of L-glutamine⁶ or crizanlizumab.⁸ Functional RBC tests like oxygen gradient ektacytometry may provide quantitative, clinically relevant biomarkers to serve as surrogate endpoints for subsequent clinical trials and for patient care.

In this study, we initiated clinical validation studies of oxygen gradient ektacytometry-derived biomarkers by investigating the relationship between these biomarkers and frequency of VOC in a multi-center study involving pediatric and adult SCD cohorts. In addition, we evaluated the ability of proposed biomarkers to detect RBC changes with initiation of hydroxyurea (HU) or transfusion therapy. Since these known effective therapies reduce PoS and increase elongation index, it is reasonable to assume that other red cell targeted effective novel SCD therapies would have a similar impact on at least one of the three

proposed biomarkers. Hence, establishment of an association between VOC frequency and these biomarkers may lead to a use of these biomarkers as surrogate endpoints for VOC, reducing the length and costs of clinical trials.

Methods

Patients

A total of 126 patients were enrolled at participating sites in The Netherlands (University Medical Center Utrecht, Erasmus Medical Center Rotterdam, Amsterdam University Medical Centers), in France (Department of Internal Medicine and Institute of Pediatric Hematology and Oncology, Hospices Civils de Lyon) or the United States (Texas Children's Hematology Center (TCHC)). Study procedures, namely collection of an additional tube of peripheral blood and review of medical records, were approved by local ethical committee/internal review boards in accordance with the Declaration of Helsinki, under registration number 17/392, 17/450, and H35473 at Baylor College of Medicine. All patients or legal guardians gave informed consent.

Peripheral blood samples from patients with no VOC in the past two years (VOC- group) were compared to patients who experienced one or more VOC (VOC+ group) in the past two years. VOC was defined as an acute pain event attributed to SCD requiring hospital admission, emergency room evaluation or an unplanned visit to the outpatient clinic. The European cohort was comprised of adult patients (n=46) with homozygous HbS (HbSS), HbS/ β^0 -thalassemia (HbS β^0) or HbS/ β^+ -thalassemia (HbS β^+). The United States cohort consisted of pediatric patients (n=80) aged 3-18 years with HbSS, HbS β^0 or HbS β^+ . Pediatric patients under three years of age were excluded because of low incidence of VOC in this age group. To assess the effect of established SCD treatments on oxygen gradient ektacytometry biomarkers, a cohort of patients were assessed before and during the first 6 months of HU therapy (n=15). Patients who received transfusion were excluded from this cohort. A second cohort was assessed before and during transfusion therapy, with variable time between blood collection and last transfusion (median 27; range 5-77 days; n=21). Additionally, in a cohort of patients receiving regular monthly transfusions, the immediate effect of a single transfusion was assessed (n=7).

Laboratory tests

Laboratory tests, including complete blood count, absolute reticulocyte count (ARC), and hemoglobin profile, were obtained as part of routine visits to the outpatient clinic prior to oxygen gradient ektacytometry measurements. Percentage dense RBCs (%DRBCs, defined as RBC with a hemoglobin concentration of 41 g/dL or higher) were measured with an ADVIA 120/2120 hematology analyzer (Siemens, Healthcare GmBH, Erlangen, Germany).

Oxygen gradient ektacytometry

Lyon or UMC Utrecht samples were measured by oxygen gradient ektacytometry after being stored at 4°C for 24hours TCHC samples were measured 8 hours after collection. Oxygen gradient ektacytometry was carried out with the Laser Optical Rotational Red Cell Analyzer

(Lorrca, RR Mechatronics, Zwaag, The Netherlands). The oxygenscan is a new add-on feature of the Lorrca which allows measurement of red cell deformability as a function of continuously changing oxygen tensions, described in detail elsewhere.^{5,9,10} Briefly, to carry out the oxygen gradient ektacytometry, 50 μL of whole blood, standardized to a fixed RBC count of 200×10^6 , is suspended in 5 mL Oxy-Iso (RR Mechatronics, osmolarity 282-286 mOsm/kg, pH 7.35-7.45 at room temperature $21 \pm 1^\circ\text{C}$).^{9,10}

Statistical Analysis

A curve fit was calculated for every individual measurement with R studio based on Pearson's correlation, generating the additional oxygen gradient ektacytometry-derived biomarkers slope and EI_0 (Figure 1). EI_0 indicates the calculated RBC deformation when oxygen tension is lowered to 0.0 mmHg. Slope reflects the rapidity of RBC sickling during deoxygenation (Figure 1).

Mann-Whitney test was performed to compare values from the VOC+ and VOC- groups and a Wilcoxon signed-rank test to compare values pre- and on therapy. All correlations were done with univariate Spearman's correlation. GraphPad Prism (version 8.0) was used in all statistical analysis except for curve fit analysis. *p-value* <0.05 was considered statistically significant.

Results

Oxygen gradient ektacytometry-derived biomarkers are associated with vaso-occlusive crisis frequency

Characteristics of VOC+ and VOC- cohorts are shown in Table 1. Overall, patient demographics and laboratory parameters were comparable between the two cohorts. Differences were noted with regard to age (significantly higher in the VOC- group of the adult cohort), percentage of patients on HU treatment (higher in the VOC+ group in the pediatric cohort), percentage of patients on HU and chronic transfusion (CTf) (higher in the VOC- group in both cohorts). Laboratory parameters were not significantly different in the pediatric cohort, but in the adult patient cohort DRBCs and bilirubin were significantly higher in the VOC+ group,

In the adult cohort, PoS differed significantly between VOC- group (median 41.6 mmHg) and VOC+ group (median 53.7 mmHg, $p=0.0008$, Figure 2A). The same was observed in the pediatric cohort ($p=0.0495$, Figure 2D), which indicates that RBCs of patients without VOC can tolerate lower oxygen tensions before sickling occurs. EI_{\min} in both cohorts was significantly lower in patients who experienced VOC (adult cohort $p=0.0178$, pediatric cohort $p=0.022$, Figure 2C and F), which highlights the fact that RBCs of patients in the VOC+ group are less deformable at the end of the deoxygenation period.

EI_{\max} was not significantly different between the VOC- and VOC+ groups in the pediatric cohort, but was significantly higher in the VOC- group in the adult cohort (Figure 2B and E), indicating that at fully oxygenated conditions RBC deformability is lower in the VOC+ group compared to the VOC- group in adult SCD patients. Slope, indicating the rapidity of RBC

Table 1. Characteristics of the adult patient cohort and pediatric patient cohort in which patients who experienced VOC were compared to patients who did not.

	Adult cohort		Pediatric cohort	
	VOC- (n=18)	VOC+ (n=28)	VOC- (n=34)	VOC+ (n=46)
Patient related				
Sex, female n (%)	11 (61)	13 (46)	15 (44)	20 (43)
Age, years, median (range)	41 (19-62)	24 (18-45) [§]	8 (3-18)	12 (4-17)
HbS/β ⁰ -thalassemia, n (%)	1 (6)	0 (0)	2 (6)	1 (2)
α-Thalassemia: 1 deletion, n (%)	4 (22)	4 (14)	nd	nd
2 deletions, n (%)	1 (6)	2 (7)	nd	nd
Splenectomy, n (%)	5 (28)	3 (11)	9 (26)	14 (30)
Current treatment				
HU, n (%)	8 (44)	11 (39)	18 (53)	34 (74)
Dose HU, fixed or mg/kg, median (range)	1000 (500-1500)	1500 (500-2000)	24 (12-35)	26 (12-36)
Duration of HU, years, median (range)	7 (4-10)	3 (1-17)	3 (1-11)	5 (1-10)
Chronic transfusion, n (%)	1 (6)	3 (11)	5 (15)	6 (13)
HU + Chronic transfusion, n (%)	5 (28)	3 (11)	7 (21)	5 (11)
Red cell characteristics				
HbF (%) ^a	15 ± 11	9 ± 9	9 ± 10	9 ± 8
HbS (%) ^a	65 ± 16	73 ± 18	50 ± 25	60 ± 28
Hb (g/dL)	9.3 ± 1.3	9.4 ± 1.1	9.0 ± 1.3	9.0 ± 1.3
ARC (10 ⁹ /L) ^b	305 ± 196	262 ± 120	423 ± 215	421 ± 155
MCV (fl)	92 ± 20	89 ± 14	90±11	94±13
MCHC (g/dL)	34 ± 2	35±1	32 ± 1	33 ± 1
Dense RBCs (%) ^c	2.2 ± 1.5	5.3 ± 3.1*	4.0 ± 2.1	5.0 ± 3.6
Other laboratory characteristics				
Platelet count (10 ⁹ /L)	367 ± 156	380 ± 181	399 ± 158	462 ± 243
Leucocytes (10 ⁹ /L)	8.8 ± 2.6	9.4 ± 3.6	9.7 ± 3.4	10.5 ± 4.7
Neutrophils (10 ⁹ /L)	4.7 ± 2.0	5.3 ± 2.8	5.0 ± 2.3	4.8 ± 2.4
Bilirubin (total (mg/dL) ^d	0.32±0.15	0.58 ± 0.32†	2.7 ± 1.8	2.5 ± 0.9
LDH (U/L) ^e	362 ± 129	463 ± 164	1197 ± 384	1305 ± 641
Ferritin (ng/mL) ^f	1035 ± 2151	300 ± 349	1345 ± 555	1913 ± 686
Creatinine (mg/dL) ^g	0.71 ± 0.23	0.65 ± 0.17	0.44 ± 0.14	0.37 ± 0.09

Patients with no history of previous VOC in the past two years (VOC-) are compared to patients who were admitted or assessed in the emergency room because of VOC in the past two years (VOC+). Numbers represent mean ± SDs or state otherwise. VOC, vaso occlusive crisis; HbS, hemoglobin S; HU, hydroxyurea; HbF, fetal hemoglobin; Hb, hemoglobin; ARC, absolute reticulocyte count, RBC, red blood cell; MCV, mean corpuscular volume; MCHC, mean corpuscular hemoglobin concentration; LDH, lactate dehydrogenase; nd, not determined; §p<0.001, †p<0.01, *p<0.05. ►

^a In the pediatric cohort, data of 28 patients available, 13 in VOC- group, 15 in VOC+ group; ^b In the adult cohort, data of 42 patients available, 15 in VOC- group, 27 in VOC+ group; ^c In the adult cohort, data of 18 patients available, 6 in VOC- group, 12 in VOC+ group; ^d In the adult cohort, data of 40 patients available, 14 in VOC- group, 26 in VOC+ group. In the pediatric cohort, data of 33 patients available, 13 in VOC- group, 20 in VOC+ group; ^e In the adult cohort, data of 39 patients available, 12 in VOC- group, 27 in VOC+ group. In the pediatric cohort, data of 22 patients available, 7 in VOC- group, 15 in VOC+ group; ^f In the adult cohort, data of 41 patients available, 14 in VOC- group, 27 in VOC+ group. In the pediatric cohort, data of 15 patients available, 9 in VOC- group, 6 in VOC+ group; ^g In the adult cohort, data of 42 patients available, 15 in VOC- group, 27 in VOC+ group. In the pediatric cohort, data of 49 patients available, 19 in VOC- group, 30 in VOC+ group.

sickling during deoxygenation, was significantly higher in the adult VOC- group ($p=0.0002$) but not significantly different in the pediatric cohort (Supplemental Figure 1A and D). Higher Slope values indicate a homogenous population of RBCs that sickle at a low oxygen tension, which is favorable for the patient. Lower Slope values indicate a heterogeneous population consisting of a percentage of sickled cells at normoxia and a population of RBCs that start to sickle at a high oxygen tension, which is unfavorable. Oxygen gradient ektactometry-derived biomarkers are population based; therefore, these findings could indicate that in the adult cohort RBCs of patients without VOC are composed of a more homogenous distribution of HbS than the pediatric cohort.

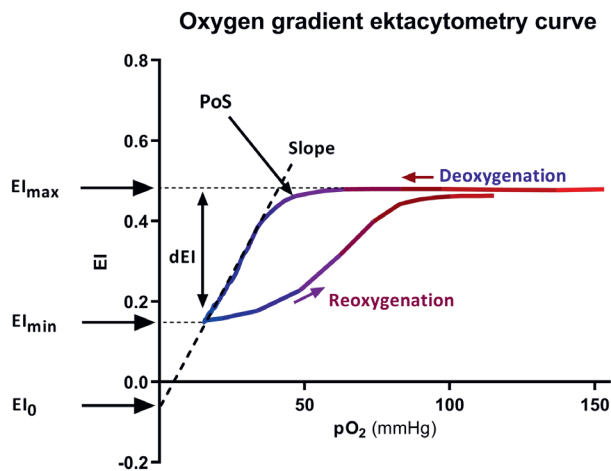


Figure 1. Representative Oxygen gradient ektactometry curve and reported biomarkers. Oxygen gradient ektactometry begins measuring deformability at normoxia, deoxygenation is achieved gradually with nitrogen gas. Deformability is measured and displayed as Elongation Index (EI). Reoxygenation with ambient air occurs rapidly when nitrogen gas valves are closed. EI_{max} is the maximum deformability measured just before deoxygenation. Point of Sickling (PoS) is the oxygen concentration at which a 5% decrease in EI occurs. EI_{min} is measured at the end of 22 minute deoxygenation cycle, and reports the deoxygenated red cell deformability. Delta EI (ΔEI) is the difference between EI_{max} and EI_{min} . Recovery is the percentage of deformability that is reached after reoxygenation in relation to the deformability before deoxygenation. Slope is calculated using a statistical program, and represents the direction coefficient of the curve between the PoS and EI_{min} and reflects the rapidity of RBC sickling during deoxygenation. EI_0 is the point the Slope intersects with the Y-axis, and indicates the calculated deformation of RBCs when oxygen tension is further lowered to 0.0 mmHg.

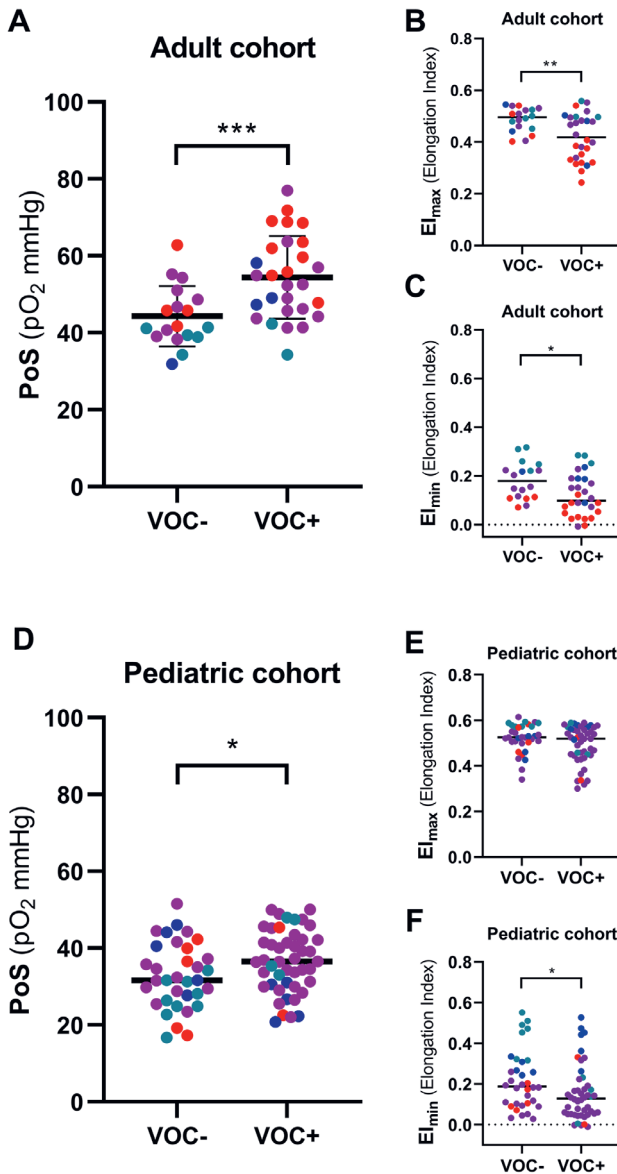


Figure 2. Oxygen gradient ektacytometry-derived biomarkers are associated with vaso-occlusive crisis.

(A) Point of Sickling (PoS) is significantly higher in patients with SCD in the adult cohort who experienced one or more VOC in the past two years. Colors show different treatment regimens: untreated (red), HU treatment (purple), chronic transfusion (turquoise). (B) Maximum deformability (EI_{max}) is significantly lower in patients in the adult cohort with VOC compared to those without. (C) Minimum deformability (EI_{min}) is significantly higher in patients who did not experience a VOC in the past two years compared to patients who did, in the adult cohort. (D) PoS is significantly higher in patients with SCD in the pediatric cohort who experienced 1 or more VOC in the past two years. Colors show different treatment regimens: untreated (red), HU treatment (purple), chronic transfusion (blue), HU and chronic transfusion (turquoise). (E) EI_{max} is not significantly different in patients in the pediatric cohort with VOC compared to those without. (F) EI_{min} is significantly higher in patients who did not experience a VOC in the past two years compared to patients who did, in the pediatric cohort. *** $p < 0.001$, ** $p < 0.01$, * $p < 0.05$

To assess the association of oxygen gradient ektactometry-derived biomarkers with RBC characteristics and known indicators of disease severity, such as HbF and HbS levels, and markers of hemolysis (Hb, lactate dehydrogenase (LDH), bilirubin and ARC), the degree of correlation between these lab parameters and the biomarkers PoS, El_{max} , El_{min} , Slope, El_0 and DeltaEI were calculated for each cohort (Supplemental Table 1 and 2). In addition, markers of inflammation and organ damage such as ferritin and creatinine were assessed for degree of correlation with oxygen gradient ektactometry-derived biomarkers as well. We found significant correlations between El_{max} , PoS and El_{min} with HbS and HbF levels. Various biomarkers correlated with ARC, bilirubin, LDH, ferritin, or creatinine in the adult cohort (Supplemental Table 1). In the pediatric cohort comparable results were found, with the strongest correlation found between El_{max} and %HbS ($r = -0.895$, $p = 0.001$; Supplemental Table 2).

Oxygen gradient ektactometry-derived biomarkers are modulated by standard of care therapy

To assess if oxygen gradient ektactometry-derived biomarkers changed in patients receiving or initiating standard of care treatment of transfusion or HU, we analyzed three patient cohorts on different treatment regimens. In the first cohort, 15 SCD patients (median age 13.0y, range 1.8-26.0, 7 female), were followed before and during HU treatment. Measurements were performed at baseline, and 1, 3 and 6 months after starting HU. Based on weight, patients were started 1000mg or 1500mg daily and titrated up by 500mg until maximum tolerated dose was achieved. During HU titration, oxygen gradient ektactometry curves showed significant changes in most biomarkers (Figure 3A). After 3 and 6 months on HU the PoS decreased significantly from 64.4 to 55.8 and 50.7 mmHg, respectively (Figure 3B; Supplemental Table 3). Accordingly, El_{max} , El_{min} and Slope increased significantly after 3 and 6 months of HU treatment (Figure 3C-E; Supplemental Table 3).

To assess the immediate effect of red cell transfusion, samples from seven SCD patients (included in The Netherlands, median age 26.2y, range 6.5-62.0; 6 female) obtained before and immediately after transfusion with 1-2 RBC units (6 patients received 2 units, 1 patient 1 unit) were analyzed by oxygen gradient ektactometry. Transfusion immediately improved El_{max} , PoS, El_{min} and El_0 (all $p < 0.05$, Figure 4, Supplemental Table 4).

We assessed the effect of chronic transfusion on biomarkers in combination with HU treatment in a subgroup of 21 patients receiving care at TCHC (median age 7.6y; range 2.1-20.9, 6 female). PoS, El_{max} and El_0 improved significantly (all $p < 0.01$, Figure 5A-C and E). El_{min} displayed the largest improvement (0.08 to 0.21 EI or 24.6% increase, $p < 0.001$, Figure 5D). Importantly, while the oxygen gradient ektactometry-derived biomarkers showed a considerable and significant change, most conventional laboratory tests did not (Supplemental Table 4), confirming that this technique provides an additional insight into the efficacy of disease modifying therapies.

Oxygen gradient ektacytometry-derived biomarkers during neonatal hemoglobin switch

To investigate how the physiologic decline in HbF in neonates changes RBC as measured by oxygen gradient ektacytometry, we analyzed the RBCs of a newborn at different time points during the first 8 months of life (Supplemental Figure 2). When HbF decreases and HbS levels increases, the PoS gradually increases, while EI_{max} and EI_{min} gradually decrease, visualizing how healthy RBCs at birth are slowly changed during the first months of life and are replaced with functionally abnormal SCD RBCs.

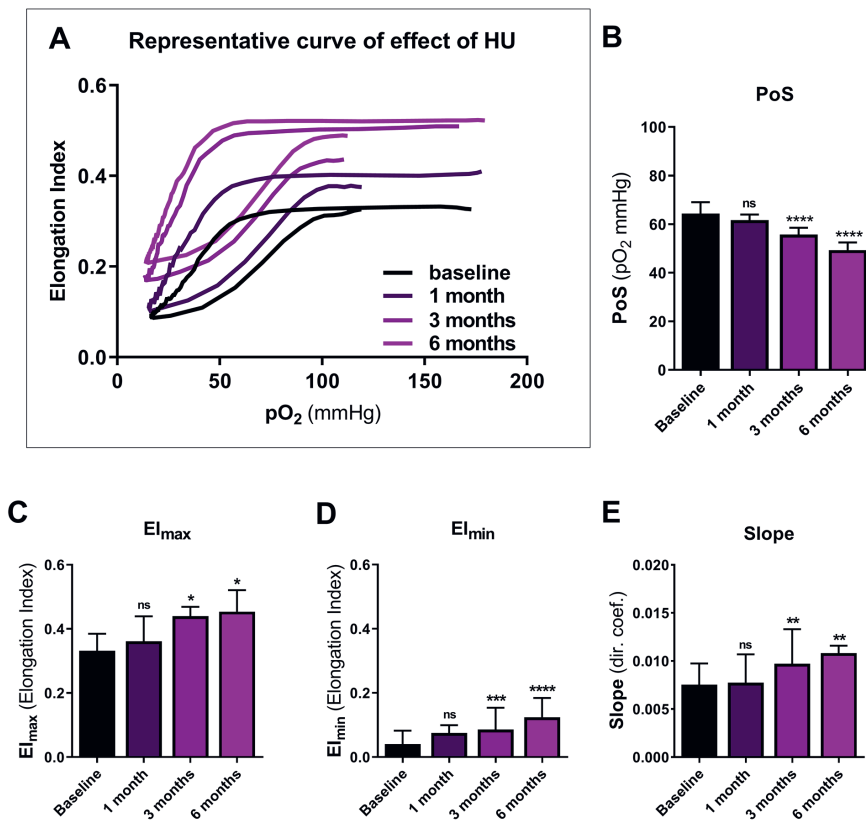


Figure 3. Hydroxyurea has a measurable effect on oxygen gradient ektacytometry-derived biomarkers.

The effect of starting HU therapy was measured in 15 patients with SCD at baseline, and after 1,3 and 6 months of HU therapy. (A) Representative curve of a patient before and during hydroxyurea (HU) titration to maximum tolerated dose. (B) Median values of Point of Sickling (PoS) before and during HU therapy. PoS significantly decreases after 3 and 6 months compared to baseline values. (C) Median values of maximum deformability before deoxygenation (EI_{max}) just before and during HU therapy. EI_{max} significantly increases after 3 and 6 months of HU compared to baseline values. (D) Median values of minimum deformability upon deoxygenation (EI_{min}) before and during HU therapy. EI_{min} significantly increases after 3 and 6 months of HU therapy compared to baseline values. (E) Median values of the directional coefficient of the deoxygenation part of the curve (Slope, see Figure 1) before and during HU therapy. Slope significantly increases after 3 and 6 months compared to baseline values. Error bars represent interquartile range. **** $p < 0.0001$, *** $p < 0.001$, ** $p < 0.01$, * $p < 0.05$

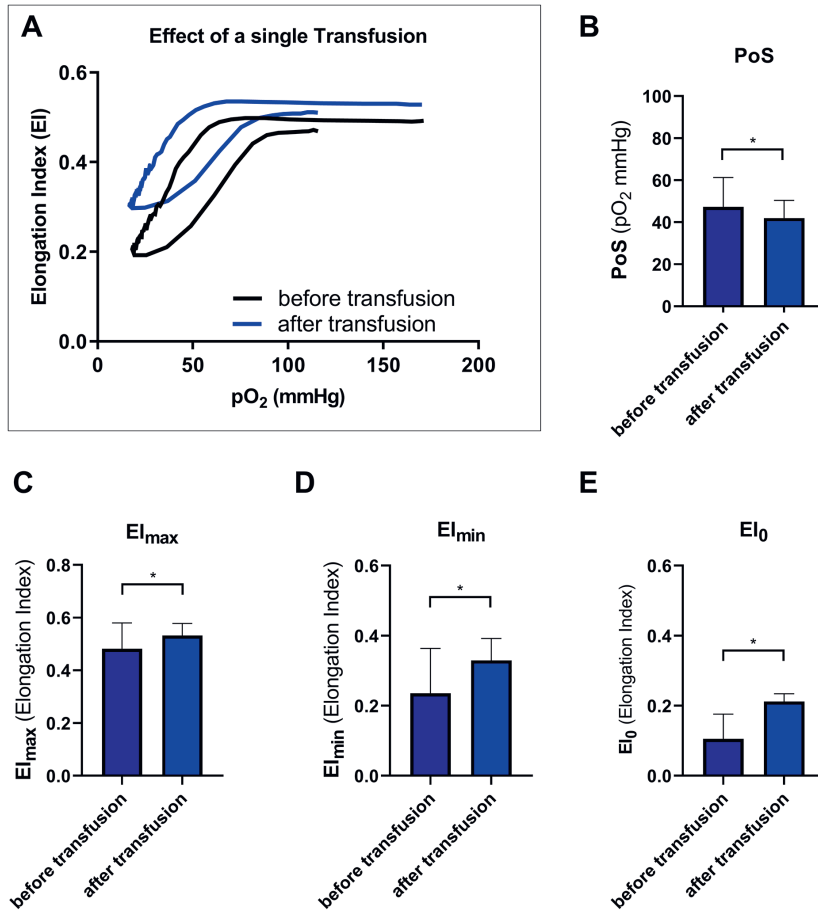


Figure 4. A single blood transfusion has a measurable effect on oxygen gradient ektactometry-derived biomarkers. Seven patients with SCD were followed just before and after transfusion therapy. (A) Representative curve that highlights how blood rheology is improved by a blood transfusion. (B) Median values of PoS are significantly decreased after transfusion, compared to before transfusion values. Median values of EI_{max} (C), EI_{min} (D) EI_0 (E) are significantly increased by transfusion. Error bars represent interquartile range. * $p < 0.05$

Discussion

Oxygen gradient ektactometry-derived biomarkers correlate with VOC frequency

We found that patients with two or more VOC in the past year had higher PoS (Figure 2A and D). Their RBCs were also less deformable when deoxygenated (EI_{min}) compared to patients in the VOC- group (Figure 2C and F). PoS was reduced and EI_{min} increased by therapies known to significantly reduce incidence of VOC, HU and CTF. These results indicate the promise of oxygen gradient ektactometry-derived biomarkers as surrogate endpoints to determine if a therapy has reduced the patient's risk of VOC.

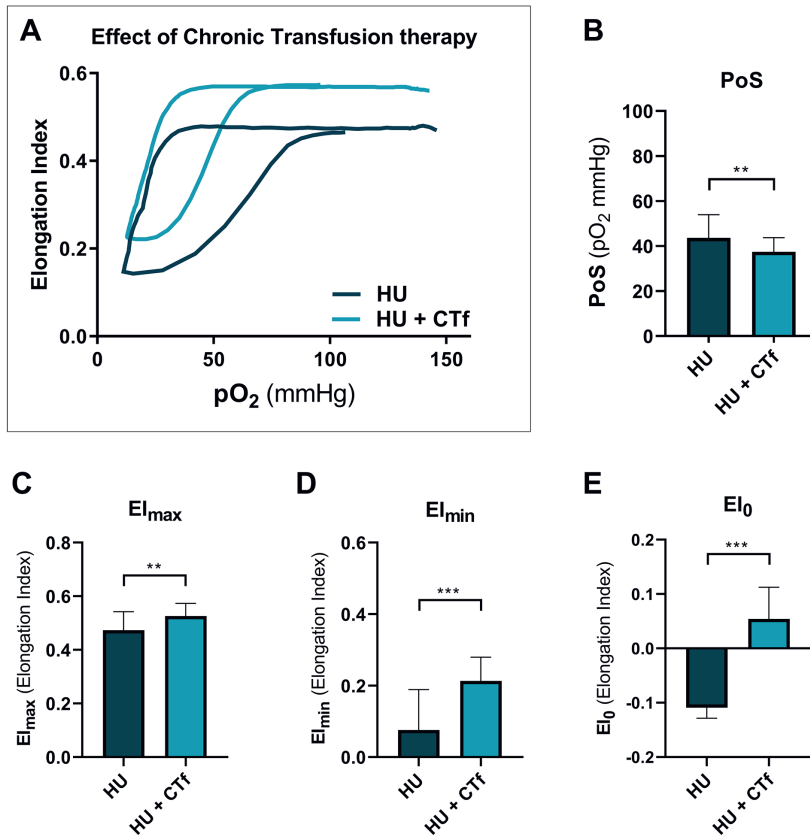


Figure 5. Chronic transfusion improves oxygen gradient ektacytometry-derived biomarkers in pediatric patients already treated with hydroxyurea therapy. Twenty-one patients with SCD were followed during HU and HU with CTf therapy. (A) Representative curve of a patient on hydroxyurea (HU) therapy before start of chronic transfusion therapy (CTf) and on CTf. (B) Median values of PoS before and on CTf, that significantly decreases during CTf. Median values of $E_{I_{max}}$ (C), $E_{I_{min}}$ (D) and E_{I_0} (E) are increased by a TF given as part of CTf. Error bars represent interquartile range. *** $p < 0.001$, ** $p < 0.01$, * $p < 0.05$

In this study we observed differences in oxygen gradient ektacytometry-derived biomarkers between cohorts. This could be due to differences in pediatric and adult SCD pathophysiology,¹¹ in particular RBC rheological characteristics, and notably RBC deformability, which has been found to be different between adults and young children.¹² In addition, other factors may also play a role, such as 1) differences in access to care (US versus Europe), 2) differences in guidelines, clinical practice and health care between adult and pediatric patients,¹³ 3) cultural differences between sites, particularly response to pain, 4) environmental factors such as climate¹⁴, or technical differences. The observed difference in PoS between VOC+ and VOC- groups seems more pronounced in the adult cohort, which could be due to the US population (and thereby pediatric cohort) of SCD patient being more heterogeneous, i.e. more admixture of Latin and Middle Eastern patient comprising of a more heterogeneous population.

In our study, specific oxygen gradient ektacytometry-derived biomarkers were associated with VOC in both cohorts, in contrast to conventional clinical laboratory parameters such as HbS and HbF levels¹⁵ and ARC.^{16,17} PoS and EI_{\min} were found to be the most reproducible clinically relevant biomarkers because they were associated with VOC in both adult and pediatric cohorts. The reproducible association observed in both cohorts, is likely due to the fact that oxygen gradient ektacytometry is a functional test that captures the combined effect of many factors contributing to RBC function, some measurable by clinical testing, like HbF and HbS levels, and some not, like the impact of 2,3-diphosphoglycerate levels, and oxidative stress.⁵

Available biomarkers of disease severity

Red cell related biomarkers such as number of irreversible sickled cells and DRBCs (%) are not consistently associated with SCD clinical complications like VOC.² The use of RBC deformability during normoxic conditions as a marker for complications is suggested as a biomarker in previous studies, which showed a correlation between an increase in RBC deformability and osteonecrosis¹⁸ or painful sickle cell crises.^{19,20} In contrast to these findings low deformability correlated with high hemolytic rate and higher risk of complications such as leg ulcers²¹, and glomerulopathy.²² More importantly, since RBC deformability is reported to be decreased during VOC²³, an increase is seen in deformability in the recovery phase of a painful VOC which was in turn a predictor of a new crisis.²⁰ Thus, in itself, RBC deformability during normoxic conditions gives varying results when different complications are assessed which makes it unsuitable to be used as biomarker for overall clinical severity.

A combination of markers of hemolysis, lactate dehydrogenase (LDH), bilirubin and ARC (i.e. hemolytic index) are associated with complications attributed to hemolysis such as pulmonary hypertension²⁴, stroke²⁵, leg ulcers, chronic kidney damage and priapism²⁶ but not with VOC.²⁷ Blood viscosity has been found to be associated with the frequency of VOC episodes both in SCD adults and children, which could indicate clinical usefulness of this parameter.²⁸ However, this biomarker does not change upon HU treatment because the increase in RBC deformability compensates for the rise in hematocrit, resulting in unchanged blood viscosity in patients²⁹, limiting the clinical usefulness of blood viscosity. The inflammatory biomarker high-sensitivity C-reactive protein (hs-CRP) was associated with the occurrence of VOC, in two studies.³⁰ TNF- α and IL-1 levels were significantly elevated in patients with frequent VOC with significant correlation with VOC frequency.³⁰ However, up till now no specific cytokine or immune cell type that is seen in patients with SCD holds the potential to serve as a biomarker for VOC frequency in SCD. This is also due to the highly complex pathophysiology that activates different immune pathways as well as the short half-life of many inflammatory cytokines.³¹

Limitations of oxygen gradient ektacytometry-derived biomarkers are that they primarily evaluate RBC function, and do not capture other factors important in SCD pathophysiology, such as inflammation, hemostatic activation, adhesion and endothelial dysfunction. Inclusion of those factors, such as soluble vascular cell adhesion molecule (sVCAM)³², or other functional tests, like adhesion to an artificial microfluidic network³³ could complement this technology. More importantly, as hemoglobin polymerization is a kinetic process that is very

strongly dependent on cell hemoglobin concentrations and the RBCs with high hemoglobin concentration will deform less even under normoxic conditions PoS might not reflect sickling ability of all circulating cells. As currently analyzed it only reflects sickling of cells that deform under normoxic conditions.

Oxygen gradient ektacytometry-derived biomarkers as surrogate endpoints in clinical trials

There are four FDA approved pharmacologic therapies available for routine SCD care in the US. The best way to choose which drug to prescribe to which patients is a topic of intense discussion. There are also several other agents currently in clinical trials on the North American continent and in Europe. Clinically relevant biomarkers, such as oxygen gradient ektacytometry, are needed for several indications: 1) to select the optimal therapy based on the patient's particular blood rheology, according to the principles of precision medicine, 2) to monitor efficacy in an objective, rapid manner rather than watching for clinical complications which can take years to emerge, and 3) to provide objective clinically relevant endpoints for clinical trials. Currently, observation of clinical complications in combination with basic hematological parameters are the outcome parameters of clinical trials to assess efficacy of new treatment for SCD. This approach requires a long observation period, and increases the cost and number of patients needed to enroll, as well as introducing a subjective endpoint that may be affected by non-SCD factors.

Biomarkers of red cell function, like those provided by oxygen gradient ektacytometry, could also be excellent ways to assess gene-based therapy outcomes. The amount of HbF induction needed to be achieved by gene therapy to effect a cure is still a topic for discussion. In most clinical trials sickling behavior is not functionally assessed, as microscopy based sickling assays are static and do not provide information on patient specific sickling characteristics.³⁴ Additionally, different gene therapy trials induce different functional hemoglobins; a functional analysis of the resulting RBC population is the best way to compare different strategies head to head. VOC is still the primary endpoint in ongoing gene therapy trials, however lack of VOC does not demonstrate a cure as organ damage may still be ongoing.

In allogeneic hematopoietic stem cell transplantation (HSCT) in SCD, HbAS or HbAA individuals, preferably related to the recipient, can serve as donors. Efficacy of HSCT, or engraftment following transplant is determined by HbS levels and donor chimerism.³⁵ The appropriate amount of donor chimerism has been reported to need to be at least 20% to reverse the sickle phenotype, based on a study of three transplanted individuals.³⁶ However, donor chimerism and HbS levels do not capture clinically relevant sickling in an individual patient, because a mixture of 60% HbAA with 40% HbSS RBCs compared to 100% HbAS RBCs give very different oxygen gradient ektacytometry-derived biomarkers results compared to that of a trait individual, even though HbS levels are the same. As a result, a severe patient might need a higher % chimerism and a lower HbS level to prevent clinically relevant sickling. Current guidelines suggest basing clinical follow-up measurements on donor chimerism and HbS level. Functional biomarkers like EI_{\min} and PoS could better assess the effectivity of these therapies in individual patients, indicating if the treatment was successful enough to prevent clinically relevant sickling.³⁷

In conclusion, oxygen gradient ektacytometry-derived biomarkers provides functional, clinically relevant next generation biomarkers that are associated with VOC. Its parameters can provide the clinician with information about patient RBC characteristics and sickling propensity that could eventually aid in clinical decision making. Moreover, oxygen gradient ektacytometry-derived biomarkers captures several RBC characteristics that have additional value over conventional laboratory tests. We have shown that oxygen gradient ektacytometry-derived biomarkers improve with known efficacious therapies and are associated VOC; therefore, these biomarkers can be an objective surrogate endpoint of disease modification.

Acknowledgements

The authors would like to thank all patients that donated blood for this study. The authors also thank the technicians of the Central Diagnostic Laboratory, Specialized Hematology, University Medical Center Utrecht. As well as the clinical research coordinators of the department of pediatric hematology at the Erasmus Medical Center Rotterdam and the department of hematology at the Amsterdam University Medical Centers.

Both M.A.E.R, M.E.H, J.G, E.N, M.H.C and E.J.vB are clinical researchers within the Sickle Cell Outcome Research (SCORE) consortium, a multicenter clinical research collaboration in the Netherlands, which gave input on the work described in this manuscript for which we value highly.

This research has been funded in part by Eurostars grant estar18105 and by an unrestricted grant provided by RR Mechatronics. This work is also funded by K08 grant from the National Institute of Diabetes and Digestive and Kidney Diseases, and by support from the Department of Pediatrics, Baylor College of Medicine.

Authorship

Contribution: M.A.E.R, R.vW., E.J.vB., and V.A.S. designed the study; M.A.E.R., M.E.H., J.G., C.R., P.J., M.B., E.N., R.F., M.H.C., E.J.vB., and V.A.S. collected clinical and laboratory data. M.A.E.R., C.K.K., J.B., B.A.vO., E.T. and J.R. and C.B. performed laboratory experiments. M.A.E.R., R.vW., P.C., E.J.vB., and V.A.S. analyzed the data and wrote the manuscript. All authors edited the manuscript and approved the final version.

Conflict-of-interest disclosure

M.A.E.R, J.B and B.A.vO. received grant funding from RR Mechatronics. R.vW received grant funding from Agios Pharmaceuticals Inc and RR Mechatronics. E.J.vB received grant funding Agios Pharmaceuticals Inc, RR Mechatronics, Novartis and Pfizer for investigator initiated research projects. V.A.S. received grant funding from Global Blood Therapeutics, Emmaus, and Novartis for investigator initiated research projects.

References

- Connes P, Alexy T, Detterich J, Romana M, Hardy-Dessources MD, Ballas SK. The role of blood rheology in sickle cell disease. *Blood Rev.* 2015;30(2):111-8.
- Kalpatthi R, Novelli EM. Measuring success: Utility of biomarkers in sickle cell disease clinical trials and care. *Hematology.* 2018;2018(1):482-92.
- Liu Y, Zhong H, Bao W, Mendelson A, An X, Shi P, et al. Patrolling monocytes scavenge endothelial-adherent sickle RBCs: A novel mechanism of inhibition of vaso-occlusion in SCD. *Blood.* 2019;134(7):579-90.
- Manwani D, Frenette PS. Vaso-occlusion in sickle cell disease: pathophysiology and novel targeted therapies. *Blood.* 2013;122(24):3892-8.
- Rab MAE, van Oirschot BA, Bos J, Merx TH, van Wesel ACW, Abdulmalik O, et al. Rapid and reproducible characterization of sickling during automated deoxygenation in sickle cell disease patients. *Am J Hematol.* 2019;94(February):575-84.
- Niihara Y, Miller ST, Kanter J, Lanzkron S, Smith WR, Hsu LL, et al. A phase 3 trial of l-glutamine in sickle cell disease. *N Engl J Med.* 2018;379(3):226-35.
- Matsui NM, Borsig L, Rosen SD, Yaghmai M, Varki A, Embury SH. P-selectin mediates the adhesion of sickle erythrocytes to the endothelium. *Blood.* 2001;98(6):1955-62.
- Ataga KI, Kutlar A, Kanter J, Liles D, Cancado R, Friedrisch J, et al. Crizanlizumab for the prevention of pain crises in sickle cell disease. *N Engl J Med.* 2017;376(5):429-39.
- Rab MAE, van Oirschot BA, Bos J, Kanne CK, Sheehan VA, van Beers EJ, et al. Characterization of Sickling During Controlled Automated Deoxygenation with Oxygen Gradient Ektacytometry. *J Vis Exp.* 2019;(153):1-10.
- Rab MAE, Kanne CK, Bos J, Boisson C, van Oirschot BA, Nader E, et al. Methodological aspects of the oxygenscan in sickle cell disease: A need for standardization. *Am J Hematol.* 2020;95(1):5-8.
- Claster S, Vichinsky EP. Managing sickle cell disease. *Br Med J.* 2003;327(7424):1151-5.
- Renoux C, Romana M, Joly P, Ferdinand S, Bertrand Y, Petras M, et al. Effect of Age on Blood Rheology in Sickle Cell Anaemia and Sickle Cell Haemoglobin C Disease : A Cross-Sectional Study. *PLoS One.* 2016;11(6):1-11.
- Blinder MA, Duh MS, Sasane M, Trahey A, Paley C, Vekeman F. Age-Related Emergency Department Reliance in Patients with Sickle Cell Disease. *J Emerg Med.* 2015;49(4):513-522.e1.
- Tewari S, Brousse V, Piel FB, Menzel S, Rees DC. Environmental determinants of severity in sickle cell disease. *Haematologica.* 2015;100(9):1108-16.
- Brousse V, El Hoss S, Bouazza N, Arnaud C, Bernaudin F, Pellegrino B, et al. Prognostic factors of disease severity in infants with sickle cell anemia: A comprehensive longitudinal cohort study. *Am J Hematol.* 2018;93(11):1411-9.
- Madhi F, Kamdem A, Jung C, Carlier-gonod A, Epaud R, Pondarre C. Identification of Clinical and Laboratory Parameters Associated with the Development of Acute Chest Syndrome during Vaso-Occlusive Episodes in Children with Sickle Cell Disease : A Preliminary Step before Assessing Specific and Early Treatment Strategies. *J Clin Med.* 2019;8(11):E1839.
- Sommet J, Alberti C, Couque N, Verlhac S, Haouari Z, Mohamed D, et al. Clinical and haematological risk factors for cerebral macrovasculopathy in a sickle cell disease newborn cohort: A prospective study. *Br J Haematol.* 2016;172(6):966-77.
- Lemonne N, Lamarre Y, Romana M, Mukisi-mukaza M, Hardy-Dessources M-D, Tarer V, Mouguel D, Waltz Xavier, Tressieres B, Lalanne-Mistrih M-L, Etienne-Julan M, Connes P. Does increased red blood cell deformability raise the risk for osteonecrosis in sickle cell anemia? *Blood.* 2013;121(15):3054-7.
- Ballas S K, Larner J, Smith ED, Surrey S, Schwartz E, Rappaport EF. Rheologic predictors of the severity of the painful sickle cell crisis. *Blood.* 1988;72(4):1216-23.
- Lande WM, Andrews DL, Clark MR, Braham N V, Black DM, Embury SH, et al. The Incidence of Painful Crisis in Homozygous Sickle Cell Disease: Correlation with Red Cell Deformability. *Blood.* 1988;72(6):2056-9.

21. Connes P, Lamarre Y, Hardy-Dessources MD, Lemonne N, Waltz X, Mougénel D, et al. Decreased hematocrit-to-viscosity ratio and increased lactate dehydrogenase level in patients with sickle cell anemia and recurrent leg ulcers. *PLoS One*. 2013;8(11):6–10.
22. Lamarre Y, Romana M, Lemonne N, Hardy-Dessources MD, Tarer V, Mougénel D, et al. Alpha thalassemia protects sickle cell anemia patients from macro-albuminuria through its effects on red blood cell rheological properties. *Clin Hemorheol Microcirc*. 2014;57(1):63–72.
23. Ballas SK, Smith ED. Red blood cell changes during the evolution of the sickle cell painful crisis. *Blood*. 1992;79(8):2154–63.
24. Kato GJ, McGowan V, Machado RF, Little JA, Taylor VI, Morris CR, et al. Lactate dehydrogenase as a biomarker of hemolysis-associated nitric oxide resistance, priapism, leg ulceration, pulmonary hypertension, and death in patients with sickle cell disease. *Blood*. 2006;107(6):2279–85.
25. Bernaudin F, Verlhac S, Chevret S, Torres M, Coïc L, Arnaud C, et al. G6PD deficiency, absence of α -thalassemia, and hemolytic rate at baseline are significant independent risk factors for abnormally high cerebral velocities in patients with sickle cell anemia. *Blood*. 2008;112(10):4314–7.
26. Novelli EM, Hildesheim M, Rosano C, Vanderpool R, Simon M, Kato GJ, et al. Elevated pulse pressure is associated with hemolysis, proteinuria and chronic kidney disease in sickle cell disease. *PLoS One*. 2014;9(12):1–14.
27. Ataga KI, Reid M, Ballas SK, Yasin Z, Bigelow C, James LS, et al. Improvements in haemolysis and indicators of erythrocyte survival do not correlate with acute vaso-occlusive crises in patients with sickle cell disease: A phase III randomized, placebo-controlled, double-blind study of the gardos channel blocker senicapoc. *Br J Haematol*. 2011;153(1):92–104.
28. Lamarre Y, Romana M, Waltz X, Lalanne MLM, Tressières B, Divialle-Doumido L, et al. Hemorheological risk factors of acute chest syndrome and painful vaso-occlusive crisis in children with sickle cell disease. *Haematologica*. 2012;97(11):1641–7.
29. Lemonne N, Charlot K, Waltz X, Ballas S.K, Lamarre Y, Lee, K; Hierso, R; Connes, C; Etienne-Julan, M; Romana, M; Connes P. Hydroxyurea treatment does not increase blood viscosity and improves red blood cell rheology in sickle cell anemia. *Haematologica*. 2015;100:e383-386.
30. Garadah TS, Jaradat AA, AlAlawi ME, Hassan AB, Sequeira RP. Pain frequency, severity and QT dispersion in adult patients with sickle cell anemia: Correlation with inflammatory markers. *J Blood Med*. 2016;7:255–61.
31. Nader E, Romana M, Connes P. The Red Blood Cell—Inflammation Vicious Circle in Sickle Cell Disease. *Front Immunol*. 2020;11(March):1–11.
32. Glassberg J, Minniti C, Cromwell C, Cytryn L, Kraus T, Skloot GS, et al. Inhaled steroids reduce pain and sVCAM levels in individuals with sickle cell disease: A triple-blind, randomized trial. *Am J Hematol*. 2017;92(7):622–31.
33. Man Y, Goreke U, Kucukal E, Hill A, An R, Liu S, et al. Leukocyte adhesion to P-selectin and the inhibitory role of Crizanlizumab in sickle cell disease: A standardized microfluidic assessment. *Blood Cells, Mol Dis*. 2020;83(February):102424.
34. Antoniani C, Meneghini V, Lattanzi A, Felix T, Romano O, Magrin E, et al. Induction of fetal hemoglobin synthesis by CRISPR/Cas9-mediated editing of the human β -globin locus. *Blood*. 2018;131(17):1960–73.
35. Stenger EO, Shenoy S, Krishnamurti L. How I treat sickle cell disease with hematopoietic cell transplantation. *Blood*. 2019;134(25):2249–60.
36. Fitzhugh CD, Cordes S, Taylor T, Coles W, Roskom K, Link M, et al. At least 20% donor myeloid chimerism is necessary to reverse the sickle phenotype after allogeneic HSCT. *Blood*. 2017;130(17):1946–8.
37. John TD, Lu M, Kanne CK, Rab MAE, van Wijk R, Shevkopyas SS, et al. Rheological Assessments of Sickle Cell Patients Post Allogeneic Hematopoietic Cell Transplant. *Blood*. 2019 Nov 13;134(Supplement_1):996.

Supplemental Table 1. Correlations of oxygen gradient ektacytometry derived-biomarkers with laboratory parameters in the adult cohort.

Laboratory parameter	Adult cohort ^a					
	Oxygen gradient ektacytometry-derived biomarkers					
	El _{max}	PoS	El _{min}	Slope	El ₀	DeltaEl
HbF (%)	0.666[‡]	-0.461[†]	-0.499[†]	0.420*	0.213	0.242
HbS (%)	-0.667[‡]	0.399*	0.650[‡]	-0.265	-0.395*	-0.285
Hb (g/dL)	0.391*	-0.198	0.276	0.118	0.255	0.278
ARC (10 ⁹ /L) ^b	-0.643[§]	0.421*	-0.330	-0.544[†]	0.123	-0.402*
MCV (fl)	0.279	-0.032	0.320	-0.163	0.660[‡]	-0.007
MCHC (g/dL)	0.071	-0.087	0.520[†]	0.246	-0.026	-0.254
Dense Cells (%) ^c	-0.950[‡]	0.736[†]	-0.447	-0.846[§]	0.332	-0.714[†]
Bilirubin (total (mg/dL) ^d	-0.593[§]	0.510[†]	-0.446*	-0.731[‡]	0.222	-0.260
LDH (U/L) ^e	-0.484[†]	0.329	-0.328	-0.408*	0.078	-0.293
Ferritin (ng/mL) ^f	0.368*	-0.232	0.410*	0.091	0.310	-0.018
Creatinine (mg/dL) ^g	-0.132	0.224	-0.213	-0.273	0.414*	-0.098

HbF, fetal haemoglobin; HbS, haemoglobin S; Hb, haemoglobin; ARC, absolute reticulocyte count; MCV, mean corpuscular volume; MCHC, mean corpuscular haemoglobin concentration; LDH, lactate dehydrogenase; TSAT, transferrin saturation;

‡p<0.0001, §p<0.001, †p<0.01, *p<0.05.

^aTotal population of this cohort was 35 adult patients with SCA who were untreated or treated with hydroxyurea. Patients on (chronic) transfusion therapy (n=11) were excluded from this analysis.

^bData of 32 patients available, 3 patients had unknown data

^cData of 13 patients available, 22 patients had unknown data

^dData of 19 patients available, 16 patients had unknown data

^eData of 33 patients available, 2 patients had unknown data

^fData of 31 patients available, 4 patients had unknown data

^gData of 19 patients available, 16 patients had unknown data

Supplemental Table 2. Correlations of oxygen gradient ektacytometry-derived biomarkers with laboratory parameters in the pediatric cohort.

Laboratory parameter	Pediatric cohort ^a					
	Oxygen gradient ektacytometry-derived biomarkers					
	El _{max}	PoS	El _{min}	Slope	El ₀	DeltaEl
HbF (%) ^b	0.699*	-0.397	0.825[†]	0.393	0.713*	0.301
HbS (%) ^b	-0.895[§]	0.811[†]	0.853[§]	-0.793[†]	-0.371	-0.587*
Hb (g/dL)	0.631[†]	-0.365[†]	0.377[†]	0.468[§]	0.104	0.417[†]
ARC (10 ⁹ /L)	-0.462[§]	0.272*	-0.269*	-0.334*	-0.033	-0.294*
MCV (fl)	-0.004	0.136	0.041	-0.231	0.333*	-0.077
MCHC (g/dL)	0.042	0.113	0.048	-0.128	0.169	0.036
Dense Cells (%)	-0.768[‡]	0.668[‡]	-0.572[‡]	-0.801[‡]	0.044	-0.295*
Bilirubin (total) (mg/dL) ^c	-0.464*	0.405*	-0.342	-0.592[†]	-0.094	-0.152
LDH (U/L) ^d	-0.296	0.122	0.058	-0.208	0.225	-0.529*
Ferritin (ng/mL)	nd	nd	nd	nd	nd	nd
Creatinine (mg/dL) ^e	0.380*	-0.258	0.110	0.328	-0.016	0.519[†]

‡p<0.0001, §p<0.001, †p<0.01, *p<0.05.

^aTotal population of this cohort was 58 pediatric patients with SCD who were untreated or treated with hydroxyurea. Patients on (chronic) transfusion therapy (n=22) were excluded from this analysis.

^bData of 12 patients available, 46 patients had unknown data

^cData of 24 patients available, 34 patients had unknown data

^dData of 21 patients available, 37 patients had unknown data

^eData of 35 patients available, 23 patients had unknown data

HbF, fetal haemoglobin; HbS, haemoglobin S; Hb, haemoglobin; ARC, absolute reticulocyte count; MCV, mean corpuscular volume; MCHC, mean corpuscular haemoglobin concentration; LDH, lactate dehydrogenase; nd, not determined

Supplemental Table 3. Median values (range) of oxygen gradient ektacytometry-derived biomarkers and laboratory parameters before (baseline) and during hydroxyurea (HU) therapy (1, 3 and 6 months) of 15 patients with SCD (adult and pediatric). Baseline values are compared to 1, 3 or 6 months.

Effect of HU	HU treated cohort (n=15)			
	baseline	1 month	3 months	6 months
Oxygen gradient ektacytometry				
PoS (mmHg)	64.4 (35.1-87.6)	61.6 (39.2-69.3)	55.8 (33.5-60.4) [§]	49.3 (37.4-56.7) [‡]
El _{min} (EI)	0.04 (0.00-0.23)	0.08 (0.03-0.20)	0.09 (0.05-0.31) [‡]	0.12 (0.07-0.22) [‡]
El _{max} (EI)	0.33 (0.22-0.56)	0.36 (0.24-0.55)	0.44 (0.31-0.55) [*]	0.45 (0.29-0.56) [*]
Slope (dir.coef.)	0.007 (0.004-0.020)	0.008 (0.005-0.021)	0.010 (0.008-0.016) [‡]	0.011 (0.008-0.021) [‡]
El ₀ (EI)	-0.09 (-0.16-0.00)	-0.10 (-0.21-0.00)	-0.08 (-0.16-0.04)	-0.06 (-0.14-0.05) [*]
DeltaEI (EI)	0.28 (0.20-0.42)	0.31 (0.20-0.38)	0.31 (0.24-0.40)	0.32 (0.20-0.35)
Laboratory parameter				
Dense Cells (%)	8.3 (2.3-11.2)	5.4 (5.0-9.9)	6.3 (4.7-12.1)	4.5 (3.2-12.1)
HbF (%)	5.2 (0.9-28.5)	7.5 (1.4-29.7)	14.5 (4.1-33.7) [‡]	17.5 (4.6-34.3) [‡]
HbS (%)	82.0 (61.9-89.3)	81.7 (60.7-88.7)	73.3 (54.3-83.4) [‡]	72.9 (56.3-83.3) [‡]
Hb (g/dL)	9.0 (7.1-11.3)	8.5 (6.9-13.0)	9.6 (7.0-11.8)	9.5 (7.3-11.5)
ARC (10 ⁹ /L)	348 (178-695)	224 (98-399) [‡]	205 (50-346) [§]	244 (48-445) [‡]
MCV (fl)	79.1 (69.4-91.2)	88.3 (75.1-116.0) [*]	98.8 (72.0-135.0) [‡]	96.6 (77.2-130.0) [‡]
MCHC (g/dL)	35.8 (34.2-40.0)	35.8 (27.9-38.5)	35.9 (32.2-38.8)	35.6 (32.4-38.0)
RDW (%)	23.0 (16.0-28.50)	23.4 (16.8-28.3)	19.6 (14.5-28.3) [‡]	18.5 (14.3-30.4) [‡]

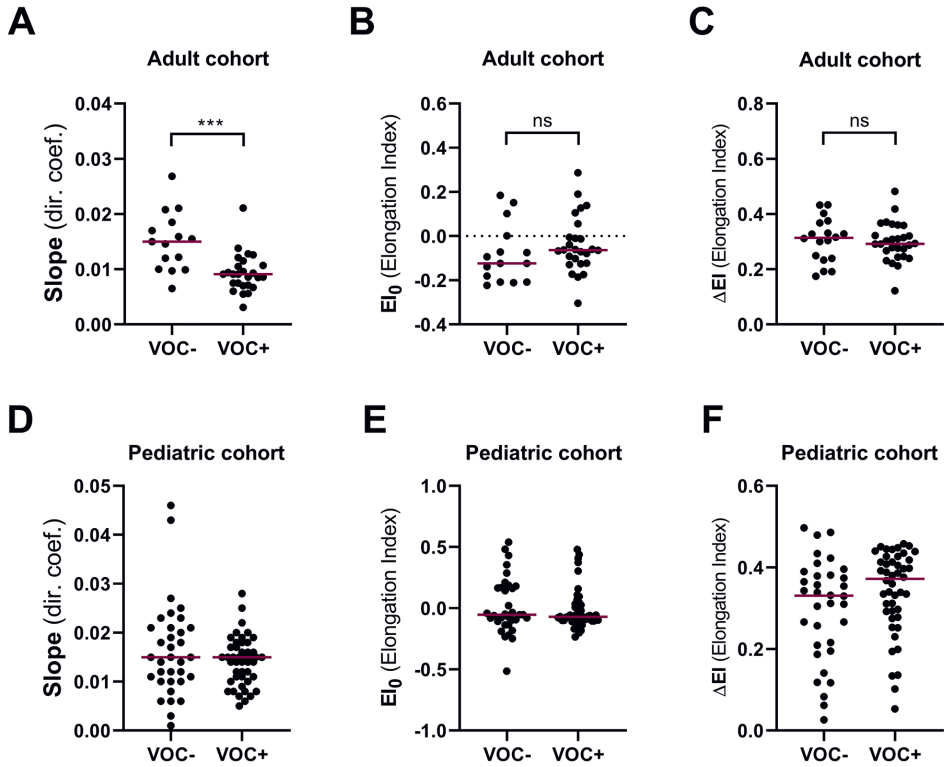
‡p<0.0001, §p<0.001, †p<0.01, *p<0.05.

HbF, fetal haemoglobin; HbS, haemoglobin S; Hb, haemoglobin; ARC, absolute reticulocyte count; MCV, mean corpuscular volume; MCHC, mean corpuscular haemoglobin concentration; RDW, red cell distribution width

Supplemental Table 4. Effect of a single transfusion or chronic transfusion therapy (pediatric cohort) on oxygen gradient ektacytometry-derived biomarkers and laboratory parameters

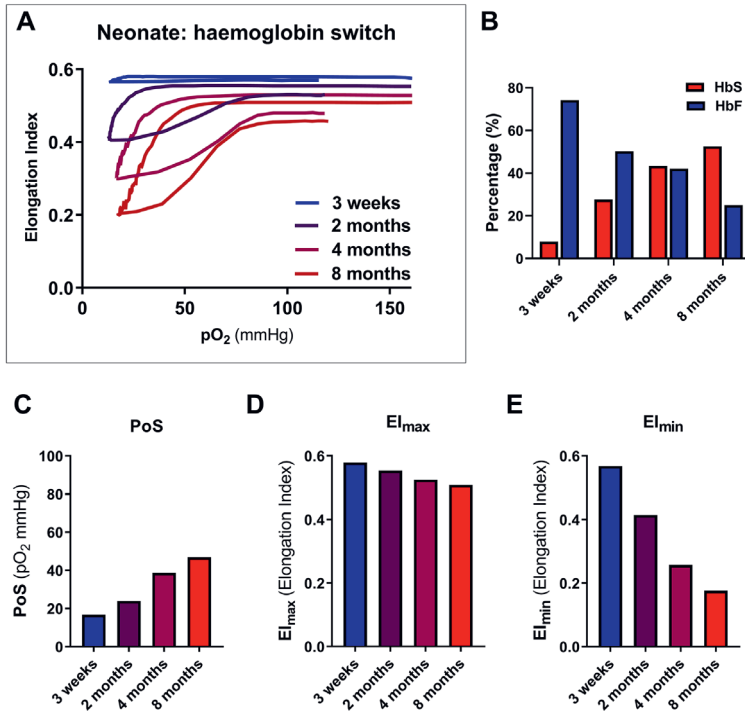
Effects of transfusion	Single transfusion N=7		Chronic transfusion N=21	
	Before (single) transfusion	After (single) transfusion	Before start of chronic transfusion	During chronic transfusion
Oxygen gradient ektacytometry				
PoS (mmHg))	47.3 (38.9-61.3)	42.0 (34.5-50.4)*	43.6 (30.9-64.0)	37.4 (28.8-53.6) [†]
El _{min} (EI)	0.24 (0.04-0.36)	0.33 (0.17-0.39)*	0.08 (-0.02-0.36)	0.21 (0.08-0.36) [§]
El _{max} (EI)	0.48 (0.27-0.58)	0.53 (0.37-0.58)*	0.47 (0.22-0.61)	0.53 (0.39-0.60) [†]
Slope (dir-coef-)	0.009 (0.003-0.011)	0.008 (0.003-0.010)	0.015 (0.007-0.031)	0.015 (0.007-0.021)
El ₀ (EI)	0.11 (-0.11-0.18)	0.22 (0.02-0.23)*	-0.11 (-0.17-0.21)	0.05 (-0.10-0.18) [§]
DeltaEI (EI)	0.24 (0.12-0.29)	0.20 (0.12-0.23)*	0.34 (0.16-0.47)	0.29 (0.20-0.45)
Laboratory parameter				
Dense Cells (%)	3.3 (1.9-10.5)	2.1 (1.9-7.2)*	5.4 (0.7-15.0)	3.5 (1.5-7.3) [†]
HbF (%)	7.7 (1.0-24.7)	4.9 (0.9-18.3)*	20.8 (10.8-41.2)	19.4 (9.0-24.6)
HbS (%)	47.6 (34.1-85.1)	28.8 (24.2-57.4)*	nd	nd
Hb (g/dL)	9.5 (7.1-10.7)	11.4 (9.7-11.8)*	8.5 (5.8-10.8)	8.3 (7.4-11.6)*
ARC (10 ⁹ /L)	228 (147-578)	189 (125-468)*	426 (205-836)	405 (171-935)
MCV (fl)	94.7 (83.7-111.0)	91.2 (86.0-103.0)	95.2 (80.6-107.3)	93.2 (79.3-107.4)*
MCHC (g/dL)	34.8 (34.3-38.4)	34.0 (33.5-36.6)	32.9 (29.4-35.1)	33.0 (29.1-34.7)
Platelet count (10 ⁹ /L)	321 (150-496)	260 (157-427)	388 (233-946)	419 (172-1465)
Neutrophils (10 ⁹ /L)	4.0 (1.4-14.3)	3.8 (1.5-11.7)	4.0 (1.3-8.8)	4.1 (1.8-6.6)

Numbers represent median (range) or state otherwise. HbF, fetal haemoglobin; HbS, haemoglobin S; Hb, haemoglobin; ARC, absolute reticulocyte count; MCV, mean corpuscular volume; MCHC, mean corpuscular haemoglobin concentration; nd, not determined. †p<0.0001, §p<0.001, †p<0.01, *p<0.05.

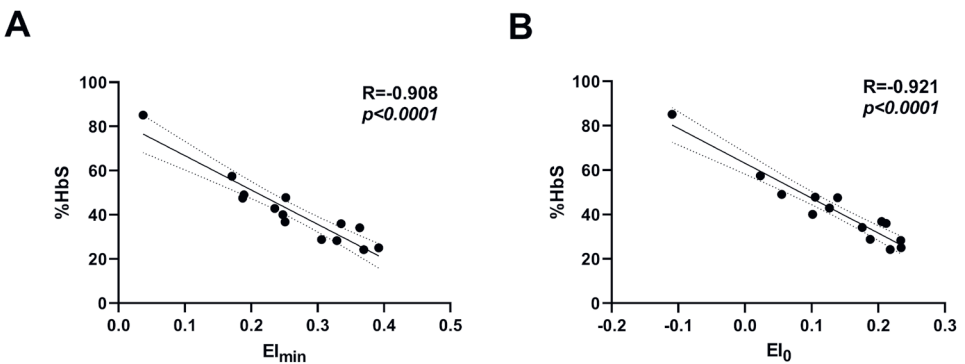


Supplemental Figure 1. Oxygen gradient ektacytometry derived-biomarkers biomarkers are associated with vaso-occlusive crisis

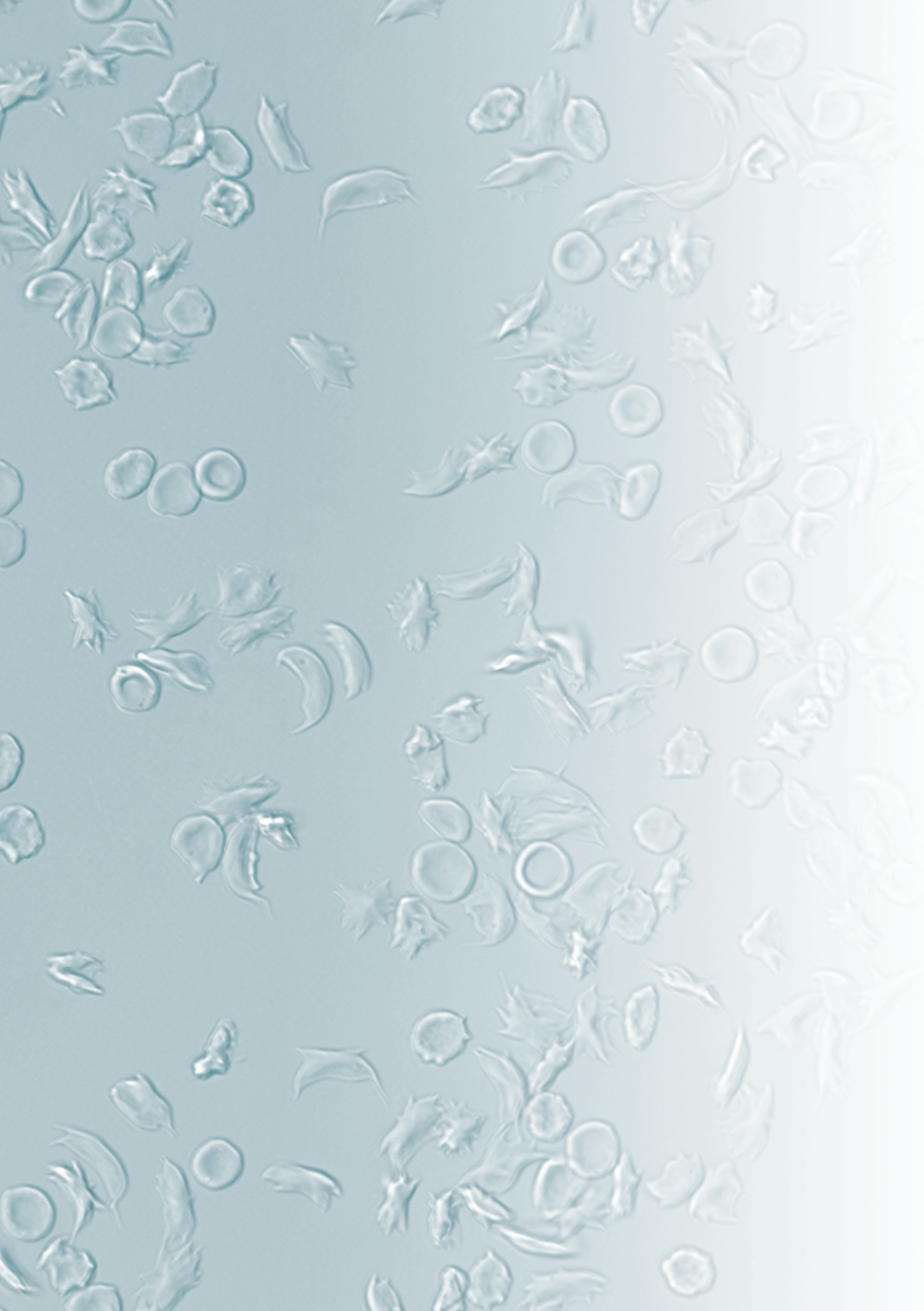
(A) Slope is significantly lower in patients with SCD in the adult cohort who experienced one or more VOC in the past two years. (B) EI_0 is not significantly lower in patients in the adult cohort with VOC compared to those without. (C) ΔEI is not significantly different in patients who did not experience a VOC in the past two years compared to patients who did, in the adult cohort. (D) Slope is not different in patients with SCD in the pediatric cohort who experienced one or more VOC in the past two years. (E) EI_0 is not significantly different in patients in the pediatric cohort with VOC compared to those without. (F) ΔEI is not significantly different in patients who did not experience a VOC in the past two years compared to patients who did, in the pediatric cohort. *** $p < 0.001$



Supplemental Figure 2. The hemoglobin switch in a neonate produces a visible deterioration of the oxygen gradient ektacytometry curve consistent with the development of the SCD phenotype. (A) Representative curve of RBCs of a neonate with HbS/Representative curve of RBCs of a neonate with HbS/ β measured after age of three weeks, two months, four months and eight months. (B) Fetal haemoglobin (%HbF, blue) and %HbS (red) levels during haemoglobin switch. (C) PoS levels gradually increases during haemoglobin switch. (D) EI_{max} gradually decreases during hemoglobin switch. (E) EI_{min} decreases rapidly during hemoglobin switch.



Supplemental Figure 3. Linear correlation of %HbS and EI_{min} in the single transfusion cohort. Seven patients were evaluated just before and immediately after transfusion was given. (A) A linear inverse correlation is observed, as RBCs are less deformable and more sickled when %HbS is given. (B) Linear inverse correlation of HbS levels and EI_0 . Dashed lines represent 95% confidence intervals.



Chapter 6

Oxygen gradient ektacytometry-derived biomarkers are associated with the occurrence of cerebral infarction, acute chest syndrome and vaso-occlusive crisis in sickle cell disease

Submitted

Minke A.E. Rab^{1,2}, Celeste K. Kanne^{3*}, Camille Boisson^{4,5*}, Jennifer Bos¹,
Brigitte A. van Oirschot¹, Maite E. Houwing⁶, Celine Renoux^{4,5,7}, Roger E.G. Schutgens²,
Marije Bartels², Erfan Nur⁸, Marjon H. Cnossen⁶, Philippe Joly^{4,5,7}, Romain Fort⁹,
Philippe Connes^{4,5}, Richard van Wijk¹, Vivien A. Sheehan^{3†} and Eduard J. van Beers^{2†}

¹ Central Diagnostic Laboratory-Research, University Medical Center Utrecht, Utrecht University, Utrecht, The Netherlands

² Van Creveldklinik, University Medical Center Utrecht, Utrecht University, Utrecht, The Netherlands

³ Department of Pediatrics Emory University School of Medicine, Children's Healthcare of Atlanta, Atlanta, Georgia, USA

⁴ Laboratory LIBM EA7424, University of Lyon 1, "Vascular Biology and Red Blood Cell" team, Lyon, France

⁵ Laboratory of Excellence GR-Ex, Paris, France

⁶ Department of Pediatric Hematology, Erasmus University Medical Center, Rotterdam, The Netherlands

⁷ Laboratory of Biochemistry and Molecular Biology, UF Biochemistry of Red Blood Cell diseases, Est Center of Biology and Pathology, Hospices Civils de Lyon, Lyon, France

⁸ Department of Hematology, Amsterdam University Medical Center, The Netherlands

⁹ Department of Internal Medicine, Hospices Civils de Lyon, Lyon, France

**These authors contributed equally*

†These authors contributed equally

Abstract

In the present study we investigated the potential of the Point of Sickling (PoS) determined by oxygen gradient ektacytometry and whole blood viscosity as biomarkers for clinical outcomes in 242 individuals with sickle cell disease (SCD); 53 adults and 189 children.

In the pediatric cohort for every 10 mmHg increase in PoS, the odds ratios (OR) for occurrence of recent (in the last two years) vaso-occlusive crises (VOC) was 1.45 ($p=0.0002$). The ORs of acute chest syndrome (ACS) or any history of cerebral infarction were 1.84 ($p<0.0001$) and 1.77 ($p=0.039$) respectively. After adjusting for age, the aORs were 1.67 ($p=0.002$) and 1.55 ($p=0.144$). In the adult cohort, for every 10 mmHg increase in PoS the OR of recent VOC was 1.95 ($p=0.036$). For any ACS or cerebral infarction the ORs were 1.75 ($p=0.061$) and 3.19 ($p=0.053$), with age adjusted aORs of 1.62 ($p=0.118$) and 3.52 ($p=0.048$) respectively. Viscosity was only studied in pediatric patients and was not associated with any of the above outcomes, but showed an OR of 1.83 for osteonecrosis ($p=0.025$), with an aOR of 1.54 ($p=0.130$) with every 1.0 cP increase in viscosity.

These results show that oxygen gradient ektacytometry is associated with ACS, VOC and cerebral infarction, suggesting that it can be used as a biomarker for clinical severity. This association does not prove causality; validation through longitudinal studies is warranted to establish whether oxygen gradient ektacytometry is able to predict clinical complications, and if improvement in its parameters predict clinical improvement after therapeutic interventions.

Introduction

Sickle cell disease (SCD) is a monogenetic disorder characterized by chronic hemolytic anemia, painful vaso-occlusive crises (VOC) and progressive organ failure. The mutation in the β -globin gene results in the formation of abnormal hemoglobin S (HbS) that polymerizes under deoxygenation leading to red blood cell (RBC) sickling.¹ Sickled RBCs are poorly deformable, and further deteriorate when deoxygenated, causing occlusion of the microvasculature together with a cascade of other factors, leading to painful events and organ damage. Two SCD sub-phenotypes are often described, one marked by high levels of hemolysis and more severe anemia, the other with higher hemoglobin and viscosity, and more vaso-occlusion.² Complications common to the high hemolysis-endothelial dysfunction phenotype are non-hemorrhagic stroke, pulmonary hypertension, priapism and leg ulceration. Complications common to the viscosity-vaso-occlusion phenotype are acute chest syndrome (ACS), VOC and osteonecrosis.^{2,3}

Fetal hemoglobin (HbF) is a known modifier of SCD clinical severity; on a population level, higher HbF levels correlate with fewer complications, although some individuals with HbF>20% still report clinical complications.⁴ Hydroxyurea (HU), as part of standard of care therapy, induces HbF production. HbF levels are often used to monitor treatment response to HU. However, as the ameliorating effects on disease burden are not always associated with increases in HbF levels following HU treatment, there is an unmet need for robust reproducible biomarkers that can assess RBC function and predict disease severity and SCD-related complications. The availability of novel biomarkers will facilitate selection and monitoring of therapy according to the principles of precision medicine. Moreover, the rapidly evolving therapeutic options that are now in development require objective and clinically relevant endpoints for clinical trials.

Biomarkers that capture RBC quality, such as number of irreversible sickled cells and dense RBCs (DRBCs) (%) are not consistently associated with SCD clinical complications like VOC.⁵ Blood viscosity has been found to be associated with the frequency of VOC episodes both in SCD adults and children, which could indicate clinical usefulness of this parameter.^{6,7} However, this biomarker does not change upon HU treatment as the increase in RBC deformability compensates for the rise in hematocrit, resulting in unchanged blood viscosity in patients.⁸ With the development of several new therapies, such as the anti-polymerization agent voxelotor, that reduce hemolysis and subsequently result in increased Hb/hematocrit^{9,10} it would be worthwhile to investigate how viscosity changes. Although *in vitro* experiments show that voxelotor directly decreases viscosity in both oxygenated and deoxygenated conditions when standardized to a fixed hematocrit¹¹, long term effects *in vivo* are still unknown. Besides blood viscosity, RBC deformability is an important factor in blood rheology. Previous studies investigated the use of RBC deformability during normoxic conditions as a marker for complications, and identified decreased deformability in patients with complications that can be attributed to the hemolytic-endothelial dysfunction phenotype.^{12,13} A relatively increased RBC deformability was found in patients with complications that can be attributed to the viscosity-vaso-occlusive phenotype.¹⁴⁻¹⁶ This limits RBC deformability at normoxic conditions for the assessment of overall clinical

severity. Since deoxygenation affects RBC deformability both *in vivo* and *in vitro* it seems reasonable to assume that RBC deformability under lower oxygen conditions might be a more informative and useful biomarker.

We previously reported that oxygen gradient ektacytometry, a next generation deformability and sickling assay, measures RBC deformability over a gradient of oxygen tensions (pO_2) generating the key parameter Point of Sickling (PoS) that reflects the patient-specific pO_2 at which polymers start to grow and sickling begins.¹⁷ Oxygen gradient ektacytometry-derived biomarkers improve with standard of care therapies HU and blood transfusion, and is associated with VOC.¹⁸ In the current study, we further establish the clinical validation of oxygen gradient ektacytometry by investigating the association of its parameters with several clinical complications. Furthermore, we examined whole blood viscosity as a complementary biomarker in pediatric individuals with SCD.

Methods

Subjects

A total of 242 individuals with SCD were included in this multicenter study. We analyzed two cohorts of SCD patients; an adult cohort of 53 individuals with SCD, enrolled at either University Medical Center Utrecht, The Netherlands (UMCU, $n=25$) or Hospital Lyon France (LIBM, $n=28$), and a pediatric cohort of 189 individuals with SCD enrolled at Texas Children's Hospital, USA (TCH). The adult and pediatric cohorts were analyzed separately as the pathophysiology of SCD complications might change with increasing age^{19,20}, and differences in RBC deformability between adults and young children have been reported.²¹

Subjects were genotyped as sickle cell anemia (HbSS or HbS/ β^0 -thalassemia) or HbS/ β^+ -thalassemia and analyzed as one population. A substantial number of subjects were on HU therapy (64.2% of adults and 85.2% of children with SCD). Subjects that received a blood transfusion less than three months prior to measurements were excluded from the study. Measurements were performed at steady state, and all subjects on HU had been on a consistent dose for at least one year.

To investigate how oxygen gradient ektacytometry-derived parameters correlate with clinical complications, the two cohorts were divided into four quartiles based on PoS values. Clinical complications included ACS, VOC, cerebral infarction (stroke or silent infarcts), osteonecrosis, retinopathy, priapism, gallstones and iron overload. VOC was predefined as a painful VOC recognized as such by the patient in the last 2 years that required hospital admission or visit to the emergency room or outpatient clinic. Occurrence of a major complication included any history of ACS and cerebral infarction and/or VOC in the past 2 years. Complication rate was defined by calculating the sum of complications that had occurred in the past within the lifetime of the individual, with the exception of VOC that was only evaluated as it occurred within the last two years.

Conventional hematologic laboratory parameters, blood viscosity and clinical complications derived from the quartile with the lowest PoS levels (1st quartile) were compared to the other quartiles. In addition, the pediatric cohort was divided into four quartiles based on

blood viscosity (measured at a shear rate of 45 s^{-1}) in order to study the relationship between viscosity and clinical complications.

Hematological laboratory parameters

Laboratory parameters, including complete blood count, absolute reticulocyte count (ARC), and HbF levels (by HPLC), were obtained at each site's clinical laboratory during routine visits to the outpatient clinic. Percentage of dense RBCs (%DRBCs), defined as RBCs with hemoglobin $>41 \text{ g/dL}$ and mean corpuscular volume (MCV) $<120 \text{ fL}$, were measured with an ADVIA 120/2120 hematology analyzer (Siemens, Healthcare GmbH, Erlangen, Germany).

Oxygen gradient ektacytometry

Oxygen gradient ektacytometry, a next generation deformability and sickling assay, measures RBC deformability over a gradient of oxygen tensions (pO_2) with an ektacytometer. Oxygen gradient ektacytometry generates three key parameters: 1) EI_{max} , RBC deformability at normoxia, before the deoxygenation cycle is initiated; 2) EI_{min} , minimum RBC deformability upon deoxygenation; and 3) the Point of Sickling (PoS): the oxygen tension at which a 5% decrease in deformability is observed during deoxygenation, reflecting the patient-specific pO_2 at which polymers start to grow and sickling begins (Figure 1A).¹⁷ Oxygen gradient ektacytometry was carried out with the Laser Optical Rotational Red Cell Analyzer (Lorrca, RR Mechatronics, Zwaag, The Netherlands) as described elsewhere.^{17,22,23} The oxygenscan module is a new add-on feature of the ektacytometer, allowing the measurement of RBC deformability during a continuously changing gradient of pO_2 . To carry out an oxygen gradient ektacytometry measurement, $50 \mu\text{L}$ of whole blood, standardized to a fixed RBC count of 200×10^6 , is mixed with 5 mL Oxy-Iso (RR Mechatronics, osmolarity 282-286 mOsm/kg, pH 7.35-7.45, viscosity 27-32 cP at room temperature $21 \pm 1^\circ\text{C}$). Detailed description of the technique and sample handling is described elsewhere.^{22,23} Samples were measured at one of the three different sites which were located in The Netherlands (Utrecht), France (Lyon) and US (Houston).

Blood viscosity

Whole blood viscosity was measured at a native hematocrit, at 37°C at a shear rate of 45 s^{-1} and 225 s^{-1} using a Brookfield DVT cone and plate viscometer (Brookfield, Massachusetts) as previously described.²⁴

Statistical Analysis

We performed a one-way ANOVA with post-hoc Dunnett's analysis to compare the 1st quartile with the other quartiles. Logistic regression analysis was performed within the four quartiles with the 1st quartile as the reference quartile. If the regression-coefficient increased in a linear manner when assessing a specific complication, a logistic regression analysis was performed for PoS and blood viscosity to calculate odds ratios (OR) for every 10 mmHg increase in PoS and every 1.0 cP increase in viscosity for that complication. ORs were corrected for age, gender and genotype if indicated. ORs were not corrected for age when association between occurrence of VOC and PoS/blood viscosity was analyzed. GraphPad Prism (version 8.3) or SPSS (version 25.0.0.2 IBM) were used in the statistical analysis. A p-value <0.05 was considered statistically significant.

Results

To explore how PoS, the key parameter of oxygen gradient ektacytometry, relates to risk of clinical complications, we analyzed quartiles of patients with different PoS values. Patient demographics of the quartiles based on PoS levels of both adult and pediatric cohorts are depicted in Table 1. In the adult cohort percentage of females was higher in the 1st quartile (lowest PoS values) compared to the 4th quartile (highest PoS values). The same was observed for HU treatment, with 85% HU treatment in the 1st quartile compared to 31% in the 4th quartile. In both cohorts, percentage of patients with the genotype HbS/ β^+ -thalassemia was highest in the 1st quartile.

Oxygen gradient ektacytometry-derived biomarkers El_{max} and El_{min} were associated with PoS values in all quartiles, i.e., both biomarkers were lower when the individual had a higher PoS, as expected, given the interrelated nature of the biomarkers. In both cohorts lower HbF and higher ARC were found in individuals with higher PoS, indicative of an association between these laboratory parameters and PoS. In the pediatric cohort, lower Hb and hematocrit were associated with higher %DRBCs, mean corpuscular volume (MCV) and PoS.

Both ACS and VOC were more prevalent in adults with higher PoS values, with a lifetime history of ACS of 8% in the 1st quartile compared to 54% in the 4th ($p=0.023$), and 46% vs 85% for VOC (during past two years) although this was not statistically significant due to low numbers ($p=0.11$). Similar results were observed in the pediatric cohort, with 36% ACS+ in the 1st quartile compared to 75% in the 4th quartile ($p=0.0005$). Similarly, 35% of 1st quartile children were VOC+ compared to 62% in the 4th quartile ($p=0.026$). There also was a higher occurrence of cerebral infarction in children in the 4th quartile compared to the 1st quartile ($p=0.054$). Altogether, these results indicate that the higher PoS values in the 4th quartile are associated with higher prevalence of ACS, cerebral infarction and VOC. The relationship between osteonecrosis incidence and rheological biomarkers tested was unclear, occurring more frequently in adults with a lower PoS, but less frequently in 1st quartile of the pediatric cohort. While the occurrence of priapism was higher in adult patients with a higher PoS (4th quartile), this could not be confirmed in the pediatric cohort, likely because of small numbers of subjects affected by priapism.

Importantly, total complication rate in the 4th quartile group was higher as compared to the 1st quartile in the pediatric cohort, 2.3 vs 1.1 ($p=0.0003$) indicating that higher PoS values are associated with the occurrence of several complications within an individual patient. Lower PoS values were associated with a milder clinical course as expressed by higher percentages of patients without any complication in the 1st quartiles compared to the 4th quartile ($p=0.002$ in pediatric cohort, Table 1).

To investigate how oxygen gradient ektacytometry results relate to the rheological biomarker blood viscosity, we divided the pediatric cohort into quartiles based on viscosity levels (Supplemental Table 1, lowest viscosity values in the 1st quartile, highest viscosity values in the 4th quartile). Older age and the HbS/ β -thalassemia genotype both seemed to be associated with higher blood viscosity. The oxygen gradient ektacytometry-derived biomarker El_{max} was lower in the 1st quartile, whereas El_{min} and PoS did not differ between

Table 1. Demographic, laboratory and clinical characteristics of adult and pediatric individuals with SCD divided into 4 quartiles based on Point of Sickling (PoS) values.

	Adult cohort				Pediatric cohort			
	Quartiles based on PoS				Quartiles based on PoS			
Patient demographics	1 st q n = 13	2 nd q n = 13	3 rd q n = 14	4 th q n = 13	1 st q n = 47	2 nd q n = 47	3 rd q n = 48	4 th q n = 47
Age (years)	31 ± 13	30 ± 9	33 ± 12	26 ± 8	7.8 ± 5.3	9.0 ± 4.5	10.5 ± 5.0*	11.3 ± 4.8†
Sex, female	62% (8/13)	38% (5/13)	43% (6/14)	31% (4/13)	45% (21/47)	49% (23/47)	44% (21/48)	38% (18/47)
HU therapy	85% (11/13)	69% (9/13)	71% (10/14)	31% (4/13)*	72% (34/47)	87% (41/47)	92% (44/48)*	89% (42/47)
HbS/β ⁰ -thal	23% (3/13)	8% (1/13)	7% (1/14)	0% (0/13)	15% (7/47)	4% (2/47)	0% (0/48)†	0% (0/47)†
α-thal: 1 deletion ^a	22% (2/9)	25% (3/12)	8% (1/12)	15% (2/13)	n/a	n/a	n/a	n/a
2 deletions ^a	11% (1/9)	33% (4/12)	8% (1/12)	8% (1/13)	n/a	n/a	n/a	n/a
Splenectomy	46% (6/13)	23% (3/13)	14% (2/14)	8% (1/13)	17% (8/47)	21% (10/47)	13% (6/48)	26% (12/47)
Oxygen gradient ektacytometry								
PoS (mmHg)	36.4 ± 4.5	44.3 ± 1.7*	50.9 ± 2.8*	64.2 ± 6.6†	25.1 ± 4.1	34.5 ± 2.5†	41.1 ± 2.0†	50.5 ± 5.1†
EI _{max} (EI)	0.51 ± 0.03	0.48 ± 0.05	0.42 ± 0.08†	0.37 ± 0.07†	0.55 ± 0.04	0.53 ± 0.05	0.48 ± 0.08*	0.39 ± 0.08*
EI _{min} (EI)	0.27 ± 0.10	0.16 ± 0.05 [§]	0.11 ± 0.05 [‡]	0.05 ± 0.03 [‡]	0.24 ± 0.1	0.17 ± 0.05 [‡]	0.11 ± 0.06 [‡]	0.05 ± 0.05 [‡]
Laboratory parameters								
HbF (%) ^b	18.9 ± 12.8	13.5 ± 10.1	12.9 ± 9.6	7.0 ± 6.1*	20.0 ± 9.9	19.7 ± 5.8	15.7 ± 4.9	8.1 ± 4.0*
Hb (g/dL)	8.8 ± 1.6	9.5 ± 1.2	9.2 ± 1.1	8.9 ± 1.0	9.9 ± 1.2	9.2 ± 1.2*	8.7 ± 1.4†	7.9 ± 1.6†
HCT (%)	27.3 ± 5.5	27.5 ± 3.0	26.0 ± 3.8	25.6 ± 2.8	30.0 ± 3.3	28.1 ± 3.3*	26.5 ± 3.7†	24.3 ± 3.4†
ARC (10 ⁹ /L)	182 ± 97	161 ± 73	231 ± 73	289 ± 108*	320 ± 159	345 ± 124	412 ± 152†	475 ± 141†
MCV (fl)	88 ± 22	83 ± 15	90 ± 22	86 ± 10	88 ± 14	94 ± 14	96 ± 14†	95 ± 11*
MCHC (g/dL)	32.6 ± 4.2	34.6 ± 1.5	35.0 ± 1.1*	34.8 ± 1.1*	32.9 ± 1.5	32.8 ± 1.0	32.7 ± 1.6	32.6 ± 0.9
DRBC (%)	n/a	n/a	n/a	n/a	2.6 ± 2.0	3.5 ± 1.9	4.8 ± 2.3*	8.1 ± 3.5*
Blood viscosity (45/s) ^c	n/a	n/a	n/a	n/a	5.2 ± 1.0	5.2 ± 0.9	5.0 ± 1.1	4.5 ± 1.2
Blood viscosity (225/s) ^c	n/a	n/a	n/a	n/a	3.6 ± 0.5	3.5 ± 0.6	3.5 ± 0.7	3.2 ± 0.8

Table 1. Continued

	Adult cohort				Pediatric cohort			
	Quartiles based on PoS				Quartiles based on PoS			
Laboratory parameters								
HVR (HCT/BV 45/s) ^f	n/a	n/a	n/a	n/a	6.0 ± 0.7	5.6 ± 0.9	5.4 ± 0.9*	5.6 ± 1.0
TCD Left MCA (cm/s) ^d	n/a	n/a	n/a	n/a	124 ± 22	125 ± 27	142 ± 25*	139 ± 26*
TCD Right MCA (cm/s) ^e	n/a	n/a	n/a	n/a	120 ± 22	121 ± 24	137 ± 20*	136 ± 33
Clinical complications								
ACS	8% (1/13)	23% (3/13)	21% (3/14)	54% (7/13)*	36% (17/47)	47% (22/47)	56% (27/48)	75% (35/47) ^g
VOC	46% (6/13)	62% (8/13)	64% (9/14)	85% (11/13)	35% (16/46)	44% (20/45)	51% (23/45)	62% (29/47)*
Cerebral infarction	0% (0/13)	0% (0/13)	7% (1/14)	15% (2/13)	6% (3/47)	2% (1/47)	4% (2/48)	19% (9/47)
Osteonecrosis	46% (6/13)	36% (4/11)	29% (4/14)	15% (2/13)	4% (2/47)	6% (3/47)	8% (4/48)	11% (5/47)
Retinopathy	31% (4/13)	55% (6/11)	7% (1/14)	15% (2/13)	6% (3/47)	6% (3/47)	4% (2/48)	4% (2/47)
Priapism (% of males)	0% (0/5)	13% (1/8)	25% (2/8)	22% (2/9)	12% (3/26)	17% (4/24)	15% (4/27)	17% (5/29)
Gallstones	31% (4/13)	45% (5/11)	62% (8/13)	38% (5/13)	17% (8/47)	13% (6/47)	19% (9/47)	30% (14/47)
Iron overload	n/a	n/a	n/a	n/a	2% (1/47)	6% (3/47)	15% (7/48)	13% (6/47)
Nr. of complications	1.7 ± 1.3	2.2 ± 1.4	2.0 ± 1.2	2.4 ± 1.4	1.2 ± 1.4	1.3 ± 1.5	1.7 ± 1.3	2.3 ± 1.5 ^h
≥1 major complication*	46% (6/13)	69% (9/13)	64% (9/14)	92% (9/13)*	54% (25/46)	67% (30/45)	74% (34/46)	87% (41/47) ⁱ
≥1 any complication	85% (11/13)	100% (12/12)	93% (13/14)	92% (12/13)	57% (25/46)	71% (32/45)	78% (35/45)*	87% (41/47) ⁱ

The 1st quartile consist of individuals with lowest PoS values, while the 4th quartile is comprised of individuals with highest PoS values. Numbers are depicted as mean ± standard deviation or stated otherwise. The 1st quartile is compared to the other quartiles. †p<0.001, ‡p<0.001, §p<0.001, ¶p<0.01, *p<0.05. HU, hydroxyurea; β-thal, β-thalassemia; n/a, not addressed; Elmax, maximum deformability; Elmin, minimum deformability; HbF, fetal hemoglobin; Hb, hemoglobin; HCT, hematocrit; ARC, absolute reticulocyte count; MCV, mean corpuscular volume; MCHC, mean corpuscular hemoglobin concentration; DRBC, dense RBC; HVR, hematocrit to viscosity ratio; TCD, trans cranial Doppler; MCA, media cerebral artery; ACS, acute chest syndrome; VOC, vaso-occlusive crisis; Nr., number. ^aData of 46 individuals available. ^bIn pediatric cohort data of 70 individuals available. ^cData of 120 individuals available. ^dData of 113 individuals available. ^eData of 115 individuals available. ^fACS, VOC or cerebral infarction

quartiles. As expected Hb levels and hematocrit were significantly lower, while ARC and %DRBC were higher in the 1st quartile, indicating that higher viscosity was accompanied by less hemolysis and presumably low occurrence of complications associated with the hemolysis endothelial dysfunction phenotype. This was confirmed by a decrease in TCD values at higher viscosity levels. ACS occurred more often in SCD patients with low viscosity (63% in the 1st quartile compared to 40% in the 4th quartile) which could be in part due to a higher percentage of HbS/ β^+ -thalassemia patients who generally have less severe anemia and less complications. In contrast, occurrence of VOC (32% vs 53%) and osteonecrosis (0% vs 20%, $p=0.014$) increased with higher viscosity values. The rate of patients with priapism also tended to increase in patients with a higher viscosity (9% in the 1st quartile compared to 35% in the 4th quartile), but not significant, presumably due to low sample size ($p=0.073$). However, complication rate and percentage of SCD individuals that did not experience any complication were not different between the 4 quartiles based on viscosity (Supplemental Table 1).

Odds ratios of PoS with clinical complications

To assess the risk of the development of a specific complication in the past, based on PoS values, we calculated odds ratios (OR) between the different quartiles (Supplemental Table 2). In the pediatric cohort ORs increased for ACS, VOC, cerebral infarction and iron overload, although the latter two complications did not reach statistical significance. In the adult cohort, risk of occurrence (positive history) of ACS and VOC was increased. Odds ratio of occurrence of ≥ 1 major complication (ACS, VOC or cerebral infarction) and of any complication in the 4th quartile were significantly higher in the pediatric cohort (OR 4.92, $p=0.002$ and OR 4.51, $p=0.003$ respectively, with the 1st quartile as the reference, but not in the adult cohort.

To further explore how these findings would relate to treatment modification of HU on PoS, i.e. how much PoS changes upon HU treatment¹⁸, we calculated ORs and adjusted ORs (aOR) for every 10 mmHg increase in PoS in the pediatric and adult cohort (Table 2). ORs were not significantly affected by sex or genotype, but age did significantly confound results and therefore adjusted ORs (aOR) were calculated. Associations were found between lifetime occurrence of ACS and PoS in both cohorts (pediatric cohort OR 1.84, $p<0.0001$; aOR 1.67, $p=0.002$; adult cohort: OR 1.75, $p=0.061$; aOR 1.62, $p=0.118$). Associations were also found with cerebral infarction (pediatric cohort: OR 1.77, $p=0.039$; aOR 1.55, $p=0.144$; adult cohort: OR 3.19, $p=0.053$; aOR 3.52, $p=0.048$) higher with every 10 mmHg PoS increase. We found a significant association for VOC in both cohorts (pediatric cohort: OR 1.45, $p=0.015$; adult cohort: OR 1.95, $p=0.036$) that was not adjusted for age since this analysis focused on the history of VOC in the past two years.

More importantly, the OR of the occurrence (positive history) of a major SCD complication (ACS, cerebral infarction or VOC) was even greater (pediatric cohort: OR 1.92, $p<0.0001$; aOR 1.67, $p=0.007$; adult cohort: OR 2.03, $p=0.034$; aOR 1.95, $p=0.069$), further supporting the hypothesis that PoS is associated with a more severe phenotype. Moreover, when occurrence of 1 or more complications (ACS, VOC, cerebral infarction, osteonecrosis, retinopathy, priapism, gallstones or iron overload) was assessed, an increased OR was found with every 10 mmHg increase in PoS (OR 1.95, $p=0.0002$, aOR 1.65, $p=0.012$) in the pediatric cohort (Table 2).

Table 2. Logistic regression analysis of PoS shows increased odds ratios for specific complications

PoS		Pediatric cohort					
<i>for every 10 mmHg increase</i>		Odds ratio			Adjusted odds ratio		
Complication	OR	95% CI	P-value	OR	95% CI	P-value	
ACS	1.84	1.35 – 2.52	<0.0001	1.67	1.19 – 2.32	0.002	
VOC	1.45	1.08 – 1.94	0.015	-	-	-	
Cerebral infarction	1.77	1.02 – 3.06	0.039	1.55	0.59 – 2.56	0.144	
Osteonecrosis	1.48	0.86 – 2.56	0.166	1.23	0.67 – 2.26	0.496	
Gallstones	1.49	1.03 – 2.16	0.036	1.23	0.80 – 1.90	0.331	
≥1 major complication*	1.92	1.35 – 2.73	<0.0001	1.67	1.15 – 2.42	0.007	
≥1 any complication	1.93	1.33 – 2.81	0.000	1.65	1.11 – 2.44	0.012	

PoS		Adult cohort					
<i>for every 10 mmHg increase</i>		Odds ratio			Adjusted odds ratio		
Complication	OR	95% CI	P-value	OR	95% CI	P-value	
ACS	1.75	0.97 – 3.15	0.061	1.62	0.88 – 2.97	0.118	
VOC	1.95	1.04 – 3.66	0.036	-	-	-	
Cerebral infarction	3.19	0.98 – 10.4	0.053	3.52	1.01 – 12.4	0.048	
Osteonecrosis	0.62	0.34 – 1.14	0.117	0.63	0.34 – 1.16	0.136	
≥1 major complication*	2.03	1.04 – 3.96	0.034	1.95	0.95 – 4.04	0.069	

Odds ratios (OR) and adjusted ORs were calculated for every 10 mmHg increase in PoS (n= 53 in the adult cohort and n=189 in the pediatric cohort) in individuals with SCD.

CI, confidence interval; ACS, acute chest syndrome; VOC, vaso-occlusive crisis;

*ACS, VOC or cerebral infarction

Odds ratios of blood viscosity and clinical complications

To explore how blood viscosity relates to the occurrence of clinical complications ORs were calculated between the different quartiles in the pediatric cohort (Supplemental Table 3). OR of priapism was higher in individuals with increased blood viscosity (4th quartile) compared to the 1st quartile, while the OR of ACS was lower in 4th quartile with the 1st quartile as reference. OR of osteonecrosis was also increased but not statistically significant. More importantly, when ORs for every 1 cP higher blood viscosity were assessed we found an OR of 1.83 (p=0.025) and an aOR 1.54 (p=0.130) for osteonecrosis (Table 3). Surprisingly, we did not find a significant risk for ACS or VOC with higher viscosity, whereas we did find a trend through higher risk for priapism (OR 1.54, p=0.091; aOR 1.40, p=0.224) although not significant (Table 3). A lower OR of 0.38 (p=0.022), with an aOR of 0.34 (p=0.011) was found for iron overload with increasing viscosity, which confirms that reduced hemolysis is accompanied with a rise in Hb and hematocrit and subsequently blood viscosity, and presumably a reduced need for transfusion.

Intra patient variability of PoS

To investigate how variable an individual's PoS levels were when measured longitudinally, we analyzed PoS values of 11 adults with SCD two or three times at routine visits during a

Table 3. Logistic regression analysis of viscosity shows increased odds ratios for specific complications.

Viscosity		Pediatric cohort					
for every 1 cP increase		Odds ratio			Adjusted odds ratio		
Complication	OR	95% CI	P-value	OR	95% CI	P-value	
ACS	0.79	0.56 – 1.10	0.156	0.72	0.51 – 1.03	0.072	
Osteonecrosis	1.83	1.08 – 3.11	0.025	1.54	0.88 – 2.67	0.130	
Priapism	1.54	0.93 – 2.56	0.091	1.40	0.81 – 2.41	0.224	
Iron overload	0.38	0.16 – 0.87	0.022	0.34	0.15 – 0.78	0.011	

Odds ratios (OR) and adjusted ORs were calculated for every 1.0 cP increase in whole blood viscosity (n=120) in pediatric individuals with SCD.

CI, confidence interval; ACS, acute chest syndrome;

1-2 year follow-up. Coefficient of variance (CV) of 6 adults without therapy and 5 adults on HU showed mean CVs of 5.1% (SD 6.9%) and 7.8% (SD 6.0%) respectively (Supplemental Table 4). These results indicate that although there is some variability, this seems to be within accepted limits for laboratory parameters.

Discussion

In this study, we report on the association of the oxygen gradient ektacytometry-derived biomarkers PoS, with important SCD-related complications such as ACS, VOC and cerebral infarction in pediatric and adult cohorts of SCD patients (Table 1). Significant higher ORs for ACS, cerebral infarction and VOC with every 10 mmHg increment in PoS were found in both cohorts (Table 2). The higher complication rate in patients with highest PoS values in both cohorts suggests a correlation between sickling at higher pO₂ and clinical complications. Oxygen gradient ektacytometry is a technique that comprehensively assesses RBC function and sickling behavior, and many factors that contribute to it. Some of these factors are easily measured, like HbF or HbS levels, while others, such as 2,3-diphosphoglycerate (2,3-DPG) and ATP levels, and oxidative stress are more challenging and time consuming.¹⁷

Red cell sickling and blood viscosity are both associated with complications attributed to the hemolytic-endothelial dysfunction and viscosity-vaso-occlusion phenotypes

Numerous studies have focused on identifying biomarkers that can predict acute and chronic complications or clinical severity; however, this goal remains a challenge, and there are no clinically validated biomarkers of global RBC function. The introduction of 2 distinct sub-phenotypes, i.e. the high hemolysis-endothelial dysfunction phenotype and the high viscosity-vaso-occlusion phenotype provides some direction in which biomarker could assess different complications. In this model cerebral vasculopathy, ischemic stroke, clinically silent infarction, pulmonary hypertension, priapism, leg ulcers and glomerulopathy are all attributed to the detrimental effects of severe chronic hemolysis on the endothelium.^{2,3,25}

Moreover, ACS, VOC and osteonecrosis are thought to be associated with increased blood viscosity and thereby attributed to the viscosity-vaso-occlusion phenotype.^{2,3} Our results are in accordance to this model when regarding the association of VOC and osteonecrosis with blood viscosity (Supplemental Table 1 and Supplemental Table 3). In contrast to this model, we found an increased occurrence of ACS in sub cohorts of patients with low blood viscosity compared to patients with high viscosity, although this could be in part be explained by inclusion of the few HbS/β+-thalassemia patients, that are generally less anemic and have fewer complications. Furthermore, priapism occurred more often (35% in 4th vs 9% in the 1st quartile) in SCD patients with high viscosity (Supplemental Table 1), which is in contrast to a previous study that found no differences in blood viscosity between patients with and without priapism.²⁶

Red cell sickling, measured with oxygen gradient ektacytometry, was associated with complications that are ranked under both hemolytic phenotype and viscosity-vaso-occlusion phenotype. This is in contrast to the proposed model where red cell sickling was thought to be pre-dominantly present in the viscosity-vaso-occlusion phenotype.² However, the two sub-phenotypes do overlap and are not completely distinct from each other.³

Differences between cohorts

We observed differences in occurrence of complications between the adult and pediatric cohorts. These findings, and observed differences in PoS (Table 1), between cohorts could be due to differences in pediatric and adult SCD pathophysiology. Although studies investigating the effect of age on clinical symptoms and signs are scarce, with age, SCD symptoms generally worsen, particularly in the transition period between adolescence and adulthood.^{19,20} This is partly due to differences in treatment, access to care (US) and differences in guidelines and clinical practice between adult and pediatric providers.^{27,28} In our study, fewer adults were on HU compared to the pediatric cohort (64.2% versus 85.2%). Regarding differences found in occurrence of clinical complications, the adult cohort was substantially smaller, making associations between biomarkers and relatively rare complications difficult to detect. Environmental factors such as climate²⁹ could also result in differences between the adult and pediatric cohort; the adult cohort is located in Europe, the pediatric in Houston, Texas. In addition, RBC rheological characteristics, and notably RBC deformability, has been found to be different between adults and young children.²¹

Emerging treatments and the need for clinically relevant biomarkers

In an era where therapeutic options are rapidly expanding, with several new drugs that do not target HbF induction, but rather aim to improve the quality or functionality of the RBC through other means, new tests and biomarker(s) must be clinically validated for use in monitoring SCD patients. For the last decade HbF, Hb, MCV and reticulocyte count have been the laboratory tools of clinicians to assess the individual's response to standard of care treatment HU and transfusion. However, voxelotor⁹, L-glutamine³⁰ and crizanlizumab³¹ are recently FDA approved therapies that target other aspects of SCD pathophysiology than HbF induction. Several other agents, e.g. pyruvate kinase activators, are currently in clinical trials on the North American continent and in Europe. Pyruvate kinase activators decrease

2,3-DPG levels, thereby increasing oxygen affinity and subsequently reducing sickling tendency (Rab et al, Blood 2021 accepted for publication).^{32,33}

Biomarkers that reflect RBC characteristics and more importantly, RBC cell function, like those provided by oxygen gradient ektacytometry, are excellent ways to assess curative therapy outcomes. The amount of HbF induction needed to be gained by gene therapy to abrogate the SCD phenotype is still a topic for discussion. In most clinical trials there is no assay included that measures RBC function, as microscopy based sickling assays are static and do not report the individual patients sickling behavior.^{34,35} VOC remains to be the primary endpoint in ongoing gene therapy trials, however absence of VOC does not necessarily mean the patient is cured, as organ damage may still be ongoing. Oxygen gradient ektacytometry-derived biomarkers provide information about RBC function beyond that of standard laboratory values such as HbF and HbS levels, MCV, reticulocyte count, and markers of hemolysis. Biomarkers like PoS and blood viscosity are needed to assess which treatment and possibly which combination of drugs is suited for the individual patient with SCD, according to the principle of precision medicine. It is reasonable to assume that certain drugs might work synergistic and patients could benefit from that. However, no patient with SCD is the same in terms of phenotype, which warrants an extended RBC characterization including sickling behavior and evaluation of other factors that contribute to pathophysiology of SCD. Ideally a single biomarker provides the clinician information on clinical severity and response to a certain therapy. However, regarding the highly complex pathophysiology of SCD it seems reasonable to assume that more than one biomarker is needed to reflect all aspects contributing to disease pathology.

Conclusion

Oxygen gradient ektacytometry provides clinically relevant next generation biomarkers that assess RBC function. We show that these biomarkers are associated with a history of ACS, cerebral infarction and VOC in individuals with SCD. This study therefore further validates the clinical usefulness of these biomarkers, particularly in relation to cerebral vasculopathy. Since our results merely describe an association and not causality, further validation is warranted to establish how well oxygen gradient ektacytometry can assess disease severity, and how well therapeutic modification of these values correlates with clinical improvement. However, its parameters can provide the clinician with information about patient RBC characteristics and sickling propensity that may aid in clinical decision making. Our results provide a rationale for further development of these biomarkers in the evaluation of novel therapies as part of clinical care, or clinical trial endpoints.

Acknowledgements

The authors would like to thank all patients that donated blood for this study. The authors also thank the technicians of the Central Diagnostic Laboratory, Specialized Hematology, University Medical Center Utrecht. The authors also thank the clinical research coordinators of the department of Pediatric Hematology at the Erasmus University Medical Center Rotterdam and the department of Hematology at the Amsterdam University Medical Centers. This work has been funded in part by Eurostars grant estar18105 and by an unrestricted grant provided by RR Mechatronics. This work is also funded in part by a K08 grant from the National Institute of Diabetes and Digestive and Kidney Diseases, and provided with support from the Department of Pediatrics, Baylor College of Medicine.

Authorship

Contribution: M.A.E.R., R.vW., V.A.S., and E.J.vB. designed the study; M.A.E.R., C.K.K., M.E.H., C.R., P.J., M.B., E.N., R.F., M.H.C., V.A.S., and E.J.vB. collected clinical and laboratory data. M.A.E.R., C.K.K., J.B., B.A.vO., E.T. and C.B. performed laboratory experiments. M.A.E.R., R.vW., P.C., V.A.S., and E.J.vB. analyzed the data and wrote the manuscript. All authors edited the manuscript and approved the final version.

Conflict-of-interest disclosure

M.A.E.R. and J.B. received grant funding from RR Mechatronics. R.vW. received grant funding from Agios Pharmaceuticals Inc and RR Mechatronics. M.H.C. received grant funding from Takeda, Shire, Baxter, Bayer, Sobi, CSL Behring, Nordic Pharma, Novo Nordisk and Pfizer. M.H. Cossen has received investigator-initiated research and travel grants over the years from The Netherlands Organisation for Scientific Research (NWO)- the Netherlands Organization for Health Research and Development (ZonMw), the Dutch "Innovatiefonds Zorgverzekeraars", Pfizer, Baxter/Baxalta/Shire, Bayer Schering Pharma, CSL Behring, Sobi Biogen, Novo Nordisk, Novartis and Nordic Pharma, and has served as a steering board member for Roche and Bayer. All grants, awards and fees go to the institution. V.A.S. received grant funding from NHLBI's Cure SCD Initiative, Global Blood Therapeutics, Beam Therapeutics, Emmaus, and Novartis for investigator-initiated research projects. E.J.vB. received grant funding Agios Pharmaceuticals Inc, RR Mechatronics, Novartis and Pfizer for investigator initiated research projects.

References

1. Kato GJ, Piel FB, Reid CD, et al. Sickle cell disease. *Nat Rev Dis Prim*. 2018;4:1-22.
2. Kato GJ, Gladwin MT, Steinberg MH. Deconstructing sickle cell disease: Reappraisal of the role of hemolysis in the development of clinical subphenotypes. *Blood Rev*. 2007;21(1):37-47.
3. Connes P, Alexy T, Detterich J, Romana M, Hardy-Dessources MD, Ballas SK. The role of blood rheology in sickle cell disease. *Blood Rev*. 2015;30(2):111-118.
4. Tolu SS, Reyes Gil M, Ogu UO, et al. High Hemoglobin F in Sickle Cell Disease: Waning Protection with Age. *Blood*. 2019;134(Supplement_1):3576.
5. Kalpatthi R, Novelli EM. Measuring success: Utility of biomarkers in sickle cell disease clinical trials and care. *Hematology*. 2018;2018(1):482-492.
6. Lamarre Y, Romana M, Waltz X, et al. Hemorheological risk factors of acute chest syndrome and painful vaso-occlusive crisis in children with sickle cell disease. *Haematologica*. 2012;97(11):1641-1647.
7. Nebor D, Bowers A, Hardy-Dessources MD, et al. Frequency of pain crises in sickle cell anemia and its relationship with the sympatho-vagal balance, blood viscosity and inflammation. *Haematologica*. 2011;96(11):1589-1594.
8. Lemonne N, Charlot, K; Waltz, X; Ballas, S.K; Lamarre, Y; Lee, K; Hierso, R; Connes, C; Etienne-Julan, M; Romana, M; Connes P. Hydroxyurea treatment does not increase blood viscosity and improves red blood cell rheology in sickle cell anemia. *Haematologica*. 2015;100:e383-386.
9. Vichinsky E, Hoppe CC, Ataga KI, et al. A Phase 3 randomized trial of voxelotor in sickle cell disease. *N Engl J Med*. 2019;381(6):509-519.
10. Howard J, Hemmaway CJ, Telfer P, et al. A phase 1/2 ascending dose study and open-label extension study of voxelotor in patients with sickle cell disease. *Blood*. 2019;133(17):1865-1875.
11. Dufu K, Patel M, Oksenberg D, Cabrales P. GBT440 improves red blood cell deformability and reduces viscosity of sickle cell blood under deoxygenated conditions. *Clin Hemorheol Microcirc*. 2018;70(1):95-105.
12. Connes P, Lamarre Y, Hardy-Dessources MD, et al. Decreased hematocrit-to-viscosity ratio and increased lactate dehydrogenase level in patients with sickle cell anemia and recurrent leg ulcers. *PLoS One*. 2013;8(11):6-10.
13. Lamarre Y, Romana M, Lemonne N, et al. Alpha thalassemia protects sickle cell anemia patients from macro-albuminuria through its effects on red blood cell rheological properties. *Clin Hemorheol Microcirc*. 2014;57(1):63-72.
14. Lemonne, N; Lamarre, Y; Romana, M; Mukisimukaza, M; Hardy-Dessources, M.-D; Tarer, V; Mouguel, D; Waltz, Xavier; Tressieres, B; Lalanne-Mistrih, M.-L.; Etienne-Julan, M; Connes P. Does increased red blood cell deformability raise the risk for osteonecrosis in sickle cell anemia? *Blood*. 2013;121(15):3054-3057.
15. Lande WM, Andrews DL, Clark MR, et al. The Incidence of Painful Crisis in Homozygous Sickle Cell Disease: Correlation with Red Cell Deformability. *Blood*. 1988;72(6):2056-2059.
16. Ballas, S K; Larner, J; Smith ED, Surrey S, Schwartz, E; Rappaport EF. Rheologic predictors of the severity of the painful sickle cell crisis. *Blood*. 1988;72(4):1216-1223.
17. Rab MAE, van Oirschot BA, Bos J, et al. Rapid and reproducible characterization of sickling during automated deoxygenation in sickle cell disease patients. *Am J Hematol*. 2019;94(February):575-584.
18. Rab MAE, Kanne CK, Bos J, et al. Oxygen gradient ektacytometry derived biomarkers are associated with vasoocclusive crises and correlate with treatment response in sickle cell disease. *Am J Hematol*. 2021;96(1):E29-E32.
19. Kanter J, Kruse-Jarres R. Management of sickle cell disease from childhood through adulthood. *Blood Rev*. 2013;27(6):279-287.
20. Claster S, Vichinsky EP. Managing sickle cell disease. *Br Med J*. 2003;327(7424):1151-1155.
21. Renoux C, Romana M, Joly P, et al. Effect of Age on Blood Rheology in Sickle Cell Anaemia and Sickle Cell Haemoglobin C Disease : A Cross-Sectional Study. *PLoS One*. 2016;11(6):1-11.
22. Rab MAE, van Oirschot BA, Bos J, et al. Characterization of Sickling During Controlled Automated Deoxygenation with Oxygen Gradient Ektacytometry. *J Vis Exp*. 2019;(153):1-10.

23. Rab MAE, Kanne CK, Bos J, et al. Methodological aspects of the oxygenscan in sickle cell disease: A need for standardization. *Am J Hematol.* 2020;95(1):5-8.
24. Baskurt OK, Boynard M, Cokelet GC, et al. New guidelines for hemorheological laboratory techniques. *Clin Hemorheol Microcirc.* 2009;42(2):75-97.
25. Connes P, Verlhac S, Bernaudin F. Advances in understanding the pathogenesis of cerebrovascular vasculopathy in sickle cell anaemia. *Br J Haematol.* 2013;161(4):484-498.
26. Cita K-C, Brureau L, Lemonne N, et al. Men with Sickle Cell Anemia and Priapism Exhibit Increased Hemolytic Rate, Decreased Red Blood Cell Deformability and Increased Red Blood Cell Aggregate Strength. *PLoS One.* 2016;11(5):e0154866.
27. Inusa, Colombatti, Rees, et al. Geographic Differences in Phenotype and Treatment of Children with Sickle Cell Anemia from the Multinational DOVE Study. *J Clin Med.* 2019;8(11):2009.
28. Blinder MA, Duh MS, Sasane M, Trahey A, Paley C, Vekeman F. Age-Related Emergency Department Reliance in Patients with Sickle Cell Disease. *J Emerg Med.* 2015;49(4):513-522.e1.
29. Tewari S, Brousse V, Piel FB, Menzel S, Rees DC. Environmental determinants of severity in sickle cell disease. *Haematologica.* 2015;100(9):1108-1116.
30. Niihara Y, Miller ST, Kanter J, et al. A phase 3 trial of l-glutamine in sickle cell disease. *N Engl J Med.* 2018;379(3):226-235.
31. Ataga KI, Kutlar A, Kanter J, et al. Crizanlizumab for the prevention of pain crises in sickle cell disease. *N Engl J Med.* 2017;376(5):429-439.
32. Xu JZ, Conrey A, Frey I, et al. Phase 1 Multiple Ascending Dose Study of Safety, Tolerability, and Pharmacokinetics/Pharmacodynamics of Mitapivat (AG-348) in Subjects with Sickle Cell Disease. *Blood.* 2020;136(Supplement 1):21-22.
33. Brown RC, Cruz K, Kalfa TA, et al. FT-4202, an Allosteric Activator of Pyruvate Kinase-R, Demonstrates Proof of Mechanism and Proof of Concept after a Single Dose and after Multiple Daily Doses in a Phase 1 Study of Patients with Sickle Cell Disease. *Blood.* 2020;136(Supplement 1):19-20.
34. Antoniani C, Meneghini V, Lattanzi A, et al. Induction of fetal hemoglobin synthesis by CRISPR/Cas9-mediated editing of the human β -globin locus. *Blood.* 2018;131(17):1960-1973.
35. Ribeil JA, Hacein-Bey-Abina S, Payen E, et al. Gene therapy in a patient with sickle cell disease. *N Engl J Med.* 2017;376(9):848-855.

Supplemental Table 1. Demographic, laboratory and clinical characteristics of pediatric individuals with SCD divided into four quartiles based on viscosity values.

Pediatric cohort				
Quartiles based on whole blood viscosity				
Patient demographics	1q n = 30	2q n = 30	3q n = 30	4q n = 30
Age (years)	9.1 ± 4.3	9.7 ± 4.3	11.1 ± 4.9	11.8 ± 4.9
Sex, female	27% (8/30)	57% (17/30)	43% (13/30)	43% (13/30)
HU therapy	83% (25/30)	90% (27/30)	83% (25/30)	83% (25/30)
HbS/β ⁺ -thal	0% (0/30)	7% (2/30)	10% (3/30)	13% (4/30)
α-thal: any deletions	n/a	n/a	n/a	n/a
Splenectomy	20% (6/30)	27% (8/30)	17% (5/30)	13% (4/30)
Oxygen gradient ektacytometry				
PoS (mmHg)	40.3 ± 10.5	39.8 ± 8.8	35.4 ± 8.8	35.2 ± 8.0
Elmax (EI)	0.45 ± 0.10	0.47 ± 0.09	0.50 ± 0.07	0.52 ± 0.06*
Elmin (EI)	0.12 ± 0.11	0.12 ± 0.07	0.15 ± 0.08	0.16 ± 0.08
Laboratory parameters				
HbF (%) ^a	12.0 ± 6.0	14.1 ± 8.3	16.3 ± 8.2	15.5 ± 8.0
Hb (g/dL)	7.9 ± 1.0	8.5 ± 1.0	9.4 ± 1.2 [‡]	10.3 ± 1.2 [‡]
HCT (%)	24.1 ± 2.9	26.0 ± 2.9	28.5 ± 3.4 [‡]	31.0 ± 3.5 [‡]
ARC (10 ⁹ /L)	407 ± 173	494 ± 144	350 ± 183	314 ± 112
MCV (fl)	94 ± 16	94 ± 12	92 ± 16	91 ± 14
DRBC (%)	6.6 ± 4.0	5.0 ± 2.5	4.4 ± 2.6*	3.3 ± 2.0 [‡]
Blood viscosity (45/s)	3.7 ± 0.4	4.5 ± 0.2 [‡]	5.2 ± 0.2 [‡]	6.5 ± 0.8 [‡]
Blood viscosity (225/s)	2.8 ± 0.3	3.2 ± 0.2*	3.5 ± 0.3 [‡]	4.3 ± 0.7 [‡]
HVR (HCT/BV 45/s)	6.5 ± 0.7	5.8 ± 0.7 [‡]	5.5 ± 0.6 [‡]	4.9 ± 0.7 [‡]
TCD Left MCA ^b	148 ± 27	134 ± 23	120 ± 30 [‡]	122 ± 22*
TCD Right MCA ^c	140 ± 35	134 ± 22	120 ± 24	116 ± 25
Clinical complications				
ACS	63% (19/30)	57% (17/30)	50% (15/30)	40% (12/30)
VOC	32% (9/28)	59% (17/29)	39% (11/29)	53% (16/30)
Cerebral infarction	10% (3/30)	7% (2/30)	7% (2/30)	7% (2/30)
Osteonecrosis	0% (0/30)	3% (1/30)	10% (3/30)	20% (6/30)*
Retinopathy	0% (0/30)	3% (1/30)	0% (0/30)	7% (2/30)
Priapism (% of males)	9% (2/22)	7% (1/13)	12% (2/17)	35% (6/17)
Gallstones	20% (6/30)	27% (8/30)	20% (6/30)	23% (7/30)
Iron overload	17% (5/30)	10% (3/30)	3% (1/30)	3% (1/30)
Nr. complications	1.5 ± 1.3	1.7 ± 1.1	1.4 ± 1.4	1.7 ± 1.3
≥1 major complication*	79% (22/28)	76% (22/29)	62% (17/29)	70% (21/30)
≥1 any complication	79% (22/28)	79% (23/29)	61% (17/28)	73% (22/30)

The first quartile consist of individuals with lowest viscosity values, while the 4th quartile is comprised of individuals with highest viscosity values.

Numbers are depicted as mean ± standard deviation or stated otherwise. The 1st quartile is compared to the other quartiles. ‡p<0.0001, §p<0.001, †p<0.01, *p<0.05.

HU, hydroxyurea; β-thal, β-thalassemia; α-thal, α-thalassemia; n/a, not addressed; Elmax, maximum deformability; Elmin, minimum deformability; HbF, fetal hemoglobin; Hb, hemoglobin, HCT, hematocrit; ARC, absolute reticulocyte count; MCV, mean corpuscular volume; MCHC, mean corpuscular hemoglobin concentration; DRBC, dense RBC; HVR, hematocrit to viscosity ratio; TCD, trans cranial Doppler; MCA, media cerebral artery; ACS, acute chest syndrome; VOC, vaso-occlusive crisis; Nr., number.

^aData of 46 individuals available. ^bData of 64 individuals available. ^cData of 65 individuals available.

*ACS, VOC or cerebral infarction

Supplemental Table 2. Logistic regression analysis of PoS values shows higher odds ratios for specific complications with higher PoS.

Point of Sickling Complication	Pediatric cohort									
	1 st q compared to 2 nd q			1 st q compared to 3 rd q			1 st q compared to 4 th q			
	OR	95% CI	P	OR	95% CI	P	OR	95% CI	P	
ACS	1.55	0.68 – 3.55	0.296	2.38	1.04 – 5.46	0.040	4.75	1.99 – 11.36	0.000	
VOC	1.50	0.64 – 3.49	0.347	2.05	0.88 – 4.79	0.096	2.86	1.24 – 6.62	0.014	
Cerebral infarction	0.32	0.03 – 3.18	0.330	0.65	0.10 – 4.09	0.648	3.39	0.86 – 13.4	0.082	
Osteonecrosis	1.54	0.24 – 9.63	0.648	2.09	0.364 – 12.0	0.408	2.62	0.48 – 14.2	0.265	
Retinopathy	1.00	0.19 – 5.23	1.000	0.65	0.10 – 4.09	0.648	0.64	0.10 – 4.00	0.631	
Priapism	1.53	0.31 – 7.69	0.603	1.39	0.28 – 6.95	0.685	1.53	0.33 – 7.15	0.586	
Gallstones	0.71	0.23 – 2.24	0.536	1.16	0.40 – 3.31	0.789	2.01	0.75 – 5.36	0.165	
Iron overload	3.14	0.31 – 31.3	0.330	8.05	0.95 – 68.3	0.056	6.57	0.76 0 56.9	0.087	
≥1 major complication*	1.68	0.72 – 3.93	0.231	2.60	1.06 – 6.35	0.036	4.92	1.83 – 13.23	0.002	
≥1 any complication	1.89	0.79 – 4.52	0.150	3.46	1.32 – 9.07	0.011	4.51	1.67 – 12.1	0.003	

Point of Sickling Complication	Adult cohort									
	1 st q compared to 2 nd q			1 st q compared to 3 rd q			1 st q compared to 4 th q			
	OR	95% CI	P	OR	95% CI	P	OR	95% CI	P	
ACS	3.60	0.32 – 40.2	0.298	3.27	0.30 – 36.3	0.334	14.0	1.39 – 141.5	0.025	
VOC	1.87	0.39 – 8.89	0.433	2.10	0.45 – 9.84	0.346	6.42	0.999-41.2	0.050	
Cerebral infarction	1.00	0.00 - ∞	1.000	1.2*10 ⁸	0.00 - ∞	0.999	2.9*10 ⁸	0.00 - ∞	0.999	
Osteonecrosis	0.67	0.13 – 3.45	0.629	0.47	0.10 – 2.29	0.348	0.21	0.03 – 1.36	0.102	
Retinopathy	2.70	0.51 – 14.3	0.244	0.17	0.02 – 1.82	0.144	0.41	0.06 – 2.77	0.360	
Priapism	2.6*10 ⁹	0.00 - ∞	0.999	5.4*10 ⁹	0.00 - ∞	0.999	4.6*10 ⁹	0.00 - ∞	0.999	
Gallstones	1.88	0.35 – 9.98	0.461	3.00	0.62 – 14.6	0.174	1.41	0.28 – 7.13	0.681	
Iron overload	n/a	n/a	n/a	n/a	n/a	n/a	n/a	n/a	n/a	
≥1 major complication*	2.63	0.53 – 13.1	0.239	2.10	0.45 – 9.84	0.346	14.0	1.39 – 141.5	0.025	
≥1 any complication	2.9*10 ⁹	0.00 - ∞	0.999	2.36	0.19 – 29.7	0.505	2.18	0.17 – 27.6	0.547	

Odds ratios (OR) were calculated for q2, q3 and q4 with q1 as reference cohort in individuals with SCD (n= 53 in adult cohort and n=189 in pediatric cohort). CI, confidence interval; q, quartile; ACS, acute chest syndrome; VOC, vaso-occlusive crisis; n/a, not addressed, P, p-value.
 *ACS, VOC or cerebral infarction

Supplemental Table 3. Logistic regression analysis of quartiles based on viscosity values shows increased odds ratios for specific complications.

Viscosity	Pediatric cohort														
	1 st q compared to 2 nd q					1 st q compared to 3 rd q					1 st q compared to 4 th q				
Complication	OR	95% CI	P	OR	95% CI	P	OR	95% CI	P	OR	95% CI	P	OR	95% CI	P
ACS	0.76	0.27 – 2.13	0.598	0.58	0.21 – 1.62	0.299	0.39	0.14 – 1.09	0.073						
VOC	2.99	1.01 – 8.84	0.048	1.37	0.46 – 4.09	0.577	2.41	0.83 – 7.03	0.106						
Cerebral infarction	0.64	0.10 – 4.15	0.643	0.64	0.10 – 4.15	0.643	0.64	0.10 – 4.15	0.643						
Osteonecrosis	5.6*10 ⁸	0.00 - ∞	0.998	1.8*10 ⁹	0.00 - ∞	0.998	4.0*10 ⁹	0.00 - ∞	0.998						
Retinopathy	5.6*10 ⁸	0.00 - ∞	0.998	1.00	0.00 - ∞	1.000	1.2*10 ⁹	0.00 - ∞	0.998						
Priapism	0.83	0.07 – 10.2	0.887	1.33	0.17 – 10.6	0.785	5.46	0.94 – 31.7	0.059						
Gallstones	1.46	0.44 – 4.86	0.543	1.00	0.28 – 3.54	1.000	1.22	0.36 – 4.17	0.754						
Iron overload	0.56	0.12 – 2.57	0.452	0.17	0.02 – 1.58	0.119	0.17	0.02 – 1.58	0.119						
≥1 major complication*	0.86	0.25 – 2.96	0.808	0.45	0.14 – 1.44	0.178	0.64	0.19 – 2.10	0.458						
≥1 any complication	1.04	0.27 – 4.09	0.951	0.39	0.11 – 1.35	0.137	0.60	0.17 – 2.11	0.424						

Odds ratios (OR) were calculated for q2, q3 and q4 with q1 as reference cohort in pediatric individuals with SCD (n=120).

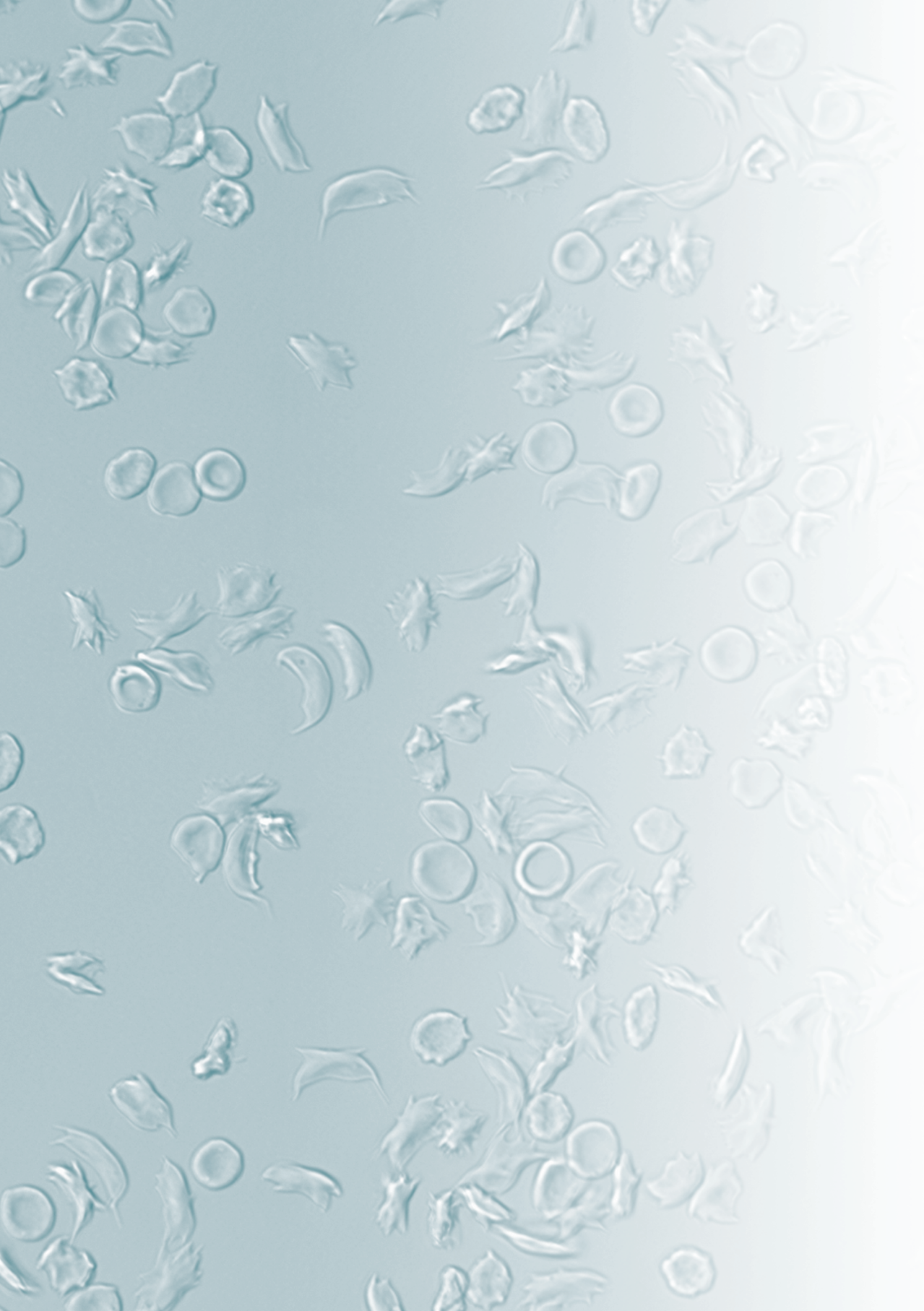
CI, confidence interval; q, quartile; ACS, acute chest syndrome; VOC, vaso-occlusive crisis; P, p-value.

* ACS, VOC or cerebral infarction

Supplemental Table 4. Intra patient variability of PoS measured at two or three different time points.

PoS	Mean CV	SD CV
No therapy (n=6)	5.1%	6.9%
Hydrea (n=5)	7.8%	6.0%
All (n=11)	6.3%	6.4%

PoS, point of sickling; CV, coefficient of variance; SD, standard deviation



Chapter 7

Use of oxygen gradient ektacytometry in the titration of hydroxyurea dosing in children with sickle cell disease

Submitted

Maite E. Houwing¹, Jennifer Bos², Sonja A.M.C. Teuben¹, Roger E.G. Schutgens², Richard van Wijk², Eduard J. van Beers³, Marjon H. Cnossen¹ and Minke A.E. Rab^{2,3}

¹ Department of Pediatric Hematology, Erasmus MC- Sophia Children's Hospital, Rotterdam, The Netherlands

² Central Diagnostic Laboratory - Research, Utrecht University, Utrecht The Netherlands

³ Van Creveldkliniek, University Medical Center Utrecht, Utrecht University, Utrecht, The Netherlands

Short summary

International guidelines recommend that hydroxyurea should be offered to all children with HbSS or HbS β^0 sickle cell disease at 9 months of age regardless of clinical course. However, there are substantial gaps in our knowledge with regard to optimal dosing, dose modifications and verification of adherence to treatment. Oxygen gradient ektacytometry-derived parameters, especially Point of Sickling (PoS) and minimum deformability after maximal deoxygenation (Elmin), provide the clinician with information on red blood cell characteristics and sickling propensity that help optimize hydroxyurea dosing in order to maximize clinical benefits.

Introduction

Sickle cell disease is an autosomal, recessive hemoglobinopathy characterized by ongoing hemolytic anemia, episodes of vaso-occlusive crises and progressive organ failure. Worldwide, approximately 312.000 neonates are born each year with this disease.¹ Sickle cell disease is caused by a single nucleotide substitution in codon 6 of the β globin gene (Glu6Val). This mutation leads to the formation of abnormal sickle hemoglobin (HbS).² When deoxygenated, HbS containing red blood cells (RBCs) develop a sickle or crescent shape. Such abnormally shaped RBCs interact with leukocytes and the vascular endothelium causing occlusion and vasculopathy, subsequently leading to a broad range of acute and chronic complications.^{3,4}

Long-term daily oral hydroxyurea treatment has consistently been shown to be clinically effective and to positively affect laboratory values in pediatric patients with sickle cell disease.⁵⁻⁸ Patients experience less frequent vaso-occlusive pain- and acute chest episodes, require fewer hospitalizations and blood transfusions and show increased levels of total hemoglobin (Hb) and fetal hemoglobin (HbF) and decreased levels of lactate dehydrogenase and bilirubin.⁵⁻⁸ However, there are substantial gaps in our knowledge with regard to optimal dosing, necessary dose modifications and verification of adherence to treatment. Laboratory values, such as Hb, HbF levels and mean corpuscular volume (MCV) are frequently used in clinical practice to assess treatment efficacy. However, none of these routine tests capture the overall effect hydroxyurea has on RBCs.^{9,10}

Oxygen gradient ektacytometry measures deformability of RBCs over a range of oxygen concentrations using a Laser Optical Rotational Red Cell Analyser (Lorrca) ektacytometer (RR Mechatronics, Zwaag, the Netherlands) with Oxygenscan module.¹¹ Oxygen gradient ektacytometry produces four key parameters: 1) EI_{max} , RBC deformability at the start of the measurement at normal oxygenation; 2) EI_{min} , deformability upon deoxygenation; 3) Point of Sickling (PoS): oxygen tension at which 5% decrease in EI is observed during deoxygenation, reflecting the patient-specific pO_2 at which cells become more rigid and sickling begins; and 4) Slope, indicating the velocity of RBC sickling during deoxygenation. RBCs that sickle more rapidly at a low oxygen tension generate higher slope values, which is favorable for patients. Lower Slope values reflect a heterogeneous population consisting of a percentage of cells already sickled at normoxia and a population of RBCs that start to sickle at a high oxygen tension, which is unfavorable. The parameters provided by oxygen gradient ektacytometry, reflect RBC characteristics that are involved in (the frequency of) vaso-occlusive crises. Moreover, oxygen gradient ektacytometry-derived parameters have been shown to change significantly as a result of hydroxyurea treatment and transfusion therapy.

Case presentation

Monozygous twin girls, six years old, attended the Sickle Cell Disease Comprehensive Care outpatients' clinic for their biannual follow-up visit in the Erasmus MC- Sophia Children's Hospital. They were diagnosed with homozygous sickle cell disease soon after birth by

neonatal screening. Except for a transient aplastic crisis associated with parvovirus B19 infection when they were four years old, they had an unremarkable medical history without frequent pain crises or organ failure, including normal transcranial Doppler values. Due to changing international guidelines regarding hydroxyurea therapy for children with sickle cell disease,¹² they both started with hydroxyurea at a dosage of 22.4 and 19.8 mg/kg respectively. Parents gave informed consent to include oxygen gradient ektacytometry measurements during regular follow-up. Patient characteristics before and during hydroxyurea treatment are described in Table 1. Results after three months of hydroxyurea therapy were promising with all three oxygen gradient ektacytometry-derived parameters improving substantially. However, after six months of hydroxyurea therapy, in both twins a decrease in EI_{\max} and EI_{\min} and an increase in PoS was noted, compared to previous oxygen gradient ektacytometry curves (Figure 1A-E). These changes in parameters were accompanied by a decrease in HbF levels and MCV. After verification of treatment adherence, it was

Table 1. Patient characteristics at baseline and on hydroxyurea therapy

Patient characteristics					
Twin 1	baseline	1 month	3 months	6 months	8 months
Laboratory parameters					
HbF (%)	9.1	14.8	18.3	14.4	22.4
HbS (%)	80.7	74.1	69.8	73.8	64.2
Hb (g/dL)	7.9	7.6	9.6	8.5	8.2
ARC ($10^9/L$)	688	200	247	445	490
MCV (fl)	91	102	104	99	114
MCHC (g/dL)	37.2	37.1	37.5	33.2	35.7
Clinical parameters					
Body weight (kg)	22.3	nd	nd	24.7	nd
BMI (kg/m^2)	15.7	nd	nd	16.3	nd
HU dosage (mg/kg)*	22.4	nd	nd	20.2	30.4
Twin 2	baseline	1 month	3 months	6 months	8 months
Laboratory parameters					
HbF (%)	7.8	11.8	16.5	9.2	18.0
HbS (%)	82.0	78.1	72.0	82.7	74.1
Hb (g/dL)	7.9	8.2	7.0	8.1	7.9
ARC ($10^9/L$)	695	315	346	586	422
MCV (fl)	90	100	106	97	111
MCHC (g/dL)	36.7	35.8	35.5	33.3	35.9
Clinical parameters					
Body weight (kg)	25.2	nd	nd	27.9	nd
BMI (kg/m^2)	17.0	nd	nd	17.9	nd

Abbreviations: HbF, fetal hemoglobin; HbS, hemoglobin S; Hb, hemoglobin; ARC, absolute reticulocyte count; MCV, mean corpuscular volume; MCHC, mean corpuscular hemoglobin concentration; BMI, body mass index; HU, hydroxyurea; nd, not determined.

hypothesized that the dosage of hydroxyurea was too low considering the body weight gain of both sisters. Indeed, hydroxyurea was now given at a dosage of 20.24 (Twin 1) and 17.92 (Twin 2) mg/kg. After dose modifications were made, oxygen gradient ektactometry-derived parameters restored in both twin sisters (Figure 1A-F).

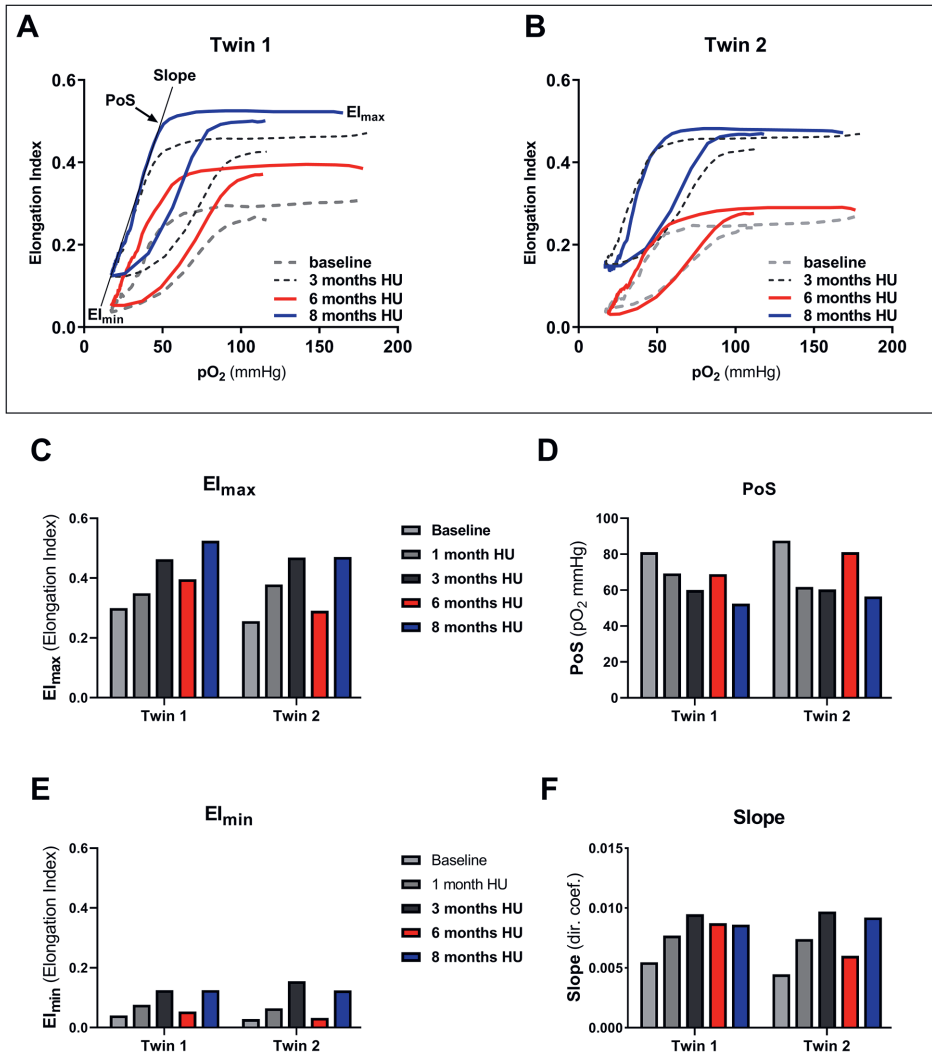


Figure 1. Oxygen gradient ektactometry curves of both twins at baseline and after start of hydroxyurea therapy. Oxygen gradient ektactometry curves of twin 1 (A) and twin 2 (B) before and during hydroxyurea therapy. (C) Maximum EI at normoxic conditions (El_{max}) of both twins before and during HU therapy. (D) Specific oxygen tension when 5% decrease of EI is observed (point of sickling (PoS)) of both twins before and during HU therapy. (E) Minimum EI measured at end of deoxygenation (El_{min}) of both twins before and during HU therapy. (F) Directional coefficient of the downward part of the curve after deoxygenation is initiated. This indicates the rapidity of sickling of RBCs upon deoxygenation and is suggested to be a reflection of the heterogeneity of the RBC population. Abbreviation: HU, hydroxyurea.

Discussion

Our case report shows that oxygen gradient ektacytometry-derived parameters can be used to assess hydroxyurea therapy efficacy and that they aid in the titration of an individual patient's dosing. Despite sufficient evidence on the safety and efficacy of hydroxyurea in sickle cell disease patients, unfortunately it is still underutilized in clinical practice.¹³⁻¹⁵ The most common provider-related barriers are concerns about patient adherence to therapy and (late) toxicities.¹⁶⁻¹⁹ Oxygen gradient ektacytometry provides visual evidence of the effects of hydroxyurea treatment that can be understood by both patients and healthcare providers. This can help with promoting and monitoring treatment adherence and is more gratifying than other methods such as pill counts. Because hydroxyurea does not typically have beneficial short-term effects, seeing oxygen gradient ektacytometry-derived parameters change from baseline till optimal dose will help patients and families realize that hydroxyurea is actually working. In addition, the clinical and laboratory benefits of hydroxyurea are the greatest when escalated to the maximum tolerated dose (MTD).²⁰ The MTD of hydroxyurea yields an average increase in HbF of 20-25%, but HbF response is known to vary widely among patients with HbF percentages ranging from 10%-15% to more than 40% HbF.^{5,21-25} Moreover, measurement of HbF in blood lysate only reflects the average HbF content across all RBCs. Due to an uneven distribution of HbF among F-cells (HbF-containing RBCs), cell-specific compartmentalization of HbF across RBCs cannot be evaluated by sole measurement of HbF percentage.²⁶ Flow cytometric quantification of F-cells is also not ideal as the threshold used for detection of F-cells is not the same threshold that defines protection against sickling.²⁷ A functional assay -such as oxygen gradient ektacytometry- that assesses all RBC characteristics, overcomes these limitations.

In conclusion, oxygen gradient ektacytometry quantifies RBC deformability and comprehensively assesses various RBC characteristics such as MCV, MCHC, HbF% and HbS% that together determine sickling behavior as influenced by hydroxyurea medication. Therefore, oxygen gradient ektacytometry-derived parameters, especially PoS and EI_{min} , provide the clinician with information on RBC characteristics and sickling propensity that help optimize hydroxyurea dosing to maximize clinical benefits.

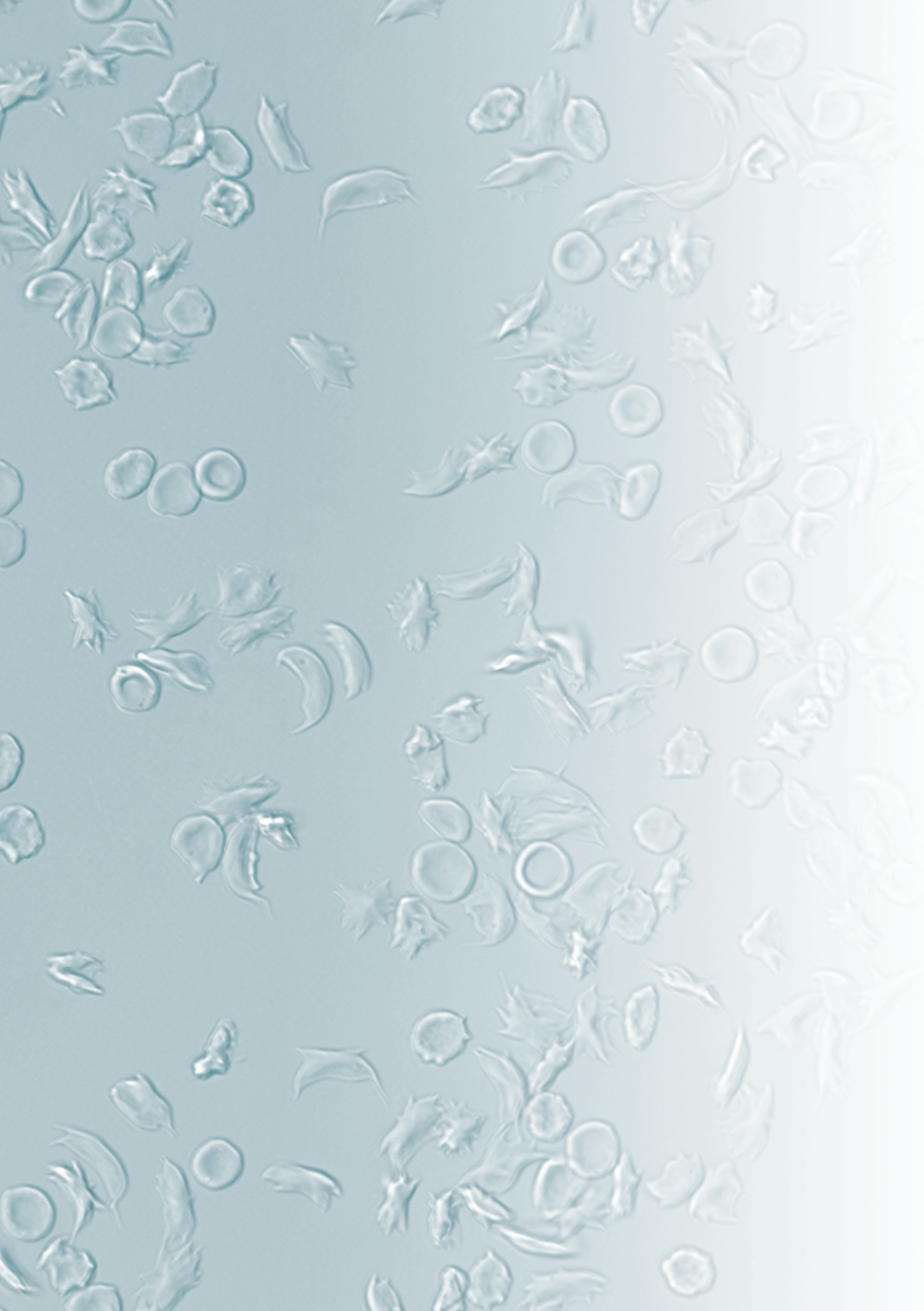
Acknowledgements

The study was in collaboration with the members of the 'SCORE' (Sickle Cell Outcome Research) consortium of the Netherlands.

References

- Piel FB, Patil AP, Howes RE, et al. Global epidemiology of sickle haemoglobin in neonates: a contemporary geostatistical model-based map and population estimates. *Lancet*. 2013;381(9861):142-151.
- Marotta CA, Forget BG, Cohne-Solal M, Wilson JT, Weissman SM. Human beta-globin messenger RNA. I. Nucleotide sequences derived from complementary RNA. *J Biol Chem*. 1977;252(14):5019-5031.
- Ataga KI, Brittain JE, Desai P, et al. Association of coagulation activation with clinical complications in sickle cell disease. *PLoS One*. 2012;7(1):e29786.
- Manwani D, Frenette PS. Vaso-occlusion in sickle cell disease: pathophysiology and novel targeted therapies. *Blood*. 2013;122(24):3892-3898.
- Kinney TR, Helms RW, O'Branski EE, et al. Safety of hydroxyurea in children with sickle cell anemia: results of the HUG-KIDS study, a phase I/II trial. Pediatric Hydroxyurea Group. *Blood*. 1999;94(5):1550-1554.
- Hoppe C, Vichinsky E, Quirolo K, van Warmerdam J, Allen K, Styles L. Use of hydroxyurea in children ages 2 to 5 years with sickle cell disease. *J Pediatr Hematol Oncol*. 2000;22(4):330-334.
- Ferster A, Tahriri P, Vermynen C, et al. Five years of experience with hydroxyurea in children and young adults with sickle cell disease. *Blood*. 2001;97(11):3628-3632.
- de Montalembert M, Brousse V, Elie C, et al. Long-term hydroxyurea treatment in children with sickle cell disease: tolerance and clinical outcomes. *Haematologica*. 2006;91(1):125-128.
- Hillery CA, Du MC, Wang WC, Scott JP. Hydroxyurea therapy decreases the in vitro adhesion of sickle erythrocytes to thrombospondin and laminin. *Br J Haematol*. 2000;109(2):322-327.
- Adragna NC, Fonseca P, Lauf PK. Hydroxyurea affects cell morphology, cation transport, and red blood cell adhesion in cultured vascular endothelial cells. *Blood*. 1994;83(2):553-560.
- Rab MAE, van Oirschot BA, Bos J, et al. Rapid and reproducible characterization of sickling during automated deoxygenation in sickle cell disease patients. *American Journal of Hematology*. 2019;94(5):575-584.
- Yawn BP, Buchanan GR, Afenyi-Annan AN, et al. Management of Sickle Cell Disease: Summary of the 2014 Evidence-Based Report by Expert Panel Members. *Jama*. 2014;312(10):1033-1048.
- Stettler N, McKiernan CM, Melin CQ, Adejoro OO, Walczak NB. Proportion of adults with sickle cell anemia and pain crises receiving hydroxyurea. *JAMA*. 2015;313(16):1671-1672.
- Reeves SL, Jary HK, Gondhi JP, Raphael JL, Lisabeth LD, Dombkowski KJ. Hydroxyurea use among children with sickle cell anemia. *Pediatric Blood & Cancer*. 2019;66(6):e27721.
- Ware RE, McGann PT, Quinn CT. Hydroxyurea for children with sickle cell anemia: Prescribe it early and often. *Pediatric Blood & Cancer*. 2019;66(8):e27778.
- Zumberg MS, Reddy S, Boyette RL, Schwartz RJ, Konrad TR, Lottenberg R. Hydroxyurea therapy for sickle cell disease in community-based practices: a survey of Florida and North Carolina hematologists/oncologists. *Am J Hematol*. 2005;79(2):107-113.
- Lanzkron S, Haywood C, Jr., Hassell KL, Rand C. Provider barriers to hydroxyurea use in adults with sickle cell disease: a survey of the Sickle Cell Disease Adult Provider Network. *J Natl Med Assoc*. 2008;100(8):968-973.
- Brandow AM, Jirovec DL, Panepinto JA. Hydroxyurea in children with sickle cell disease: practice patterns and barriers to utilization. *Am J Hematol*. 2010;85(8):611-613.
- Brandow AM, Panepinto JA. Hydroxyurea use in sickle cell disease: the battle with low prescription rates, poor patient compliance and fears of toxicities. *Expert Rev Hematol*. 2010;3(3):255-260.
- Ware RE, Aygun B. Advances in the use of hydroxyurea. *Hematology*. 2009;2009(1):62-69.
- Charache S, Terrin ML, Moore RD, et al. Effect of hydroxyurea on the frequency of painful crises in sickle cell anemia. Investigators of the Multicenter Study of Hydroxyurea in Sickle Cell Anemia. *N Engl J Med*. 1995;332(20):1317-1322.
- Steinberg MH, Lu ZH, Barton FB, Terrin ML, Charache S, Dover GJ. Fetal hemoglobin in sickle cell anemia: determinants of response to hydroxyurea. Multicenter Study of Hydroxyurea. *Blood*. 1997;89(3):1078-1088.

23. Bakanay SM, Dainer E, Clair B, et al. Mortality in sickle cell patients on hydroxyurea therapy. *Blood*. 2005;105(2):545-547.
24. Zimmerman SA, Schultz WH, Davis JS, et al. Sustained long-term hematologic efficacy of hydroxyurea at maximum tolerated dose in children with sickle cell disease. *Blood*. 2004;103(6):2039-2045.
25. Heeney MM, Ware RE. Hydroxyurea for children with sickle cell disease. *Pediatr Clin North Am*. 2008;55(2):483-501
26. Quinn CT, Niss O, Pfeiffer A, et al. Pharmacokinetics-Guided Dosing of Hydroxyurea Can Achieve Near-Pancellular Fetal Hemoglobin Expression in Sickle Cell Anemia: F-Cell Analysis As a Benchmark for Disease-Modifying Therapy. *Blood*. 2019;134(Supplement_1):892-892.
27. Fertrin KY, van Beers EJ, Samsel L, et al. Imaging flow cytometry documents incomplete resistance of human sickle F-cells to ex vivo hypoxia-induced sickling. *Blood*. 2014;124(4):658-660.



Chapter 8

Decreased activity and stability of pyruvate kinase in sickle cell disease: a novel target for therapy by mitapivat

Blood 2021 May 27;137(21):2997-3001

Minke A.E. Rab^{1,2}, Jennifer Bos¹, Brigitte A. van Oirschot¹, Stephanie van Straaten³, Penelope A. Kosinski⁴, Victor Chubukov⁴, Hyeryun Kim⁴, Heidi Mangus⁴, Roger E.G. Schutgens², Gerard Pasterkamp¹, Lenny Dang⁴, Charles Kung⁴, Eduard J. van Beers², and Richard van Wijk¹

¹ Central Diagnostic Laboratory - Research, University Medical Center Utrecht, Utrecht University, Utrecht, The Netherlands

² Van Creveldkliniek, University Medical Center Utrecht, Utrecht University, Utrecht, The Netherlands

³ Sophia Children's Hospital, Erasmus Medical Center, Rotterdam, The Netherlands

⁴ Agios Pharmaceuticals Inc., Cambridge, MA, USA

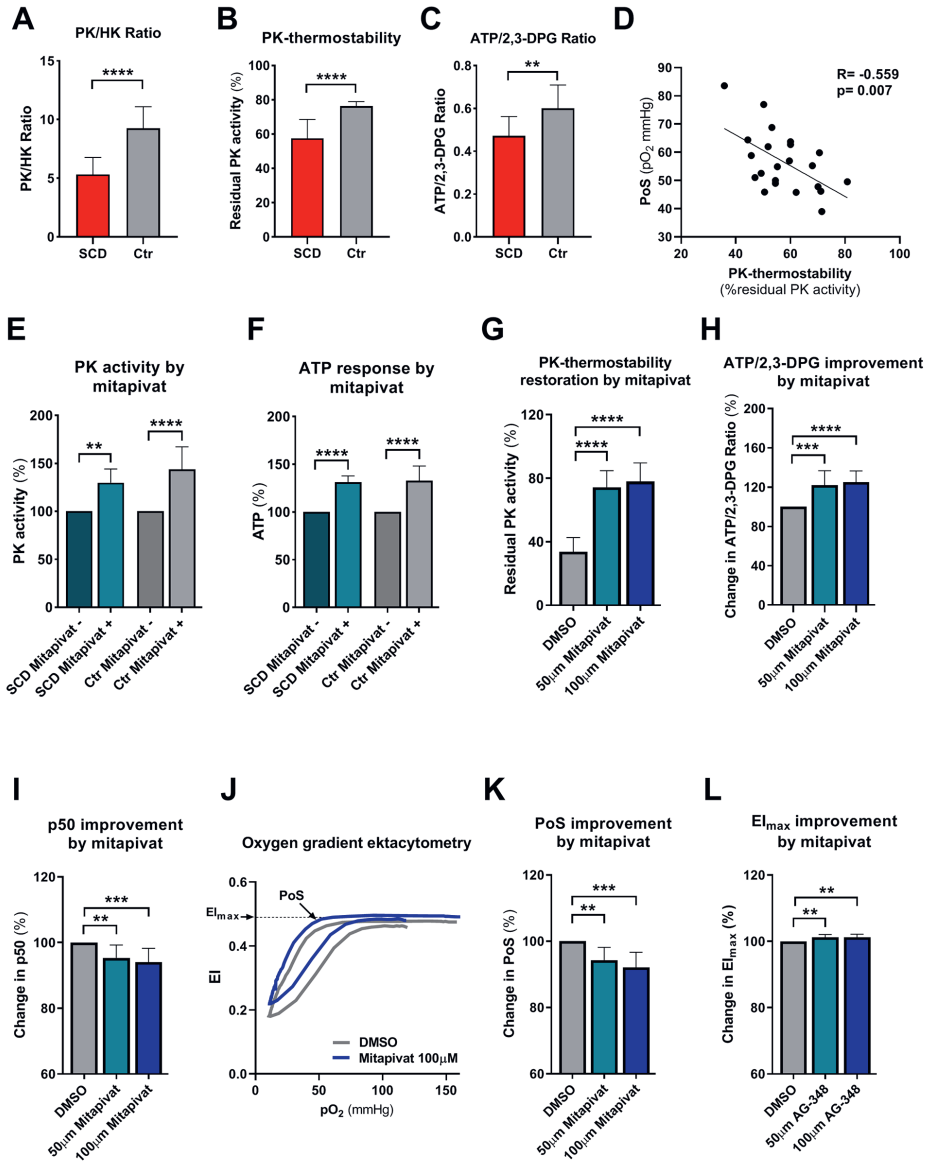
To the editor

Sickle cell disease (SCD) is a devastating disease characterized by a single nucleotide mutation in the beta-globin chain, encoding the production of an abnormal type of hemoglobin: hemoglobin S (HbS). HbS polymerizes upon deoxygenation causing red blood cells (RBC) to sickle. Sickled RBCs are poorly deformable, which leads to vaso-occlusion and hemolytic anemia. In addition, increased red cell adhesion, endothelial dysfunction, inflammation, oxidative stress, hemostatic activation, and rheological abnormalities all contribute to the complex pathophysiology of SCD.¹ Among the factors that influence sickling are RBC metabolic intermediates, in particular levels of 2,3-diphosphoglycerate (2,3-DPG) and ATP. 2,3-DPG is produced in the Rapoport-Luebering shunt, a unique RBC-specific glycolytic bypass, and serves as an important regulator of oxygen affinity of hemoglobin. The increased intracellular 2,3-DPG levels lower oxygen affinity, thereby promoting polymerization of HbS upon deoxygenation and, hence, sickling.² ATP is critical for maintaining RBC membrane integrity and deformability, and approximately 50% of the cell's ATP is generated in the last step of glycolysis catalyzed by pyruvate kinase (PK). Decreased levels of ATP have been reported in SCD mice,³ and ATP-depletion has been associated with an increased number of irreversibly sickled cells.⁴ Interestingly, these metabolic changes are strongly reminiscent of key metabolic changes observed in PK deficiency, a rare inherited glycolytic enzymopathy which is caused by mutations in the *PKLR* gene and associated with non-spherocytic hemolytic anemia.⁵ PK deficiency results in decreased levels of ATP whereas retrograde accumulation of glycolytic intermediates leads to increased levels of 2,3-DPG.⁶ Mitapivat is an allosteric activator of PK and currently in phase 3 clinical trials for PK-deficiency (NCT02476916, NCT03548220, NCT03559699, NCT03853798) and phase 1 trial for SCD (NCT4000165). This small molecule directly targets PK by binding in a pocket at the dimer-dimer interface, resulting in enhanced activity of both wild type and mutant PK.⁷ Both phase I and II studies in healthy volunteers and PK-deficient patients demonstrated glycolytic pathway activation upon treatment with mitapivat and confirmed safety and efficacy.^{8,9} In this study we investigated key properties of PK in SCD, and the effect of *ex vivo* treatment with mitapivat on PK properties, metabolic features and sickling behavior.

Whole blood from SCD patients and healthy controls was collected according to protocol, approved by the ethical committee of UMC Utrecht (17-450/M and 17-392/M). Unless stated otherwise, blood was collected in EDTA. Routine hematological parameters were measured using the Cell-Dyn Sapphire (Abbott Diagnostics). Fetal hemoglobin (HbF) and HbS levels were measured by HPLC (Tosoh G8) during routine visits to the outpatient clinic. PK and hexokinase (HK) activity measurements, PK protein levels and thermostability were performed on RBCs purified from whole blood using microcrystalline cellulose- α -cellulose.¹⁰ PK-thermostability was measured on lysates after 1 hour of incubation (53°C), and expressed as percentage residual enzymatic activity (final substrate concentration 5 mM) after incubation.⁶ PK protein levels were determined by Mesoscale Assay (MesoScale Discovery) as described.⁶ Quantitative analysis of ATP and 2,3-DPG was performed as described.⁶ Sickling behavior was assessed on whole blood, standardized to a fixed RBC count of $200 \times 10^6/5$ ml Oxy-iso by oxygen gradient ektacytometry on the Laser Optical Rotational Red

Cell Analyzer (Lorrc, RR Mechatronics) with oxygenscan add-on.^{11,12} The Point-of-Sickling (PoS) indicates the specific pO_2 at which RBCs start to sickle. For *ex vivo* treatment with mitapivat purified RBCs were incubated for 24 hours at 37°C in presence or absence of 10 μ M mitapivat as described.⁶ After 24 hours PK activity and ATP levels (CellTiterGlo; Promega) were measured. Oxygen gradient ektacytometry, ATP/2,3-DPG levels, p50 (Hemox analyzer TCS), and PK-thermostability⁶ measurements (final substrate concentration 0.5 mM) were performed on buffy coat-depleted whole blood (0.2 hematocrit), collected in CPDA and incubated for 22 hours in AGAM buffer,⁶ in presence or absence of 50 or 100 μ M mitapivat. Incubation was performed overnight (18 hours) at 4°C after which samples were allowed to recover at RT (1 hour), and 37°C (3 hours).

Baseline patient characteristics, RBC features and PK features of 22 SCD patients and 10 healthy controls are shown in Table 1. Reticulocytosis in SCD patients was accompanied by increased activity of HK but PK activity, which is also age-related, was found to be decreased, as reflected by a decreased PK/HK ratio^{13,14} (Table 1, Figure 1A). This deficiency of PK was accompanied by a substantial decrease in PK-thermostability in SCD patients (Table 1, Figure 1B), and a decreased ATP/2,3-DPG ratio (Table 1, Figure 1C). At the same time PK protein levels were increased (Table 1), likely because of the relatively young age of the RBC population (positive correlation with reticulocyte count, $r=0.655$, $p<0.0001$ and inverse correlation with Hb, $r=-0.785$, $p<0.0001$). Together, these findings imply that enzyme activity and stability, as well as red cell metabolism, is compromised in SCD, similar to what is observed in PK-deficient patients.⁶ PK-thermostability inversely correlated with reticulocytes, *i.e.* patients displaying the lowest degree of PK stability had the highest reticulocyte count ($R=-0.797$, $p<0.0001$). This suggests that a lower degree of PK stability is associated with more severe anemia, which is underlined by the correlation with Hb ($r=0.731$, $p<0.0001$). In addition, PK-thermostability also inversely correlated with PoS, indicating that decreased PK-thermostability is associated with sickling at a higher pO_2 ($r=-0.559$, $p=0.007$, Figure 1D). Notably, this association between PK-thermostability and clinical severity was not observed in SCD patients followed after starting hydroxyurea (HU) therapy: Despite significant decreases in PoS of 16% and 19% compared to baseline after 3 and 6 months, respectively (Supplemental Figure 1A), PK-thermostability remained unchanged (baseline: 51%, 3 months, 54%, 6 months 55%, Supplemental Figure 1B). This indicates that the clinical benefit of HU is independent of PK properties. We next investigated if PK activity from SCD patients could be enhanced by mitapivat and whether this would be associated with an improvement of RBC metabolism and functional properties. Upon *ex vivo* treatment with mitapivat an increase in PK activity was seen in purified RBCs of patients and controls, with a mean increase of 129% in SCD patients (range 113-148%), and 144% in controls (range 111-188%, Figure 1E). Accordingly, mean ATP levels increased 131% in SCD patients (range 123-139%), and 133% in controls (range 101-155%, Figure 1F). This shows that mitapivat is able to bind PK from SCD patients similar to healthy controls, and that this small molecule activator can elicit an allosteric response upon binding, resulting in enhanced production of ATP. Further evidence for functional improvement was obtained from a series of experiments on buffy coat-depleted whole blood from both non-transfused as well as transfused SCD patients. This showed that *ex vivo* treatment with mitapivat considerably restored PK-thermostability



Pyruvate kinase (PK) activity, thermostability and cellular metabolism is compromised in red blood cells (RBCs) from patients with sickle cell disease (SCD) and correlates with markers of clinical severity (A-D). (A) PK/HK ratio, as a means to evaluate PK activity in the presence of high number of reticulocytes, is decreased in RBCs from SCD patients (red, N=22) compared to healthy controls (Ctr, grey, N=10), indicating a deficiency of PK. (B) The deficiency of PK is accompanied by a decrease in PK-thermostability in RBCs of SCD patients (N=22) compared to controls (N=10), as well as a decrease in ATP/2,3-DPG ratio in SCD patients (N=14) compared to healthy controls (N=10). (D) PK-thermostability correlates with Point of Sickling (PoS, pO₂ at which RBCs start to sickle) in SCD patients (N=22), a novel potential biomarker of clinical severity determined by oxygen gradient ektactometry.²⁰ **Ex vivo treatment of purified SCD RBCs with mitapivat increases PK activity and ATP levels (E-F).** PK activation and ATP response (%) were assessed from purified RBCs of SCD patients (turquoise, N=7) and 14 healthy controls (Ctr, grey, N=14) after 24 hours incubation in presence (light turquoise and light grey) or absence (dark turquoise and dark grey) of 10 µM mitapivat. ▶

(E) An increase in PK activity is seen in SCD patients (mean increase 129%, range 113-148%) and controls (mean increase 144%, range 111-188%). (F) This increase is accompanied by an increase in ATP response in SCD patients (mean increase 131%, range 123-139%) and controls (mean increase 133%, range 101-155%). **Ex vivo treatment of buffy coat-depleted whole blood with mitapivat restores PK-thermostability, increases ATP/2,3-DPG ratio, decreases p50 and PoS and increases membrane health (G-L).** (G) PK-thermostability (% residual PK activity), after 22 hours incubation in presence of 50 μM (light turquoise) and 100 μM (dark blue) mitapivat is restored to 79% (100 μM) compared to vehicle controls (32%, DMSO control, grey, N=11), causing a 25% increase in ATP/2,3-DPG ratio (N=11, panel H) and a 5% decrease in p50 (N=11, panel I). (J) Representative oxygen gradient ektacytometry curve shows improved PoS and $E_{I_{\max}}$ after incubation in presence of 100 μM mitapivat (dark blue) compared to vehicle control (grey). (K-L) PoS and $E_{I_{\max}}$ of 9 SCD patients improve with 9% and 2%, respectively, after 22 hours incubation in presence of 100 μM (dark blue) mitapivat compared to vehicle controls (grey).
 HK, hexokinase; 2,3-DPG, 2,3-diphosphoglycerate; ATP, adenosine triphosphate; PoS, point of sickling; Error bars represent standard deviation. **** $p < 0.0001$, *** $p < 0.001$, ** $p < 0.01$

(79% residual activity compared to 32% for vehicle control, Figure 1G) and led to a 25% increase in ATP/2,3-DPG ratio (Figure 1H). This was mainly due to a 17% decrease in 2,3-DPG levels (Supplemental Figure 2A), whereas the 5% increase in ATP was non-significant under these conditions (Supplemental Figure 2B). In line with the decrease in 2,3-DPG there was 5% decrease in p50 (Figure 1I), which, most importantly, was accompanied by a functional improvement of SCD RBCs, as illustrated by a significant 9% decrease in PoS compared to untreated samples (Figure 1K, representative curve depicted in Figure 1J). In addition we observed a modest but significant 2% increase in RBC deformability at normoxic conditions ($E_{I_{\max}}$), indicative of improved RBC membrane health of SCD RBCs treated with mitapivat (Figure 1L). Importantly, these results did not differ between non-transfused and transfused patients (Supplemental Figure 3A-J), suggesting that the positive effects can be attributed to improved functional properties of sickle RBCs.

In summary, we report on a novel finding in SCD RBCs: PK is less stable and less active compared to healthy control RBCs. The mechanism involved is yet to be determined, but could involve altered intracellular redox state and subsequent inhibition of the enzyme through oxidation of cysteine residues.^{15,16} Defective PK function and, hence, compromised RBC metabolism therefore could contribute to the complex pathophysiology of SCD. Notably, the importance of PK function in SCD is underlined by a case report on a combination of PK deficiency and sickle cell trait causing an acute sickling syndrome.¹⁷ Our findings furthermore demonstrate that *ex vivo* treatment with mitapivat restores PK activity and PK-thermostability, reduces 2,3-DPG levels, decreases p50, and subsequently reduces sickling behavior. Targeting PK by mitapivat treatment therefore represents a potential novel therapeutic option for SCD,^{18,19} either by itself or, because HU treatment does not affect PK properties, synergistic with HU treatment or transfusion. Clinical trials are warranted to investigate whether mitapivat treatment will ameliorate clinical features such as hemolysis, vaso-occlusive episodes and anemia.

Table 1. Baseline characteristics of patients with SCD and controls

	SCD patients* (n=22)	Controls (n=10)
Patient related features		
Sex, female n (%)	9 (40.9)	9 (90.0)
Age, years	23 (7-57)	48 (26-63)
α -Thalassemia, n (%)	3 (13.6)	n/d
Splenectomy, n (%)	1 (4.5)	n/d
HU, n (%)	13 (59.1)	n/d
Chronic transfusion, n (%)	0 (0.0)	n/d
Red cell features		
HbF (%)	7.4 (0.6-28.8)	0.5 (0.4-0.6)
HbS (%)	81.3 (59.4-89.3)	0.0 (0.0-0.0)
Hb (g/dL)	9.4 (7.1-12.3)	14.5 (12.3-17.4)
Reticulocytes (%)	9.1 (4.0-21.9)	1.4 (0.7-2.3)
RBC count ($10^{12}/L$)	2.9 (2.2-4.4)	4.7 (3.7-5.4)
MCV (fl)	82.3 (69.4-125)	92.7 (83.8-105)
MCHC (g/dL)	34.9 (33.4-38.2)	34.4 (31.9-37.5)
Pyruvate kinase features		
PK activity (U/gHb)	13.7 (7.5-22.4)‡	7.9 (5.3-8.7)
HK activity (U/gHb)	2.6 (1.2-4.9)‡	0.8 (0.5-1.0)
PK/HK ratio	5.1 (2.5-9.9)‡	8.9 (7.4-14.0)
PK-thermostability (% residual activity)	54.9 (35.8-80.8)‡	76.3 (72.6-80.9)
PK protein (AU/gHb)	146 (105-176)‡	102 (78-124)
<i>PKLR</i> mutations	none detected	n/d
Metabolic features*		
2,3-DPG ($10^{-3}ug/gHb$)	4.6 (3.5-6.3) ‡	3.3 (2.8-4.1)
ATP ($10^{-3}ug/gHb$)	2.0 (1.9-3.0)	2.0 (1.6-2.5)
ATP/2,3-DPG ratio	0.44 (0.34-0.67)†	0.57 (0.46-0.81)

Numbers represent median (range), unless stated otherwise. HU, hydroxyurea; HbF, fetal hemoglobin; Hb, hemoglobin; HbS, hemoglobin S; RBC, red blood cell; MCV, mean corpuscular volume; MCHC, mean corpuscular hemoglobin concentration; PK, pyruvate kinase; HK, hexokinase; 2,3-DPG, 2,3-diphosphoglycerate; ATP, adenosine triphosphate; n/d, not determined; ‡p<0.0001, †p<0.01

*Metabolic features were obtained from 14/22 SCD patients

Acknowledgements

The authors sincerely wish to thank the patients who participated in this study.

Authorship contributions

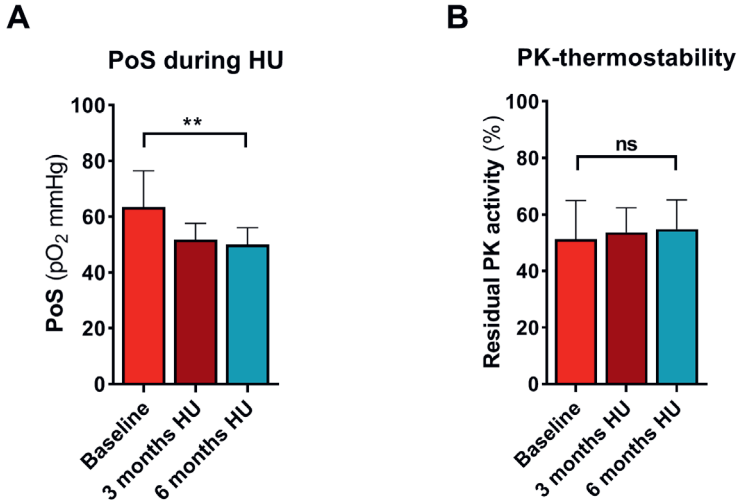
The concept and design of the study was developed by MAER, SS, LD, CK, EJB and RW; MAER, JB, BAO, PAK, and CK developed methodology; MAER, JB, BAO, PAK, VC, HK, and HM acquired data; MAER, JB, BAO, PAK, VC, HK, HM, LD, CK and RW analyzed and interpreted data; MAER and EJB provided patient data; MAER and RW wrote the manuscript; JB, BAO, SS, PAK, HM, REG, GP, LD, CK, and EJB reviewed and/or revised the manuscript.

Disclosure of conflicts of interest

This research has been funded in part by Agios Pharmaceuticals Inc. and the Eurostars program (SCOOP, ESTAR18105). EJB and RW are consultant for Agios Pharmaceuticals.

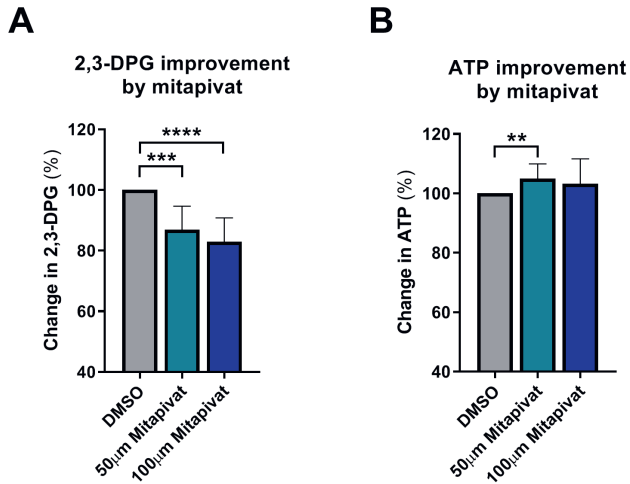
References

- Piel FB, Steinberg MH, Rees DC. Sickle Cell Disease. *N Engl J Med*. 2017;376(16):1561-1573.
- Charache S, Grisolia S, Fiedler AJ, Hellegers AE. Effect of 2,3-diphosphoglycerate on oxygen affinity of blood in sickle cell anemia. *J Clin Invest*. 1970;49(4):806-812.
- Banerjee T, Kuypers FA. Reactive oxygen species and phosphatidylserine externalization in murine sickle red cells. *Br J Haematol*. 2004;124(3):391-402.
- Jensen M, Shohet SB, Nathan DG. The role of red cell energy metabolism in the generation of irreversibly sickled cells in vitro. *Blood*. 1973;42(6):835-842.
- Grace RF, Zanella A, Neufeld EJ, et al. Erythrocyte pyruvate kinase deficiency: 2015 status report. *Am J Hematol*. 2015;90(9):825-830.
- Rab MAE, van Oirschot BA, Kosinski PA, et al. AG-348 (Mitapivat), an allosteric activator of red blood cell pyruvate kinase, increases enzymatic activity, protein stability, and ATP levels over a broad range of PKLR genotypes. *Haematologica*. 2020.
- Kung C, Hixon J, Kosinski PA, et al. AG-348 enhances pyruvate kinase activity in red blood cells from patients with pyruvate kinase deficiency. *Blood*. 2017;130(11):1347-1356.
- Yang H, Merica E, Chen Y, et al. Phase 1 Single- and Multiple-Ascending-Dose Randomized studies of the Safety, Pharmacokinetics, and Pharmacodynamics of AG-348, a First-in-Class Allosteric Activator of Pyruvate Kinase R, in Healthy Volunteers. *Clin Pharmacol Drug Dev*. 2019;8(2):246-259.
- Grace RF, Rose C, Layton DM, et al. Safety and Efficacy of Mitapivat in Pyruvate Kinase Deficiency. *N Engl J Med*. 2019;381(10):933-944.
- Beutler E. Red cell metabolism. A manual of biochemical methods (ed 3rd). Orlando: Grune & Stratton; 1984.
- Rab MAE, van Oirschot BA, Bos J, et al. Rapid and reproducible characterization of sickling during automated deoxygenation in sickle cell disease patients. *Am J Hematol*. 2019;94(5):575-584.
- Rab MAE, Kanne CK, Bos J, et al. Methodological aspects of the oxygenscan in sickle cell disease: A need for standardization. *Am J Hematol*. 2020;95(1):E5-E8.
- Bianchi P, Fermo E, Glader B, et al. Addressing the diagnostic gaps in pyruvate kinase deficiency: Consensus recommendations on the diagnosis of pyruvate kinase deficiency. *American journal of hematology*. 2019;94(1):149-161.
- Al-Samkari H, Addonizio K, Glader B, et al. The pyruvate kinase (PK) to hexokinase enzyme activity ratio and erythrocyte PK protein level in the diagnosis and phenotype of PK deficiency. *Br J Haematol*. 2020.
- Sprengers ED, van Berkel TJ, Koster JF, Staal GE. Influence of the rebox state of glutathione upon pyruvate kinase in the intact erythrocyte. *Clin Chim Acta*. 1977;80(3):495-502.
- Anastasiou D, Pouligiannis G, Asara JM, et al. Inhibition of pyruvate kinase M2 by reactive oxygen species contributes to cellular antioxidant responses. *Science*. 2011;334(6060):1278-1283.
- Alli N, Coetzee M, Louw V, et al. Sickle cell disease in a carrier with pyruvate kinase deficiency. *Hematology*. 2008;13(6):369-372.
- Nardo-Marino A, Brousse V, Rees D. Emerging therapies in sickle cell disease. *Br J Haematol*. 2020;190(2):149-172.
- Salinas Cisneros G, Thein SL. Recent Advances in the Treatment of Sickle Cell Disease. *Front Physiol*. 2020;11:435.
- Rab, MAE, Kanne, CK, Bos J et al. Oxygen gradient ektacytometry derived-biomarkers are associated with vaso-occlusive crises and correlate with treatment response in sickle cell disease. *Am J Hematol*. 2021;96(1):E29-E32



Supplemental Figure 1. Clinical benefit of hydroxyurea (HU) therapy in SCD patients is independent of PK properties

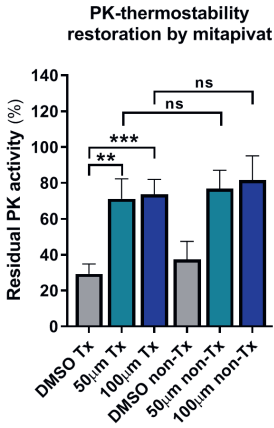
(A) SCD patients (N=5) followed after starting HU therapy show a significant decrease in PoS after 3 (dark red bar) and 6 months (light turquoise), compared to baseline (red). (B) SCD patients (N=5) followed after starting HU therapy show no significant increase in mean PK-thermostability levels. Error bars represent standard deviation. $**p<0.01$; ns, not significant.



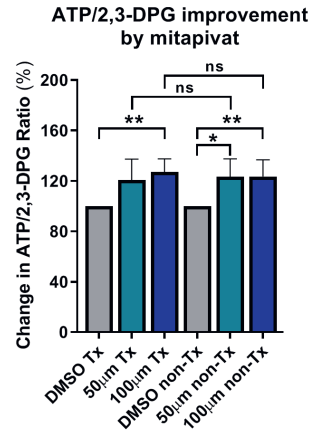
Supplemental Figure 2. Ex vivo treatment with mitapivat decreases 2,3-DPG levels

2,3-diphosphoglycerate (2,3-DPG, panel A) and adenosine triphosphate (ATP) (levels (panel B) after 22 hours incubation of buffy coat-depleted blood of SCD patients (N=11) in presence of 50 μ M (light turquoise) and 100 μ M (dark blue) mitapivat shows, respectively, a significant decrease of 17% in 2,3-DPG levels and a non-significant increase of 5% in ATP compared to vehicle controls (DMSO control, grey, N=11). Mean values are reported, error bars represent standard deviation. $****p<0.0001$, $***p<0.001$, $**p<0.01$

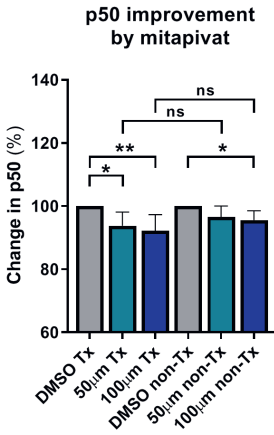
A



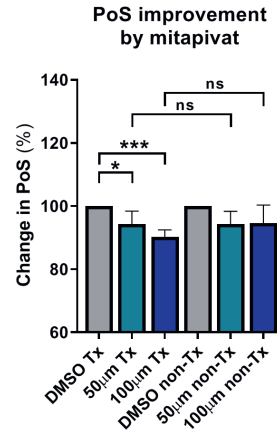
B



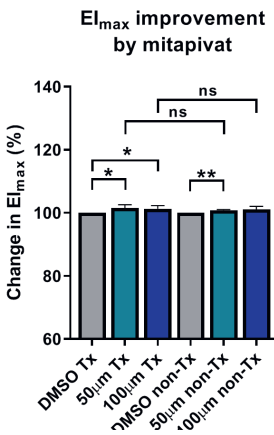
C



D

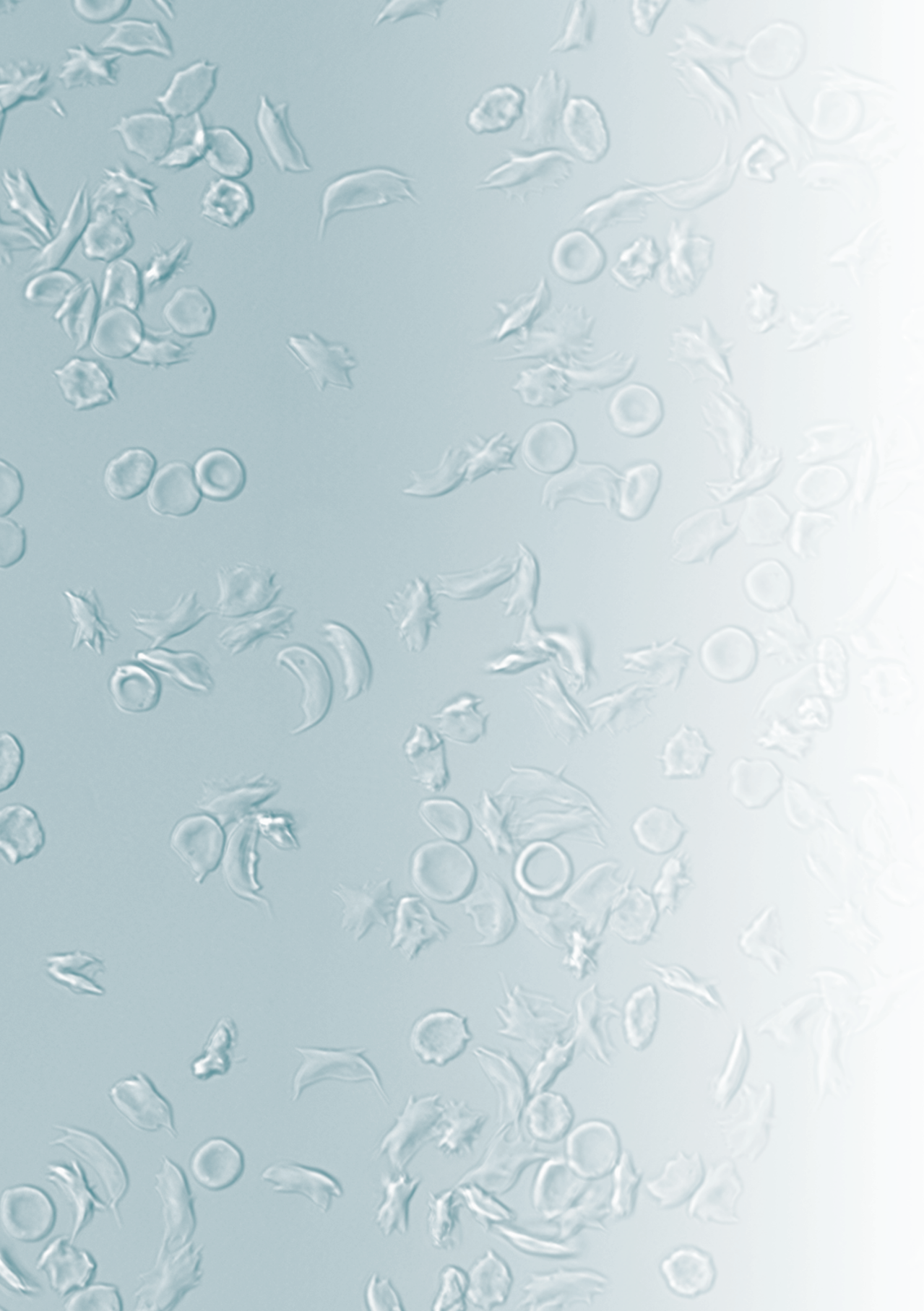


E



Supplemental Figure 3. Comparable response to *ex vivo* treatment with mitapivat between non-transfused and transfused patients

PK-thermostability (panel A), ATP/2,3-DPG ratio (panel B), p50 (panel C), PoS (panel D) and EI_{max} (panel E) were measured on RBCs from SCD patients (N=11, except for PoS and EI_{max}: N=9) after 22 hours incubation of buffy coat-depleted blood in presence of 50 µM (light turquoise) and 100 µM (dark blue) mitapivat. The increases in PK-thermostability, ATP/2,3-DPG ratio, and EI_{max} as well as the decreases in p50 and PoS, compared to vehicle controls (DMSO control, grey, N=11), were comparable and statistically not different between non-transfused and transfused SCD patients. Mean values are reported, error bars represent standard deviation. ****p*<0.0001, ***p*<0.001, **p*<0.05



Chapter 9

Identification of biomarkers that are associated with clinical complications of hemoglobin SC disease and sickle cell anemia

Manuscript in preparation

Minke A.E. Rab^{1,2}, Celeste K. Kanne³, Mitchel Berrevoets¹, Jennifer Bos¹,
Brigitte A. van Oirschot¹, Erik Teske⁴, Roger E.G. Schutgens², Gerard Pasterkamp¹,
Richard van Wijk¹, Eduard J. van Beers^{2*} and Vivien A. Sheehan^{3*}

¹ Central Diagnostic Laboratory - Research, University Medical Center Utrecht, Utrecht University, Utrecht, The Netherlands

² Van Creveldkliniek, University Medical Center Utrecht, Utrecht University, The Netherlands

³ Department of Pediatrics Emory University School of Medicine, Children's Healthcare of Atlanta, Atlanta, Georgia, USA,

⁴ Department of Clinical Sciences, Faculty of Veterinary Medicine, Utrecht University, Utrecht, The Netherlands

** These authors contributed equally*

Abstract

Sickle cell disease (SCD) is an umbrella term used to describe inherited anemias that originate from a mutation in *HBB*, the gene coding for β -globin, that causes the formation of the abnormal hemoglobin S (HbS). The two most common genotypes are HbSS, termed sickle cell anemia (SCA) and HbSC, termed hemoglobin SC disease. Due to the higher prevalence and more severe clinical symptoms in SCA, attention focused on this latter group of patients. Patients with HbSC disease who report significant SCD related symptoms are treated largely the same as SCA patients, despite differences in disease pathophysiology. We analyzed an adult (n=30) and pediatric cohort (n=226) of SCA and HbSC individuals to assess differences in RBC characteristics, including dense red blood cells (dense RBCs), blood viscosity and ektacytometry-derived parameters, including the recently developed oxygen gradient ektacytometry. We found that in particular dense RBCs, blood viscosity and point of sickling (PoS), an oxygen gradient ektacytometry-derived biomarker that reflects the oxygen tensions when sickling is initiated, are notably different in HbSC disease compared to SCA. Subsequently, we assessed in the pediatric cohort (189 SCA and 37 HbSC individuals) if PoS, dense RBCs or blood viscosity are associated with clinical complications. We found that biomarkers that relate to clinical complications in SCA, such as PoS, are not applicable for HbSC disease: In SCA, PoS was associated with occurrence of acute chest syndrome (ACS, for every 10mmHg increase OR 1.84, $p < 0.0001$, adjusted OR 1.67, $p = 0.002$), but no such association was found in children with HbSC. In contrast, we found an association of blood viscosity and ACS (OR 9.3, $p = 0.012$; adjusted OR 13.5, $p = 0.015$) in HbSC children, while we found no such association in SCA. We conclude that sickling is a key factor in the pathophysiology of SCA, whereas in HbSC disease blood viscosity might play a crucial role in development of certain complications like ACS. This study confirms that SCA and HbSC disease are separate disease entities that warrant a distinct treatment approach.

Introduction

Sickle cell disease (SCD) is a generic term used to describe a heterogeneous group of inherited anemias that originates from mutations in the *HBB* gene responsible for the synthesis of the beta subunit of hemoglobin.^{1,2} The two most common single nucleotide mutations result in the replacement of glutamic acid with either valine or lysine in the β globin chain, leading to the formation of either the abnormal hemoglobin S (HbS) or hemoglobin C (HbC). Inheritance of two alleles coding for HbS results in sickle cell anemia (SCA) the most common form of SCD with an estimated number of 217 331 newborns affected annually worldwide.³ Co-inheritance of a β^S and a β^C allele results in hemoglobin SC disease (HbSC), the second most common form of SCD with an estimated number of 54 736 newborns annually worldwide.³

HbS polymerizes under deoxygenated conditions leading to the formation of crescent or sickle-shaped red blood cells (RBC) with altered rheological properties.⁴⁻⁷ This results in hemolytic anemia, blockage of blood vessels, and affiliated clinical symptoms like vaso-occlusive crises (VOC), acute chest syndrome (ACS), stroke, and organ damage.^{1,2,7} The pathophysiology of HbSC disease is notably different. HbC does not sickle, and HbCC individuals are generally asymptomatic. However, in combination with HbS, HbC causes the formation of intracellular crystals, which ultimately induces RBC dehydration through the loss of intracellular K^+ and water. This raises intracellular hemoglobin concentration up to levels sufficiently high to induce SCA-like polymerization and resulting pathology.⁸⁻¹¹ In comparison with individuals with SCA, those with HbSC have generally lower prevalence of sickle specific complications like VOCs, stroke, and leg ulcers, and a higher prevalence of chronic organ complications like proliferative retinopathy and sensorineural otological disorders.^{8,9,12} Several prior studies reported differences in the pathophysiology of HbSC disease and SCA.^{8,9,12} The K-Cl Cotransporter (KCC) appears to play a key role in the dehydration of RBCs in HbSC disease^{13,14}, while the Gardos channel (KCNN4) and deoxygenation-induced cation conductance play a greater role in SCA.¹³ This leads to differences in cation homeostasis and results in a higher number of dense and dehydrated RBCs in HbSC disease.^{8,15,16} Despite the higher number of dense dehydrated RBCs in HbSC compared to SCA, the total HbSC RBC population is less rigid and more deformable compared with SCA.^{7,17}

Conventional laboratory parameters such as hemoglobin, fetal hemoglobin (HbF), reticulocyte count and mean corpuscular volume (MCV) are widely used to monitor patients with SCD. However, the extent to which these laboratory parameters can be applied for HbSC disease remains to be elucidated. Research that aims to identify and implement biomarkers for HbSC disease severity or association with certain complications is scarce. K-Cl cotransport activity is clinically relevant in HbSC, and is a promising drug target.¹⁴ It is essential that we identify more markers of disease severity in HbSC, in order to identify patients in need of early intervention, and to develop novel therapies targeting HbSC specific pathophysiology.

The increasing number of FDA approved therapeutic options, including voxelotor¹⁸, l-glutamine¹⁹ and crizanlizumab²⁰, is promising for the treatment of SCD, but it is important to note that most drugs were approved based on the results found in individuals with SCA and relatively little is known about the effects of these drugs in individuals with HbSC disease.^{21,22} Recently, we developed a novel assay, oxygen gradient ektacytometry, that characterizes sickling behavior in SCD.⁵ Previously we showed that the oxygen gradient ektacytometry-derived biomarkers Point of Sickling (PoS) and Elmin (minimum elongation index upon deoxygenation) are associated with occurrence of VOC and are modified by standard of care therapy hydroxyurea (HU) and blood transfusion in SCA.²³

In this study, we explored whether the previously described associations found between the occurrence of clinical complications and oxygen gradient ektacytometry-derived parameters in SCA could be extended to HbSC disease. Furthermore, we investigated how the characteristics and rheological properties of RBCs in both adults and children with either SCA or HbSC disease differ. To identify possible biomarkers for HbSC, we studied different RBC and rheological characteristics, including sickling behavior, in an adult and pediatric cohort, and assessed which RBC characteristics were associated with clinical complications.

Methods

Patients

Twenty-two adults with SCA, eight adults with HbSC, and nine healthy controls (HC) were enrolled in the University Medical Centre Utrecht (UMCU) for evaluation of RBC characteristics. Two additional pediatric patient cohorts were included to assess the potency of studied parameters as possible biomarkers. One cohort was comprised of 189 children enrolled at Texas Children's Hematology Center (TCHC) with either HbSS or HbS/ β -thalassemia, and one cohort was comprised of 37 pediatric HbSC individuals also enrolled at TCHC. All blood samples were obtained at steady state, and patients that received blood transfusions <3 months prior to blood sampling were excluded from the study.

Study procedures, which included collection of an additional tube of peripheral blood and review of medical records, were approved by local ethical committee or internal review board in accordance with the Declaration of Helsinki (registered under 17/392 and 17/450 at UMCU, and H35473 at Baylor College of Medicine). Informed consent was obtained for all patients. Blood samples of healthy controls were obtained by the minidonordienst (MDD) from the UMCU, The Netherlands.

History of clinical complications was collected on subjects in both adult and pediatric cohorts. Clinical complications included ACS, VOC, cerebral infarction (stroke or silent infarcts), osteonecrosis, retinopathy, priapism, gallstones and iron overload. VOC was defined as occurrence of a painful event unexplained by any other cause in the last 2 years that required hospital admission or visit to the emergency room or outpatient clinic. Complication rate was defined as the sum of complications that had occurred in the past within the lifetime of the individual, with the exception of VOC that was only counted if it had occurred within the last two years. All other complications were included if they occurred in the patient's lifetime.

Laboratory parameters

Routine laboratory parameters, i.e. complete blood count, were analyzed using the Abbott Cell-Dyn Sapphire hematology analyzer (Abbott Diagnostics Division, Santa Clara, CA, USA) or the Advia 120/2120 hematology analyzer (Siemens Healthcare Diagnostics, NY, USA). The percentage of dense RBCs was analyzed using the Advia 120/2120 hematology analyzer (Siemens Healthcare Diagnostics, NY, USA). We defined RBCs with a hemoglobin concentration >41 g/dL and a volume of 60 to 120 fL as normocytic dense RBCs (normo DRBC), RBCs with a hemoglobin concentration >41 g/dL and a volume < 60 fL as microcytic dense RBCs (micro DRBC), and RBCs with a hemoglobin concentration of >41 g/dL and a volume below 120 fL as the total percentage of dense RBCs (total DRBC).

Ektacytometry

RBC deformability and sickling behavior was analyzed by the laser optical red cell analyzer (Lorrc MaxSis, RR Mechatronics, Zwaag, The Netherlands) as described elsewhere.²⁴ Briefly, the sample solution, containing a mixture of whole blood and isotonic polyvinylpyrrolidone (PVP) was injected between a static inner cylinder (BOB) and a rotating outer cylinder (CUP) to generate a predefined shear stress. The change in the laser diffraction pattern from circular to elliptical is captured by a camera and the accompanying vertical (A) and horizontal (B) axis is used to calculate the elongation index (EI) by the formula $(A-B)/(A+B)$. This calculated EI reflects RBC deformability.

Osmotic gradient ektacytometry

Osmotic gradient ektacytometry measurements were performed as described elsewhere.^{24,25} Briefly, 250-350 μ L of whole blood, standardized to a fixed RBC count of 1000×10^6 , was added to 5 ml of isotonic PVP. Elongation index (EI) was continuously measured under a fixed shear stress (30 Pa) as a function of increasing osmolality (40-600 mOsm/kg). Four key parameters are generated by osmotic gradient ektacytometry: The osmolality at minimal EI in the hypotonic range (O_{\min}), maximal EI (EI_{\max}), osmolality at 50% of the maximal EI in the hypertonic region (O_{hyper}), and area under the curve (AUC) were determined.

Cell membrane stability test (CMST)

The CMST measurements were performed according to the manufacturer's instructions and are described in detail elsewhere.²⁶ Briefly, 300×10^6 RBCs (50-100 μ L of whole blood), was added to 5 ml of isotonic PVP. This sample solution is injected into the gap between the bob and the cup and subsequently exposed to a shear stress of 100 Pa for 1800 seconds. The change in the EI (ΔEI) was determined by calculating the difference between the median EI of the first and the last 100 seconds of the CMST. The ΔEI is considered to reflect RBC membrane health and shows the capacity of RBCs to shed membrane.

Oxygen gradient ektacytometry

Oxygen gradient ektacytometry, a next generation deformability and sickling assay, measures RBC deformability over a gradient of oxygen tensions (pO_2). Oxygen gradient ektacytometry generates three key parameters: 1) EI_{\max} , RBC deformability at normoxia, before the deoxygenation cycle is initiated; 2) EI_{\min} , minimum RBC deformability upon

deoxygenation; and 3) the Point of Sickling (PoS): the oxygen tension at which a 5% decrease in deformability is observed during deoxygenation, reflecting the patient-specific pO_2 at which polymers start to grow and sickling is initiated. In addition, the parameter Recovery reflects the unsickling process and is calculated as the percentage of EI_{max} (Figure 2A).⁵ The oxygenscan module is a new add-on feature of the Lorrca ektacytometer, allowing the measurement of RBC deformability during a continuously changing gradient of pO_2 . To carry out an oxygen gradient ektacytometry measurement, whole blood, standardized to a fixed RBC count of 200×10^6 , is mixed with 5 mL Oxy-Iso (RR Mechatronics, osmolarity 282-286 mOsm/kg, pH 7.35-7.45 at room temperature $21 \pm 1^\circ\text{C}$, viscosity 28-30 cP). Detailed description of the technique and sample handling is described elsewhere.^{27,28} Samples were measured at one of the two different sites which were located in The Netherlands (UMCU) and US (TCHC).

Blood viscosity

Whole blood viscosity was measured at a native hematocrit, at 37°C at a shear rate of 45 s^{-1} and 225 s^{-1} using a Brookfield DVT cone and plate viscometer (Brookfield, Massachusetts) as previously described.²⁹

Statistical analysis

Analysis was performed by using GraphPad Prism version 8.3.0 for Windows (GraphPad Software, San Diego, CA, USA) or SPSS (version 25.0.0.2 IBM). Normality tests were conducted using the Kolmogorov-Smirnov test. The sample means of the groups were compared using a two-tailed, unpaired t-test analysis, or Mann-Whitney test when appropriate. Logistic regression analysis was performed in both pediatric SCA cohort and pediatric HbSC cohort. If the regression-coefficient increased in a linear manner when assessing a specific complication, a logistic regression analysis was performed for PoS, blood viscosity and micro DRBCs to calculate odds ratios (OR) for every 10 mmHg increase in PoS, every 1.0 cP increase in viscosity or every 1.0% in micro DRBC for that complication. ORs were corrected for age, gender and genotype if indicated. A p -value < 0.05 was considered statistically significant.

Results

An adult cohort consisting of 22 individuals with SCA and eight individuals with HbSC, and a pediatric cohort comprised of 189 children with SCA and 37 with HbSC were studied. In the adult cohort, the majority of HbSC patients were female (Table 1). Forty-one percent of adults with SCA were treated with HU compared to 13% of adults with HbSC. This was reflected by low values of HbF in the latter group (1.3% compared to 9.9% in adults with SCA). In the pediatric cohort 85% of children with SCA were on HU therapy compared to 41% of children with HbSC (Table 2) which was confirmed by HbF levels of 15.6% and 1.4% respectively.

Routine laboratory parameters confirmed previously reported differences in red cell characteristics between SCA and HbSC patients (Table 1 and 2). Occurrence of acute and chronic complications of SCD were considerably different between the genotypes, with ACS, and retinopathy as the most pronounced difference in both cohorts. In addition, rate of

Table 1. Characteristics

	Adult cohort	
	SCA (n=22)	HbSC (n=8)
Patient related		
Sex, female, % (n)	45% (10/22)	88% (7/8)
Age, years, mean (range)	28 (16 - 57)	24 (17 - 34)
HbS/ β -thalassemia, % (n)	14% (3/22)	0% (0/8)
Splenectomy, % (n)	9% (2/22)	0% (0/8)
HU, % (n)	41% (9/22)	13% (1/8)
Red cell characteristics		
HbF (%)	9.9 \pm 8.7	1.3 \pm 0.5
HbS (%)	77.5 \pm 8.7	43.5 \pm 1.4
HbC (%)	0.0 \pm 0.0	45.8 \pm 1.4
Hb (g/dL)	9.4 \pm 1.2	12.9 \pm 1.2
HCT (%)	26.6 \pm 3.5	34.0 \pm 2.8
ARC ($10^9/L$)	251 \pm 97	154 \pm 100
RBC count ($10^{12}/L$)	3.0 \pm 0.6	4.6 \pm 0.5
MCV (fl)	90.0 \pm 16.7	75.5 \pm 13.5
MCHC (g/dL)	35.7 \pm 1.7	35.6 \pm 1.5
Clinical complications		
ACS	36% (8/22)	13% (1/8)
VOC	73% (16/22)	63% (5/8)
Cerebral infarction	9% (2/22)	0% (0/8)
Osteonecrosis	18% (4/22)	0% (0/8)
Retinopathy	18% (4/22)	63% (5/8)
Priapism	25% (3/12)	100% (1/1)
Gallstones	45% (10/22)	25% (2/8)
Iron overload	9% (2/22)	0.0% (0/8)
Complication rate	2.2 \pm 1.4	1.6 \pm 1.3
No complications	9% (2/22)	13% (1/8)

Numbers represent mean \pm SD, unless stated otherwise. SCA, sickle cell anemia; HbS, hemoglobin S; HU, hydroxyurea, HbF, fetal hemoglobin; Hb, hemoglobin; ARC, absolute reticulocyte count, RBC, red blood cell; MCV, mean corpuscular volume; MCHC, mean corpuscular hemoglobin concentration; n/a, not applicable; ACS, acute chest syndrome; VOC, vaso-occlusive crisis

complications, i.e. number of different complications that had occurred in the individual, was markedly higher in both adults and children with SCA. Moreover, the percentage of children without complications was substantially higher in the HbSC group compared to the SCA group (49% and 28% respectively). This was much less apparent in the adult cohort, which could indicate that although HbSC is considered a milder form of SCD, all kinds of complications do occur during a lifetime, but at a slower pace.

In our search for biomarkers reflecting HbSC disease severity and/or clinical complications we measured several RBC characteristics including total percentage of dense RBCs and the sub fractions normo DRBCs and micro DRBCs. Micro DRBCs were significantly higher in adults and children with HbSC disease compared to SCA (Figure 1B and E), while normo DRBCs were only significantly higher in children with HbSC disease compared to SCA (Figure 1A and D). Total DRBCs were significantly lower in individuals with SCA compared to HbSC

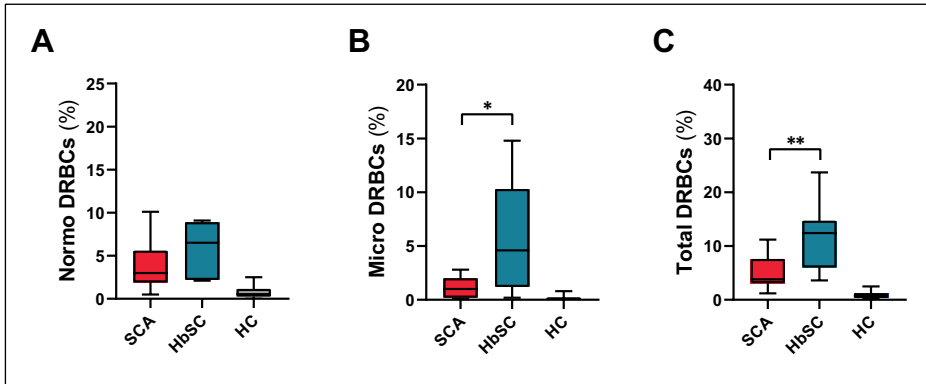
Table 2. Characteristics

	Pediatric cohort	
	SCA (n=189)	HbSC (n=37)
Patient related		
Sex, female, % (n)	44% (83/189)	35% (13/37)
Age, years, mean (range)	10 (2 - 19)	10 (2 - 18)
HbS/β-thalassemia, % (n)	11% (21/189)	0% (0/37)
Splenectomy, % (n)	19% (36/189)	5% (2/37)
HU, % (n)	85% (161/189)	41% (15/37)
Red cell characteristics		
HbF (%)	15.6 ± 8.3	1.4 ± 1.2
HbS (%)	80.5 ± 8.1	48.9 ± 1.0
HbC (%)	0.0 ± 0.0	46.0 ± 0.8
Hb (g/dL)	8.9 ± 1.4	10.9 ± 1.0
HCT (%)	27.3 ± 4.0	31.4 ± 2.4
ARC (10 ⁹ /L)	388 ± 156	207 ± 71
RBC count (10 ¹² /L)	3.0 ± 0.7	4.3 ± 0.7
MCV (fl)	93.4 ± 14.0	75.2 ± 11.7
MCHC (g/dL)	32.7 ± 1.3	34.8 ± 1.4
Clinical complications		
ACS	53% (101/189)	24% (9/37)
VOC	48% (88/183)	42% (14/33)
Cerebral infarction	8% (15/189)	5% (2/37)
Osteonecrosis	7% (14/189)	11% (4/37)
Retinopathy	5% (10/189)	11% (4/37)
Priapism	15% (16/106)	13% (3/24)
Gallstones	20% (37/189)	11% (4/37)
Iron overload	9% (17/189)	0.0% (0/37)
Complication rate	1.6 ± 0.3	1.1 ± 1.2
No complications	28% (52/189)	49% (18/37)

Numbers represent mean ± SD, unless stated otherwise. SCA, sickle cell anemia; HbS, hemoglobin S; HU, hydroxyurea, HbF, fetal hemoglobin; Hb, hemoglobin; ARC, absolute reticulocyte count, RBC, red blood cell; MCV, mean corpuscular volume; MCHC, mean corpuscular hemoglobin concentration; n/a, not applicable; ACS, acute chest syndrome; VOC, vaso-occlusive crisis

in both cohorts (Figure 1C and F). These results indicate that RBCs from HbSC patients are denser compared to SCA RBCs, which is especially evident by the increase in micro DRBCs. This confirms previously reported findings of dense and dehydrated RBCs in patients with HbSC disease.

Adult cohort



Pediatric cohort

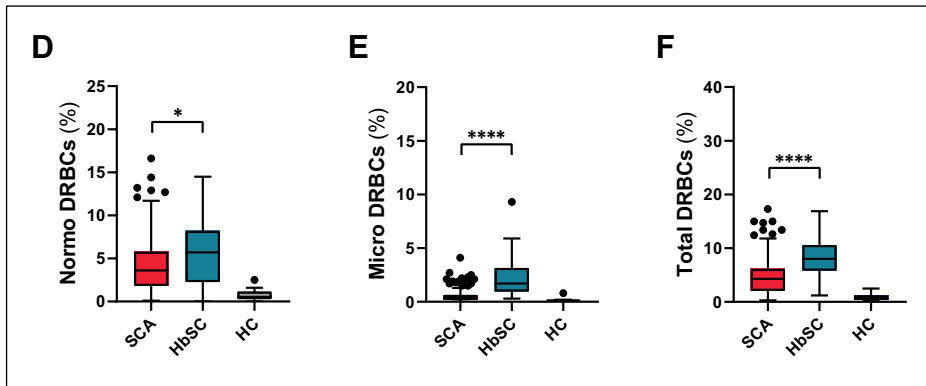


Figure 1. Dense red blood cells and sub fractions in adult and pediatric cohorts comprised of SCA and HbSC patients. Median values of normocytic dense red blood cells (normo DRBC) are depicted in panel A and D. Median values of microcytic DRBCs are shown in B (adults) and E (children). Median values of total DRBCs are depicted in C (adults) and F (children).

Whiskers represent Tukey. **** $p < 0.0001$, ** $p < 0.01$, * $p < 0.05$.

SCA, sickle cell anemia; HbSC, hemoglobin SC disease; HC, healthy control

Oxygen gradient ektacytometry-derived biomarkers are more favorable in HbSC disease

Oxygen gradient ektacytometry was performed to study to what extent sickling behavior was different in HbSC disease compared to SCA. The representative curves of the two patient groups are displayed in Figure 2A. The PoS, reflecting the patient specific pO_2 when sickling is initiated, occurred at a significantly lower oxygen tension in both children and adults with HbSC when compared with SCA (Figure 2C and F).

EI_{max} was not different between the genotypes in the adult cohort (Figure 2D), while in the pediatric HbSC cohort EI_{max} was lower, which is unfavorable (Figure 2G). EI_{min} was significantly higher, which is more favorable, in individuals with HbSC compared to SCA in the pediatric cohort (Figure 2H), but no such difference was found in the adult cohort (Figure 2E). In the adult cohort an additional parameter, recovery, that reflects the unsickling process, was calculated showing a substantial lower percentage of RBCs that was able to regain their initial degree of deformability upon reoxygenation (Figure 2B).

These combined results highlight the fact that RBCs in HbSC disease display different sickling behavior compared to RBCs in SCA, likely due to the crystallization of hemoglobin C.

Osmotic gradient ektacytometry-derived parameters indicate a more dehydrated RBC population in HbSC disease

The deformability of RBCs in SCA and HbSC adults was also studied with osmotic gradient ektacytometry, and representative curves of both SCA and HbSC are shown in Figure 3A. The surface-area-to-volume ratio (O_{min}) and the cytoplasmic viscosity or hydration state (O_{hyper}) were significantly decreased in adults with SCA and HbSC disease. This decrease was more pronounced in adults with HbSC disease (Figure 3B and D). This indicates that RBCs in HbSC patients are more dehydrated with a reduced surface-area-to-volume ratio. In contrast, the maximum deformability (EI_{max}) was not statistically different (Figure 3C), reflecting a similar loss of deformability in SCA and HbSC adults. The area under the curves (AUC) displayed no significant difference between the two groups (Figure 3E).

CMST in patients with SCA and HbSC disease

The cell membrane stability test (CMST), that involves exposure of RBCs to a long period of supraphysiological shear stress was performed to investigate membrane stability and the ability to shed membrane in adults with SCA and HbSC disease. Representative curves of both SCA and HbSC disease and healthy controls (HC) are displayed in Figure 4A. The ΔEI was higher (i.e. more negative) in adults with HbSC (median -0.07, IQR 0.17) when compared with adults with SCA (median -0.12, IQR 0.16), although this was not significant ($p=0.161$, Figure 4B). This suggests that the membrane of RBCs from adults with HbSC are better able to shed membrane when compared to RBCs obtained from adults with SCA. These findings indicate that even though RBCs obtained from HbSC patients are more dehydrated, this does not result in a decreased ability to shed membrane.

Blood viscosity is higher in children with HbSC disease

Blood viscosity measured at two different shear rates (45 s^{-1} and 225 s^{-1}) was significantly higher in children with HbSC disease compared to SCA (Figure 5A and B). Factors that could contribute to higher blood viscosity in HbSC disease could be higher hemoglobin and hematocrit levels (Table 2) in relation to a slightly lower RBC deformability in HbSC (Figure 2G).

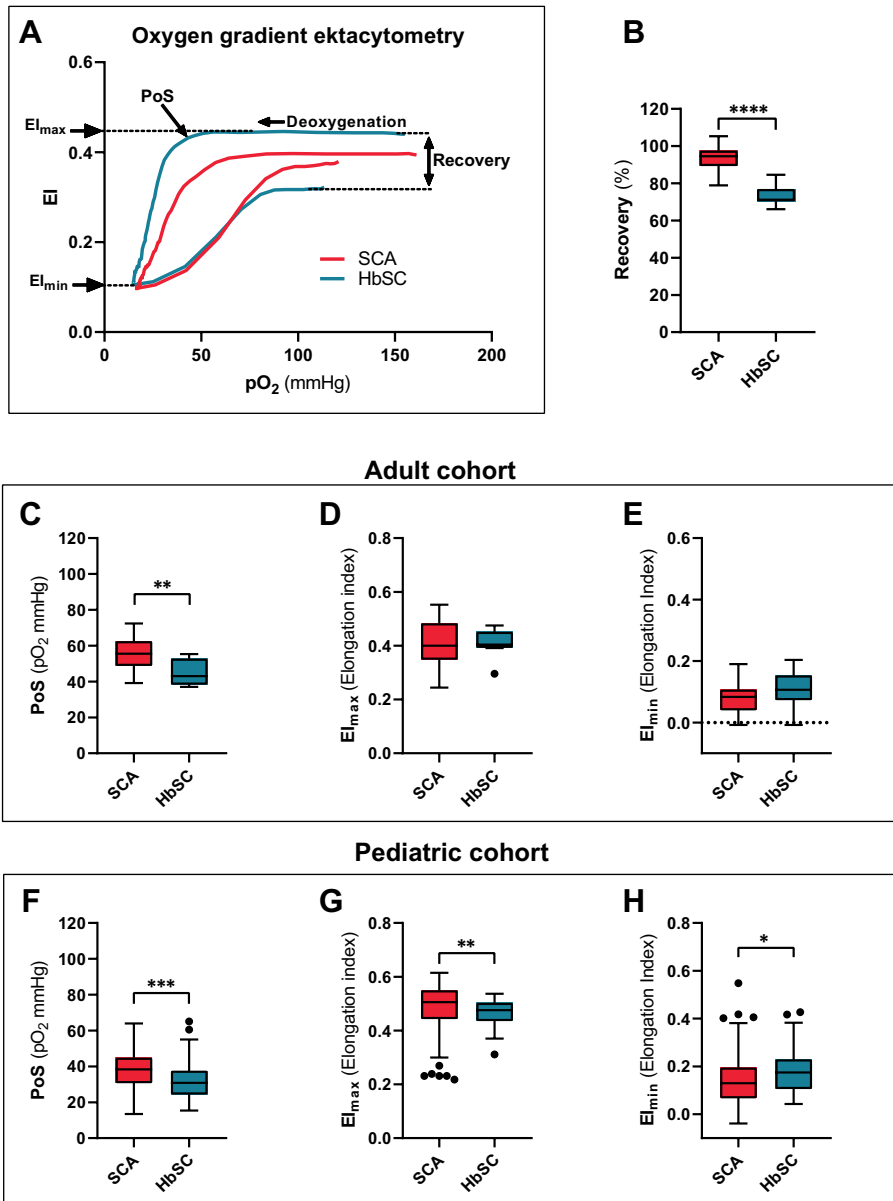


Figure 2. Oxygen gradient ektactometry-derived parameters are different in HbSC disease compared to SCA in both children and adults. Representative oxygen gradient ektactometry curves are shown in panel A.

Median values of PoS are lower in HbSC compared to SCA in both adults (C) and children (F). Median values of El_{max} , reflecting RBC deformability at normoxia, are not different in adults with HbSC compared to adults with SCA (D). Median values of El_{min} , reflecting the minimum deformability at the end of the deoxygenation cycle, are comparable in adults with SCA or HbSC (E) and higher in children with HbSC (H). Median values of recovery, reflecting the unsickling process upon reoxygenation is lower in adults with HbSC compared to SCA (E). Median values of El_{max} are lower in children with HbSC (G). Whiskers represent Tukey. **** $p < 0.0001$, *** $p < 0.001$, ** $p < 0.01$, * $p < 0.05$. SCA, sickle cell anemia; HbSC, hemoglobin SC disease; PoS , point of sickling.

The potential of PoS as biomarker for clinical complications

To explore how PoS is associated with occurrence of clinical complications of both SCA and HbSC we analyzed the pediatric cohort with logistic regression analysis. We found a positive association between the OR of clinical complications and PoS in the pediatric SCA cohort (Table 3). ORs were not significantly affected by sex or genotype, but age did significantly confound results and therefore adjusted ORs (aOR) were calculated. ORs for ACS (SCA cohort OR 1.84, $p < 0.0001$; aOR 1.67, $p = 0.002$), VOC (OR 1.45, $p = 0.015$; aOR 1.28, $p = 0.118$), cerebral infarction (OR 1.77, $p = 0.039$; aOR 1.55, $p = 0.144$) were higher with every 10 mmHg PoS increment. More importantly, the OR of the occurrence (positive history) of a major SCD complication (ACS, cerebral infarction or VOC) was even greater (pediatric cohort: OR 1.92,

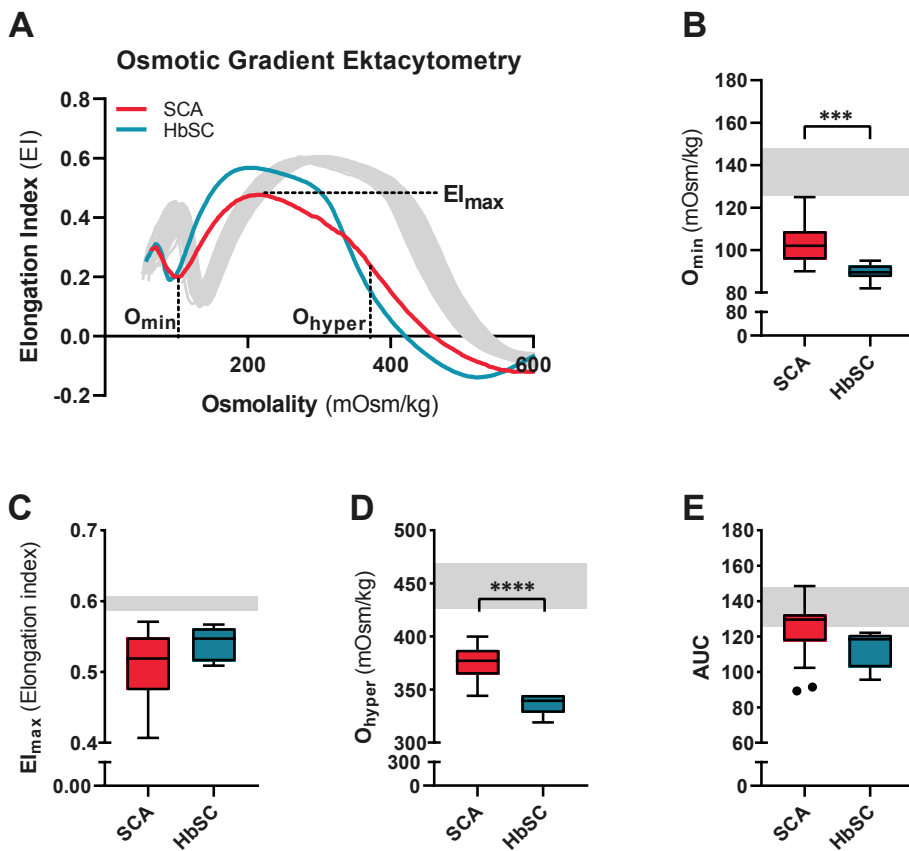


Figure 3. Osmotic gradient ektacytometry-derived parameters are different in HbSC disease compared to SCA in adults. Representative osmotic gradient ektacytometry curves are shown in panel A. Median values of O_{min} , reflecting membrane surface area to volume ratio, are lower in HbSC compared to SCA in adults (B). Median values of EI_{max} , reflecting maximum RBC deformability, are not different in adults with HbSC compared to adults with SCA (C). Median values of O_{hyper} , reflecting RBC hydration are lower in adults with HbSC (D). Median values of area under the curve (AUC) are not different in adults with HbSC compared to SCA (E).

Whiskers represent Tukey. Grey area represents range of healthy controls. **** $p < 0.0001$, *** $p < 0.001$. SCA, sickle cell anemia; HbSC, hemoglobin SC disease; AUC, area under the curve.

$p < 0.0001$; aOR 1.67, $p = 0.007$), further supporting the hypothesis that PoS is associated with a more severe phenotype in SCA. Moreover, when occurrence of 1 or more complications (ACS, VOC, cerebral infarction, osteonecrosis, retinopathy, priapism, gallstones or iron overload) was assessed, OR was higher when the PoS was higher, in increments of 10 mmHg, (OR 1.93, $p = 0.0002$, aOR 1.65, $p = 0.012$) in the pediatric SCA cohort (Table 3). When ORs were calculated for PoS and clinical complications in the pediatric HbSC cohort no significant OR or aOR was found (Table 4), indicating that sickling behavior is not a major determinant in the occurrence of clinical complications.

Table 3. Logistic regression analysis of PoS, blood viscosity and micro DRBCs shows increased or decreased odds ratios for specific complications in SCA. Odds ratios (OR) and adjusted ORs were calculated for every 10 mmHg increase in PoS (n=189), every 1.0 cP increase in blood viscosity (n=120), and for every 1.0% increase in micro DRBCs (n=189) in children with SCA.

Pediatric SCA cohort						
PoS (n=189)						
for every 10 mmHg increase		Odds ratio			Adjusted odds ratio	
Complication	OR	95% CI	P-value	OR	95% CI	P-value
ACS	1.84	1.35 – 2.52	<0.0001	1.67	1.19 – 2.32	0.002
VOC	1.45	1.08 – 1.94	0.015	1.28	0.93 – 1.76	0.118
Cerebral infarction	1.77	1.02 – 3.06	0.039	1.55	0.59 – 2.56	0.144
Osteonecrosis	1.48	0.86 – 2.56	0.166	1.23	0.67 – 2.26	0.496
Gallstones	1.49	1.03 – 2.16	0.036	1.23	0.80 – 1.90	0.331
≥1 major complication*	1.92	1.35 – 2.73	<0.0001	1.67	1.15 – 2.42	0.007
≥1 any complication	1.93	1.33 – 2.81	0.0002	1.65	1.11 – 2.44	0.012
Blood viscosity (n=120)						
for every 1 cP increase		Odds ratio			Adjusted odds ratio	
Complication	OR	95% CI	P-value	OR	95% CI	P-value
ACS	0.79	0.56 – 1.10	0.156	0.72	0.51 – 1.03	0.072
Osteonecrosis	1.83	1.08 – 3.11	0.025	1.54	0.88 – 2.67	0.130
Priapism	1.54	0.93 – 2.56	0.091	1.40	0.81 – 2.41	0.224
Iron overload	0.38	0.16 – 0.87	0.022	0.34	0.15 – 0.78	0.011
Micro DRBCs (n=189)						
for every 1% increase		Odds ratio			Adjusted odds ratio	
Complication	OR	95% CI	P-value	OR	95% CI	P-value
Osteonecrosis	2.26	1.15 – 4.44	0.018	1.75	0.88 – 3.46	0.108
Retinopathy	0.53	0.11 – 2.58	0.428	0.53	0.12 – 2.43	0.415
Priapism	1.04	0.47 – 2.29	0.926	0.80	0.37 – 1.73	0.574
Iron overload	0.90	0.36 – 2.25	0.820	0.79	0.35 – 1.79	0.569
≥1 any complication	1.09	0.61 – 1.95	0.766	0.91	0.48 – 1.93	0.912

PoS, point of sickling; SCA, sickle cell anemia; CI, confidence interval; ACS, acute chest syndrome; VOC, vaso-occlusive crisis; cP, centipoise; Micro DRBC, microcytic dense red blood cells.

*ACS, VOC or cerebral infarction

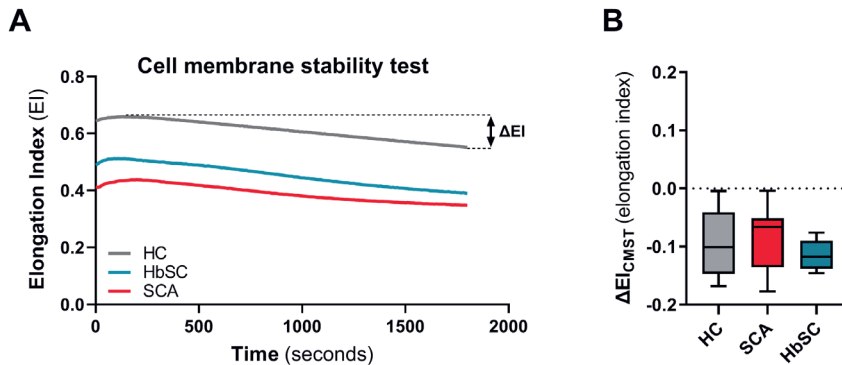


Figure 4. The cell membrane stability test (CMST) in adults with SCA or HbSC disease. (A) Representative curves of the cell membrane stability test (CMST) that shows how RBCs of SCA and HbSC patients respond to a prolonged exposure to high levels of shear stress (100Pa). (B) Median levels of ΔEI , reflecting membrane health, i.e. the ability to shed membrane in vitro.

Whiskers represent Tukey.

SCA, sickle cell anemia; HbSC, hemoglobin SC disease; HC, healthy control.

The potential of blood viscosity as biomarker for clinical complications

To determine if there was an association between blood viscosity and occurrence of clinical complications in SCA and HbSC, ORs of clinical complications were calculated for every 1.0 cP increase. We did not find a significant risk for VOC with higher viscosity in the pediatric SCA cohort, whereas we did find a higher risk for osteonecrosis (OR 1.83, $p=0.025$; aOR 1.54, $p=0.130$) and priapism (OR 1.54, $p=0.091$; aOR 1.40, $p=0.224$) although the latter was not significant (Table 3). A lower OR of 0.38 ($p=0.022$), with an aOR of 0.34 ($p=0.011$) was found for iron overload with increasing viscosity in SCA, which confirms that reduced hemolysis is accompanied by a rise in Hb and hematocrit and subsequently blood viscosity. We did find a trend for ACS with an aOR of 0.72 ($p=0.072$; OR 0.79, $p=0.156$) which could indicate that low blood viscosity protects against the occurrence of this severe, or even fatal complication.

In the HbSC cohort we found a markedly increased OR for ACS and blood viscosity (OR 9.3, $p=0.012$; aOR 13.5, $p=0.015$). Although we found increased ORs for several complications and blood viscosity, including VOC, cerebral infarction, retinopathy and priapism, they did not reach significance, possibly due to low events in this smaller cohort (Table 4). A trend was seen when occurrence of a major complication (OR 2.33, $p=0.087$; aOR 2.24, $p=0.107$) or any complication (OR 2.32, $p=0.071$; aOR 2.09, $p=0.122$) was assessed. These findings imply that blood viscosity plays an important role in development of acute and chronic complications in HbSC, but not in SCA.

The potential of micro DRBCs as biomarker for clinical complications

Since RBC dehydration is a hallmark pathophysiological feature of HbSC, we further explored the potential of using micro DRBCs as a biomarker of clinical complications. A positive association was found between complications and % micro DRBC; for every 1.0% higher micro DRBCs, higher ORs were found for osteonecrosis (OR 2.26, $p=0.018$; aOR 1.75, $p=0.108$)

Table 4. Logistic regression analysis of PoS, blood viscosity and micro DRBCs shows increased or decreased odds ratios for specific complications in HbSC. Odds ratios (OR) and adjusted ORs were calculated for every 10 mmHg increase in PoS (n=37), every 1.0 cP increase in blood viscosity (n=32), and for every 1.0% increase in micro DRBCs (n=37) in children with SCA.

Pediatric HbSC cohort						
PoS (n=37)						
<i>for every 10 mmHg increase</i>		Odds ratio			Adjusted odds ratio	
Complication	OR	95% CI	P-value	OR	95% CI	P-value
ACS	0.96	0.29 – 1.53	0.334	0.94	0.21 – 1.51	0.253
Priapism	1.06	0.72 – 4.06	0.214	1.09	0.83 – 7.16	0.103
Blood viscosity (n=32)						
<i>for every 1 cP increase</i>		Odds ratio			Adjusted odds ratio	
Complication	OR	95% CI	P-value	OR	95% CI	P-value
ACS	9.3	1.64 – 52.4	0.012	13.5	1.65 – 109.9	0.015
Retinopathy	1.81	0.40 – 8.30	0.444	1.83	0.41 – 8.21	0.432
Priapism	1.70	0.38 – 7.58	0.488	1.85	0.47 – 7.33	0.380
Gallstones	1.30	0.38 – 4.50	0.677	0.79	0.14 – 4.43	0.791
≥1 major complication*	2.33	0.89 – 6.12	0.087	2.24	0.84 – 5.95	0.107
≥1 any complication	2.32	0.93 – 5.79	0.071	2.09	0.82 – 5.32	0.122
Micro DRBCs (n=37)						
<i>for every 1% increase</i>		Odds ratio			Adjusted odds ratio	
Complication	OR	95% CI	P-value	OR	95% CI	P-value
ACS	1.23	0.84 – 1.80	0.288	1.54	0.96 – 2.47	0.076
Retinopathy	0.94	0.51 – 1.73	0.834	1.01	0.53 – 1.92	0.989
Gallstones	0.56	0.19 – 1.64	0.289	0.59	0.17 – 2.06	0.404

PoS, point of sickling; HbSC, hemoglobin SC disease; CI, confidence interval; ACS, acute chest syndrome; cP, centipoise; Micro DRBCs, microcytic dense red blood cells.

*ACS, VOC or cerebral infarction

in the cohort comprised of children with SCA (Table 3). In contrast to these findings a trend was seen in the occurrence of ACS in relation to micro DRBCs (OR 1.23, $p=0.288$; aOR 1.54, $p=0.076$) in children with HbSC disease. No other complications were significantly associated with micro DRBCs. Our results indicate that although increased density seems to pathognomonic for HbSC only ACS might be associated with increasing levels of micro DRBCs in HbSC disease. On the contrary, in SCA the higher micro DRBCs seem to be associated with other complications suggesting a different pathophysiology.

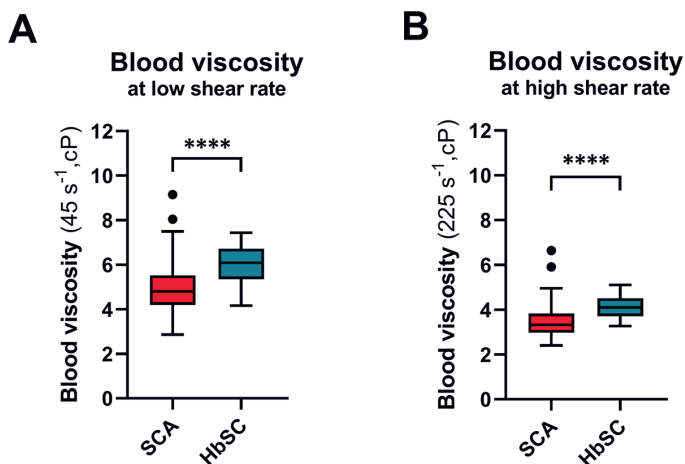


Figure 5. Blood viscosity in children with SCA or HbSC disease. (A) Median values of blood viscosity measured at shear rate of 45 S^{-1} are higher in HbSC compared to SCA in children. (B) Median values of blood viscosity measured at shear rate of 225 S^{-1} are higher in HbSC compared to SCA in children.

Whiskers represent Tukey. **** $p < 0.0001$

SCA, sickle cell anemia; HbSC, hemoglobin SC disease; cP, centipoise.

Discussion

In this study, we report on the differences in RBC properties between SCA and HbSC disease. Our results indicate a profound difference in pathophysiology that has been previously addressed in prior studies, but are further extended by this study. We report on novel functional assays that reflect RBC characteristics such as deformability and sickling behavior and found considerable differences in HbSC disease and SCA. While osmotic gradient ektacytometry measurements indicate reduced hydration of HbSC RBCs, this does not result in decreased membrane health, i.e. a reduced ability to shed membrane in vitro, as is reported in HS.²⁶ More importantly, sickling tendency, reflected by PoS, was significantly increased in both adults and children with SCA compared to HbSC. Whereas PoS proved to be an important biomarker for ACS, VOC, cerebral infarction and development of a major or any complication in children with SCA (*Rab et al, submitted*) this did not apply for children with HbSC disease. These findings could indicate that RBC sickling is not a crucial factor in the development of severe clinical complications in HbSC. In contrast, blood viscosity did show an association with ACS in the pediatric HbSC cohort.

Potential biomarkers that could be further explored

The question of which laboratory parameters or functional assays could be potent biomarkers for HbSC disease severity is still unanswered. The association of K-Cl cotransport activity with pain-related hospital visits/admittance supports its potential as a clinically relevant biomarker.¹⁴ However, apart from being clinically relevant, biomarkers should be measurements that are relatively fast and easy to perform, and should refrain from the use

of hazardous chemicals. Only this ensures implementation in diagnostic laboratories. Blood viscosity measurements and oxygen gradient ektacytometry are meeting the criteria to be available in hospital laboratories, although the latter might be reserved for large or academic hospitals only. Although the association of blood viscosity with ACS is of interest, the association between major complication or any complication and whole blood viscosity was not significant, which is possibly due to a low sample size in the HbSC cohort, along with variability in viscosity test values, particularly with low shear rates.

Identification of biomarkers associated with clinical complications in HbSC will enhance our knowledge of the pathophysiology of HbSC, and potentially also HbCC disease. HbCC is a rare, generally benign disorder which is characterized by mild hemolytic anemia, mild reticulocytosis, hyperchromic microcytosis, and dense, dehydrated RBCs.³⁰ Even though RBC deformability is considerably impaired and blood viscosity is equally increased in HbCC compared to HbSC, this does not lead to occurrence of ACS or VOC.³¹ This raises the question which abnormal RBC or vascular properties are crucial for the development of ACS or VOC in HbSC disease. Proposed differences between HbCC and HbSC disease that ameliorate clinical phenotype in HbCC are the profound microcytosis³¹ and less adhesion to the vascular wall. Larger studies are warranted to elucidate how blood viscosity, markers of RBC dehydration (i.e. O_{hyper}), MCV and adherence of RBC to the endothelium relate to occurrence of clinical complications in HbSC.

Blood viscosity is associated with complications in HbSC, in contrast to sickling: implications for therapy

While PoS showed significant ORs and aORs for several complications in SCA no significant increased/decreased ORs were found for PoS in HbSC. In contrast, blood viscosity was associated with occurrence of ACS in HbSC. This raises the question of whether anti-sickling or anti-polymerization agents such as voxelotor are suitable for individuals with HbSC. More importantly, particularly in the already high Hb, high viscosity HbSC, if voxelotor increases blood viscosity as a result of the rise in Hb, as was reported in patients with SCA, HbSC subjects could experience increased rates of viscosity related complications.¹⁸ The effect of voxelotor on whole blood viscosity *in vivo* has not been investigated, and if voxelotor will have a similar effect on HbSC RBC rheology as it has been described for SCA remains to be elucidated. Even though *in vitro* experiments in SCA show that voxelotor directly decreases viscosity in both oxygenated and deoxygenated conditions when standardized to a fixed hematocrit³², long term effects are still unknown.

The efficacy of HU has been extensively studied in cohorts comprised of adults and children with SCA,^{33,34} but such studies have not been performed on patients with HbSC disease and the effect of HU on laboratory parameters and clinical complications in this patient group is scarce.^{33,35} It is reasonable to assume that it's efficacy might be predominantly due to improved RBC hydration and decreasing sickling tendency due to increased HbF levels. Our findings on blood viscosity further strengthens the proposed therapeutic benefit of phlebotomy in HbSC disease.^{12,36,37} Another potential approach to ameliorate clinical complications in HbSC might be iron restriction³⁸ which would presumably increase microcytosis and decrease blood viscosity as a result of decreased hematocrit levels. This strategy has been proposed for SCA and was, even though it had other effects, found to be beneficial in SCA mice.³⁹

Differences between cohorts

We observed differences in occurrence of complications between the adult and pediatric cohorts (Table 1 and 2). These findings, as well as the observed differences in laboratory parameters and oxygen gradient ektacytometry-derived biomarkers (Figure 2) between cohorts could be due to differences in pediatric and adult SCD pathophysiology. Although studies investigating the effect of age on clinical symptoms and signs are scarce, with age, SCD symptoms generally worsen, particularly in the transition period between adolescence and adulthood.^{40,41} This is partly due to differences in treatment, access to care (US) and differences in guidelines and clinical practice between adult and pediatric providers.^{42,43} In our study, fewer adults were treated with HU compared to the pediatric cohort (SCA 41% versus 85.2%; HbSC 13% versus 41%). The differences in occurrence of clinical complications could be due to the substantially smaller adult cohort, making associations between biomarkers and relatively rare complications more difficult to detect. Environmental factors such as climate⁴⁴ could also result in differences between the adult and pediatric cohort; the adult cohort is located in The Netherlands, in Europe, the pediatric cohort in Houston, in the US. In addition, RBC rheological characteristics, and notably RBC deformability, are known to be different between adults and young children.⁴⁵ Limitations of this study include low sample size in the HbSC cohorts, in particular the adult cohort. More importantly it would have been informative to have blood viscosity values of the adult cohorts and osmotic gradient ektacytometry and CMST measurements of the pediatric cohorts.

Conclusion

We report on blood viscosity as a new potential biomarker associated with risk of ACS in individuals with HbSC disease. Blood viscosity was significantly higher in HbSC compared to SCA and was associated with the occurrence of ACS in children with HbSC but not SCA. In addition, we found that PoS, that reflects sickling tendency, was not associated with the occurrence of clinical complications in HbSC in contrast to SCA. Based on these findings and previous studies, we state that HbSC disease should be regarded as an independent disease entity and, hence, warrants a different treatment approach.

References

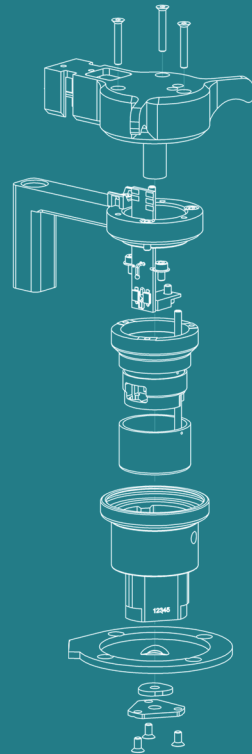
1. Rees DC, Williams TN, Gladwin MT. Sickle-cell disease. *Lancet*. 2010;376:2018-2031. doi:10.1016/S0140-6736(10)61029-X
2. Kato GJ, Piel FB, Reid CD, et al. Sickle cell disease. *Nat Rev Dis Prim*. 2018;4:1-22. doi:10.1038/nrdp.2018.10
3. Weatherall DJ. The inherited diseases of hemoglobin are an emerging global health burden. *Blood*. 2010;115(22):4331-4336. doi:10.1182/blood-2010-01-251348
4. Connes P, Lamarre Y, Waltz X, et al. Haemolysis and abnormal haemorheology in sickle cell anaemia. *Br J Haematol*. 2014;165(4):564-572. doi:10.1111/bjh.12786
5. Rab MAE, van Oirschot BA, Bos J, et al. Rapid and reproducible characterization of sickling during automated deoxygenation in sickle cell disease patients. *Am J Hematol*. 2019;94(Febuary):575-584. doi:10.1002/ajh.25443
6. Lu M, Rab MAE, Shevkopyas SS, Sheehan VA. Blood rheology biomarkers in sickle cell disease. *Exp Biol Med*. 2020;0:1-11. doi:10.1177/1535370219900494
7. Connes P, Alexy T, Detterich J, Romana M, Hardy-Dessources MD, Ballas SK. The role of blood rheology in sickle cell disease. *Blood Rev*. 2015;30(2):111-118. doi:10.1016/j.blre.2015.08.005
8. Nagel RL, Fabry ME, Steinberg MH. The paradox of hemoglobin SC disease. *Blood Rev*. 2003;17(3):167-178. doi:10.1016/S0268-960X(03)00003-1
9. Pecker LH, Schaefer BA, Luchtman-Jones L. Knowledge insufficient: the management of haemoglobin SC disease. *Br J Haematol*. 2017;176(4):515-526. doi:10.1111/bjh.14444
10. Bunn HF, Noguchi CT, Hofrichter J, Schechter GP, Schechter AN, Eaton WA. Molecular and cellular pathogenesis of hemoglobin SC disease. *Proc Natl Acad Sci U S A*. 1982;79(23 1):7527-7531. doi:10.1073/pnas.79.23.7527
11. Ballas SK, Lewis CN, Noone AM, Krasnow SH, Kamarulzaman E, Burka ER. Clinical, hematological, and biochemical features of Hb SC disease. *Am J Hematol*. 1982;13(1):37-51. doi:https://doi.org/10.1002/ajh.2830130106
12. Lionnet, Francois; Hammoudi, Nadjib; Stankovic Stojanovic, Katja; Avellino, Virginie; Grateau, Gilles; Girot, Robert; Haymann J-P. Hemoglobin sickle cell disease complications : a clinical study of 179 cases. *Haematologica*. 2012;97(8):1136-1141. doi:10.3324/haematol.2011.055202
13. Hannemann A, Rees DC, Tewari S, Gibson JS. Cation Homeostasis in Red Cells From Patients With Sickle Cell Disease Heterologous for HbS and HbC (HbSC Genotype). *EBio-Medicine*. 2015;2(1 1):1669-1676. doi:10.1016/j.ebiom.2015.09.026
14. Rees DC, Thein SL, Osei A, et al. The clinical significance of K-CL cotransport activity in red cells of patients with HbSC disease. *Haematologica*. 2015;100(5):595-600. doi:10.3324/haematol.2014.120402
15. Ballas SK, Lerner J, Smith ED, Surrey S, Schwartz E, Rappaport EF. The Xerocytosis of Hb SC disease. *Blood*. 1987;69(1):124-130.
16. Lawrence C, Fabry ME, Nagel RL. The unique red cell heterogeneity of SC disease: Crystal formation, dense reticulocytes, and unusual morphology. *Blood*. 1991;78(8):2104-2112. doi:10.1182/blood.v78.8.2104.bloodjournal7882104
17. Lemonne N, Billaud M, Waltz X, et al. Rheology of red blood cells in patients with HbC disease. *Clin Hemorheol Microcirc*. 2014;61:571-577. doi:10.3233/CH-141906
18. Vichinsky E, Hoppe CC, Ataga KI, et al. A Phase 3 randomized trial of voxelotor in sickle cell disease. *N Engl J Med*. 2019;381(6):509-519. doi:10.1056/NEJMoa1903212
19. Niihara Y, Miller ST, Kanter J, et al. A phase 3 trial of l-glutamine in sickle cell disease. *N Engl J Med*. 2018;379(3):226-235. doi:10.1056/NEJMoa1715971
20. Ataga KI, Kutlar A, Kanter J, et al. Crizanlizumab for the prevention of pain crises in sickle cell disease. *N Engl J Med*. 2017;376(5):429-439. doi:10.1056/NEJMoa1611770
21. Salinas Cisneros G, Thein SL. Recent Advances in the Treatment of Sickle Cell Disease. *Front Physiol*. 2020;11(May):1-15. doi:10.3389/fphys.2020.00435
22. Nardo-Marino A, Brousse V, Rees D. Emerging therapies in sickle cell disease. *Br J Haematol*. 2020;190(2):149-172. doi:10.1111/bjh.16504

23. Rab MAE, Kanne CK, Bos J, et al. Oxygen gradient ektactometry derived-biomarkers are associated with vaso-occlusive crises and correlate with treatment response in sickle cell disease. *Am J Hematol*. 2021;96(1):E29-E32. doi:10.1002/ajh.26031
24. DaCosta L, Suner L, Galimand J, et al. Diagnostic tool for red blood cell membrane disorders : Assessment of a new generation ektactometer. *Blood Cells, Mol Dis*. 2016;56(1):9-22. doi:10.1016/j.bcmd.2015.09.001
25. Lazarova E, Gulbis B, Oirschot B Van, Van Wijk R. Next-generation osmotic gradient ektactometry for the diagnosis of hereditary spherocytosis: Interlaboratory method validation and experience. *Clin Chem Lab Med*. 2017;55(3):394-402. doi:10.1515/cclm-2016-0290
26. Berrevoets MC, Bos J, Huisjes R, et al. Ektactometry Analysis of Post-splenectomy Red Blood Cell Properties Identifies Cell Membrane Stability Test as a Novel Biomarker of Membrane Health in Hereditary Spherocytosis. *Front Physiol*. 2021;12(March):1-10. doi:10.3389/fphys.2021.641384
27. Rab MAE, van Oirschot BA, Bos J, et al. Characterization of Sickling During Controlled Automated Deoxygenation with Oxygen Gradient Ektactometry. *J Vis Exp*. 2019;(153):1-10. doi:10.3791/60213
28. Rab MAE, Kanne CK, Bos J, et al. Methodological aspects of the oxygenscan in sickle cell disease: A need for standardization. *Am J Hematol*. 2020;95(1):5-8. doi:10.1002/ajh.25655
29. Baskurt OK, Boynard M, Cokelet GC, et al. New guidelines for hemorheological laboratory techniques. *Clin Hemorheol Microcirc*. 2009;42(2):75-97. doi:10.3233/CH-2009-1202
30. Charache S, Conley CL, Waugh DF, Ugoretz RJ, Spurrell JR. Pathogenesis of hemolytic anemia in homozygous hemoglobin C disease. *J Clin Invest*. 1967;46(11):1795-1811. doi:10.1172/JCI105670
31. Lemonne N, Billaud M, Waltz X, et al. Rheology of red blood cells in patients with HbC disease. *Clin Hemorheol Microcirc*. 2016;61(4):571-577. doi:10.3233/CH-141906
32. Dufu K, Patel M, Oksenberg D, Cabrales P. GBT440 improves red blood cell deformability and reduces viscosity of sickle cell blood under deoxygenated conditions. *Clin Hemorheol Microcirc*. 2018;70(1):95-105. doi:10.3233/CH-170340
33. Nevitt S, Jones A, Howard J. Hydroxyurea (hydroxycarbamide) for sickle cell disease. *Cochrane Database Syst Rev*. 2017;4(4):CD002202. doi:10.1002/14651858.CD002202.pub2.www.cochranelibrary.com
34. Charache S, Terrin ML, Moore RD, et al. Effect of hydroxyurea on the frequency of painful crises in sickle cell anemia. *N Engl J Med*. 1995;332(20):1317-1322. doi:10.1056/NEJM199505183322001
35. Luchtman-Jones L, Pressel S, Hilliard L, et al. Effects of hydroxyurea treatment for patients with hemoglobin SC disease. *Am J Hematol*. 2016;91(2):238-242. doi:10.1002/ajh.24255
36. Summirell CCG, Sheehan VA. Use of hydroxyurea and phlebotomy in pediatric patients with hemoglobin SC disease. *Exp Biol Med*. 2016;241(7):737-744. doi:10.1177/1535370216639737
37. Markham MJ, Lottenberg R, Zumberg M. Role of phlebotomy in the management of hemoglobin SC disease: Case report and review of the literature. *Am J Hematol*. 2003;73(2):121-125. doi:10.1002/ajh.10328
38. Lionnet F, Hammoudi N, Stankovic Stojanovic K, et al. Iron restriction is an important treatment of hemoglobin SC disease. *Am J Hematol*. 2016;91(7):E319-E320. doi:10.1002/ajh.24379
39. Parrow NL, Violet P-C, Ajit George N, et al. Dietary Iron Restriction Improves Markers of Disease Severity in Murine Sickle Cell Anemia. *Blood*. Published online 2020. doi:10.1182/blood.2020006919
40. Kanter J, Kruse-Jarres R. Management of sickle cell disease from childhood through adulthood. *Blood Rev*. 2013;27(6):279-287. doi:10.1016/j.blre.2013.09.001
41. Claster S, Vichinsky EP. Managing sickle cell disease. *Br Med J*. 2003;327(7424):1151-1155. doi:10.1136/bmj.327.7424.1151
42. Inusa, Colombatti, Rees, et al. Geographic Differences in Phenotype and Treatment of Children with Sickle Cell Anemia from the Multinational DOVE Study. *J Clin Med*. 2019;8(11):2009. doi:10.3390/jcm8112009
43. Blinder MA, Duh MS, Sasane M, Trahey A, Paley C, Vekeman F. Age-Related Emergency Department Reliance in Patients with Sickle Cell Disease. *J Emerg Med*. 2015;49(4):513-522.e1. doi:10.1016/j.jemermed.2014.12.080

44. Tewari S, Brousse V, Piel FB, Menzel S, Rees DC. Environmental determinants of severity in sickle cell disease. *Haematologica*. 2015;100(9):1108-1116. doi:10.3324/haematol.2014.120030
45. Renoux C, Romana M, Joly P, et al. Effect of Age on Blood Rheology in Sickle Cell Anaemia and Sickle Cell Haemoglobin C Disease : A Cross-Sectional Study. *PLoS One*. 2016;11(6):1-11. doi:10.1371/journal.pone.0158182

Part III

Ektacytometry in other hereditary hemolytic anemias



Chapter 10

AG-348 (mitapivat), an allosteric activator of red blood cell pyruvate kinase, increases enzymatic activity, protein stability, and ATP levels over a broad range of PKLR genotypes

Haematologica 2021 Jan 1;106(1):238-249

Minke A.E. Rab^{1,2*}, Brigitte A. van Oirschot^{1*}, Penelope A. Kosinski³, Jeffrey Hixon^{3,4}, Kendall Johnson³, Victor Chubukov³, Lenny Dang³, Gerard Pasterkamp¹, Stephanie van Straaten¹, Wouter W. van Solinge¹, Eduard J. van Beers², Charles Kung^{3†}, and Richard van Wijk^{1†}

¹ Laboratory of Clinical Chemistry & Haematology, University Medical Center Utrecht, Utrecht University, Utrecht, The Netherlands

² Van Creveldkliniek, University Medical Center Utrecht, Utrecht University, Utrecht, The Netherlands

³ Agios Pharmaceuticals, Inc., Cambridge, MA, United States

⁴ Current affiliation: KSQ Therapeutics, Cambridge, MA, United States

* These authors contributed equally

† These authors contributed equally

Abstract

Pyruvate kinase (PK) deficiency is a rare hereditary disorder affecting red cell (RBC) glycolysis, causing changes in metabolism including a deficiency in ATP. This affects red cell homeostasis, promoting premature removal of RBCs from the circulation. In this study we characterized and evaluated the effect of AG-348, an allosteric activator of PK that is currently in clinical trials for treatment of PK deficiency, on RBCs and erythroid precursors from PK-deficient patients. In 15 patients ex vivo treatment with AG-348 resulted in increased enzymatic activity in all patient cells after 24 hours (mean increase 1.8-fold, range 1.2-3.4). ATP levels increased (mean increase 1.5-fold, range 1.0-2.2) similar to control cells (mean increase 1.6-fold, range, 1.4-1.8). Generally, PK thermostability was strongly reduced in PK-deficient RBCs. Ex vivo treatment with AG-348 increased residual activity 1.4 to >10-fold than residual activity of vehicle-treated samples. Protein analyses suggests that a sufficient level of PK protein is required for cells to respond to AG-348 treatment ex-vivo, as treatment effects were minimal in patient cells with very low or undetectable levels of PK-R. In half of the patients, ex vivo treatment with AG-348 was associated with an increase in RBC deformability. These data support the hypothesis that drug intervention with AG-348 effectively upregulates PK enzymatic activity and increases stability in PK-deficient RBCs over a broad range of PKLR genotypes. The concomitant increase in ATP levels suggests that glycolytic pathway activity may be restored. AG-348 treatment may represent an attractive way to correct the underlying pathologies of PK deficiency. (AG-348 is currently in clinical trials for the treatment of PK deficiency. ClinicalTrials.gov: NCT02476916, NCT03853798, NCT03548220, NCT03559699).

Introduction

Pyruvate kinase (PK) deficiency is a rare hereditary disorder affecting red blood cell (RBC) glycolysis resulting in life long chronic hemolytic anemia.¹ It is the most common cause of chronic hereditary nonspherocytic hemolytic anemia, although its exact prevalence is unknown.²⁻⁴ PK deficiency is an autosomal recessive disease that occurs worldwide. It is caused by mutations in *PKLR*, the gene encoding the red blood cell and liver specific isoforms PK-R and PK-L, respectively.^{5,6} Humans express two additional PK isoforms, PK-M1 and PK-M2, both encoded by the *PKM* gene. PK-M2 is expressed in early fetal tissues and most adult tissues, including early stage erythroblasts, whereas expression of PK-M1 is confined to muscle.

To date, more than 370 mutations have been reported in *PKLR* associated with PK deficiency (van Wijk, in preparation). Most of these mutations are missense mutations encoding single amino acid changes that affect the enzyme's structure, stability or catalytic function.^{7,8} Only a few mutations occur relatively frequently, implying that the majority of patients harbor a unique combination of mutations.⁹

PK is an allosterically regulated homotetrameric enzyme that catalyzes the conversion of phosphoenol pyruvate (PEP) to pyruvate in the final step of glycolysis, thereby producing energy in the form of ATP. PK-deficient RBCs are characterized by changes in metabolism associated with defective glycolysis, including a build-up of the upstream metabolite 2,3-disphosphoglycerate (2,3-DPG) and deficiency in the PK product ATP. Since RBCs rely totally on glycolysis for ATP production it is hypothesized that insufficient energy production affects red cell homeostasis, promoting premature removal of PK-deficient RBCs from the circulation by the spleen. Increased RBC dehydration resulting from increased activity of the Gardos channel, and consequent potassium efflux¹⁰⁻¹²; as well as ATP depletion-mediated changes in RBC membrane integrity have been proposed as mechanisms triggering this premature clearance.^{13,14} In addition, ineffective erythropoiesis may contribute to the pathophysiological consequences of PK deficiency.¹⁵⁻¹⁷

Clinically, PK deficiency manifests as chronic hemolytic anemia of highly variable clinical severity. Patients may present with severe neonatal anemia requiring exchange transfusion, whereas at the other end of the spectrum patients are diagnosed later in life with fully compensated hemolysis. The ongoing Pyruvate Kinase Deficiency Natural History Study showed that apart from anemia, the most frequent reported complications were iron overload and gallstones. However, other complications such as aplastic crises, osteoporosis, extramedullary hematopoiesis, post-splenectomy sepsis, pulmonary hypertension, and leg ulcers are not uncommon. Typically, worsening of hemolysis occurs during infections, stress, and pregnancy.¹⁸

Current treatment for PK deficiency is generally supportive, with splenectomy, blood transfusion and iron chelation as the main therapies, focusing on the anemia and iron overload state.¹⁹ Splenectomy is effective for the majority of PK-deficient patients, in that it reduces transfusion burden and improves baseline hemoglobin levels post splenectomy by an average of 1.6 g/dL. Fourteen percent of patients who underwent splenectomy however continued to require regular transfusions.¹⁸ Curative treatment possibilities include stem cell transplantation (SCT) or experimental gene therapy.^{20,21}

Recently, it was shown that AG-348 is an allosteric activator of PK-R. This small molecule directly targets PK-R by binding in a pocket at the dimer-dimer interface, distinct from the allosteric activator fructose-1,6-bisphosphate binding domain (FBP). This induces the active R-state conformation of the PK-R tetramer, resulting in enhanced activity of both wild type and mutant PK-R.²² Phase I studies in healthy volunteers demonstrated glycolytic pathway activation upon treatment with AG-348 demonstrating its potential for treating PK deficiency.²³ Data from a Phase II study in PK deficiency patients treated with AG-348 showed that approximately half of treated subjects experienced a rise in hemoglobin.²⁴ In this study we further evaluated the effect of *ex vivo* treatment with AG-348 on PK deficient red cells with a broad range of patient genotypes, including effects on enzyme activity and ATP levels. In particular, for the first time we report the effects of AG-348 on PK thermostability in red cell lysates, PK-R protein level, RBC deformability and the effect of AG-348 during *in vitro* PK-deficient erythropoiesis.

Methods

This study was approved by the ethical committee of the University Medical Center Utrecht (Protocol 14-571/M).

Metabolic Profiling

Frozen whole blood samples were extracted with hot 70% ethanol, dried and resuspended in water. Relative abundance of central carbon metabolites was performed by UPLC-MS with high resolution accurate mass detection on a QExactive™ Orbitrap mass spectrometer (Thermo Fisher Scientific).²⁵ Peak identification and integration was done with Maven software.²⁶ Quantitative analysis of ATP and 2,3-DPG was performed as described previously.²⁷

PK activity, protein levels, and thermostability.

RBCs were purified using microcrystalline α -cellulose columns.^{28,29} PK and hexokinase activity was measured as described.^{28,29} PK thermostability was measured as described³⁰ after 0, 5, 10, 20, 40 and 60 minutes of incubation (53°C). PK activity after *ex vivo* treatment with AG-348 was measured using low substrate (0.5 mM). PK-R protein levels were determined by Mesoscale Assay (MesoScale Discovery) as described²² using Goat anti-PKLR antibody (Aviva) and Mouse anti-PKLR antibody (Abcam). SULFO-TAG goat anti-mouse (Mesoscale discovery) was used as detection antibody. Protein level was determined by normalizing light intensity of the SULFO-TAG electrochemiluminescence to lysate protein concentration. Western blot of PK-R and PK-M2 was performed as described³¹ using polyclonal antibodies against PK-L³² and monoclonal antibodies against PK-M2 (PodiCeps). Alexa Fluor® 680-conjugated goat anti-mouse and goat anti-rabbit antibodies (Li-Cor, Invitrogen) were used as detection antibodies.

Ex vivo treatment with AG-348

Purified RBCs or whole blood of patients and controls were incubated for 3, 6 and 24 hours at 37°C in presence or absence of AG-348 in phosphate-buffered saline containing 1% glucose, 170 mg/L adenine, and 5.25 g/L mannitol (AGAM, pH 7.40). RBCs were incubated

with different dosages of AG-348 (up to 10 μM) up to 24 hours, at 37°C. After 6 and 24 hours PK-R activity and ATP levels (CellTiterGlo; Promega, Madison, WI) were measured. For thermostability, RBC lysates were incubated for 2 hours with AG-348.

Osmoscan and deformability

Osmoscan and deformability measurements were performed using the Lorrca (RR Mechatronics).^{33,34} AGAM buffer was added to whole blood (1:10), and supplemented with either AG-348 (20 μM) or DMSO (untreated). Samples were incubated 24 hours at 37°C before measurements.

AG-348 treatment during in vitro erythropoiesis

Erythroid cells were produced from peripheral blood mononuclear cells (PBMC).³⁵ For proliferation, cells were cultured 10 days in CellQuin medium (Sanquin), supplemented with Stem Cell Factor (100ng/mL, Amgen), Epo (2U/mL, EPREX), dexamethasone (1 μM , Sigma), and 1ng/mL IL-3 (R&D systems). After 10 days, cells were reseeded (2E⁶ cells/mL) in CellQuin medium supplemented with EPO (10 U/mL, Eprex), heparine (5U/mL, Leo Pharmacy), human AB plasma (3%, Sigma). At day 5 CellQuin was replaced by RetQuin medium (Sanquin). AG-348 (2 $\mu\text{mol/L}$) was added at days 0, 1, 3-10 during proliferation and day 0, 2, and 4 during differentiation.

Statistical Analysis

Statistical analysis was performed using Graphpad Prism (v7.04). T-test, Mann-Whitney test or Wilcoxon test was used when appropriate. One-way ANOVA was carried out or a Kruskal-Wallis test, followed by Dunn's tests for post-hoc analysis. Pearson's correlation was used to determine correlations of laboratory parameters with enzyme activity measurements.

Results

Fifteen adult, transfusion independent, PK-deficient patients were enrolled for this study (median age 44.0 years, range 20.0-51.5). PK deficiency was confirmed by demonstrating compound heterozygosity or homozygosity for mutations in *PKLR* (Sanger sequencing). Whole blood from 15 healthy volunteers was used as control samples.

Baseline patient characteristics displayed varying degrees of anemia (Table 1). In addition, most patients had strongly elevated reticulocyte counts, a prominent feature of PKD patients in particular after splenectomy.¹¹ Most patients showed reduced red cell PK activity (Figure 1A) and reduced PK thermal stability (Figure 1C). Since the activity of many red cell enzymes is red cell age-dependent,³⁶ we also compared PK activity to hexokinase (HK) activity (Table 1 and Figure 1B). This PK/HK ratio was clearly decreased in all patients, indicating a relatively strong decrease in activity of PK ($r=-0.677$, $p<0.01$, Figure 1B). When causative mutations were classified as missense (M) or non-missense (NM) a genotype to phenotype correlation was identified.¹⁸ All four patients without splenectomy were of the M/M genotype, which is in line with the lower likelihood of splenectomy in this group.¹⁸ Similarly, these patients had generally higher hemoglobin levels and lower reticulocyte counts (Table 1).

Table 1 Genotypes and baseline characteristics of PK-deficient patients

Nr.	Sex	PKLR mutation	Amino acid change	Geno- type	Splene-ctomy	Hb (g/dL)	Ret. (%)	PK (U/gHb)	HK (U/gHb)	PK/HK ratio
P1	F	c.1121T>C:c.1456C>T	p.(Leu374Pro)/p.(Arg486Trp)	M/M	Yes	9.7	10.0	9.0	5.0	1.8
P2	M	c.331G>A:c.1456C>T	p.(Gly111Arg)/p.(Arg486Trp)	M/M	No	11.2	7.0	3.1	1.7	1.8
P3	M	c.1178A>G:c.1456C>T	p.(Asn393Ser)/p.(Arg486Trp)	M/M	Yes	9.4	>35.0	16.9	6.2	2.7
P4	F	c.1462C>T:c.1529G>A	p.(Arg488*)/p.(Arg510Gln)	M/NM	Yes	6.6	>34.0	15.9	7.4	2.1
P5	F	c.1121T>C:c.1706G>A	p.Leu374Pro/p.(Arg569Gln)	M/M	No	10.9	7.0	2.1	1.5	1.4
P6	F	c.507+1G>A:c.1436G>A	p.[*; 0]/p.(Arg479His)	M/NM	Yes	7.7	75.0	1.9	6.0	0.3
P7	M	c.376-2A>C:c.1529G>A	p.(Glu125_Tyr126ins32;Tyr126Alafs*83)/p.(Arg510Gln)	M/NM	Yes	8.0	55.0	1.7	5.6	0.3
P8	F	c.331G>A:c.1456C>T	p.(Gly111Arg)/p.(Arg486Trp)	M/M	No	11.9	5.0	2.2	1.4	1.6
P9	M	c.331G>A:c.1492C>T	p.(Gly111Arg)/p.(Arg498Cys)	M/M	Yes	10.3	40.0	2.5	4.1	0.6
P10	M	c.1154G>A:c.1529G>A	p.(Arg385Lys)/p.(Arg510Gln)	M/M	No	13.4	15.0	2.7	2.0	1.3
P11	M	c.721G>T:c.1529G>A	p.(Glu241*)/p.(Arg510Gln)	M/NM	Yes	8.2	85.0	2.2	6.1	0.4
P12	M	c.142_159del/c.494G>T	p.(Thr48_Thr53del)/p.(Gly165Val)	M/NM	Yes	12.9	20.0	10.0	3.5	2.8
P13	M	c.1269G>A:c.1654G>A	p.([Met373_Ala423del; 0])/p.(Val552Met)	M/NM	Yes	9.7	55.0	1.8	5.8	0.3
P14	F	c.401T>A:c.1529G>A	p.(Val134Asp)/p.(Arg510Gln)	M/M	Yes	9.6	60.0	1.2	5.2	0.2
P15	M	c.1529G>A:c.1529G>A	p.(Arg510Gln)/p.(Arg510Gln)	M/M	Yes	12.8	40.0	1.6	2.8	0.6
Contr					No	14.1 (1.3)	1.18(0.3)	12.7(2.3)	1.1(0.2)	11.9(2.1)
						Reference range values:				
						M: 13.8-17.2	1.0-2.0	9.2-16.9	0.9-1.4	9.0-16.6
						F: 11.9-15.5				

Genotypes, amino acid change, splenectomy status and laboratory parameters are shown for all fifteen PK-deficient patients included in this study. Enzyme activity of PK was decreased or normal. HK activity was almost always increased due to reticulocytosis. PK/HK ratio was strongly decreased in all cases, indicative of PK deficiency. Mean values (standard deviation) of 15 healthy controls are shown. Reference range values of the UMC Utrecht population are also included. M: male, F: female. Hb, hemoglobin. Ret., reticulocytes. PK, pyruvate kinase. U, units. HK, hexokinase. M/M: missense/missense, M/NM: missense/nonmissense.

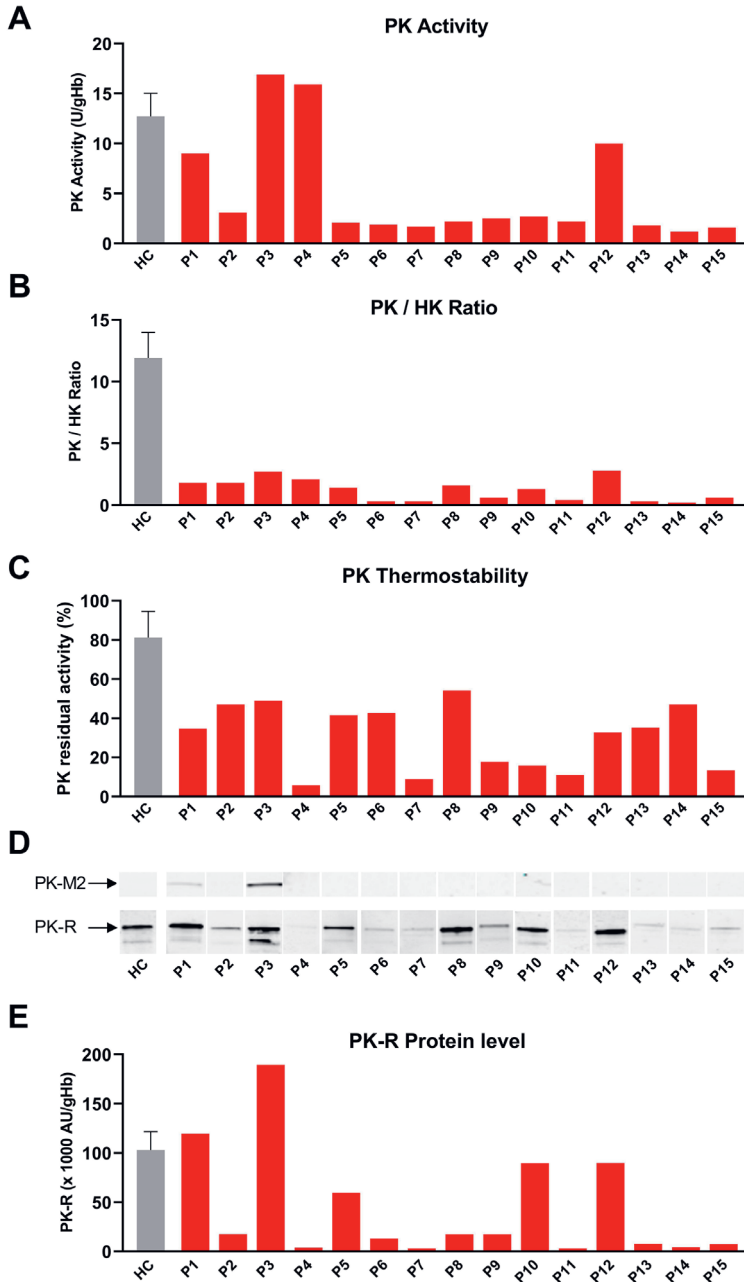


Figure 1. Baseline levels of PK activity, PK/Hexokinase (HK) ratio, PK thermostability, and PK-R protein levels in PK-deficient patients and controls. (A) PK activity of PK deficient patients (red) and healthy controls (grey). (B) PK/HK Ratio in patients (red) and healthy controls (grey), as a means to evaluate PK activity in the presence of high number of reticulocytes, reflected by increased HK activity. (C) PK-thermostability of patients (red) and controls (grey). (D) PK-R protein levels of patients (P#) and controls (HC) measured by western blot. (E) PK-R protein levels of patients (red) and controls (grey) measured by MSD. PK: pyruvate kinase, HK: hexokinase, ECL: electrochemiluminescence.

PK-R protein levels correlate with PK activity

Protein levels of PK-R were measured by both western blot and MSD. PK-R protein levels were variable between patients (Figure 1C and D). In general, PK-activity correlated well positively with PK-R protein levels. The most notable exception was patient 4. RBCs from this patient contained very low levels of protein, as measured by both Western Blot and ELISA, but repeated measurements showed high levels of PK-activity (Table 1, Figure 1A, D and E). Low levels of PK-R protein in this patient could result from combined instability of the p.Arg510Gln³⁷ mutant as well as the truncated p.(Arg488*) PK-R nonsense mutant. In line with this, PK thermostability was also strongly reduced in this patient (Figure 1C). The reason for the high PK activity in this patient remains unknown however.

Increased PK-M2 expression, that could perhaps compensate for the loss in PK-R³⁸ activity was not detected, except for patient 3, and to a lesser degree in RBCs from patient 1 (Figure 1D).

PK-deficient red blood cells show glycolytic intermediates levels that are consistent with decreased pyruvate kinase activity.

Metabolic profiling of PKD patients was performed by LC-MS/MS on whole blood. Consistent with a decrease in PK activity at the final step of glycolysis, levels of phosphoenol pyruvate (PEP) were significantly increased ($p < 0.0001$) whereas levels of pyruvate and ATP were significantly decreased (both $p < 0.0001$, Figure 2). In addition, dihydroxyacetone phosphate (DHAP) and 2,3-DPG levels were increased ($p < 0.001$ and $p < 0.0001$), indicative of retrograde accumulation of upstream glycolytic intermediates.

Ex vivo incubation with AG-348 increases PK activity and ATP in a dose dependent manner

Ex vivo treatment of PK-deficient and healthy control RBCs with increasing dose of AG-348 showed an increase in PK-activity and ATP levels. Illustrative PK activity dose response curves of two patients are shown in figure 3A and B. Incubations with 10 μM AG-348 showed a mean 1.3 fold increase (range 1.0-2.0) in PK-activity in PK-deficient RBCs after 6 hours ($p < 0.0001$) and of 1.8 (range 1.2-3.4) after 24 hours ($p < 0.0001$, figure 3E). Similar values were obtained from control cells 1.4 after 6 hours ($p < 0.01$, range 0.9-1.9) and 2.3 (range, 1.2-7.1) after 24 hours ($p < 0.0001$).

ATP levels increased accordingly in a dose dependent manner (figure 3C and D). AG-348 treatment significantly increased mean ATP levels in PK-deficient RBCs to 1.4 fold (range 1.0-2.3) after six hours ($p < 0.01$) and 1.5 fold (range 1.0-2.2) after 24 hours ($p < 0.0001$). The mean increase in ATP levels in control cells was 1.5 fold (range 1.3-1.7) after 6 hours ($p < 0.001$) and 1.6 fold (range 1.4-1.8) after 24 hours ($p < 0.0001$). We observed no differences in PK activity and ATP response between PK-deficient patients with M/M and M/NM genotypes (Table 1, Figure 3E and F). Since glycolysis in RBCs is known to be regulated by band 3³⁹ we verified RBC band 3 expression levels by Western Blot analysis. We observed no differences in band 3 expression levels of PK-deficient patients compared to healthy controls (Supplemental Figure 1). Collectively, these results are consistent with previous reports,²² and illustrate the ability of AG-348 to stimulate PK activity in patient samples with a range of genotypes.

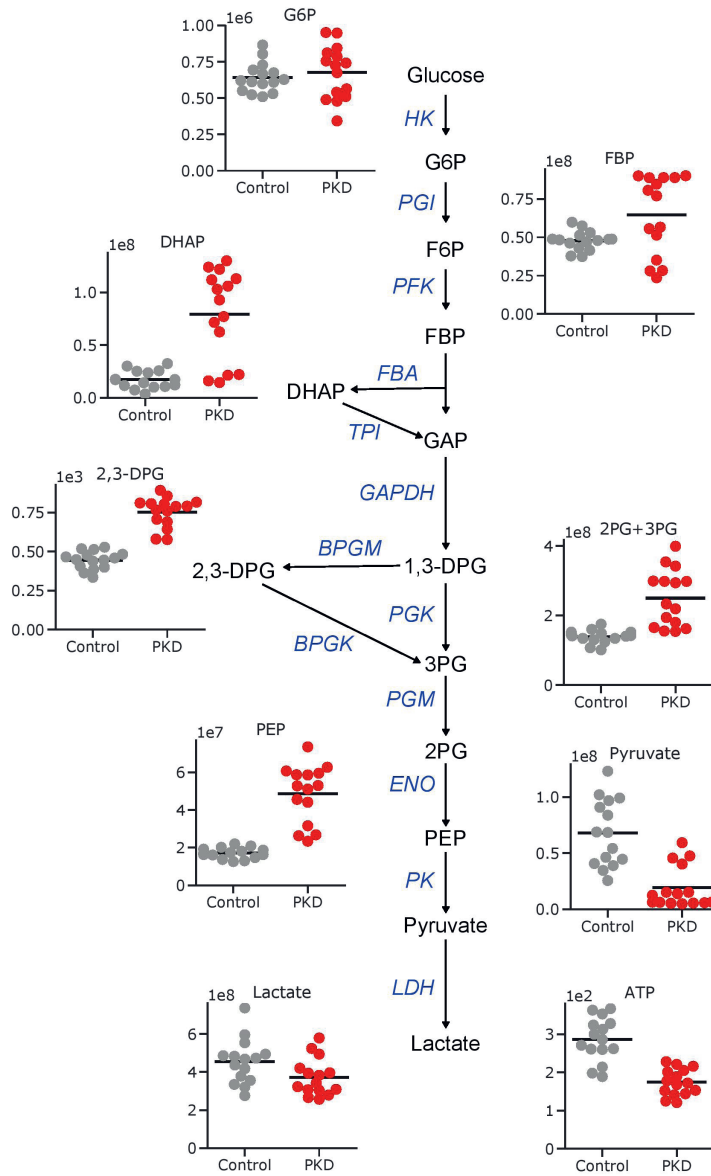


Figure 2. PK-deficient patients show glycolytic intermediates levels that are consistent with decreased pyruvate kinase activity. Upstream intermediates of PK of PK-deficient patients (red) are significantly increased compared to values of health controls (grey), with for example an almost 2-fold increase in 2,3-DPG. Downstream targets, pyruvate and ATP, are significantly decreased compared to healthy controls. PKD: pyruvate kinase deficiency, G6P: glucose-6-phosphate, DHAP: dihydroxyacetone phosphate, 2,3-DPG: 2,3-diphosphoglycerate, PEP: phosphoenol pyruvate, FBP: fructose biphosphate, 2PG: 2-phosphoglycerate, 3PG: 3-phosphoglycerate, GAP: glyceraldehyde phosphate, 1,3-DPG: 1,3-diphosphoglycerate, HK: hexokinase, PGI: phosphogluco isomerase, PFK: phosphofructokinase, FBA: fructose biphosphate aldolase, TPI: triosephosphate isomerase, GAPDH: glyceraldehyde phosphate dehydrogenase, BPGM: bisphosphoglycerate mutase, PGK: phosphoglycerate kinase, BPKG: bisphosphoglycerate kinase, PGM: phosphoglycerate mutase, ENO: enolase, LDH: lactate dehydrogenase.

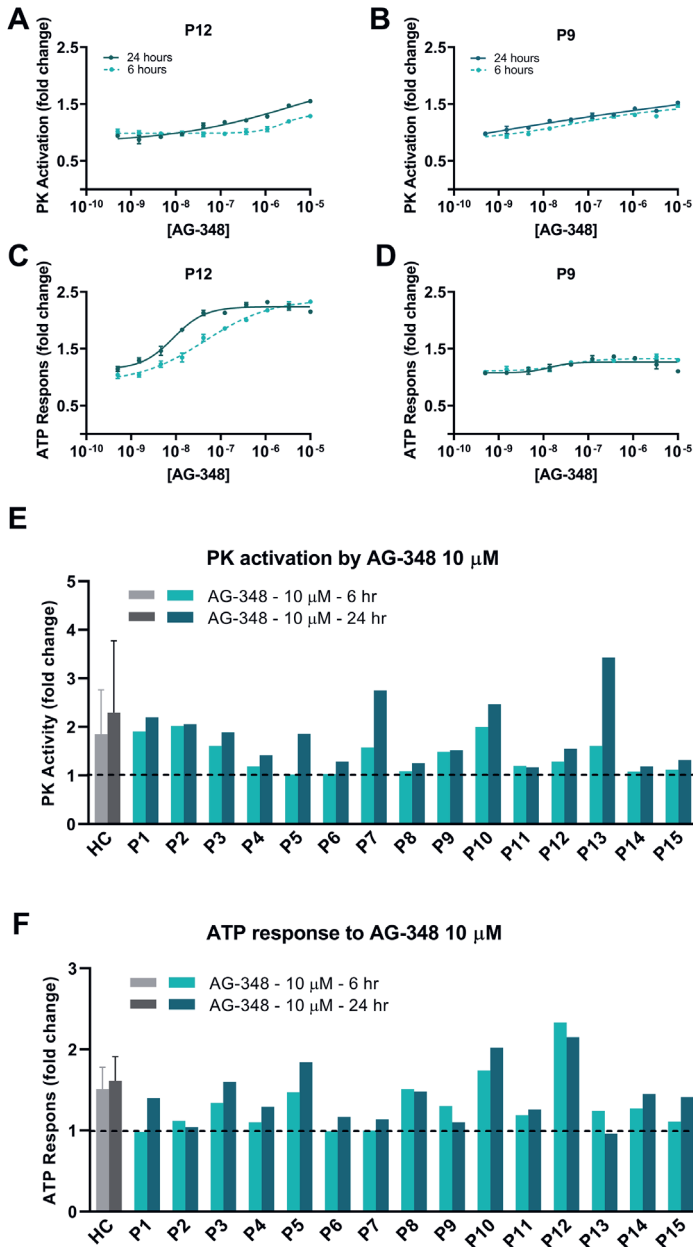


Figure 3. Ex vivo AG-348 treatment of RBCs increase PK activity and ATP levels in a dose dependent manner. (A and B) representative patient dose response curves of PK activity, expressed as fold activation compared to incubation without AG-348, as measured in RBCs of patients 12 (A) and 9 (B) after 6 (turquoise) and 24 hour (dark green) incubation with AG-348. (C and D) representative patient ATP dose response curves, expressed as fold activation compared to incubation without AG-348, as measured in RBCs of patients 12 (C) and 9 (D) after 6 (turquoise) and 24 hour (dark green) incubation with AG-348. (E) PK activation in RBCs of 15 PK deficient patients after six (turquoise) and 24 hours (dark green) incubation with 10 μ M AG-348. Mean PK fold activation of healthy controls after six (light gray) and 24 hours (dark gray) incubation with AG-348 10 μ M is shown on the left of the graph. ▶

(F) ATP response (fold activation) of 15 PK deficient patients after six (turquoise) and 24 hours (dark green) incubation with 10 μM AG-348. Mean ATP response of healthy controls is shown on the left of the graph (gray bars). Error bars represent standard deviation. Dashed turquoise line represents 6 hour incubation with AG-348, solid dark green line represents 24 hour incubation.

Ex vivo treatment with AG-348 restores PK thermostability

At baseline, PK-R thermostability was strongly reduced in all PK-deficient patients (figure 4C). Whereas RBCs from healthy controls showed a mean residual activity of 81% (range 64-108%) after incubation at 53 °C for 60 minutes, the mean residual PK-R activity in PK-deficient patients was significantly decreased under these conditions to only 30% (range 6-54%, $p < 0.0001$). This confirms earlier observations³⁰ and shows that PK thermostability is a common feature of many different mutant forms of PK-R, and not just restricted to known unstable variants like p.Arg510Gln. Treating PK-deficient RBCs *ex vivo* with AG-348 (2 μM) prior to this assay showed a clear effect on stability of the enzyme (Fig 4C, illustrative examples of RBCs from patients 12 and 9 are displayed in Figure 4A and B). *Ex-vivo* treatment with AG-348 lead to a mean residual PK activity of 58% (range 0-115%, $p < 0.001$) in RBCs from PK-deficient patients and 106% in controls (range 99-111%, $p = 0.13$). We observed no differences in PK thermostability response between PK-deficient patients with M/M and M/NM genotypes (Table 1, Figure 4C).

Effect of ex vivo AG-348 treatment on deformability of PK-deficient RBCs

Because RBC deformability is partly ATP dependent^{40,41} we investigated the effect of *ex vivo* AG-348 treatment on this important RBC functional property by osmotic gradient ektacytometry (osmoscan) and deformability measurements. Figure 5A shows osmoscan curves of the 15 healthy control samples (gray) and that of patient 7 (red) as an example. At baseline, maximum deformability (EI_{max}) of PK-deficient RBCs was significantly decreased compared to controls, although the difference was small ($p < 0.01$, figure 5D). Similarly, O_{min} and O_{hyper} , reflecting RBC surface-to-volume ratio and hydration status,⁴² respectively, were significantly different in PK-deficient patients ($p = 0.039$ and 0.047 , figure 5C and E). This implies that PK-deficient RBCs are somewhat less deformable than normal RBCs, possibly due to a slightly lower surface to volume ratio and a slight increase in RBC hydration.

When PK-deficient patients were divided according to genotype (Table 1) there was a significant difference between M/M and M/NM genotypes, indicating that a more severe genotype results in lower maximal RBC deformability (EI_{max} , $p = 0.039$, figure 5B).

After 24 hours of *ex vivo* treatment with AG-348, an improvement in RBC deformability was observed in about half of the PK-deficient patients (Figure 5F, patients 1, 3, 4, 6, 7, 8, and 9) compared to their untreated RBCs. The effect of these changes were similar in magnitude to the baseline difference in deformability observed between PK-deficient RBCs and control RBCs (Figure 5C). Taken in aggregate, however, there was no overall significant improvement of deformability.

Effect of ex vivo AG-348 treatment on PK-R-deficient erythroid development

During erythropoiesis PK-M2 levels are gradually replaced by PK-R^{43,44} and AG-348 has been described to also activate PK-M2.²² Because, PK deficiency has been associated with

ineffective erythropoiesis¹⁵⁻¹⁷ we next investigated the effect of *ex vivo* AG-348 treatment on erythroid development from four PK-deficient patients and controls. Morphologically there were no major abnormalities in erythroid development between healthy controls and PK-deficient patients (Figure 6A). This was supported by absence of differences in erythroid surface marker expression³⁵ (supplemental Figure 2A). There was no difference in erythroid differentiation with or without AG-348 treatment. This was observed in both healthy control cells as well as PK-deficient cells (Supplemental Figure 2B and C). In presence of AG-348 (2 μ M) we did note however a small increase in cell number in both normal controls and patients after proliferation for 10 days, although the difference was not significant ($p=0.059$, Figure 6B).

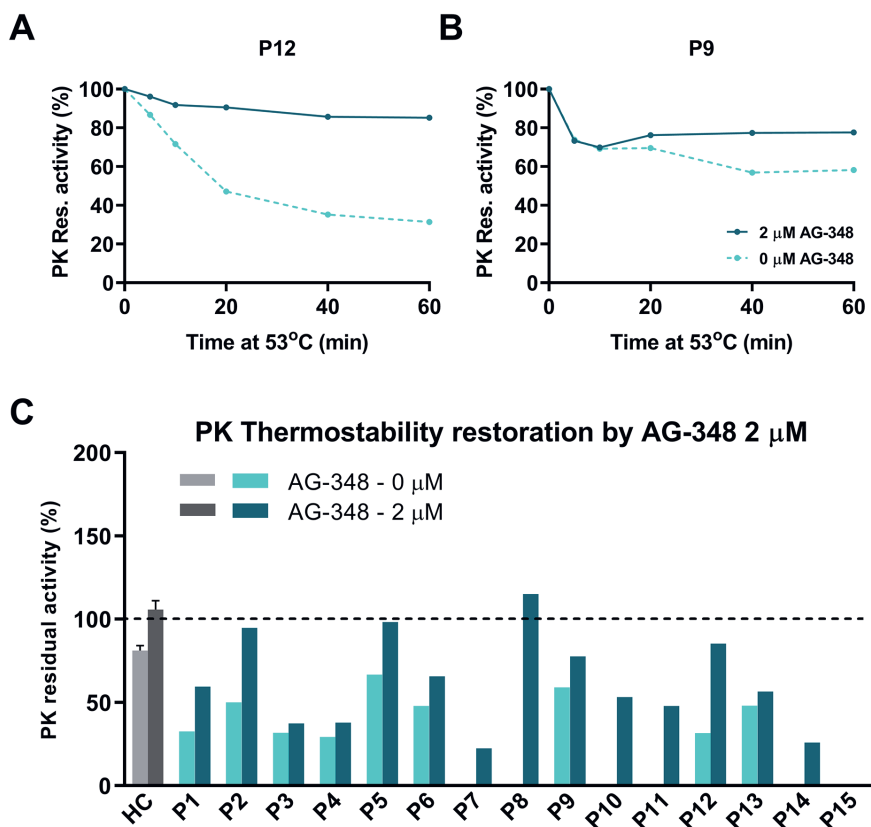


Figure 4. PK thermostability is restored upon *ex vivo* treatment with AG-348. (A and B) Representative PKD patient's PK thermostability of RBC lysates of patients 12 (A) and 9 (B) pre-incubated in absence (dashed line) or presence (solid line) of 2 μ M AG-348 for 2 hours at 37°C. For PK thermostability, residual PK activity (%) is measured after 5, 10, 20, 40 and 60 minutes of heat treatment at 53°C. (C) Residual PK activity (%) after 60 minutes of heat treatment of 15 PK deficient pre-incubated in absence (light turquoise) and presence (dark turquoise) of 2 μ M AG-348. Levels are normalized to baseline levels of PK-activity before heat treatment. Absence of bars indicate that PK residual activity was below the detection limit. Error bars represent standard deviation.

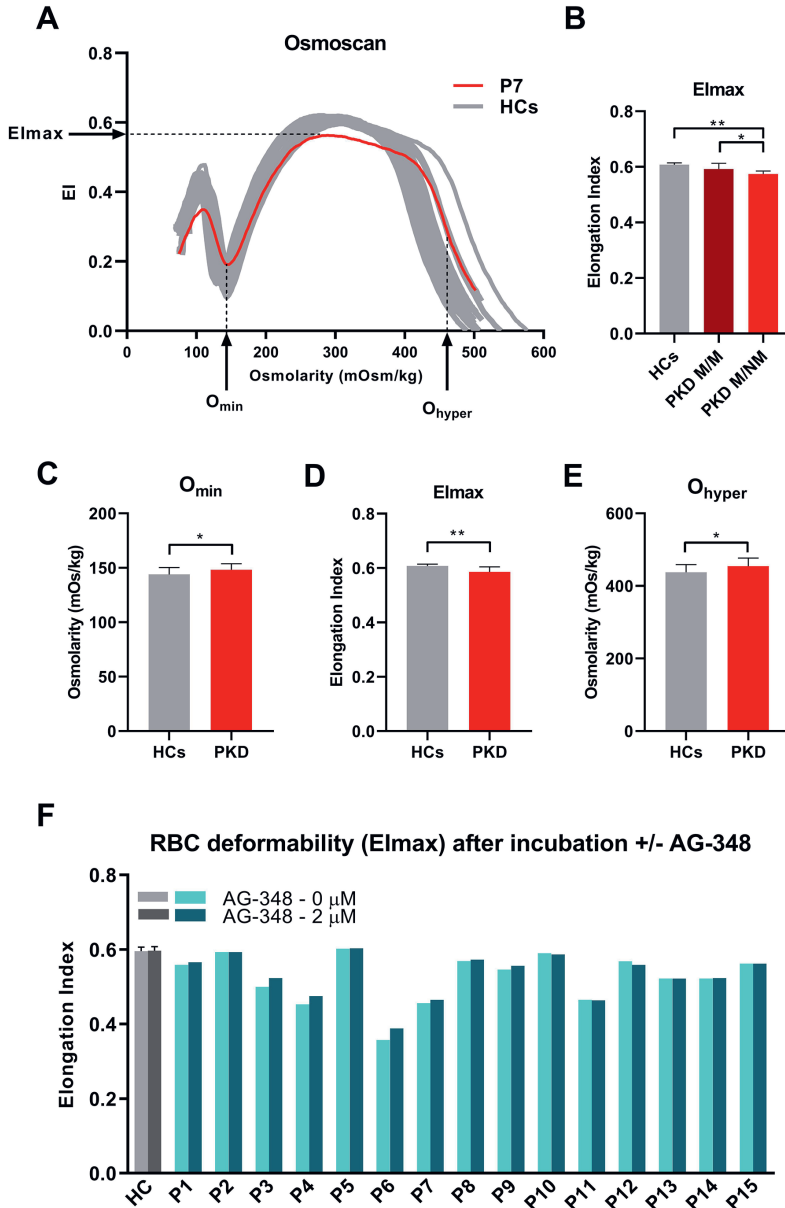
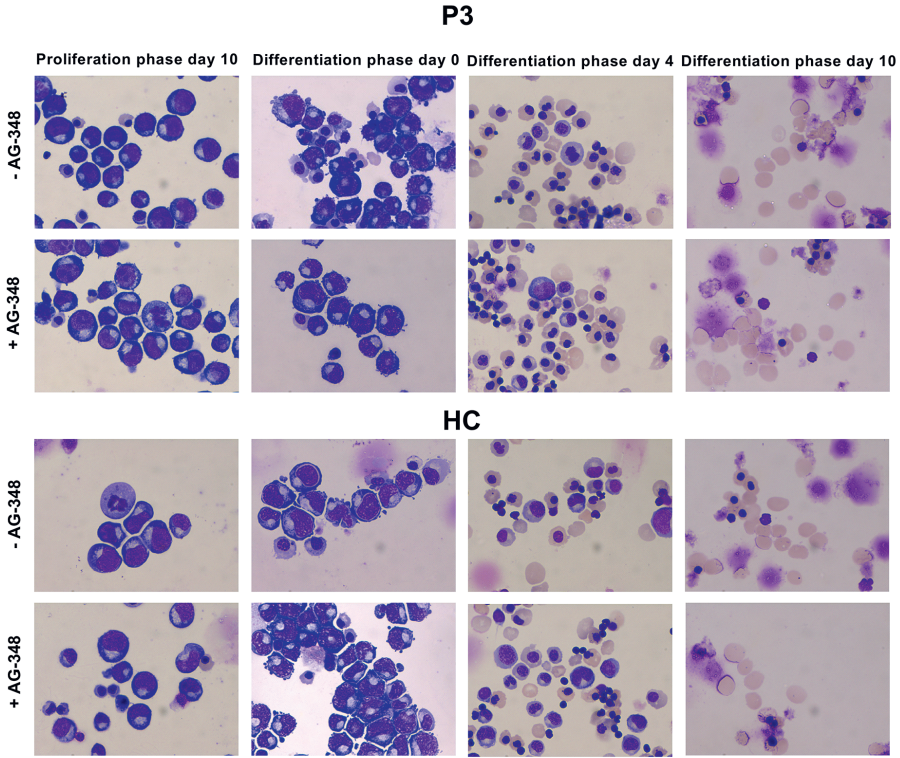
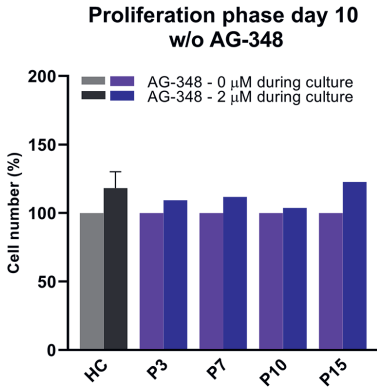


Figure 5. Red blood cell deformability in PK-deficient patients is slightly decreased. (A) Osmoscan curve of patient 7 (red) and 15 healthy controls (grey). (B) Maximum deformability (Elmax) is slightly decreased in PK deficiency compared to controls. When grouped according to genotype, i.e. M/M versus M/NM there is a significant difference, indicating that a more severe genotype results in lower maximal RBC deformability. (C) O_{min} is slightly increased in PK-deficient patients compared to healthy controls. (D) Elmax is slightly decreased in PK-deficient patients compared to healthy controls. (E) O_{hyper} is slightly increased in PK-deficient patients compared to healthy controls. (F) After 24 hours of *ex vivo* treatment with 20 μ M AG-348 in about half of the PK-deficient patients an improvement in RBC deformability was observed (patients 1, 3, 4, 6, 7, 8, and 9) compared to their untreated RBCs. PKD: pyruvate kinase deficiency, HCs: healthy controls, M/M: missense/missense, M/NM: missense/non-missense, Error bars represent standard deviation. ** $p < 0.01$, * $p < 0.05$.

A



B



C

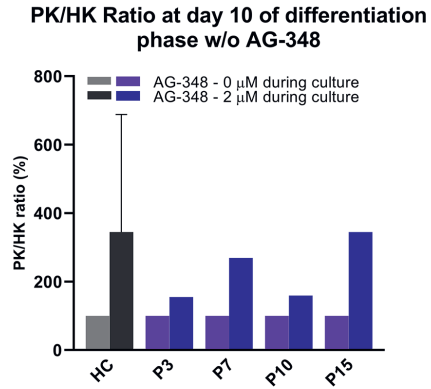


Figure 6. Ex vivo treatment with AG-348 does not evidently affect PK-deficient ex vivo erythroid proliferation and differentiation. (A) Morphology of ex vivo cultured erythroid cells of a PK-deficient patient (P3) and a healthy control at the final stage of proliferation (day 10) and on various days during differentiation (day 0, 4 and 10). (B) Ex vivo erythroid proliferation (cell numbers in %) was slightly higher when cells were cultured in presence of 2 μM AG-348 (dark purple) compared to 0 μM AG-348 (light purple). This was also observed for healthy controls. (C) PK/HK ratio of erythroid cells of PK-deficient patients (purple) and healthy controls (grey) cultured in presence (dark) or absence (light) of 2 μM AG-348 respectively was increased compared to cells cultured without AG-348. W/o: with/without, HC: healthy control, P: patient. Error bars represent standard deviation.

Western Blot analysis of PK-R and PK-M2 protein levels of healthy control samples clearly showed an increase of expression of PK-R and a decrease of PK-M2 during differentiation (Supplemental Figure 3). The decrease in PK-M2 was also observed in all patient samples, whereas a clear increase in PK-R expression was seen only in samples from patients 7 and 15 (Supplemental Figure 3). PK-R protein levels were low or inconclusive in patients 3 and 10. Presence of AG-348 during *ex vivo* erythropoiesis was associated with higher levels of PK-R in patients 7 and 15. There was no effect of AG-348 on PK-M2 expression. On the level of enzymatic activity the PK/HK ratio from cultured red cells was higher in presence of AG-348 in both patients and healthy controls, although this effect did not meet statistical significance ($p=0.064$, Figure 6C).

Discussion

In this study we characterized and evaluated the effect of AG-348, a recently reported first-in-class allosteric activator of PK-R^{22,23} that is currently in clinical trials for the treatment of PK deficiency (ClinicalTrials.gov: NCT02476916, NCT03853798, NCT03548220, NCT03559699). Our findings indicate that *ex vivo* treatment with AG-348 effectively increases PK-R activity over a broad range of *PKLR* genotypes as assessed by enzymatic activity as well as cellular ATP levels. Our findings are consistent with those previously reported by Kung et al.,²² and further extend those findings through the evaluation of a substantially larger cohort of PK-deficient blood samples, including a comprehensive baseline metabolomics analysis, and assessment for the first time of the effects of PK deficiency on parameters such as red cell deformability and *ex-vivo* expansion of erythroid progenitors.

Our cohort shows an overall mean 1.8-fold increase in PK activity in response to *ex vivo* treatment with AG-348 (range 1.2 – 3.4, Figure 3E). This is very similar to the previously reported mean fold increase of 2.1 (range 1.3 – 3.4). Similarly, the 1.5-fold increase in ATP levels we observed in PK-deficient RBCs (range 1.0 – 2.2) was comparable to previously reported results (mean fold increase 1.7; range 1.3 – 2.4).

PK-thermostability was found to be significantly improved upon *ex vivo* treatment with AG-348 even though there was a high variability in response among the different genotypes (Figure 4). An interesting subset comprised six PK-deficient patients (patients 4, 7, 10, 11, 14, and 15) who had the common PK-R mutation c.1529G>A p.(Arg510Gln), previously shown to have little defect in catalytic activity but to be highly unstable. Five of these patients had unmeasurably low PK activity in the thermostability test, and the activity of four could be restored by pre-incubating RBCs with AG-348 (Figure 4, patients 7, 10, 11 and 14). These four patients carried the p.(Arg510Gln) mutation *in trans* to a splice site mutation (patient 7), a missense mutation (patients 10 and 14), and a nonsense mutation (patient 11). A significant outlier was patient 15, who was homozygous for p.(Arg510Gln), suggesting the possibility that it may be more difficult to stabilize this mutation in the homozygous condition. Another outlier was patient 4, who had p.(Arg510Gln) paired with the nonsense mutation p.(Arg488*) yet had a relatively modest loss of activity in the thermostability test. Collectively these data illustrate that AG-348 has the potential to stabilize a diverse range

of different mutant PK-R molecules *in vitro*, but also demonstrate the complex variability that is introduced by the compound heterozygous state of most patients.

One surprising result was that the effects of AG-348 were variable across the different patient samples and that overall increases in PK-activity, ATP and thermostability were not observed in concert in some patients. For example patient 13 shows a clear response in terms of PK activity after AG-348 treatment for 24 hours whereas the ATP response was present at 6 hours and back to baseline by 24 hours. However we did observe that residual PK-R protein levels at baseline are important for the response to AG-348. When grouping patients according to their response in PK activity or ATP levels (i.e. >1.5-fold versus <1.5-fold response) PK-R protein levels at baseline (Figure 1E) were found to be higher in the patients that showed a >1.5-fold increase upon *ex vivo* treatment with AG-348 (Figure 7). This suggests that the amount of PK-R protein is an important determinant for the *in vitro* activity of AG-348, and is consistent with its mechanism of action via direct binding and stimulation of mutant enzyme.

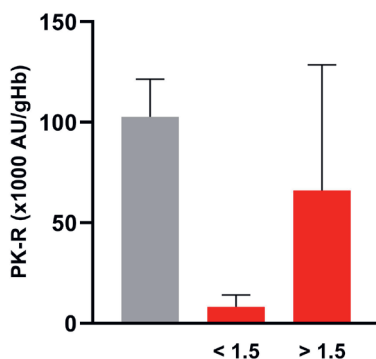


Figure 7. PK-deficient red cells with higher PK-R protein levels are more likely to show an increase in ATP levels and/or PK-R activity after *ex vivo* treatment with AG-348. Base line PK-R protein levels in patients showing a response in PK activity or ATP levels (i.e. >1.5-fold response versus <1.5-fold response, red bars) upon *ex vivo* treatment with AG-348 PK-R levels of healthy controls are shown in grey. ECL: Electrochemiluminescence, gHb: gram hemoglobin. Error bars represent standard deviation.

While the *in vitro* assessments as presented in this study provide clear evidence that AG-348 can stimulate the activity of mutant PKR enzymes in a variety of contexts, the central question is whether changes in these parameters would be associated with increased likelihood of clinical response to AG-348. Recently, data from the Phase 2 study of AG-348 in PK deficient patients have been published.²⁴ Analysis of those results suggests some parallels between our data and the response observed in treated patients. For instance, the clinical manuscript demonstrates that higher baseline PK-R protein levels in patients is associated with Hb increases, which parallels the findings described here. Similarly to the effects on thermostability noted above in patients with the p.(Arg510Gln) mutation, such patients in Phase 2 had variable Hb responses.²⁴

For the first time, we report here on the effects of AG-348 on *ex vivo* produced PK-R deficient red blood cells. In presence of AG-348 we observed a trend towards a slightly improved proliferation of erythroid progenitor cells in both healthy controls and PK-deficient patients of various *PKLR* genotypes (Figure 5B). Further studies are warranted to establish this more firmly, but it could indicate that, apart from acting on mature RBCs in the circulation, AG-348 could have a potential beneficial effect on both normal and PK-deficient early stage erythroid development. In addition, we show that *ex vivo* produced (mutant) PK-R can be activated to a similar degree as (mutant) PK-R from RBCs from patients and healthy controls (Figure 6C). This was particularly evident for patients 7 and 15, who also showed the most pronounced effect of AG-348 on PK-R protein levels (Supplemental Figure 3).

At the same time, based on cell count, morphology, and erythroid differentiation markers we did not observe major differences between normal and PK-deficient *ex vivo* erythroid proliferation. This is in contrast with previous reports that suggest ineffective erythropoiesis is a pathophysiological feature of PK deficiency, based on increased numbers of apoptotic early erythroid progenitor cells in the spleen of one PK-deficient patient,¹⁶ and similar findings in the spleen from a mouse model of PK deficiency.¹⁵ Regarding this observed discrepancy between our findings and previous studies, a possible confounder is that we grew erythroid cells from a fixed number of PBMCs. There likely will be variation between patients and controls in terms of PBMC composition, in particular the number of CD34⁺ cells. This may influence the eventual outcome of cellular proliferation. More importantly, genotype-phenotype correlations could explain these conflicting results as different genotypes result in different complications,¹⁸ indicating that different mutations could result in a large variability in the occurrence of ineffective hematopoiesis.

A limitation of this study is the absence of a functional assay that could directly measure the effect of ATP increase. We did observe an improvement of red blood cell deformability as measured by osmotic gradient ektacytometry after *ex vivo* treatment with AG-348 in half of the patients (figure 5F). However, this technique likely underestimates the effect of ATP increase by AG-348. Although ektacytometry is an important and established method in the diagnosis of RBC membrane and hydration disorders^{33,34,45,46} it has some limitations. Ektacytometry reflects the passive deformation of RBCs in contrast to filter based assays or microfluidics which forces RBCs to actively deform. The latter is thought to be more dependent on ATP.^{14,41} This could explain the finding of only a small correlation with ATP levels and deformability measured in RBC concentrates intended for transfusion.⁴⁰

Our results show only a slight difference in RBC deformability between PK-deficient patient and healthy controls, with the lowest deformability observed in M/NM patients (figure 5B). This is in line with recent findings⁴⁵ using the same technique, but contrasts with earlier findings based on a filtration based assay.⁴⁷ We also observed normal deformability in the splenectomized PK-deficient patients compared to a small decrease in EI_{\max} in non-splenectomized patients, which correlated inversely to reticulocyte count ($r=-0.740$, $p=0.0016$). These results are in line with previous studies, that show that reticulocytes of PK-deficient patients are preferentially removed by the spleen,¹¹ probably due to their

compromised deformability as a result of insufficient ATP-levels.⁴⁷ It has been suggested that such a decreased deformability could be due to the decreased hydration as a result of K^+ efflux through PIEZO1 mediated Ca^{2+} influx and activation of Gardos channels.¹² However, the osmoscan data show no signs of dehydration of RBCs (i.e. decreased O_{hyper}), which is clearly measurable on RBCs of patients with hereditary xerocytosis, where dehydration is thought to occur through the same mechanism.⁴⁸

Collectively, the data presented in this study support the hypothesis that drug intervention with AG-348 effectively upregulates PK-R enzymatic activity and increases stability in PK-deficient RBCs over a broad range of PKLR genotypes. The concomitant increase in ATP levels suggests that glycolytic pathway activity may be restored. AG-348 treatment may therefore represent an attractive way to correct the underlying pathologies of PK deficiency.

Author contributions

CK, BAO, PAK and RW designed the experiments. BAO, SS, KJ, VC and PAK recruited, and collected samples and/or performed experiments. PAK, JH, LD and CK provided AG-348. MAER, and RW analyzed the data and wrote the manuscript with input and revisions of BAO, PAK, GP, VC, WWS, EJB and CK.

Funding

This research has been supported by AGIOS Pharmaceuticals, and in part by an unrestricted grant provided by RR Mechatronics.

Acknowledgements

The authors would like to thank all the PK-deficient patients that participated in this study.

References

- Koralkova P, Van Solinge WW, Van Wijk R. Rare hereditary red blood cell enzymopathies associated with hemolytic anemia - pathophysiology, clinical aspects, and laboratory diagnosis. *Int J Lab Hematol*. 2014;36(3):388-397.
- Beutler E, Gelbart T. Estimating the prevalence of pyruvate kinase deficiency from the gene frequency in the general white population. *Blood*. 2000;95(11):3585-3588.
- Carey PJ, Chandler J, Hendrick A, et al. To the editor: Prevalence of pyruvate kinase deficiency in a northern European population in the north of England. *Blood*. 2000;96(12):4005-4007.
- de Medicis E, Ross P, Friedman R, et al. Hereditary nonspherocytic hemolytic anemia due to pyruvate kinase deficiency: a prevalence study in Quebec (Canada). *Hum Hered*. 1992;42(3):179-183.
- Kanno H, Fujii H, Miwa S. Structural Analysis of Human Pyruvate Kinase L-Gene and Identification of the Promoter Activity in Erythroid Cells ' Hitoshi KANNO ', Hisaichi FUJII ' and Shiro MIWA '. *Biochem Biophys Res Commun*. 1992;188(2):516-523.
- Kanno H, Fujii H, Hirono A, Miwa S. cDNA cloning of human R-type pyruvate kinase and identification of a single amino acid substitution (Thr384 --> Met) affecting enzymatic stability in a pyruvate kinase variant (PK Tokyo) associated with hereditary hemolytic anemia. *Proc Natl Acad Sci*. 1991;88(September):8218-8221.
- Zanella A, Fermo E, Bianchi P, Chiarelli LR, Valentini G. Pyruvate kinase deficiency: The genotype-phenotype association. *Blood Rev*. 2007;21(4):217-231.
- Van Wijk R, Huizinga EG, Van Wesel ACW, Van Oirschot BA, Hadders MA, Van Solinge WW. Fifteen novel mutations in PKLR associated with pyruvate kinase (PK) deficiency: Structural implications of amino acid substitutions in PK. *Hum Mutat*. 2009;30(3):446-453.
- Canu G, De Bonis M, Minucci A, Capoluongo E. Red blood cell PK deficiency: An update of PK-LR gene mutation database. *Blood Cells, Mol Dis*. 2016;57:100-109.
- Glader B. Salicylate-induced injury of pyruvate-kinase-deficient erythrocytes. *N Engl J Med*. 1976;294(17):916-918.
- Mentzer WC, Baehner RL, Schmidt-Schönbein H, Robinson SH, Nathan DG. Selective reticulocyte destruction in erythrocyte pyruvate kinase deficiency. *J Clin Invest*. 1971;50(3):688-699.
- Koller CA, Orringer EP, Parker JC. Quinine protects pyruvate kinase deficient red cells from dehydration. *Am J Hematol*. 1979;7(3):193-199.
- Park Y, Best CA, Badizadegan K, et al. Measurement of red blood cell mechanics during morphological changes. *Proc Natl Acad Sci*. 2010;107(15):6731-6736.
- Weed RI, LaCelle PL, Merrill EW. Metabolic dependence of red cell deformability. *J Clin Invest*. 1969;48(5):795-809.
- Aizawa S, Harada T, Kanbe E, et al. Ineffective erythropoiesis in mutant mice with deficient pyruvate kinase activity. *Exp Hematol*. 2005;33(11):1292-1298.
- Aizawa S, Kohdera U, Hiramoto M, et al. Ineffective erythropoiesis in the spleen of a patient with pyruvate kinase deficiency. *Am J Hematol*. 2003;74(1):68-72.
- Aisaki K ichi, Aizawa S, Fujii H, Kanno J, Kanno H. Glycolytic inhibition by mutation of pyruvate kinase gene increases oxidative stress and causes apoptosis of a pyruvate kinase deficient cell line. *Exp Hematol*. 2007;35(8):1190-1200.
- Grace RF, Bianchi P, van Beers EJ, et al. The clinical spectrum of pyruvate kinase deficiency: data from the Pyruvate Kinase Deficiency Natural History Study. *Blood*. 2018;131(20):blood-2017-10-810796. doi:10.1182/blood-2017-10-810796
- Grace RF, Mark Layton D, Barcellini W. How we manage patients with pyruvate kinase deficiency. *Br J Haematol*. 2019;(January):721-734.
- van Straaten S, Bierings M, Bianchi P, et al. Worldwide study of hematopoietic allogeneic stem cell transplantation in pyruvate kinase deficiency. *Haematologica*. 2018;103(e83).
- Garcia-Gomez M, Calabria A, Garcia-Bravo M, et al. Safe and efficient gene therapy for pyruvate kinase deficiency. *Mol Ther*. 2016;24(7):1187-1198.
- Kung C, Hixon J, Kosinski PA, et al. AG-348 enhances pyruvate kinase activity in red blood cells from patients with pyruvate kinase deficiency. *Blood*. 2017;130(11):1347-1356.

23. Yang H, Merica E, Chen Y, et al. Phase 1 Single- and Multiple-Ascending-Dose Randomized Studies of the Safety, Pharmacokinetics, and Pharmacodynamics of AG-348, a First-in-Class Allosteric Activator of Pyruvate Kinase R, in Healthy Volunteers. *Clin Pharmacol Drug Dev.* 2019;8(2):246-259.
24. Grace RF, Rose C, Layton M, et al. Safety and Efficacy of Mitapivat in Pyruvate Kinase Deficiency. *N Engl J Med.* 2019;381(10):933-944.
25. Allen EL, Ulanet DB, Pirman D, et al. Differential Aspartate Usage Identifies a Subset of Cancer Cells Particularly Dependent on OGDH. *CellReports.* 2016;17(3):876-890.
26. Clasquin MF, Melamud E, Rabinowitz JD. LC-MS Data Processing with MAVEN: A Metabolomic Analysis and Visualization Engine. *Curr Protoc Bioinforma.* 2012;37(14).
27. Kim H, Kosinski P, Kung C, Dang L, Chen Y, Yang H. A fit-for-purpose LC-MS/MS method for the simultaneous quantitation of ATP and 2,3-DPG in human K2EDTA whole blood. *J Chromatogr B.* 2017;1061-1062:89-96.
28. Beutler E, Blume K, Kaplan J, Lohr G, Ramot B, Valentine W. International Committee for Standardization in Haematology: Recommended Methods for Red-Cell Enzyme Analysis. *Br J Haematol.* 1977;35(August 1977):331-340.
29. Beutler E. *Red Cell Metabolism. A Manual of Biochemical Methods.*; 1980.
30. Blume KG, Arnold H, Lohr GW, Beutler E. Additional diagnostic procedures for the detection of abnormal red cell pyruvate kinase. *Clin Chim Acta.* 1973;43(3):443-446.
31. van Oirschot BA, Francois JJM, Van Solinge WW, et al. Novel type of red blood cell pyruvate kinase hyperactivity predicts a remote regulatory locus involved in PKLR gene expression. *Am J Hematol.* 2014;89(4):380-384.
32. Rijksen G, Veerman AJP, Schipper-Kester GPM, Staal GEJ. Diagnosis of Pyruvate Kinase Deficiency in a Transfusion-Dependent Patient With Severe Hemolytic Anemia. *Am J Hematol.* 1990;35(3):187-193.
33. Lazarova E, Gulbis B, Oirschot B Van, Van Wijk R. Next-generation osmotic gradient ektacytometry for the diagnosis of hereditary spherocytosis: Interlaboratory method validation and experience. *Clin Chem Lab Med.* 2017;55(3):394-402.
34. DaCosta L, Suner L, Galimand J, et al. Diagnostic tool for red blood cell membrane disorders : Assessment of a new generation ektacytometer. *Blood Cells, Mol Dis.* 2016;56(1):9-22.
35. van den Akker E, Satchwell TJ, Pellegrin S, Daniels G, Toye AM. The majority of the in vitro erythroid expansion potential resides in CD34 - cells, outweighing the contribution of CD34 + cells and significantly increasing the erythroblast yield from peripheral blood samples. *Haematologica.* 2010;95(9):1594-1598.
36. Jansen G, Koenderman L, Rijksen G, Cats BP, Staal GEJ. Characteristics of hexokinase, pyruvate kinase, and glucose-6-phosphate dehydrogenase during adult and neonatal reticulocyte maturation. *Am J Hematol.* 1985;20(3):203-215.
37. Wang C, Chiarelli LR, Bianchi P, et al. Human erythrocyte pyruvate kinase: Characterization of the recombinant enzyme and a mutant form (R510Q) causing nonspherocytic hemolytic anemia. *Blood.* 2001;98(10):3113-3120.
38. Diez A, Gilsanz F, Martínez J, Pérez-Benavente S, Meza NW, Bautista JM. Life-threatening nonspherocytic hemolytic anemia in a patient with a null mutation in the PKLR gene and no compensatory PKM gene expression. *Blood.* 2005;106(5):1851-1856.
39. Rogers SC, Ross JGC, D'Avignon A, et al. Sickle hemoglobin disturbs normal coupling among erythrocyte O2 content, glycolysis, and antioxidant capacity. *Blood.* 2013;121(9):1651-1662.
40. Karger R, Lukow C, Kretschmer V. Deformability of red blood cells and correlation with atp content during storage as leukocyte-depleted whole blood. *Transfus Med Hemotherapy.* 2012;39(4):277-282.
41. Fischer DJ, Torrence NJ, Sprung RJ, Spence DM. Determination of erythrocyte deformability and its correlation to cellular ATP release using microbore tubing with diameters that approximate resistance vessels in vivo. *Analyst.* 2003;128(9):1163-1168.
42. Clark R, Rossi E. Osmotic gradient ektacytometry: comprehensive characterization of red cell volume and surface maintenance. *Blood.* 1983;61(5):899-911.
43. Nijhof W, Wierenga PK, Staal GEJ, Jansen G. Changes in activities and isozyme patterns of glycolytic enzymes during erythroid differentiation in vitro. *Blood.* 1984;64(3):607-613.

44. Takegawa S, Fujii H, Miwa S. Change of pyruvate kinase isozymes from M2- to L-type during development of the red cell. *Br J Haematol.* 1983;54(3):467-474.
45. Zaninoni A, Fermo E, Vercellati C, et al. Use of laser assisted optical rotational cell analyzer (LoRRca MaxSis) in the diagnosis of RBC membrane disorders, enzyme defects, and congenital dyserythropoietic anemias: A monocentric study on 202 patients. *Front Physiol.* 2018;9(APR):1-12.
46. Llaudet-Planas E, Vives-Corrans JL, Rizzuto V, et al. Osmotic gradient ektacytometry: A valuable screening test for hereditary spherocytosis and other red blood cell membrane disorders. *Int J Lab Hematol.* 2018;40(1):94-102.
47. Leblond PF, Coulombe L, Lyonnais J. Erythrocyte Populations in Pyruvate Kinase Deficiency Anaemia Following Splenectomy. *Br J Haematol.* 1978;39(1):63-70.
48. Cahalan SM, Lukacs V, Ranade SS, Chien S, Bandell M, Patapoutian A. Piezo1 links mechanical forces to red blood cell volume. *Elife.* 2015;4:1-12.

Supplemental methods

Whole blood from patients with PKD was collected according to protocol that was approved by the ethical committee of the University Medical Center Utrecht (Protocol 14-571/M). Whole blood of healthy controls was collected through the Mini Donor Service, which is approved by the ethical committee of the University Medical Center Utrecht and in accordance to the declaration of Helsinki.

Hematological laboratory parameters

Routine hematological parameters were measured using the Abbott Cell-Dyne Sapphire (Abbott Diagnostics, Santa Clara, CA, USA).

Metabolic Profiling

Relative abundance of central carbon metabolites was performed by UPLC-MS. Frozen whole blood samples were thawed on ice and 10 μ L aliquots were extracted with 120 μ L of hot 70% ethanol containing 100 ng/mL L-glutamate (13C5, D5, 15N) as an internal standard. Samples were vortexed and centrifuged at 14000 rpm for 10 minutes at 4° C; supernatants were dried down and resuspended in water with 2-ketobutyrate (13C4, D2) internal standard. Metabolites were analyzed by high resolution accurate mass detection (HRAM) on a QExactive™ Orbitrap mass spectrometer (Thermo Fisher Scientific) as described previously.¹ Peak identification and integration was done with Maven software.² Quantitative analysis of ATP and 2,3-DPG was performed as described previously.³

PK activity measurements, protein levels, and thermostability tes

RBCs were purified from whole blood using a microcrystalline cellulose- α -cellulose column according to standardized methods.^{4,5} Columns were centrifuged and washed twice with NaCl 0.9% before further experiments. PK and hexokinase (HK) activity was measured in lysates of purified RBCs as described.^{4,5} PK thermostability was measured essentially as described⁶ on the same hemolysates, after 0, 5, 10, 20, 40 and 60 minutes of incubation at 53°C. Aliquots were chilled for 5 minutes and centrifuged for 3 minutes at 600 g.

PK activity measurements after *ex vivo* treatment with AG-348 were performed at low substrate conditions (final concentration phosphoenol pyruvate (PEP) 0.5 mM). Protein levels of PK-R were determined by Mesoscale Assay (MesoScale Discovery) as described⁷ using Goat anti-PKLR antibody (Aviva) and Mouse anti-PKLR antibody (Abcam) both in Tris buffered saline + 0.5% Tween 20 (TBS-T) as sandwich antibodies in a multi-array 96 well plate. SULFO-TAG goat anti-mouse (Mesoscale discovery) was used as the detection antibody and the signal was measured using a MesoScale Discovery instrument. The PKR protein level was determined by normalizing the light intensity of the SULFO-TAG electrochemiluminescence (ECL) to the protein concentration of the lysate (final units: ECL/g of protein).

Western blot analysis of PK-R and PK-M2 was performed as previously described⁸ using polyclonal antibodies directed against PK-L⁹ and monoclonal antibodies raised against PK-M2 (PodiCeps, Utrecht, The Netherlands). Blots were visualized using Alexa Fluor®

680-conjugated goat anti-mouse and goat anti-rabbit antibodies (Li-Cor, Invitrogen) and quantified using the Odyssey Infrared Imaging System (LI-COR Biosciences, Lincoln, NE).

Ex vivo treatment of wild type and PK-deficient RBCs with AG-348

Purified RBCs or whole blood of patients and controls were incubated for 3, 6 and 24 hours at 37°C in presence or absence of AG-348. Purified RBCs or whole blood was added to phosphate-buffered saline containing 1% glucose, 170 mg/L adenine, and 5.25 g/L mannitol (pH 7.40) (AGAM buffer) prior to incubation. Purified RBCs from patients and healthy control subjects were incubated with different dosages of AG-348 (up to 10 µM) up to 24 hours at 37°C. After 6 and 24 hours PK-R activity and ATP levels (CellTiterGlo; Promega, Madison, WI) were measured. For determination of PK-R thermostability, RBC lysates were incubated for 2 hours with AG-348 (37°C) prior to testing. Because in the latter case AG-348 does not need to cross the membrane, a lower concentration of AG-348 was used (2 µM).

Band 3 expression levels

Western blot analysis of band 3 and glyceraldehyde-3-phosphate dehydrogenase (GAPDH) was performed on purified RBCs using monoclonal antibodies directed against human band 3 (Sigma) and polyclonal anti-human GAPDH antibodies (Sigma). Blots were visualized using Alexa Fluor® 680-conjugated goat anti-mouse and goat anti-rabbit antibodies (Li-Cor, Invitrogen) and quantified using the Odyssey Infrared Imaging System (LI-COR Biosciences, Lincoln, NE). Band 3/GAPDH ratio was calculated to evaluate band 3 expression levels.

Osmotic gradient ektacytometry (osmoscan) and deformability measurements

Osmotic gradient ektacytometry (osmoscan) and deformability measurements were performed using the Laser Optical Rotational Red Cell Analyzer (Lorrcra, RR Mechatronics, Zwaag, The Netherlands) as described.^{10,11} Elongation index (EI) was calculated from height and width of the diffraction pattern and reflects RBC deformability. To study the effect of AG-348 AGAM buffer was added to whole blood (1:10 ratio), and supplemented with either AG-348 (final concentration 20 µM) or DMSO (untreated samples). Samples were incubated for 24 hours at 37°C, after which deformability was measured.

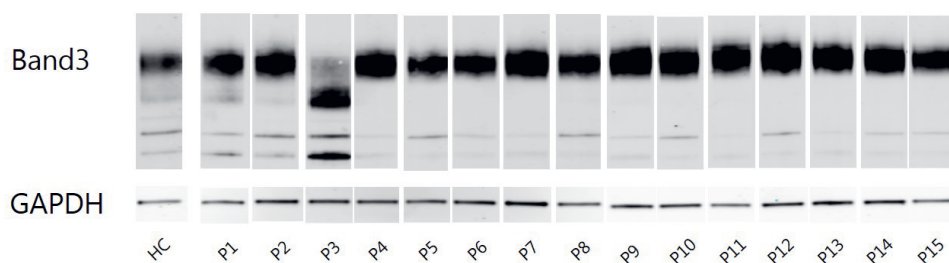
Ex vivo production of red blood cells and treatment with AG-348

Erythroid cells from PK-deficient patients and healthy controls were produced from peripheral blood mononuclear cells (PBMC) as described.¹² Briefly, PBMCs were isolated from peripheral blood by density purification using Percoll (GE Healthcare, Little Chalfont, UK). For proliferation, cells were cultured for 10 days in CellQuin medium (kind gift from Emile van den Akker, Sanquin, Amsterdam, The Netherlands), supplemented with Stem Cell Factor (100ng/mL, Amgen), Epo (2U/mL, EPREX), dexamethasone (1µM, Sigma), and 1 ng/mL IL-3 (R&D systems). After 10 days, cells were washed three times with PBS and reseeded at 2E⁶ cells/mL in CellQuin medium supplemented with EPO (10 U/mL, Eprex), heparin (5U/mL, Leo Pharmacy), human blood group AB plasma (3%, Sigma). At day 5 of differentiation CellQuin medium was replaced by RetQuin medium (Emile van den Akker, Sanquin, Amsterdam, The Netherlands). AG-348 was added at a final concentration of 2 µmol/L at days 0, 1, 3-10 during proliferation and day 0, 2, and 4 during differentiation. Under these

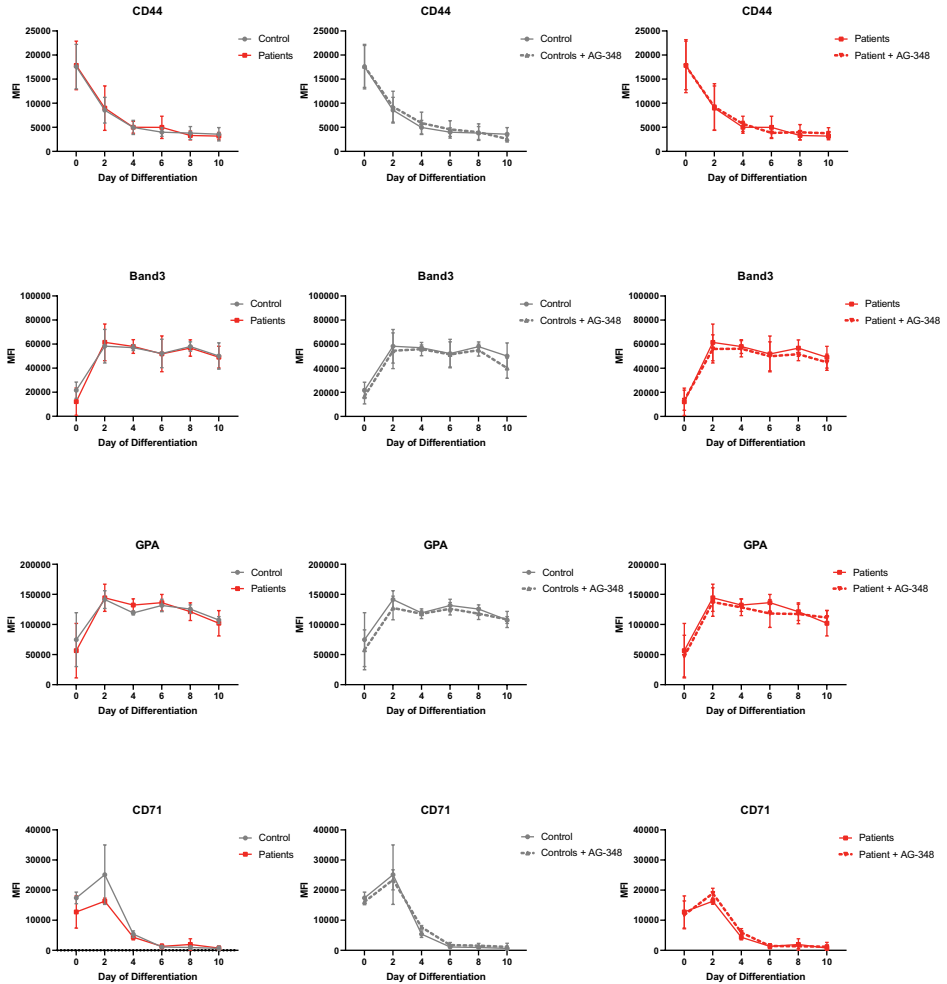
conditions mean AG-348 levels in medium are 2.4 $\mu\text{mol/L}$ (range 1.4 - 3.8 $\mu\text{mol/L}$) as determined by a validated liquid chromatography with tandem mass spectrometry (LC-MS/MS) method.¹³

Statistical Analysis

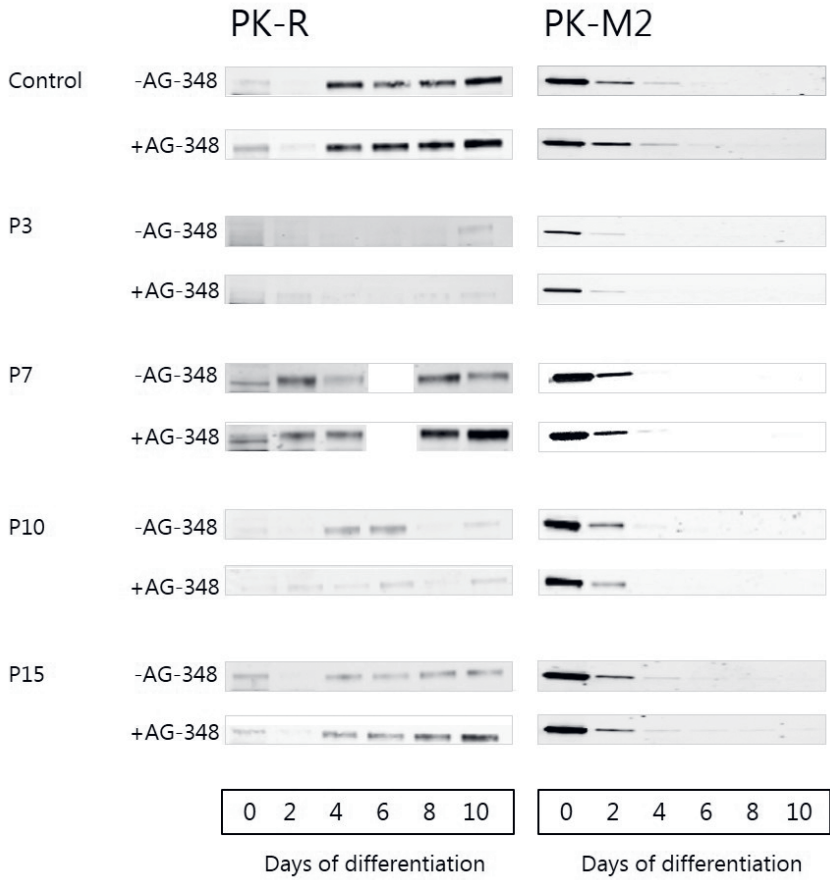
Statistical analysis was performed using Graphpad Prism (v7.04). T-test, Mann-Whitney test or Wilcoxon test was used when appropriate. One-way ANOVA (Post-hoc Tukey's test or Dunnett's test) was carried out or a Kruskal-Wallis test, followed by Dunn's tests for post-hoc analysis was used when appropriate. Pearson's correlation was used to determine correlations of laboratory parameters with enzyme activity measurements. A *p*-value of <0.05 was considered statistical significant.



Supplemental Figure 1. Band 3 expression levels are comparable between PK-deficient patients and healthy controls. Erythroid surface marker Band 3 and glyceraldehyde-3-phosphate dehydrogenase (GAPDH) levels were determined by Western Blot analysis and the Band 3/GAPDH ratio was used to evaluate band 3 expression levels. Band 3 expression levels of PK-deficient patients (median band3/GAPDH ratio: 2.7, range 1.0-4.8, n=14) were comparable to healthy controls (median ratio: 2.3, range 1.9-2.7, n=3). Patient 3 was excluded from this analysis because this sample may be degraded. A mutated form of band 3 is unlikely because of an essentially normal osmoscan profile as measured on this patient (not shown).



Supplemental Figure 2. Erythroid surface marker expression during erythroid differentiation is comparable between PK-deficient patients and healthy controls and is not influenced by AG-348. (A) Erythroid surface markers CD44, Band 3, glycophorin A (GPA) and CD71 were measured on day 0, 2, 4, 6, 8 and 10 of differentiation in cultured erythroid cells of PK-deficient patients and healthy controls. (B) Erythroid surface markers measured during differentiation in erythroid cells from healthy controls cultured in absence (solid grey line) and presence of AG-348 (dashed grey line). (C) Erythroid surface markers measured during differentiation in erythroid cells of PK-deficient patients cultured in absence (solid red line) and presence of AG-348 (dashed red line).



Supplemental Figure 3. PK-R and PK-M2 expression during ex vivo erythropoiesis is not influenced by AG-348. PK-R and PK-M2 levels were determined by Western Blot analysis on consecutive days during erythroid differentiation. Levels of PK-M2 gradually decreased during differentiation whereas PK-R levels increased, although not evidently recapitulated in all patients. Erythroid cells from healthy controls, and patient samples 7 and 15 showed an increase in PK-R expression when grown in presence of AG-348.

References

- Allen EL, Ulanet DB, Pirman D, et al. Differential Aspartate Usage Identifies a Subset of Cancer Cells Particularly Dependent on OGDH. *CellReports*. 2016;17(3):876-890. doi:10.1016/j.celrep.2016.09.052
- Clasquin MF, Melamud E, Rabinowitz JD. LC-MS Data Processing with MAVEN: A Metabolomic Analysis and Visualization Engine. *Curr Protoc Bioinforma*. 2012;37(14). doi:10.1002/0471250953.bi1411s37.LC-MS
- Kim H, Kosinski P, Kung C, Dang L, Chen Y, Yang H. A fit-for-purpose LC-MS/MS method for the simultaneous quantitation of ATP and 2,3-DPG in human K2EDTA whole blood. *J Chromatogr B*. 2017;1061-1062:89-96. doi:10.1016/j.jchromb.2017.07.010
- Beutler E, Blume K, Kaplan J, Lohr G, Ramot B, Valentine W. International Committee for Standardization in Haematology: Recommended Methods for Red-Cell Enzyme Analysis. *Br J Haematol*. 1977;35(August 1977):331-340.
- Beutler E. *Red Cell Metabolism. A Manual of Biochemical Methods*; 1980.
- Blume KG, Arnold H, Lohr GW, Beutler E. Additional diagnostic procedures for the detection of abnormal red cell pyruvate kinase. *Clin Chim Acta*. 1973;43(3):443-446. doi:10.1016/0009-8981(73)90487-7
- Kung C, Hixon J, Kosinski PA, et al. AG-348 enhances pyruvate kinase activity in red blood cells from patients with pyruvate kinase deficiency. *Blood*. 2017;130(11):1347-1356. doi:10.1182/blood-2016-11-753525
- van Oirschot BA, Francois JJM, Van Solinge WW, et al. Novel type of red blood cell pyruvate kinase hyperactivity predicts a remote regulatory locus involved in PKLR gene expression. *Am J Hematol*. 2014;89(4):380-384. doi:10.1002/ajh.23647
- Rijksen G, Veerman AJP, Schipper-Kester GPM, Staal GEJ. Diagnosis of Pyruvate Kinase Deficiency in a Transfusion-Dependent Patient With Severe Hemolytic Anemia. *Am J Hematol*. 1990;35(3):187-193.
- Lazarova E, Gulbis B, Oirschot B Van, Van Wijk R. Next-generation osmotic gradient ektacytometry for the diagnosis of hereditary spherocytosis: Interlaboratory method validation and experience. *Clin Chem Lab Med*. 2017;55(3):394-402. doi:10.1515/cclm-2016-0290
- DaCosta L, Suner L, Galimand J, et al. Diagnostic tool for red blood cell membrane disorders : Assessment of a new generation ektacytometer. *Blood Cells, Mol Dis*. 2016;56(1):9-22. doi:10.1016/j.bcmd.2015.09.001
- van den Akker E, Satchwell TJ, Pellegrin S, Daniels G, Toye AM. The majority of the in vitro erythroid expansion potential resides in CD34 - cells, outweighing the contribution of CD34 + cells and significantly increasing the erythroblast yield from peripheral blood samples. *Haematologica*. 2010;95(9):1594-1598. doi:10.3324/haematol.2009.019828
- Yang H, Merica E, Chen Y, et al. Phase 1 Single- and Multiple-Ascending-Dose Randomized Studies of the Safety, Pharmacokinetics, and Pharmacodynamics of AG-348, a First-in-Class Allosteric Activator of Pyruvate Kinase R, in Healthy Volunteers. *Clin Pharmacol Drug Dev*. 2019;8(2):246-259. doi:10.1002/cpdd.604

Chapter 11

Ektacytometry analysis of post-splenectomy red blood cell properties identifies cell membrane stability test as a novel biomarker of membrane health in hereditary spherocytosis

Frontiers in Physiology; 2021 Mar 25;12:641384

Berrevoets M.C¹, Bos J¹, Huisjes R¹, Merx T.H¹, van Oirschot B.A¹, van Solinge W.W¹, Verweij J.W.², Lindeboom M.Y.A², van Beers E.J³, Bartels M^{3†}, van Wijk R^{1†} and Rab M.A.E.^{1,3}

¹ Central Diagnostic Laboratory-Research, University Medical Center Utrecht, Utrecht, The Netherlands

² Department of Pediatric Surgery, University Medical Center Utrecht, Utrecht, The Netherlands

³ Van Creveldkliniek, University Medical Center Utrecht, Utrecht, The Netherlands

† These authors contributed equally and share penultimate authorship

Abstract

Hereditary spherocytosis (HS) is the most common form of hereditary chronic hemolytic anemia. It is caused by mutations in red blood cell (RBC) membrane and cytoskeletal proteins, which compromise membrane integrity, leading to vesiculation. Eventually, this leads to entrapment of poorly deformable spherocytes in the spleen. Splenectomy is a procedure often performed in HS. The clinical benefit results from removing the primary site of destruction, thereby improving RBC survival. But whether changes in RBC properties contribute to the clinical benefit of splenectomy is unknown. In this study we used ektacytometry to investigate the longitudinal effects of splenectomy on RBC properties in five well-characterized HS patients at four different time points and in a case-control cohort of 26 HS patients. Osmotic gradient ektacytometry showed that splenectomy resulted in improved intracellular viscosity (hydration state) whereas total surface area and surface-to-volume ratio remained essentially unchanged. The cell membrane stability test (CMST), which assesses the *in vitro* response to shear stress, showed that after splenectomy, HS RBCs had partly regained the ability to shed membrane, a property of healthy RBCs, which was confirmed in the case-control cohort. In particular the CMST holds promise as a novel biomarker in HS that reflects RBC membrane health and may be used to assess treatment response in HS.

Contribution to the field

Hereditary spherocytosis (HS) is characterized by poorly deformable spherocytes with increased density. These RBCs with reduced deformability are prematurely cleared by the spleen. Therefore, splenectomy is an effective treatment, and removal of the primary site of RBC destruction generally improves clinical symptoms. The effects of splenectomy on cellular level are unknown. In this study we assess changes in RBC properties measured with osmotic gradient ektacytometry upon splenectomy. Our results indicate that the osmotic gradient ektacytometry-derived parameter O_{hyper} showed that splenectomy resulted in improved intracellular viscosity (hydration state). More importantly we describe the Cell Membrane Stability Test (CMST), a new developed ektacytometry-based assay. The CMST reflects an yet-undescribed distinct RBC characteristic that correlates with the effect of splenectomy. Hence, it holds promise as a novel biomarker for membrane health in HS that may be used to assess the effect of other treatments such as embolization and partial splenectomy, and that may be related to clinical severity.

Introduction

Hereditary spherocytosis (HS) is a heterogeneous group of inherited anemias that originates from defective anchoring of transmembrane proteins to the cytoskeletal network of the red blood cell (RBC). The defective anchoring is predominantly caused by a mutation in the genes coding for ankyrin (ANK1), α -spectrin (SPTA1), β -spectrin (SPTB), band-3 (SLC4A1) or protein 4.2 (EPB42).¹ These mutations compromise the vertical linkages between the lipid bilayer and the cytoskeletal network, leading to destabilization of the membrane, increased vesiculation and subsequent membrane loss. The progressive membrane loss leads to formation of dense spherical-shaped RBCs (spherocytes) with reduced deformability.²⁻⁴

The spleen plays an intricate role in the pathophysiology of HS. Normally, this organ functions as a quality control for RBCs. During the 120-day lifespan of healthy RBCs, membrane surface area, surface area-to-volume ratio, and deformability decrease because of release of essentially hemoglobin-free microvesicles. RBCs with increased density and reduced deformability are eventually trapped in the narrow endothelial slits of the spleen, leading to clearance of aged RBCs.^{2,5} The compromised vertical linkages in HS accelerate the loss of membrane and deformability, leading to premature destruction of RBCs in the spleen. Therefore, splenectomy is an effective treatment, and removal of the primary site of RBC destruction generally improves clinical symptoms.^{1,2,6} Nevertheless, the risks and benefits should be carefully assessed as splenectomy results in a permanently increased risk of infections caused by encapsulated bacteria and long term risk for cardiovascular events.^{1,7}

The effects of splenectomy on RBC rheology and RBC related parameters in HS have been studied to a limited extent. It is known that splenectomy improves the RBC count, hemoglobin (Hb) levels, and hematocrit, and that it reduces mean corpuscular hemoglobin concentration (MCHC) and the percentage of reticulocytes.⁸⁻¹¹ On a cellular level it has been shown that the size of RBCs increases following splenectomy, and that microspherocytes can no longer be detected.¹² However, splenectomy has little effect on correcting the cytoskeletal membrane defect.¹¹ More recent studies have shown that RBC deformability as measured by osmotic gradient ektacytometry was not improved after splenectomy.^{9,10} An important limitation of these studies was the fact that they compared cohorts of splenectomized and non-splenectomized patients; longitudinal studies on the response to splenectomy of individual HS patients are scarce.⁸

In this study, we investigated individual responses to splenectomy in a group of five HS patients, with particular focus on RBC functional properties as determined by ektacytometry. Our results indicate that the Cell Membrane Stability Test (CMST), which measures the RBCs response to high shear stress, is able to detect substantial functional improvement of the RBC membrane after splenectomy, by showing a partly restored ability to shed membrane, a feature of healthy RBCs. We suggest that the CMST represents a novel biomarker of RBC membrane health in HS, and may be used to assess the efficacy of treatment.

Methods

Patients

Two groups of patients were enrolled in this study. The first group consisted of five patients (one male and four females, aged between 13 and 43 years) diagnosed with HS, and scheduled to undergo splenectomy. Detailed characteristics are provided in Supplemental Table 1. Left-over material of blood collected before splenectomy and at different time points after splenectomy (i.e. 1 week, 1 month and ≥ 3 months) was used for laboratory measurements. Informed consent was obtained from all patients and/or legal guardians. The second group consisted of a patient cohort of 26 HS patients: 18 non-splenectomized patients, 8 patients who underwent splenectomy ≥ 1 year prior to enrollment, and 26 healthy controls (HC). Blood samples of this cohort were obtained after inclusion in the CoMMiTMeNT-study which was approved by the Medical Ethical Research Board of the University Medical Center Utrecht, the Netherlands (15/426M) or from anonymized left-over material. Blood from healthy control individuals was obtained by means of the institutional blood donor service.

Surgical procedure

Laparoscopic total splenectomy was performed in all five patients. The patients were positioned in right lateral decubitus. Four trocars were used. The lesser sac was entered and the short gastric vessels were divided. After full mobilization of the spleen, the hilar vessels were controlled by using a linear cutting stapler. The spleen was extracted using a retrieval bag.

Laboratory parameters

Routine hematological laboratory parameters were analyzed on an Abbott Cell-Dyn Sapphire hematology analyzer (Abbott Diagnostics Division, Santa Clara, CA, USA).

Ektacytometry

Deformability of RBCs was measured with the Lorrca (Laser Optical Rotational Red Cell Analyzer, RR Mechatronics, Zwaag, The Netherlands). In this ektacytometer, RBCs are exposed to shear stress in a viscous solution (Elon-Iso), forcing the cells to elongate into an elliptical shape. The diffraction pattern, that is generated by a laser beam is measured by a camera. The vertical axis (A) and the horizontal axis (B) of the ellipse are used to calculate the elongation index (EI) by the formula $(A-B)/(A+B)$. The EI reflects the deformability of the total population of RBCs.

Osmotic gradient ektacytometry

Osmotic gradient ektacytometry measurements of RBCs of healthy controls and HS patients before and after splenectomy were obtained using the osmoscan module on the Lorrca according to the manufacturer's instructions and as described elsewhere.^{13,14} Briefly, whole blood was standardized to a fixed RBC count of 1000×10^6 and mixed with 5 mL of Elon-Iso (RR Mechatronics). RBCs in the viscous solution (Elon-Iso) were exposed to an osmolarity gradient from approximately 60 mOsmol/L to 600 mOsmol/L, while shear stress was kept constant (30 Pa).

Cell membrane stability test (CMST)

The cell membrane stability test (CMST) was performed using the CMST module on the ektacytometer. To perform a CMST, whole blood was standardized to a fixed RBC count of 200×10^6 and mixed with 5 mL of Elon-Iso. In the CMST RBCs are exposed to a shear stress of 100 Pa for 3600 seconds (1 hour) while the EI is continuously measured. The change in the elongation index (ΔEI) was calculated by determining the median of the first and the last 100 seconds of the CMST and subsequently calculating the difference between the medians. The ΔEI depicts the capacity of the RBCs to shed membrane and resist shear stress.

Microscopic analysis on a subset of samples was performed with the use of a camera microscope (1/1.8" Sony CMOS Global IMX265LLR imaging sensor, long working distance VS-Technology 50X Plan LWD, VS-MS-COL tube) which was placed on outside of the rotating cup of the Lorrca. A power-LED flash (415nm) coupled to a fiber-optic, in bright field illumination, from the inside of the cup into a 45 degrees mirror and diffusor lens directed at the microscope, was used for proper lighting of the RBCs. A flash time of 214 ns was used to get less than 1% motion blur. The rotating cup was modified with 15 thin and small glass windows circumferential in the cup. Images were taken with Image Capture software during a CMST measurement.

Density separation

To assess the effect of splenectomy on the composition of the RBC population a density separation was carried out before splenectomy and approximately 1 month after in one HS patient. A total of 20 mL whole blood was placed on top of 3 layers with different percentage percoll (GE Healthcare) 1.130 ± 0.005 g/mL in 8 different columns (2mL whole blood/column). RBCs were fractioned according to density (i.e. cellular age) using this density gradient of percoll with addition of HEPES, NaCl, KCL and NaOH as described in detail elsewhere.¹⁵ Cells were centrifuged at 1665g for 15 minutes, after which four fractions could be obtained (Supplemental Figure 1A). Fraction 1, containing the RBCs with the lowest density, was present on top of the 59% percoll layer, and was only present and subsequently obtained from the pre-splenectomy blood sample (Supplemental Figure 1A). Because of the limited amount of RBCs in fraction 1 only a subset of measurements could be performed. Fraction 2 was obtained from the top of the 70% percoll layer. Fraction 3 was obtained from the top of the 78% percoll layer. The 4th fraction, containing the most dense RBCs was obtained from the bottom of the tube (Supplemental Figure 1A).

Digital microscopy

Peripheral blood smears were analyzed using the CellaVision digital microscope DM96 (software 5.0.1build11). Analysis was performed using a neuronal network which classifies RBCs based on morphological characteristics such as shape, color, and texture. Spherocytes, microcytes and macrocytes (%) were calculated as a percentage of total RBCs as quantified by the software.¹⁶

Statistical analysis

All the data were analyzed using GraphPad Prism version 8.3.0 for Windows (GraphPad Software, San Diego, CA, USA). A paired T-test (two-tailed) was used to assess the values

before and after splenectomy. An one-way ANOVA, with post-hoc Tukey analysis was used to assess the differences between HC and HS patients, and non-splenectomized and splenectomized HS patients. In addition, a correlation analysis between RBC related parameters and the change in elongation index (ΔEI) was conducted using the Spearman's rank correlation coefficient. A p-value below 0.05 was considered statistically significant.

Results

Routine hematological parameters show a decrease in RBC density and increased RBC homogeneity after splenectomy

Following splenectomy, routine hematology parameters showed a significant improvement in RBC count, Hb, and reticulocyte count after 1 and ≥ 3 months (Figure 1A-C, Supplemental Table 1). Mean corpuscular volume (MCV) increased in the first week after splenectomy, but returned to pre-surgery levels in the following months (Figure 1D). This suggests that cell volume is not altered by splenectomy. At the same time, we observed a significant decrease in MCHC and the percentage of hyperchromic cells, indicating a decline in RBC density following splenectomy (Figure 1E and F). At the same time, spherocytes and microcytes as assessed by digital microscopy also declined, except for spherocytes in patient 1 (Supplemental Table 1). When RBCs of one HS patient were separated according to density (Supplemental Figure 1A), we noted that the MCHC before splenectomy seemed determined mainly by density fraction 4, containing the most dense RBCs, whereas after splenectomy density fractions 3 and 4 seem to contribute equally to the MCHC (Supplemental Figure 1B). This implies a more homogeneous RBC population after splenectomy, which was also reflected by a more equal distribution of the different fractions after splenectomy (Supplemental Figure 1A). Hyperchromic cells were predominantly present in fraction 4 before splenectomy, and their number decreased substantially after splenectomy (Supplemental Figure 1C).

Osmotic gradient ektacytometry-derived parameters indicate increased cellular hydration after splenectomy

Osmotic gradient ektacytometry was performed to determine the effect of splenectomy on RBC total surface area (EI_{max}), surface area-to-volume ratio (O_{min}), and RBC hydration state (O_{hyper}). In addition, the area under the curve was calculated.¹⁷ A representative curve of the effect of splenectomy after 1 month is shown in Figure 2A.

Post-splenectomy values for O_{min} and EI_{max} did not change significantly compared to pre-splenectomy values, indicating that after splenectomy HS RBCs still had reduced surface area-to-volume ratio and total surface area (Figure 2B and 2C, respectively). In contrast, the hydration state or cytoplasmic viscosity (O_{hyper}) showed a significant increase towards normal values after already one week and this was maintained after 1 and ≥ 3 months (Figure 2D). This is in line with the decrease in number of hyperchromic cells and MCHC (Figure 1E and 1F). The increase in O_{hyper} was accompanied by an increase in the AUC, although values remained lower than normal controls (Figure 2E).

Additional osmotic gradient ektacytometry measurements on the different density fractions showed that following splenectomy the variability between the curves from each density fraction is less, again indicating a more homogeneous RBC population (Supplemental Figure 1D and E). These analyses also showed that only O_{hyper} of density fraction 4 improved. Therefore, the increase in O_{hyper} after splenectomy seemed mainly determined by this fraction, containing the most dense RBCs. O_{hyper} of fractions 2 and 3 decreased after splenectomy, most presumably due to a decrease in reticulocytes in both fractions (Supplemental Figure 1D-G).

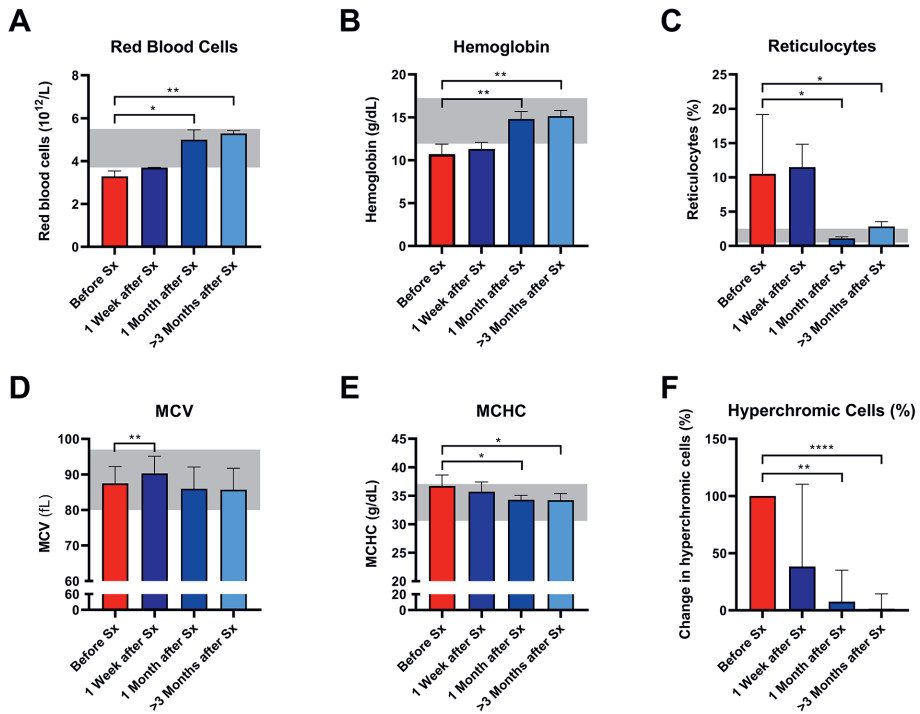


Figure 1. Red blood cell related parameters of patients with hereditary spherocytosis (HS) before and after splenectomy (Sx). Whole blood of HS patients (n=5) was analyzed before and 1 week, 1 month and 3 months after splenectomy. (A) Red Blood Cells significantly increased after splenectomy. (B) Mean hemoglobin values significantly increased after 1 and 3 months after splenectomy. (C) Mean values of reticulocytes decreased 1 and 3 months after splenectomy. (D) mean values of mean corpuscular volume (MCV) increased significantly 1 week after splenectomy but decreased 1 and 3 months after splenectomy. (E) Mean values of mean corpuscular hemoglobin concentration (MCHC) decreased significantly 1 and 3 months after splenectomy. (F) Mean change in hyperchromic cells (%) after splenectomy. The laboratory reference ranges (2SD) of the University Medical Center Utrecht (UMCU) are depicted in the light grey area. Error bars represent standard deviation. ****p<0.0001, ***p<0.001, **p<0.01, *p<0.05

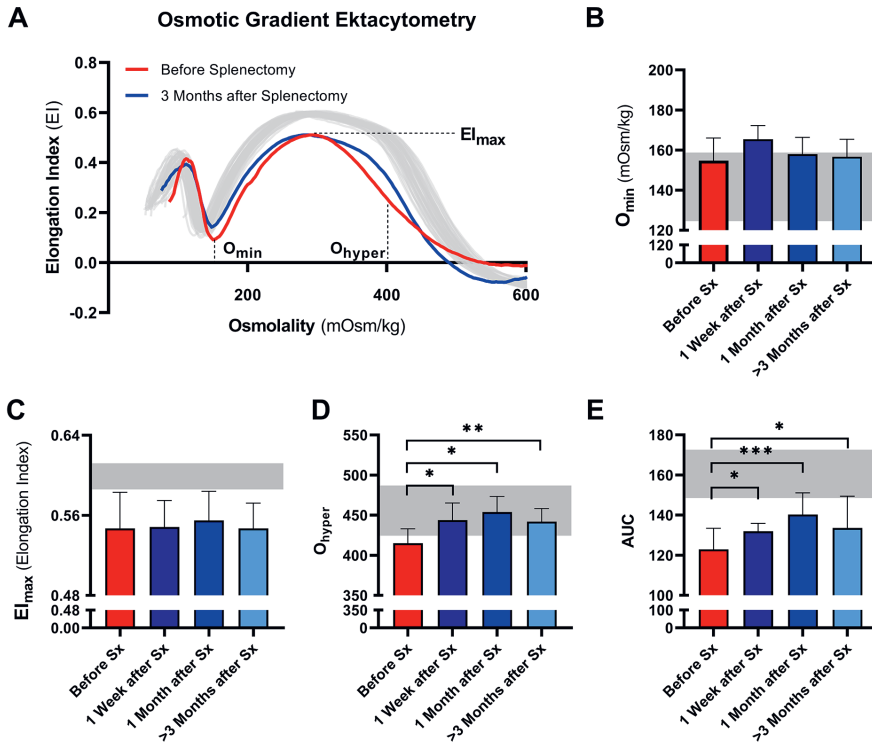


Figure 2. Osmotic gradient ektactometry curve (Osmoscan) and the corresponding parameters of 5 patients with HS before and after splenectomy (Sx). (A) Representative example of the osmotic gradient ektactometry curve in P03 before and 3 months after splenectomy. The osmotic gradient ektactometry curves of healthy controls (n=40) are depicted by the grey lines. The changes in (B.) the surface area to volume ratio of red blood cells (Omin), (C.) the maximum deformability (Elmax), (D.) the hydration state or cytoplasmic viscosity (Ohyper) and (E.) the area under the curve (AUC) are depicted above. The HS patients (n=5) were grouped and the results are displayed as the mean (SD) of the combined values. The mean (2SD) of healthy controls (n=74) are depicted in the light grey area (B-E). Error bars represent standard deviation. ****p<0.0001, ***p<0.001, **p<0.01, *p<0.05

The Cell Membrane Stability Test (CMST) reveals that HS RBCs have regained the ability to shed membrane after splenectomy, reflecting improved membrane health

We next investigated RBC rigidity and its ability to respond to mechanical stress by performing CMST measurements. The CMST exposes RBCs to a high, supraphysiological, shear stress (100Pa) for the duration of 1 hour. Healthy RBCs showed a gradual decrease in deformability under these conditions (Representative curve, Figure 3A), reflected by a negative ΔEI . The loss of deformability likely results from increased vesiculation *in vitro* and consequent membrane loss under shear. In contrast, HS RBCs showed a significantly lower ΔEI before splenectomy compared to healthy controls ($p<0.01$, Figure 3B; representative curve Figure 3A). This suggests that RBCs of HS patients are more rigid and less able to shed membrane *in vitro* compared to healthy RBCs. After splenectomy, ΔEI increased until it was no longer significantly different from healthy controls ≥ 3 months after splenectomy (Figure

3B). Hence, splenectomy results in a less rigid cell population that has for a large part regained the ability to shed membrane. These findings were strengthened by microscopic analysis of RBCs during the CMST. Figure 3C shows how RBCs obtained from a healthy control were fully elongated and elliptical at the start of the CMST ($t=10s$), then turning into dense and less elongated RBCs at the end of the measurement ($t=3590s$). In contrast, RBCs of an HS patient without splenectomy were already dense and unable to elongate fully at the start of the CMST, remaining like this throughout the measurement. Notably, reticulocyte count and hyperchromic cells both correlated with ΔEI ($r=0.660$, $p<0.01$ and $r=0.668$, $p<0.01$ respectively, Figure 3D and E), indicating that these cells strongly influence the outcome of CMST measurements.

Additional CMST measurements on the density fractions suggest that the increase in ΔEI post-splenectomy are determined by density fractions 2 and 3 (Supplemental Figure 1H).

Membrane-shedding as measured by the CMST represents a novel pathophysiological property of HS RBCs

To further explore its added value we performed CMST measurements on a large HS cohort consisting of 18 non-splenectomized, 8 splenectomized patients, and 26 HCs. These results confirmed the findings observed in our longitudinal study, showing that the CMST was able to distinguish splenectomized HS patients from non-splenectomized HS patients ($p=0.028$), in addition to the clear distinction between HS patients in general and HCs (both $p<0.001$). Similarly, also in this large cohort there was a correlation of ΔEI and reticulocyte count ($R=0.606$, $p<0.01$, Figure 4F) and hyperchromic cells ($R=0.521$, $p<0.01$ Figure 4G).

We next evaluated osmotic gradient ektacytometry measurements in this case-control cohort. In agreement with our findings in the longitudinal study (Figure 2B), O_{min} was not different in splenectomized patients (Figure 4B). Also EI_{max} and AUC were not significantly different in splenectomized HS patients (Figure 4C and E). In contrast, O_{hyper} was the only parameter that showed improvement when comparing splenectomized to non-splenectomized HS patients ($p<0.01$, Figure 4D). Furthermore, O_{hyper} correlated with hyperchromic cells although less clear than ΔEI ($R=-0.461$, $p<0.05$, Supplemental Figure 2), but not with reticulocyte count (Figure 4H). Importantly, ΔEI and O_{hyper} showed no correlation (Figure 4I), suggesting that both biomarkers reflect different features of HS RBCs.

Together, these findings confirm that a decreased ability to shed membrane *in vitro* as measured by the CMST is a novel pathophysiological feature of HS RBCs. It likely reflects membrane health and improves after splenectomy, thereby rendering a novel biomarker that is distinct from the improved density/cell hydration as measured by osmotic gradient ektacytometry.

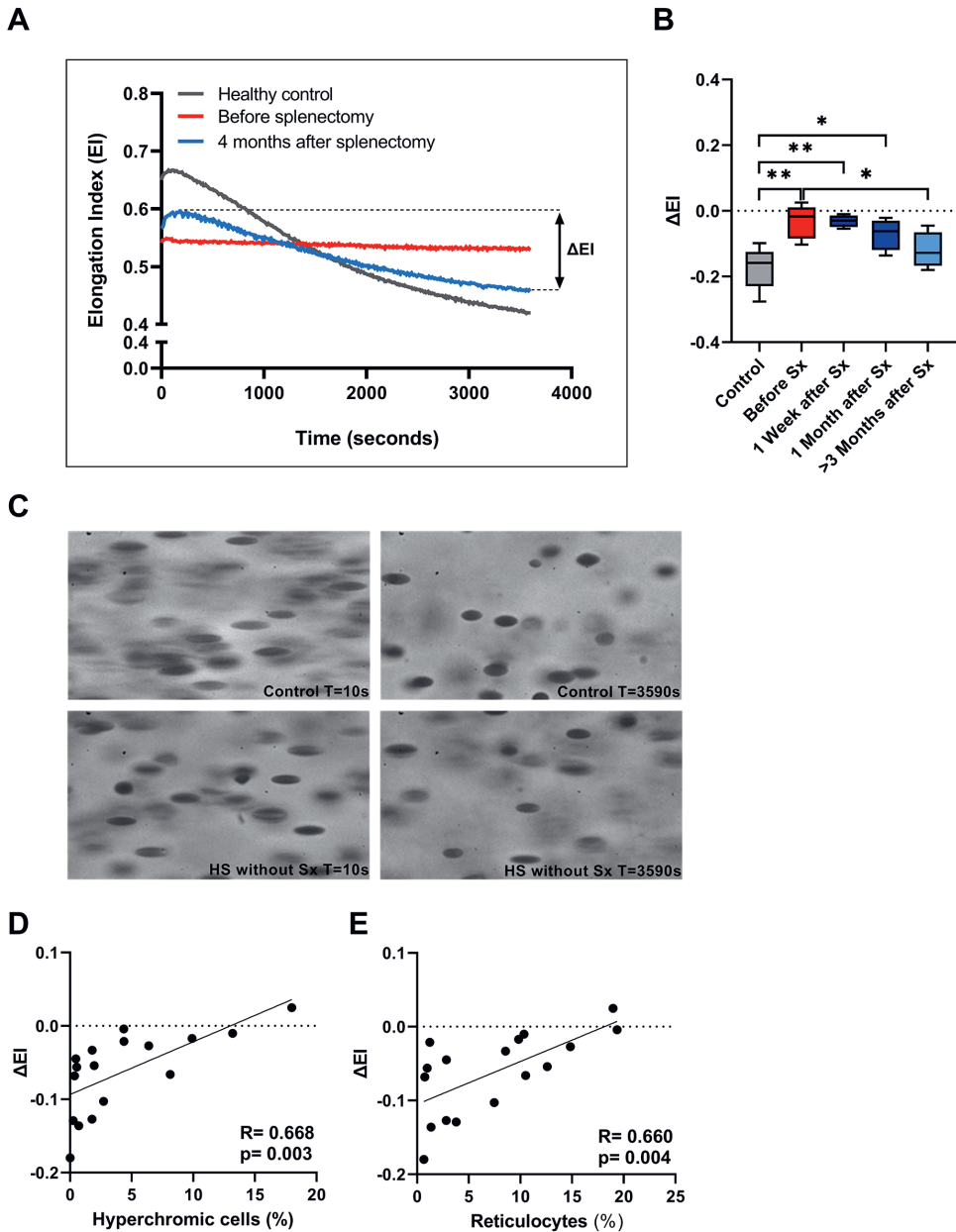


Figure 3. The Cell membrane stability test (CMST) and the calculated parameter (ΔEI) improves after splenectomy in a longitudinal study of 5 HS patients. (A) Representative example of the CMST before (red line) and 4 months after splenectomy (light blue line) compared to a healthy control (dark grey line). (B) The mean values of ΔEI of HS patients ($n=5$) before and after splenectomy. (C) Microscopic images of the RBCs during a CMST. Start of the measurement ($T=10s$) compared to the end of the measurement ($T=3590s$) in a control and HS patient without splenectomy. (D) Correlation between ΔEI and hyperchromic red blood cells. (E) Correlation between ΔEI and reticulocytes (%). Error bars represent standard deviation. **** $p < 0.0001$, *** $p < 0.001$, ** $p < 0.01$, * $p \leq 0.05$. Sx, splenectomy; HS, hereditary spherocytosis; T, time; s, seconds.

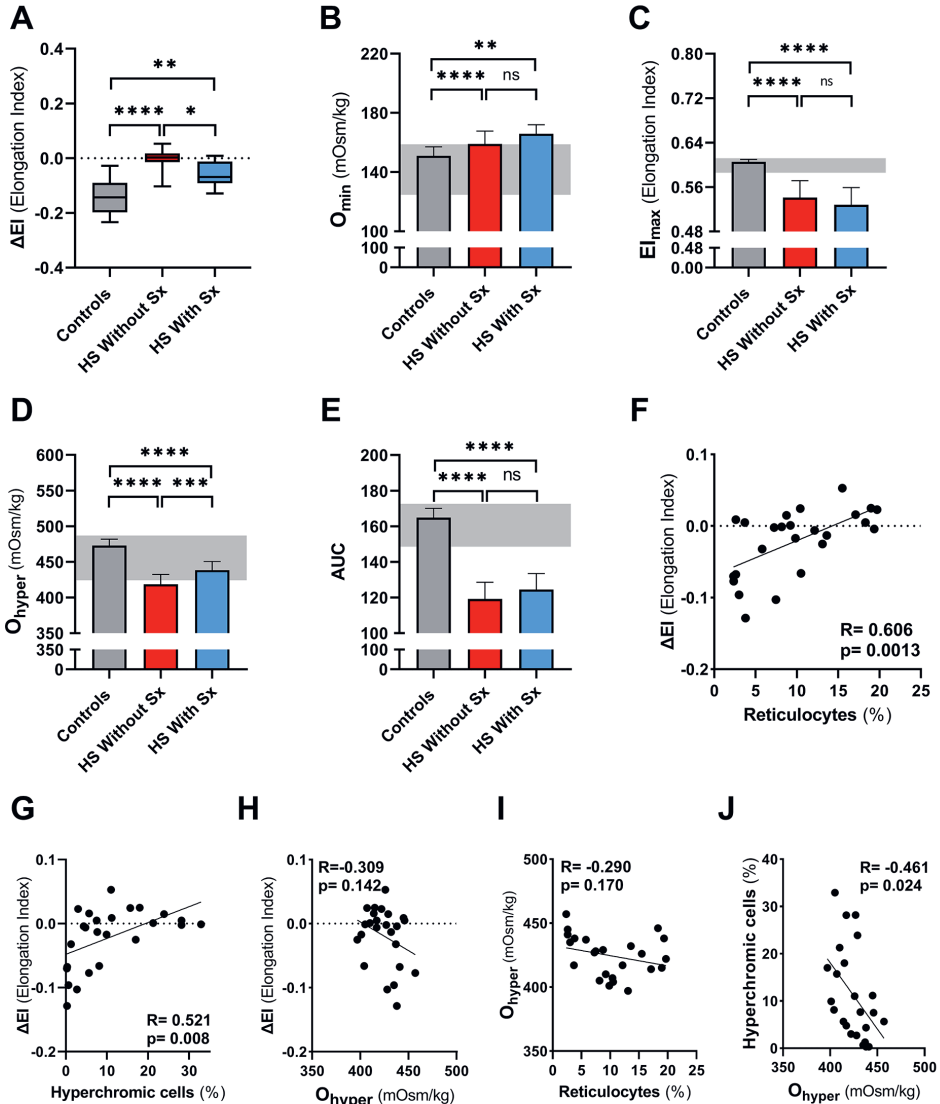


Figure 4. Cell membrane stability test (CMST) and the calculated parameter (ΔEI) shows improvement in splenectomized patients with HS in a case-control study. CMST-derived parameter ΔEI (panels A, F, G, H, I), osmotic gradient ektactometry-derived parameters (panels B-E, H, I, J), reticulocytes and hyperchromic cells were assessed in 18 non-splenectomized HS patients, 8 non-splenectomized HS patients and 26 healthy controls (HC). (A) Mean ΔEI of HS patients without splenectomy compared to patients with splenectomy, both groups were compared to HCs. (B) Mean values of O_{min} are increased in splenectomized patients compared to HCs or non-splenectomized HS. (C) Mean values of E_{lmax} are decreased in splenectomized HS patient RBCs, compared to HC and non-splenectomized HS RBCs. (D) Mean values of O_{hyper} are significantly different between the 3 groups mentioned above. (E) Mean values of AUC show no significant differences between non-splenectomized and splenectomized HS RBCs. (F) Linear correlation between reticulocytes (%) and ΔEI of HS patients. (G) Linear correlation between hyperchromic cells (%) and ΔEI of HS patients. (H) Linear correlation between O_{hyper} and ΔEI . (I) Linear correlation between reticulocytes (%) and O_{hyper} . (J) Linear correlation between hyperchromic cells and O_{hyper} . Error bars represent standard deviation. **** $p < 0.0001$, *** $p < 0.001$, ** $p < 0.01$, * $p < 0.05$, ns non-significant. Sx, splenectomy; HS, hereditary spherocytosis; AUC, area under the curve.

Discussion

In the present study, we report on the longitudinal effects of splenectomy in 5 HS patients. We specifically focused on cellular properties related to membrane health with the use of two different forms of ektacytometry: osmotic gradient ektacytometry and the CMST. In particular the CMST results revealed a novel feature of HS RBCs, i.e. the loss of the ability to shed membrane, and improvement of this *in vitro* cellular property following splenectomy. Membrane-shedding capacity in this test is assessed by the loss of deformability that occurs during prolonged exposure of RBCs to high shear stress. We suggest that improved membrane-shedding capacity after splenectomy reflects improved RBC membrane health, and ΔEI as measured by the CMST may thus serve as a novel clinically relevant biomarker.

The longitudinally observed increase in RBC count, Hb and reticulocyte count after splenectomy corresponds well with results from previous studies where splenectomized and non-splenectomized patient groups were compared.^{9,10} In addition, our patients also showed a decrease in MCHC directly after splenectomy, which continued to decrease in the following months. This implicates that the internal viscosity or cellular density of HS RBCs is reduced after splenectomy, which is supported by the reduction in the percentage of hyperchromic cells. Little is known about the effect of splenectomy on *in vivo* RBC vesiculation in HS, an important pathophysiological feature, but previous studies demonstrated that RBC vesiculation caused an increase in internal viscosity (MCHC) through shedding of RBC-derived microvesicles.^{18–20} Hence, both the decrease in MCHC and hyperchromic cells could indicate that *in vivo* vesiculation of RBCs in HS is reduced after splenectomy. In turn this could explain the observed improvement in ΔEI in the CMST after splenectomy, which reflects improved ability to shed membrane *in vitro*.

More detailed analysis of the longitudinal effects of splenectomy was obtained by osmotic gradient ektacytometry. This technique is generally considered as the gold standard in the diagnosis of HS,^{10,13,14,21} and its parameters EI_{max} , O_{min} , and O_{hyper} are considered biomarkers of, respectively, total membrane surface area, surface area to volume ratio, and RBC hydration status. Upon splenectomy most of these parameters were not affected, only O_{hyper} was significantly increased (Figure 2D and 4D). O_{hyper} and MCHC are known to have an inverse correlation with each other.¹⁰ Both the increase in O_{hyper} and the decrease in MCHC indicate that splenectomy improves the hydration state/intracellular viscosity. In line with this, an increase in the AUC was observed in the longitudinal cohort, whereas AUC remained unchanged after splenectomy in the case-control cohort. Our findings partly contradict with previous studies where both O_{hyper} and AUC remained unaltered after splenectomy,^{9,10} This could be explained by the non-longitudinal design of these latter studies in which individual differences in response to splenectomy become less apparent.

We next investigated the effect of splenectomy on the ability of HS RBCs to respond to mechanical stress. For this we used the CMST, an ektacytometry based test that was previously used to study membrane stability in HS by studying resealed RBC ghosts.^{22,23} We demonstrate that RBCs from non-splenectomized HS patients show no or only a modest

decrease in EI after prolonged exposure to shear stress, in contrast to healthy control RBCs which display a substantial decrease in EI under these conditions. We hypothesize that HS RBCs from non-splenectomized HS patients are more dense and rigid due to *in vivo* vesiculation that is accelerated by the spleen, and, therefore are less able to shed membrane *in vitro*.²⁴ This is confirmed by the microscopic evaluation of HS RBCs during CMST measurement, which shows that, in contrast to healthy RBCs, HS RBCs do not change morphologically (Figure 3C). Further support for this hypothesis is obtained from the significant correlation of ΔEI and hyperchromic cells (Figure 3D).

Following splenectomy HS RBCs showed an increase in ΔEI (Figure 3B) and after more than three months ΔEI was not significantly different compared to healthy controls. This suggests that after splenectomy HS RBCs have regained part of the ability to shed membrane *in vitro*, which may be related to a partly restored ability of HS RBCs for de novo synthesis of lipids.^{12,25,26} The increase in ΔEI could also indicate a change in RBC population due to the absence of the quality control function of the spleen; Instead of shedding micro vesicles *in vivo* in the spleen (i.e. splenic conditioning), this now occurs *in vitro* under the supraphysiological conditions in the CMST. In both cases cellular characteristics as obtained by the CMST measurements indicate an improvement after splenectomy, in a sense that they behave more like normal healthy RBCs. Furthermore, the degree of increase in ΔEI after splenectomy we observed could also be dependent on genetic defect^{11,27} Our findings were strengthened by CMST results on a large cohort of HS patients that showed that this test was able to discriminate between splenectomized and non-splenectomized HS patients (Figure 4A). This implies that the CMST may represent a novel biomarker of HS, which was further supported by the correlation of ΔEI and % reticulocytes ($r=0.66$, $p=0.004$). The ability to distinguish splenectomized patients from non-splenectomized patients can be valuable in an era where different types of splenectomy are explored. Partial splenectomy, either through embolization of splenic arteries or through (laparoscopic) removal of a part of the spleen, might ameliorate symptoms and improve anemia while maintaining splenic phagocytic function.^{28,29} However, data of several small studies are inconclusive regarding the remaining immunological capacity of the spleen after partial splenectomy even though hemolysis is decreased.³⁰ Larger studies that also include functional analysis of the spleen and functional analysis of RBCs, i.e. the CMST, are warranted to accurately assess the efficacy of (partial) splenectomy or embolization, and to investigate whether changes in RBC properties or the nature of the underlying molecular defect^{11,27} contribute to the clinical benefit of splenectomy.

In conclusion, we report on the longitudinal effects of splenectomy on HS RBC characteristics and function as studied by ektacytometry. Our data shows that before splenectomy the HS RBC population is more heterogeneous, cells are more rigid, have increased intracellular viscosity and reduced deformability. Functional analysis of HS RBCs using osmotic gradient ektacytometry and CMST further shows that splenectomy improves the hydration state of HS RBCs and allows cells to regain the ability to shed membrane. In particular the CMST reflects an yet-undescribed distinct RBC characteristic and holds promise as a novel biomarker for membrane health in HS that could be helpful, together with a comprehensive

clinical evaluation and appropriate follow-up, to assess the effect of different treatments such as embolization and (partial) splenectomy, and that may be related to clinical severity given the correlation of ΔEI and reticulocyte count. Larger studies are warranted to establish if the CMST can be used to improve the assessment of clinical severity and/or is able to contribute to a better understanding of phenotypic differences in HS.

Acknowledgements

The authors would like to thank all patients that donated blood for this study.

Authorship

Contribution: R.H., M.B., R.vW., and M.A.E.R. designed the study; R.H., J.W.V., M.Y.A.H., M.B., E.J.vB., and M.A.E.R. collected clinical and laboratory data. J.B., R.H., T.H.M., B.A.vO., and M.A.E.R. performed laboratory experiments. M.C.B., R.vW., and M.A.E.R. analyzed the data and wrote the manuscript. All authors edited the manuscript and approved the final version.

Conflict-of-interest disclosure

M.A.E.R, J.B, and T.H.M received grant funding from RR Mechatronics. R.vW received grant funding from Agios Pharmaceuticals Inc and RR Mechatronics. E.J.vB received grant funding Agios Pharmaceuticals Inc, RR Mechatronics, Novartis and Pfizer for investigator initiated research projects.

Funding

The research has received funding from the European Seventh Framework Program under grant agreement number 602121 (CoMMITMenT) and was partially funded by an unrestricted grant from RR Mechatronics.

References

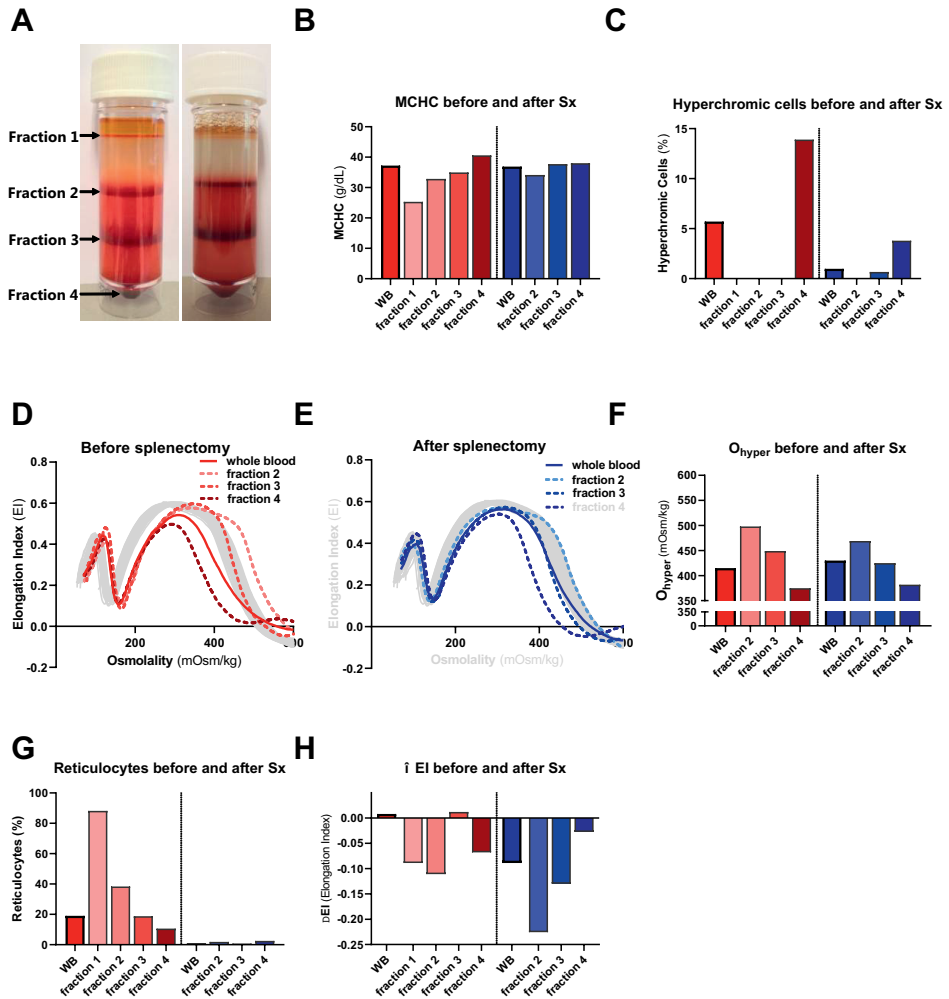
- Perrotta S, Gallagher PG, Mohandas N. Hereditary spherocytosis. *Lancet*. 2008;372(9647):1411-1426. doi:10.1016/S0140-6736(08)61588-3
- Eber SW, Lux SE. Hereditary spherocytosis-defects in proteins that connect the membrane skeleton to the lipid bilayer. *Semin Hematol*. 2004;41(2):118-141.
- Chasis JA, Agre P, Mohandas N. Decreased membrane mechanical stability and in vivo loss of surface area reflect spectrin deficiencies in hereditary spherocytosis. *J Clin Invest*. 1988;82(2):617-623. doi:10.1172/JCI113640
- Huisjes R, Bogdanova A, van Solinge WW, Schiffelers RM, Kaestner L, van Wijk R. Squeezing for life - Properties of red blood cell deformability. *Front Physiol*. 2018;9(JUN):1-22.
- Mebius RE, Kraal G. Structure and function of the spleen. *Nat Rev Immunol*. 2005;5(8):606-616.
- Musser G, Lazar G, Hocking W, Busuttill W. Splenectomy for hematologic disease. The UCLA experience with 306 patients. *Ann Surg*. 1984;200(1):40-45.
- Schilling RF, Gangnon RE, Traver MI. Delayed adverse vascular events after splenectomy in hereditary spherocytosis. *J Thromb Haemost*. 2008;6(8):1289-1295.
- Li Y, Lu L, Li J. Topological Structures and Membrane Nanostructures of Erythrocytes after Splenectomy in Hereditary Spherocytosis Patients via Atomic Force Microscopy. *Cell Biochem Biophys*. 2016;74(3):365-371.
- Huisjes R, Makhro A, Llaudet-Planas E, et al. Density, heterogeneity and deformability of red cells as markers of clinical severity in hereditary spherocytosis. *Haematologica*. 2020;105(2):338-347.
- Zaninoni A, Fermo E, Vercellati C, et al. Use of laser assisted optical rotational cell analyzer (LoRRca MaxSis) in the diagnosis of RBC membrane disorders, enzyme defects, and congenital dyserythropoietic anemias: A monocentric study on 202 patients. *Front Physiol*. 2018;9(APR):1-12.
- Reliene R, Mariani M, Zanella A, et al. Splenectomy prolongs in vivo survival of erythrocytes differently in spectrin/ankyrin- and band 3-deficient hereditary spherocytosis. *Blood*. 2002;100(6):2208-2215.
- Sugihara T, Miyashima K, Yawata Y. Disappearance of microspherocytes in peripheral circulation and normalization of decreased lipids in plasma and in red cells of patients with hereditary spherocytosis after splenectomy. *Am J Hematol*. 17(2):129-139.
- DaCosta L, Suner L, Galimand J, et al. Diagnostic tool for red blood cell membrane disorders : Assessment of a new generation ektacytometer. *Blood Cells, Mol Dis*. 2016;56(1):9-22.
- Lazarova E, Gulbis B, Oirschot B Van, Van Wijk R. Next-generation osmotic gradient ektacytometry for the diagnosis of hereditary spherocytosis: Interlaboratory method validation and experience. *Clin Chem Lab Med*. 2017;55(3):394-402.
- Rennie CM, Thompson S, Parker AC, Maddy A. Human erythrocyte fractionation in "percoll" density gradients. *Clin Chim Acta*. 1979;98(1-2):119-125.
- Huisjes R, Solinge WW, Levin MD, Wijk R, Riedl JA. Digital microscopy as a screening tool for the diagnosis of hereditary hemolytic anemia. *Int J Lab Hematol*. 2017;40(2):159-168.
- Van Vuren A, Van Der Zwaag B, Huisjes R, et al. The Complexity of Genotype-Phenotype Correlations in Hereditary Spherocytosis: A Cohort of 95 Patients: Genotype-Phenotype Correlation in Hereditary Spherocytosis. *HemaSphere*. 2019;3(4).
- Alaarg A, Schiffelers RM, Van Solinge WW, Van Wijk R. Red blood cell vesiculation in hereditary hemolytic anemia. *Front Physiol*. 2013;4 DEC(December):1-15.
- Bosman GJCGM. Survival of red blood cells after transfusion: Processes and consequences. *Front Physiol*. 2013;4 DEC(December):1-8.
- Bosch, FH Werre, JM Schipper, L Roerdinkholder-Stoelwinder, B Huls, T Willekens, FLA Wichers, G Halie M. Determinants of red blood cell deformability in relation to cell age. *Eur J Haematol*. 1994;52(1):35-41.
- Llaudet-Planas E, Vives-Corróns JL, Rizzuto V, et al. Osmotic gradient ektacytometry: A valuable screening test for hereditary spherocytosis and other red blood cell membrane disorders. *Int J Lab Hematol*. 2018;40(1):94-102.

22. Chasis JA, Mohandas N. Erythrocyte membrane deformability and stability: Two distinct membrane properties that are independently regulated by skeletal protein associations. *J Cell Biol.* 1986;103(2):343-350.
23. Mohandas N, Clark MR, Health BP, et al. A technique to detect reduced mechanical stability of red cell membranes: relevance to elliptocytic disorders. *Blood.* 1982;59(4):768-774.
24. Waugh RE, La Celle PL. Abnormalities in the membrane material properties of hereditary spherocytes. *J Biomech Eng.* 1980;102(3):240.
25. Takashi S, Yoshihito Y. Observations on plasma and red cell lipids in hereditary spherocytosis. *Clin Chim Acta.* 1984;137(2):227-232.
26. Cooper RA, Jandl JH. The role of membrane lipids in the survival of red cells in hereditary spherocytosis. *J Clin Invest.* 1969;48(4):736-744.
27. Ingrosso D, D'Angelo S, Perrotta S, et al. Cytoskeletal behaviour in spectrin and in band 3 deficient spherocytic red cells: Evidence for a differentiated splenic conditioning role. *Br J Haematol.* 1996;93(1):38-41.
28. Pratl B, Benesch M, Lackner H, et al. Partial splenic embolization in children with hereditary spherocytosis. *Eur J Haematol.* 2008;80(1):76-80.
29. Tchernia G, Gauthier F, Mielot F, et al. Initial assessment of the beneficial effect of partial splenectomy in hereditary spherocytosis. *Blood.* 1993;81(8):2014-2020.
30. Guizzetti L. Total versus partial splenectomy in pediatric hereditary spherocytosis: A systematic review and meta-analysis. *Pediatr Blood Cancer.* 2016;63(10):1713-1722.

Supplementary Table 1.

Patient characteristics	Patient 1		Patient 2		Patient 3		Patient 4		Patient 5	
	Pre-Sx	Post-Sx	Pre-Sx	Post-Sx	Pre-Sx	Post-Sx	Pre-Sx	Post-Sx	Pre-Sx	Post-Sx
Age (years)	12		14		13		30		43	
Gene	<i>ANK1</i>		<i>SPTB</i>		<i>SPTB</i>		<i>SPTA1</i>		<i>SLC4A1</i>	
Mutation	c.5201_5202insTCAG p.(Thr1734fs)		c.4542dup p.(Leu1515fs)		c.647G>A p.(Arg216Gln)		c.3257dup p.(Leu1086fs)		c.2494C>T p.(Arg832Cys)	
Transfusions	0		5		1		0		0	
Red cell characteristics										
Hb (g/dL)	8.2	15.5	13.2	15.5	10.7	15.8	9.2	13.1	12.1	15.3
RBC ($\times 10^{12}/L$)	3.1	5.8	4.1	5.3	3.3	5.0	2.9	4.2	3.6	4.7
MCV (fL)	76.0	81.0	84.0	82.0	87.5	87.0	92.5	92.5	92.0	93.8
MCHC (g/dL)	35.1	33.3	38.2	35.9	37.2	35.7	35.0	33.5	36.7	35.0
Reticulocytes (%)	19.4	2.3	10.0	2.8	19.0	4.9	7.5	0.6	10.5	1.0
Hypochromic cells (%)	15.7	9.4	N.A.	2.4	3.0	0.8	11.7	36.1	3.1	1.3
Hyperchromic cells (%)	4.4	0.3	9.9	1.8	18.0	0.3	2.7	0.0	8.1	0.5
Red cell morphology										
Spherocytes (%)	0.2	8.9	4.8	4.4	1.7	0.1	0.05	N.A.	0.2	0.003
Microcytes (%)	59.8	24.3	51.3	19.3	37.6	0.02	7.9	N.A.	14.2	0.01
Macrocytes (%)	0.2	0.03	0.09	0.0	1.2	0.01	3.5	N.A.	0.3	0.02
Osmotic gradient ektacytometry										
Omin	172	166	150	152	160	163	147	147	145	165
Elmax	0.547	0.532	0.510	0.510	0.542	0.558	0.582	0.577	0.584	0.591
Ohyper	438	469	401	421	415	438	428	451	404	465
AUC	122.9	139.1	107.6	117.6	117.3	133.2	138.6	154.6	128.3	152.3
Cell membrane stability test										
ΔEI	-0.004	-0.07	-0.017	-0.127	0.025	-0.129	-0.103	-0.18	-0.066	-0.056

Detailed overview of patients genotypes, red cell characteristics and morphology, osmotic gradient ektacytometry-derived parameters and Cell Membrane Stability Test results of pre- of post splenectomy (>3 months) blood samples of the patients described in this study. All patients were heterozygous for the indicated mutations. In addition to the *SPTB* mutation Patient HS02 also carried the Variant of Unknown clinical Significance (VUS) c.3565C>T p.(His1189Tyr) in *SPTA1*. *Also known as the *SPTA1* alpha-LELY low expression allele. N.A. Not Available



Supplemental Figure 1. Osmotic gradient curves and parameters, CMST parameter (ΔEI) and routine laboratory parameters of fractions with different HS densities, before and 1 month after splenectomy (Sx). (A) Percoll gradient density separations of a HS patient before (left) and 1 month after splenectomy (right). (B) Mean corpuscular hemoglobin concentration (MCHC) and hyperchromic cells (C) show changes after splenectomy. (D) Osmotic gradient curves of whole blood (solid line) are plotted together with the different density separated fractions (dashed lines) before splenectomy and compared to curves 1 month after splenectomy (E). (F) O_{hyper} measured in whole blood increases after splenectomy in contrast to fraction 2 that decreases compared to pre-splenectomy values, which is mostly due to decrease in reticulocytes, in all fractions, but most pronounced in fraction 1 and 2 after splenectomy (G). (H) DeltaEI increase substantially after splenectomy which was also found in the different fractions with the exception of fraction 4. WB, whole blood;

Chapter 12

Red cell dehydration is associated with distinctive alterations of red cell metabolism in hereditary xerocytosis caused by PIEZO1 and KCNN4 defects

Manuscript in preparation

Minke A.E. Rab^{1,2}, Birgit van Dooijeweert^{1,2}, Jennifer Bos¹, Brigitte A. van Oirschot¹, Penelope A. Kosinski³, Annet van Wesel¹, Stephanie van Straaten⁴, Roger E.G. Schutgens², Judith J.M. Jans⁵, Marije Bartels², Paola Bianchi⁶, Lenny Dang³, Charles Kung³, Eduard J. van Beers² and Richard van Wijk¹

¹ Central Diagnostic Laboratory - Research, University Medical Center Utrecht, Utrecht University, Utrecht, The Netherlands

² Van Creveldkliniek, University Medical Center Utrecht, Utrecht University, The Netherlands;

³ Agios Pharmaceuticals Inc., Cambridge, MA, USA

⁴ Sophia Children's Hospital, Erasmus Medical Center, Rotterdam, The Netherlands

⁵ Section Metabolic Diagnostics, Department of Genetics, University Medical Center Utrecht, Utrecht, The Netherlands

⁶ UOC Oncoematologia, UOS, Fisiopatologia delle Anemie Fondazione IRCCS Ca' Grande Ospedale Maggiore Policlinico, Milano, Italy

Abstract

Hereditary xerocytosis (HX) is a rare red blood cell (RBC) disorder associated with hemolysis and iron overload. Mutations in either *PIEZO1*, the gene coding for the mechanosensitive cation channel PIEZO1, or *KCNN4*, the gene encoding for the Gardos channel, a calcium-dependent potassium channel cause inappropriate Gardos channel activation, ultimately leading to dehydration of the red cell.

PIEZO1-HX defective RBCs show a left shifted curve with osmotic gradient ektacytometry, reflecting cellular dehydration and increased surface area to volume ratio. Interestingly, KCNN4-HX defective RBCs generally fail to show this left-shift. The differences in osmotic gradient ektacytometry and hemocytometry parameters regarding RBC hydration suggest differences in pathophysiology that could reflect altered ATP-dependent RBC volume control. We therefore assessed RBC hydration status and metabolism in ten PIEZO1-HX patients, three patients with a KCNN4 mutation and healthy controls (HC). Analysis of metabolism, and in particular glycolysis, with both untargeted and targeted metabolomics found significantly lower 2,3-diphosphoglycerate levels in PIEZO1-HX while ATP was normal. Further analysis of the key glycolytic enzyme pyruvate kinase (PK), revealed a secondary PK deficiency that was more pronounced in PIEZO1-HX patient RBCs. Moreover, PK stability and protein levels were decreased compared to KCNN4-HX and HC RBCs. More importantly, the degree of dehydration correlated with PK activity and stability, ATP/2,3-DPG ratio, and reticulocyte count, suggesting a direct link between cellular hydration, PK function and ATP/2,3-DPG ratio, and reticulocyte count. Our results indicate that altered PK function could contribute to the pathophysiology of PIEZO1-HX through yet-unknown mechanisms. KCNN4-HX RBCs have a less compromised PK function and are only slightly dehydrated, indicating other pathophysiological pathways in this specific RBC channelopathy. Collectively, our results suggest both channelopathies should be considered distinct red cell disorders. Our findings enhance our understanding of both PIEZO1 channelopathy and Gardos channelopathy pathophysiology, and may offer novel opportunities for therapeutic strategies.

Introduction

Hereditary xerocytosis (HX) is a rare red blood cell (RBC) disorder also known as dehydrated stomatocytosis due the presence of stomatocytes on peripheral blood smears. This autosomal dominant disorder is associated with hemolysis and iron overload. HX is caused by mutations in *PIEZO1*, the gene coding for the mechanosensitive cation channel PIEZO1^{1,2}, or *KCNN4*, the gene encoding for the Gardos channel, a calcium-dependent potassium channel.³⁻⁵ Gain of function mutations in *PIEZO1* lead to (temporarily) increased intracellular calcium levels.⁵⁻⁸ This sudden peak increase in intracellular calcium activates the calcium sensitive Gardos channel, eventually resulting in loss of potassium and water. Similarly, gain of function mutations in the *KCNN4* gene, result in over activation of the Gardos channel and increased calcium levels⁵, in turn also leading to decreased intracellular potassium and water concentrations. Consequently, in both cases, this causes an imbalance of volume homeostasis, and, hence, dehydration of the red cell.⁹

PIEZO1-HX patients often present with a marked reticulocytosis, iron overload and a fully compensated hemolysis. *KCNN4* patients present with hemolytic anemia with concomitant reticulocytosis and often substantial iron overload without a history of transfusions¹⁰, although occasional transfusions may be required at early age.⁵

The mechanism by which HX RBCs are cleared from the circulation is unknown. However, in contrast to other hereditary hemolytic anemias, such as hereditary spherocytosis, splenectomy is contraindicated in PIEZO1-HX patients due to the increased risk of thromboembolic complications post-splenectomy in about 75% of patients.¹⁰⁻¹³ The exact mechanism that results in post-splenectomy thrombosis remains to be elucidated. Proposed causative factors are increased platelet aggregation¹⁴, RBC membrane phospholipid abnormalities, high level of circulating microparticles, high rate of phosphatidylserine expressing RBCs¹⁰, decreased RBC deformability⁵, and increased (reticulocyte) adherence to the endothelium.^{15,16} Whether patients with a Gardos channelopathy also have an increased risk of post-splenectomy thromboembolic complications is still unknown, although the limited data available suggests the risk is lower in *KCNN4* mutations compared to PIEZO1.¹⁰

Diagnosis of HX can be challenging since osmotic gradient ektacytometry, the gold standard, is a technique that is available in only in few laboratories, thereby often delaying prompt diagnosis. PIEZO1-defective RBCs show a left shifted curve with this technique, reflecting cellular dehydration and increased surface area to volume ratio¹⁷. Interestingly, most mutations associated with a *KCNN4* channelopathy affect residues in close proximity to the calmodulin binding site, and such RBCs fail to show this left-shift.⁴ The diagnosis is even more difficult since the phenotype of HX varies considerably¹⁸, and therefore no other test other than DNA analysis, often by means of next generation sequencing, is ultimately required to establish the diagnosis.⁵

The differences observed in osmotic gradient ektacytometry and laboratory parameters reflecting RBC hydration suggest differences in pathophysiology between PIEZO1-HX and *KCNN4*-HX. RBC volume is controlled by two ATP dependent pumps, the sodium pump

(ATP1) and the plasma membrane calcium pump (PMCA).⁹ A previous study found metabolic requirements to be high in HX, indicating that in order to maintain proper RBC volume and deformability, high ATP levels are needed.^{19,20}

Hence, we hypothesize that altered RBC metabolism might contribute to the observed differences in RBC hydration between PIEZO1-HX and KCNN4-HX (Gardos channelopathy) patients. Previously we reported that decreased activity and thermostability of pyruvate kinase (PK), a key regulatory enzyme of red cell glycolysis, is a feature of various forms of hereditary hemolytic anemia such as sickle cell disease.²¹ We now show that RBC dehydration, a prominent feature of HX, is also associated with altered PK properties and metabolic alterations in a way that is distinct from sickle cell disease or hereditary deficiency of PK.

Methods

Patients

Ten adult patients with PIEZO1-HX and three patients with KCNN4-HX were enrolled in this study. Blood samples were obtained after inclusion in the Tapir-study which was approved by the Medical Ethical Research Board of the University Medical Center Utrecht, the Netherlands (17/450M) and in accordance to the declaration of Helsinki. Informed consent was obtained from all patients. Blood from healthy control individuals was obtained by means of the institutional blood donor service.

Conventional laboratory parameters

Routine hematological laboratory parameters were analyzed on an Abbott Cell-Dyn Sapphire hematology analyzer (Abbott Diagnostics Division, Santa Clara, CA, USA). Ferritin levels were measured on routine chemistry analyzer.

Digital microscopy

Peripheral blood smears were analyzed using the CellaVision digital microscope DM96 (software 5.0.1build11). Analysis was performed using a neuronal network which classifies RBCs based on morphological characteristics such as shape, color, and texture. Stomatocytes (%) were calculated as a percentage of total RBCs as quantified by the software.²²

Ektacytometry

RBC deformability was measured with the Laser Optical Rotational Red Cell Analyzer, (Lorcca, RR Mechatronics, Zwaag, The Netherlands). In this next generation ektacytometer, RBCs in a viscous solution (Elon-Iso) are exposed to shear stress, forcing the cells to elongate into an elliptical shape. The laser beam generates the diffraction pattern, that is measured by a camera. The vertical axis (A) and the horizontal axis (B) of the ellipse are used to calculate the elongation index (EI) by the formula $(A-B)/(A+B)$. The EI reflects the deformability of the total population of RBCs.

Osmotic gradient ektacytometry

Osmotic gradient ektacytometry measurements of RBCs of healthy controls and HX patients were obtained using the osmoscan module on the Lorcca according to the manufacturer's

instructions and as described elsewhere.^{17,23} Briefly, whole blood was standardized to a fixed RBC count of 1000×10^6 and mixed with 5 mL of Elon-Iso (RR Mechatronics), and subsequently exposed to a constant shear stress (30Pa) and an osmolarity gradient from approximately 60 mOsmol/kg to 600 mOsmol/kg.

Cell membrane stability test (CMST)

The cell membrane stability test (CMST) was performed using the CMST module on the ektacytometer. To perform a CMST, whole blood was standardized to a fixed RBC count of 300×10^6 and mixed with 5 mL of Elon-Iso. In the CMST RBCs are exposed to a shear stress of 100 Pa for 1800 seconds (30 minutes) while the EI is continuously measured. The change in the elongation index (ΔEI) was calculated by determining the median EI of the first and the last 100 seconds of the CMST and subsequently calculating the difference between the medians. The ΔEI depicts the capacity of the RBCs to shed membrane and reflects membrane health (Berrevoets et al, *Frontiers in physiology*, accepted/Chapter 11 of this thesis).

Untargeted metabolomics on dried blood spots

Sample preparation, direct infusion high resolution mass spectrometry (DI-HRMS) and data processing was performed as previously reported.^{24,25} Features were defined using a peak calling bioinformatics developed in R programming software (<http://github.com/UMCUGenetics/DIMS>). Mass peak intensities were averaged over technical triplicates. In addition, as DI-HRMS is unable to separate isomers, mass peak intensities consisted of summed intensities of these isomers. Metabolite annotation was performed based on the human metabolome database (version 3.6) allowing for up to 5 ppm deviation. This resulted in 3565 metabolite annotations corresponding to 1770 unique metabolite features.²⁶ To compare the metabolic profiles between HX and HC (n=50), mass peak intensities for each identified feature were converted to Z-scores (as samples were distributed over several DI-HRMS runs). These scores, based on metabolic control samples that were added to each DI-HRMS run, were calculated by the following formula:

$$Z - score = \frac{(Mass\ peak\ intensity\ of\ Pt\ or\ HC\ sample - Mean\ mass\ peak\ intensities\ of\ control\ samples)}{Standard\ deviation\ mass\ peak\ intensities\ of\ metabolic\ control\ samples \ddagger}$$

‡Metabolic controls exist of a batch of banked dried blood spots (DBS) samples from individuals in whom an inborn error of metabolism (IEM) was excluded after an extensive diagnostic workup.

RBC pyruvate kinase (PK) activity, stability and protein levels

RBCs were purified from whole blood with the use of a cellulose column according to standardized methods.²⁷ Subsequently, PK and hexokinase (HK) activity was measured in lysates of purified RBCs as previously described elsewhere.^{27,28} PK thermostability was measured on the same RBC lysates at 0, 5, 10, 20, 40 and 60 minutes of incubation at 53°C.²⁹

Protein levels of PK-R were determined by Mesoscale Assay (MesoScale Discovery) as described³⁰ using Goat anti-PKLR antibody (Aviva) and Mouse anti-PKLR antibody (Abcam)

both in PBS buffered saline + 0.5% Tween 20 + BSA 1% as sandwich antibodies in a multi-array 96 well plate. SULFO-TAG goat anti-mouse (Mesoscale discovery) was used as the detection antibody and the signal was measured using a MSD reader (Quickplex S120). The PKR protein level was determined by normalizing the light intensity of the SULFO-TAG electrochemiluminescence (ECL) to the protein concentration of the lysate (final units: au/gHb).

Targeted metabolomics

Relative abundance of central carbon metabolites was performed by UPLC-MS. Frozen whole blood samples were thawed on ice and 10 μ L aliquots were extracted with 120 μ L of hot 70% ethanol containing 100 ng/mL L-glutamate (13C5, D5, 15N) as an internal standard. Samples were vortexed and centrifuged at 14000 rpm for 10 minutes at 4° C; supernatants were dried down and resuspended in water with 2-ketobutyrate (13C4, D2) internal standard. Metabolites were analyzed by high resolution accurate mass detection (HRAM) on a QExactive™ Orbitrap mass spectrometer (Thermo Fisher Scientific) as described previously.³¹ Peak identification and integration was done with Maven software.³² Quantitative analysis of ATP and 2,3-DPG was performed as described previously.³³

Statistical analysis

Data was analyzed with GraphPad Prism version 8.3.0 for Windows (GraphPad Software, San Diego, CA, USA). An unpaired T-test or Mann Whitney U test was used to assess the differences between HCs, PIEZO1 patients and KCNN4 patients when appropriate. A Spearman ranks coefficient was used for correlation analysis. A p-value <0.05 was considered statistically significant. Analyses of untargeted metabolomics data were conducted in MetaboAnalyst. No further data filtering or normalization was applied. Multivariate principal component analysis (PCA) and partial least squares discriminant analysis (PLS-DA), in which the number of features is reduced by combining them into fewer explanatory variables, were used to explore the variation in metabolic fingerprints between patients and controls. In contrast to PCA, PLS-DA takes group label into account to maximize the variance between groups. Plots are displayed with 95% confidence regions.

Results

Ten PIEZO1-HX patients (median age 30 years, range 18-75), three KCNN4-HX patients (median age 33 years, range 20-55) and nine healthy controls (HC, median age 41 years, range 26-59) were studied. The PIEZO1-HX patient cohort was comprised of patients harboring 4 different heterozygous mutations in the *PIEZO1* gene resulting in four different amino acid changes (Table 1). Two patients (20%) with a PIEZO1 mutation were splenectomized and five patients (50%) are regularly phlebotomized because of iron overload. None of the patients with a KCNN4 mutation had a splenectomy or had been treated with a phlebotomy previously. Hereditary deficiency of PK was excluded by DNA sequence analysis of *PKLR*.

Table 1. Genotypes and baseline characteristics of patients with HX

Nr.	Sex	PIEZO1 mutation	Amino acid change	Splenectomy	Phlebotomy	Hb (g/dL)	Ret. (%)	MCHC (g/dL)	Stomato-cytes (%)	Ferritin (µg/L)
P1	M	c.6262C>G	p.Arg2088Gly	No	Yes	14.8	19.4	38.5	3.2	94
P2 ^s	F	c.7367G>A	p.Arg2456His	Yes	No	13.2	7.9	36.4	7.2	170
P3 ^s	M	c.7367G>A	p.Arg2456His	No	No	16.6	19.8	36.4	1.9	107
P4 ^s	M	c.7367G>A	p.Arg2456His	No	Yes	9.8	11.0	32.9	2.5	17
P5	M	c.1792G>A	p.Val598Met	Yes	No	15.6	11.3	34.6	0.7	591
P6 ^s	F	c.7367G>A	p.Arg2456His	No	No	13.4	12.1	37.5	0.5	70
P7 ^s	F	c.7367G>A	p.Arg2456His	No	Yes	12.7	12.7	35.9	0.2	128
P8 ^s	F	c.7367G>A	p.Arg2456His	No	Yes	15.0	9.0	38.8	1.1	332
P9 ^s	F	c.7367G>A	p.Arg2456His	No	Yes	11.0	16.3	35.5	0.7	232
P10	M	c.6503_6508del	p.Lys2168_2169del	No	No	17.7	3.2	38.0	0.5	271
Nr.	Sex	KCNN4 mutation	Amino acid change	Splenectomy	Phlebotomy	Hb (g/dL)	Ret. (%)	MCHC (g/dL)	Stomato-cytes (%)	Ferritin (µg/L)
P11*	F	c.1055G>A	p.Arg352His	No	No	10.4	7.8	36.7	5.2	306
P12*	M	c.1055G>A	p.Arg352His	No	No	10.7	8.6	34.6	5.6	574
P13	M	c.611C>G	p.Pro204Arg	No	No	13.0	7.8	34.2	1.2	639
Contr.						14.6 (1.53)	1.5 (0.5)	34.3 (2.0)	2.2 (3.7)	43 (14)
						M: 13.8-17.2 F: 11.9-15.5	1.0-2.0	30.6-37.1		25-250

Genotypes, amino acid change, splenectomy status, phlebotomy status and laboratory parameters are shown for ten PIEZO1 patients and three KCNN4 patients included in this study. Mean values (standard deviation) of nine healthy controls are shown. Reference range values of the UMC Utrecht population are also included. M, male; F, female. Hb, hemoglobin; Ret., reticulocytes. MCHC, mean corpuscular hemoglobin concentration

^s Patients are from the same family. Patients are from the same family

Routine laboratory parameters show a marked reticulocytosis in HX and anemia in KCNN4 patients but not in PIEZO1 patients

Routine laboratory parameters showed anemia in KCNN4-HX patients, but not in PIEZO1-HX patients (Figure 1A). In contrast there was an inappropriate reticulocytosis in both types of HX, as reflected by a significantly higher reticulocyte production index in both types (data not shown). The percentage reticulocytes was significantly higher in PIEZO1-HX patients, especially considering the absence of anemia in this patient group (Figure 1B). Mean corpuscular volume (MCV), mean corpuscular hemoglobin concentration (MCHC) and red cell distribution width (RDW) seemed to be higher in both types of HX, although only MCHC was significant, indicating that the RBC population was generally more heterogeneous, with larger and more dehydrated RBCs (Figure 1C-E). Percentage hypochromic cells seemed to be lower in both conditions, although not significant, and most pronounced in PIEZO1-HX patients (Figure 1F). In contrast, the number of hyperchromic cells was substantially higher in PIEZO1-HX patients and modestly increased in KCNN4-HX patients (Figure 1G). In line with previous reports¹⁰ stomatocytes were found in low numbers in peripheral blood smears of HX patients and HCs, with the highest levels found in KCNN4-HX patients (Figure 1H). Ferritin levels were found to be higher in KCNN4-HX patients, most presumably because of the frequent phlebotomies in 50% of the PIEZO1-HX patients (Figure 1I). Altogether, our results show that PIEZO-HX patients show brisk reticulocytosis, despite absence of anemia, increased MCHC and hyperchromic RBCs, both indicating cellular dehydration. In contrast, KCNN4-HX patients, are mainly anemic. Their RBCs do not show the same features that characterizes PIEZO1-HX RBCs.

PIEZO1-HX RBCs are more dehydrated and have an increased surface area-to-volume ratio compared to KCNN4-HX RBCs

Osmotic gradient ektacytometry measurements showed the typical left shift of the curve in PIEZO1-HX patients whereas this was absent in KCNN4-HX patients (Figure 2A). In particular, the surface area-to-volume ratio (O_{min}) of RBCs was substantially higher, as reflected by a low O_{min} in PIEZO1-HX compared to KCNN4-HX and HC (Figure 2B), while EI_{max} , representing the total membrane surface area, was slightly decreased in the two types of HX (Figure 2C). O_{hyper} was strongly decreased in PIEZO1-HX, indicating that the RBC population was more dehydrated compared to KCNN4-HX (Figure 2D). The identified differences in particular in the PIEZO1-HX RBCs also resulted in a decreased area under the curve (AUC), whereas there was only a slight decrease in AUC in KCNN4-HX compared to HC (Figure 2E). In line with these findings, PIEZO1-HX and not KCNN4-HX RBCs also behaved differently in the cell membrane stability test (CMST), a novel test to measure membrane health.³⁴ During the CMST, RBCs are exposed to a high shear stress during a fixed time (30 minutes), and the loss in deformability during this test is depicted by ΔEI , which reflect the ability to shed membrane *in vitro*. A representative curve of a PIEZO1-HX patient, KCNN4-HX patient and a HC are shown in Figure 2F. This ability to shed membrane *in vitro* was significantly increased in PIEZO1-HX patients compared to KCNN4-HX and HC (Figure 2G). Combined, the results of osmotic gradient ektacytometry and CMST measurements indicate that PIEZO1-HX RBCs are more dehydrated and have an increased surface area-to-volume ratio compared to KCNN4-HX, with an increased ability to shed membrane *in vitro*.

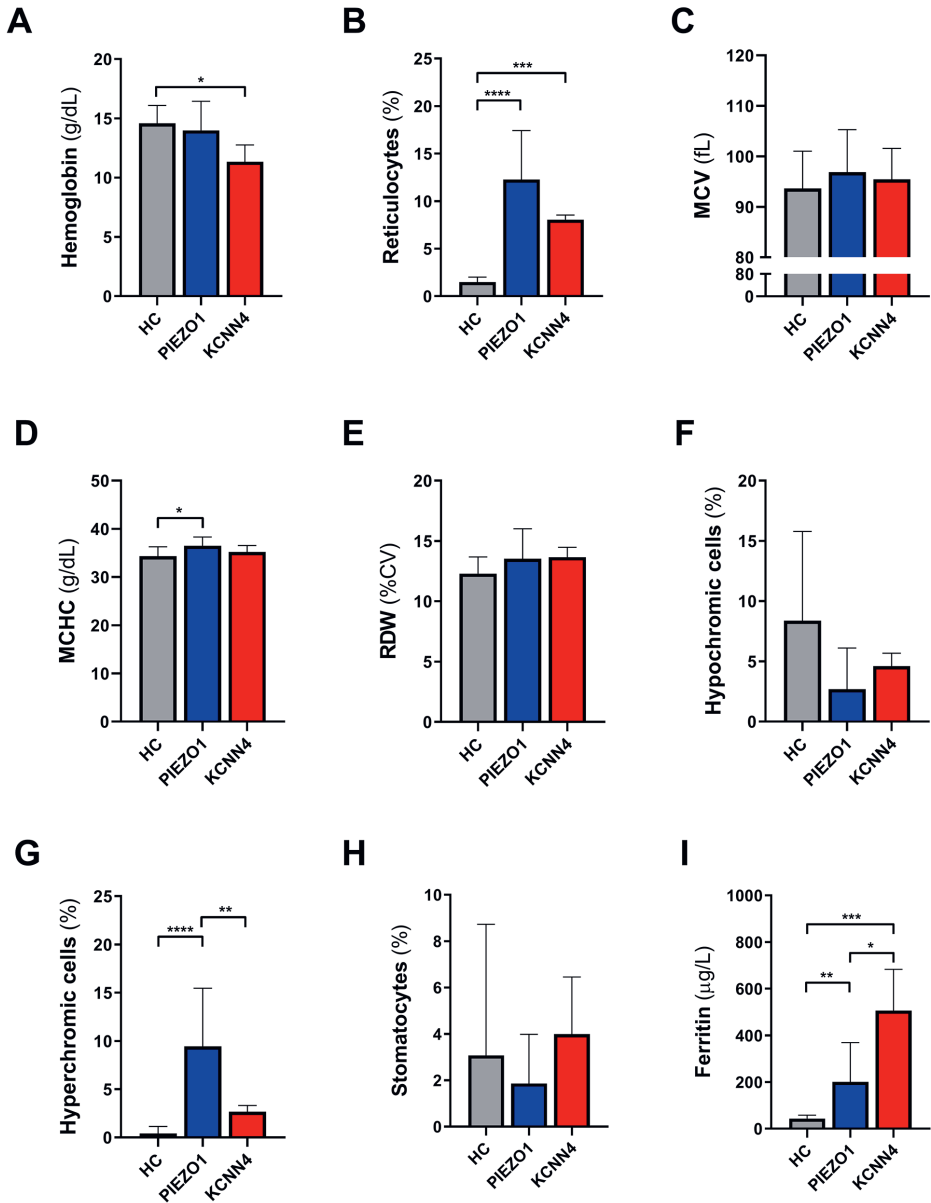


Figure 1. Routine hematological parameters, ferritin and stomatocytes of HX patients with a PIEZO1 or KCNN4 mutation. Mean values of routine hematological parameters of hemoglobin (A), reticulocytes (B), MCV (C), MCHC (D), Ferritin levels (I) of 10 patients with a PIEZO1 mutation, 3 patients with a KCNN4 mutation and 9 healthy controls (HC) are shown. Additional parameters were measured, including red cell distribution width (RDW, panel E), hypochromic cells (F), hyperchromic cells (G) and stomatocytes (H). Error bars represent standard deviation. **** $p < 0.0001$, *** $p < 0.001$, ** $p < 0.01$, * $p < 0.05$. HC, healthy control; MCV, mean corpuscular volume; MCHC, mean corpuscular hemoglobin concentration; RDW, red cell distribution width.

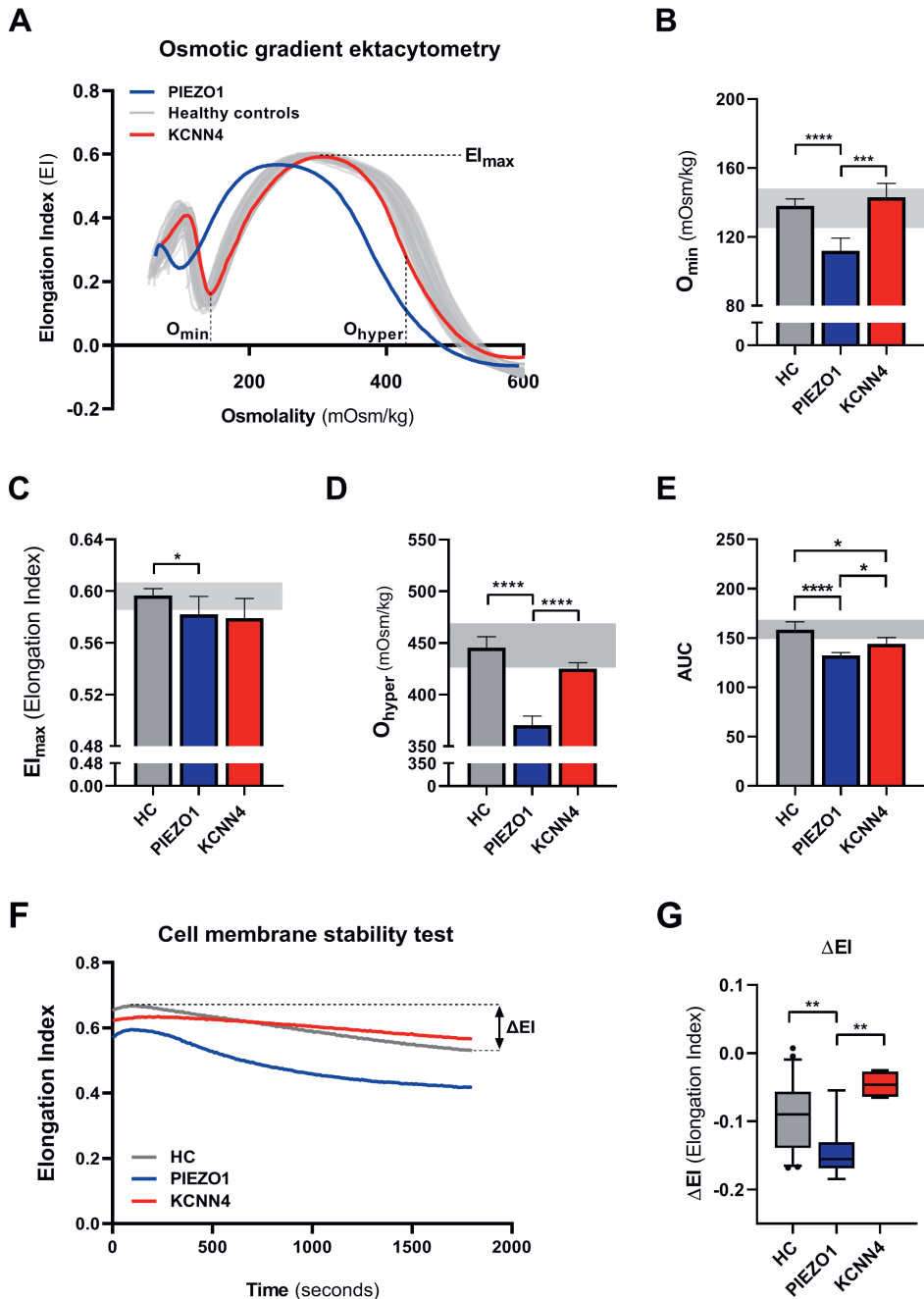


Figure 2. Red blood cell deformability measured by osmotic gradient ektactometry and the Cell membrane stability test. (A) Representative curve of a PIEZO1 patient (blue) and a KCNN4 patient (red) in relation to healthy controls (grey, n=40). (B) Mean values of O_{min}, representing surface to volume ratio, of ten PIEZO1 patients, three KCNN4 patients and 9 healthy controls (HC). (C) Mean values of E_I_{max}, representing the total surface area of the RBC population. (D) Mean values of O_{hyper}, representing the hydration of RBCs. (E) Mean values of area under the curve (AUC). (F) Mean values of area under the curve (AUC). (G) Mean values of area under the curve (AUC). ▶

(F) Representative curves of the cell membrane stability test (CMST) that shows how RBCs of PIEZO1-HX and KCNN4-HX patients respond to a prolonged exposure to high levels of shear stress (100Pa). (G) mean levels of ΔE_i , representing membrane health, i.e. the ability to shed membrane in vitro. The mean (2SD) of healthy controls (n=74) are depicted in the light grey area (B-E). Error bars represent standard deviation. ****p<0.0001, ***p<0.001, **p<0.01, *p<0.05.

Explorative untargeted metabolomics

To assess the variation and separation between HX in general and HC, broad data exploration was performed by the dimension-reducing algorithms of principal component analysis (PCA) and partial least square discriminant-analysis (PLS-DA). The unsupervised PCA reveals evident visual separation, while supervised PLS-DA, taking into account the group label (HX or control), confirmed robust separation of patient samples from controls (data not shown). Both analyses indicate a distinct metabolic profile for the investigated groups. Repetition of these analyses, now stratified for the subgroups of PIEZO-1 HX and KCNN4-HX, demonstrates natural separation in the PCA plot (Figure 3A), and a remarkable separation between the two subgroups of HX in the PLS-DA plot (Figure 3B). Although numbers in particularly for the KCNN4 group are low, this confirms that PIEZO1-HX and KCNN4-HX patients show distinct metabolic profiles in dried blood spots. Exploration of glycolytic metabolites from the untargeted dried blood spot metabolomics showed a significant decrease in 2,3-DPG for PIEZO1-HX. In addition, glyceraldehyde-3-phosphate was significantly increased in PIEZO1-HX, with also a trend to significance for KCNN4-HX. Lastly, a significant yet minimal decrease was observed for pyruvate in PIEZO1-HX compared to controls (Figure 4).

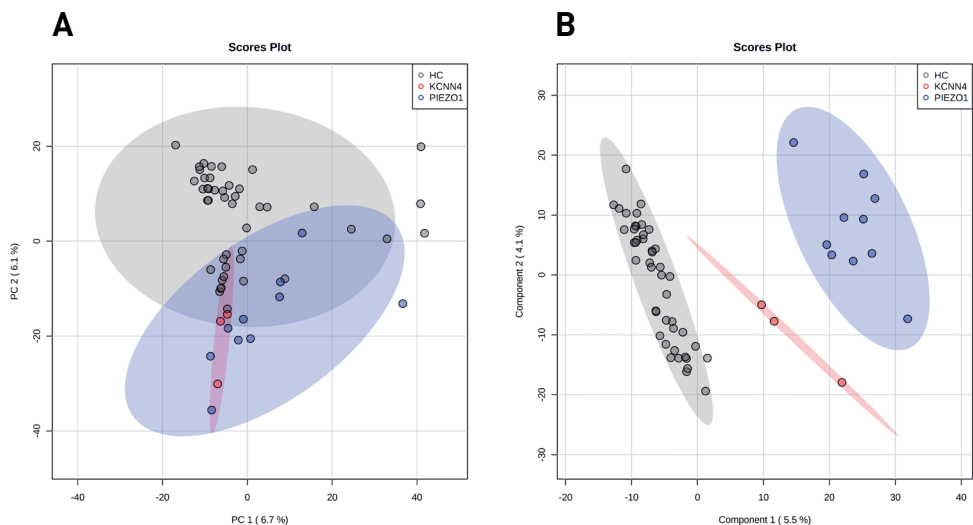


Figure 3. Explorative untargeted metabolomics. (A) Principal component analysis of hereditary xerocytosis and healthy controls, divided per subgroup of PIEZO-1 (n=10) and KCNN4 (n=3) displayed with 95% confidence interval. **(B)** Partial least squares discriminant analysis of the respective groups displayed with 95% confidence interval.

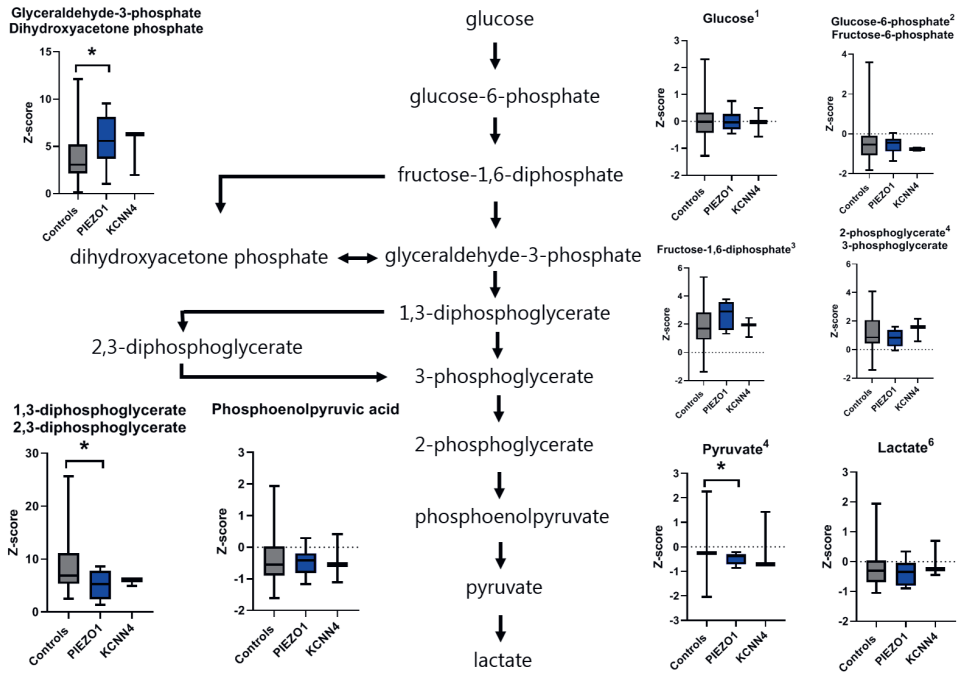


Figure 4. Schematic representation of glycolysis in red blood cells. Z-scores of glycolytic intermediates (and glycolytic isomers) are plotted for healthy control (n=45) and HX-samples (PIEZO 1 n=9; KCNN4 n=3) in a boxplot with Tukey whiskers. Additional isomers of glycolytic intermediates include: 1) D-Galactose, D-Mannose, Myoinositol, 3-Deoxyarabinohexonic acid, Beta-D-Glucose, D-Fructose, Alloose, L-Sorbose, Alpha-D-Glucose, D-Tagatose, Beta-D-Galactose, Scyllitol, L-Gulose, L-Galactose. 2) Myo-inositol 1-phosphate, Galactose 1-phosphate, Dolichyl phosphate D-mannose, Fructose 1-phosphate, Mannose 6-phosphate, D-Myo-inositol 4-phosphate, Glucose 1-phosphate, Inositol phosphate, Beta-D-Glucose 6-phosphate, Beta-D-Fructose 6-phosphate, D-Tagatose 1-phosphate, D-Mannose 1-phosphate, Sorbose 1-phosphate, Beta-D-Fructose 2-phosphate, 1D-myo-Inositol 3-phosphate, D-Tagatose 6-phosphate, D-fructose 1-phosphate. 3) 1D-Myo-inositol 1,4-bisphosphate, D-fructose 2,6-bisphosphate, Alpha-D-Glucose 1,6-bisphosphate, 1D-Myo-inositol 1,3-bisphosphate, 1D-Myo-inositol 3,4-bisphosphate, D-Tagatose 1,6-bisphosphate, D-Mannose 1,6-bisphosphate, beta-D-Fructose 1,6-bisphosphate. 4) 2-Phospho-D-glyceric acid, (2R)-2-Hydroxy-3-(phosphonatoxy)propanoate. 5) Malonic semialdehyde. 6) Hydroxypropionic acid, Glyceraldehyde, D-Lactic acid, Dihydroxyacetone, Methoxyacetic acid. * p<0.05.

Red blood cell glycolysis is altered in HX in particular in PIEZO1

We next explored if altered RBC glycolysis could be attributed to altered, i.e. decreased function of PK. PK activity itself was normal (Supplemental Table 1) but significantly decreased when compared to HK activity in PIEZO1-HX RBCs (median PK/HK ratio 4.6) and KCNN4-HX patients (median ratio 6.3) compared to HC (median ratio 8.6) (Figure 5A). This relative deficiency of PK was accompanied by a significant substantial decrease in PK thermostability in HX RBCs (median residual activity 39% and 63% for PIEZO1-HX and KCNN4-HX, respectively) compared to HC (median residual activity 78%, Figure 5B). The decrease was most pronounced in PIEZO1-HX RBCs, which also had lower PK-R protein levels (129 au/gHb, Figure 5C) compared to HCs (174 au/gHb) and KCNN4-HX RBCs (168 au/gHb). Subsequent quantitative analysis of red cell ATP and 2,3-DPG levels showed a modest

decrease in ATP levels in both types of HX, although not significant (Figure 5D). Furthermore, we found decreased levels of 2,3-DPG in RBCs from in PIEZO1-HX patients, whereas they were normal in KCNN4 RBCs (Figure 5E), thereby confirming the untargeted metabolomics results. Hence, the ATP/2,3-DPG ratio was significantly increased in PIEZO1-HX RBCs compared to KCNN4-HX RBCs and HC RBCs (Figure 5F).

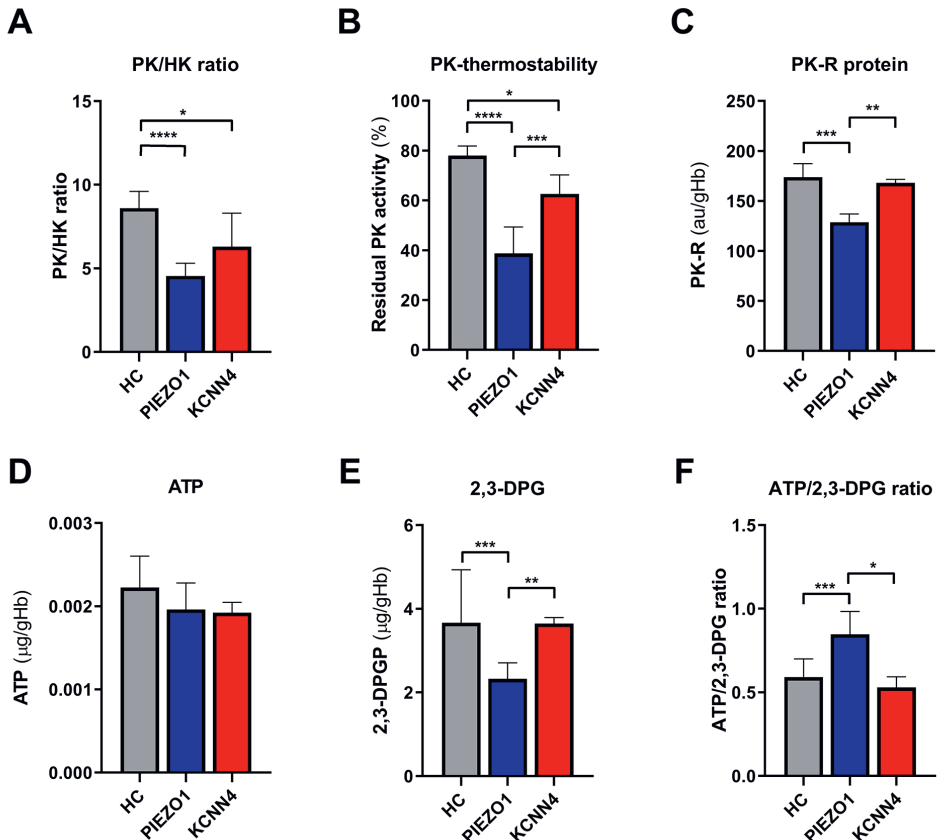


Figure 5. Pyruvate kinase activity, stability, protein levels and ATP/2,3-DPG levels. (A) mean values of PK/HK Ratio, as a means to evaluate PK activity in the presence of high number of reticulocytes, reflected by increased HK activity, of RBCs of ten PIEZO1 patients (blue), three KCNN4 patients (red) and healthy controls (grey). (B) Mean values of residual PK activity in the PK-thermostability test (C) PK-R protein levels of HX patients and healthy controls. (D) Mean values of ATP, corrected for hemoglobin. (E) Mean values of 2,3-diphosphoglycerate (2,3-DPG) corrected for hemoglobin. (F) mean values of ATP/2,3-DPG ratio. Error bars represent standard deviation. ****p<0.0001, ***p<0.001, **p<0.01, *p<0.05. PK, pyruvate kinase; HK, hexokinase; HC, healthy control; 2,3-DPG, 2,3-diphosphoglycerate.

Biomarkers of RBC dehydration are correlated with reticulocytes and PK properties

To explore if, and possibly how RBC dehydration, the hallmark finding in HX, is related to RBC glycolysis, and in particular PK function, we performed a correlation analysis (Figure 6). Hyperchromic cells, representing a dense subpopulation, showed an inverse correlation with both PK/HK ratio and PK stability (Figure 6A and B). In addition, there was a positive correlation with ATP/2,3-DPG ratio and hyperchromic cells (Figure 6C). The same correlations

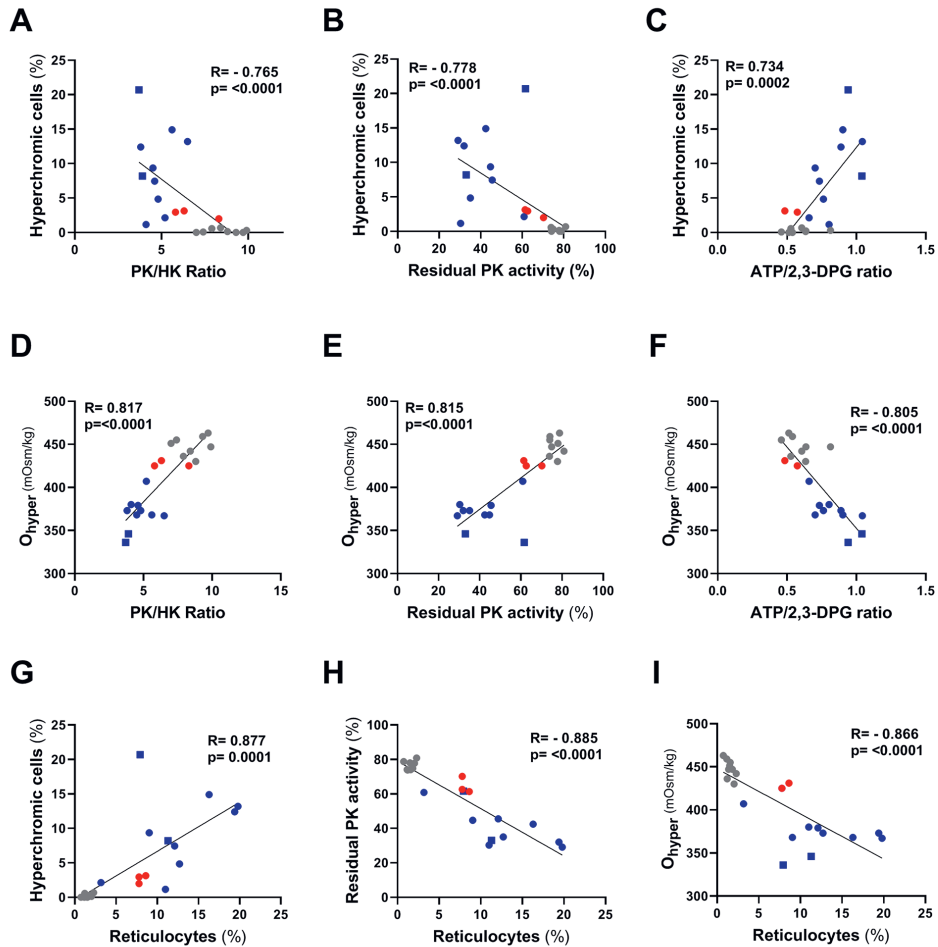


Figure 6. Biomarkers of RBC hydration are correlated with reticulocytes and PK properties. Linear correlations of ten PIEZO1-HX patients (blue dots, splenectomized PIEZO1-HX patients are depicted in blue squares), three KCNN4 patients (red dots) and eight HCs (grey dots). Linear correlations are shown of hyperchromic cells (%) and PK/HK ratio (A), PK-thermostability (B) and ATP/2,3-DPG ratio (C). Linear correlations are shown between Ohyper and PK/HK ratio (D), PK-thermostability (E) and ATP/2,3-DPG ratio (F). Linear correlations are shown between reticulocytes (%) and hyperchromic cells (%) (G), Residual PK activity (H) and Ohyper (I).

PK, pyruvate kinase; HK, hexokinase; 2,3-DPG, 2,3-diphosphoglycerate

were observed for O_{hyper} , a parameter that represent overall hydration status of the RBC population (Figure 6D-F). These findings imply a direct link between dehydration of the red cell, PK stability and function and, as a consequence, a shift in ATP/2,3-DPG ratio. Hyperchromic cells, O_{hyper} and PK stability also showed a strong correlation with reticulocyte count (Figure 6G-I) indicating that the disproportional increase in reticulocytes is related to RBC dehydration and PK properties.

Discussion

In this study we report on differences and similarities of RBC properties, metabolism and deformability between PIEZO1-HX and KCNN4-HX.

Surprisingly, KCNN4-HX RBCs are less dehydrated, with a metabolic profile which is almost normal. In addition, the cells are more deformable compared to PIEZO1-HX RBCs. This seems counterintuitive as patients with KCNN4-HX have chronic hemolysis and a substantial degree of anemia, in contrast to PIEZO1-HX patients that generally present with reticulocytosis but hemoglobin levels in the normal range. The cause of this inappropriate reticulocytosis alongside normal to high hemoglobin levels remains to be elucidated but previous work suggests that reticulocyte maturation is delayed in PIEZO1-HX patients.^{35,36} The previously reported increased intracellular calcium levels in these patients might play a role in the delay in reticulocyte maturation. In addition, it is hypothesized that increased intracellular calcium levels accelerate clearance in the spleen by the activation of scramblase, resulting in an increased phosphatidylserine exposure on the outer membrane.⁶

RBC PK activity, stability and protein levels are compromised in HX, in particular in PIEZO1

We show that absolute levels of PK enzyme activity are normal, but compared to HK activity³⁷ PK activity and stability are compromised in HX, in particular in PIEZO1-HX patients (Figure 5A and B), indicating a secondary partial deficiency of this rate limiting enzyme of glycolysis. In PIEZO1-HX, but not KCNN4-HX RBCs, this was associated with decreased levels of PK-R protein (Figure 5C), indicating different mechanisms involved in partial PK deficiency in the two forms of HX. Metabolic analysis of PIEZO1-HX RBCs showed almost normal ATP and decreased 2,3-DPG levels (Figure 5D and E). This contrasts with the decrease in ATP and increase in 2,3-DPG as the key metabolic hallmarks of hereditary PK deficiency, suggesting complex metabolic (dys)regulation in RBCs with defective PIEZO1 function. The decreased levels of 2,3-DPG increases oxygen affinity of hemoglobin and likely explains the erythrocytosis seen in PIEZO1-HX patients^{38,39}, as well as the marked reticulocytosis. Interestingly, in KCNN4-HX RBCs the loss of PK activity and thermostability was not associated with altered levels of 2,3-DPG and ATP, highlighting an yet unknown difference between the two channelopathies.

The interplay between increased dehydration and metabolic abnormalities

We found significant correlations between biomarkers of RBC dehydration (hyperchromic cells and O_{hyper}) and PK activity, stability and ATP/2,3-DPG ratio (Figure 6A-F). These findings

indicate that with increasing density and dehydration PK activity and, presumably, glycolysis is impaired. It is also reasonable to assume that besides inappropriate Gardos channel activation, the increase of intracellular calcium levels in RBCs of PIEZO1 patients affects other processes in the red cell, such as scramblase activation, calpain cleavage, and flippase inhibition, which ultimately may contribute to premature clearance and, perhaps, to increased risk of post-splenectomy thrombosis.⁵

We have previously found secondary PK deficiency to be a feature of other hemolytic anemias, such as sickle cell disease²¹, in which intracellular calcium levels are also found to be increased^{40,41}. In SCD it has been shown that intracellular calcium mediates reactive oxygen species by downstream activation of NADPH oxidase thereby contributing to the increased oxidative stress that is reported in this devastating disease.⁴² The same downstream effects of pathophysiological increased Ca^{2+} influx could enhance ROS formation and oxidative stress in PIEZO1-HX RBCs. This hypothesis is further supported by preliminary data of the RBC proteome obtained from P1 (patient 1, Table 1), which showed downregulation of the redox regulators glutathione peroxidase 1, and glutathione S-transferase, and modest downregulation of superoxide dismutase (manuscript in preparation). Since oxidative stress is known to affect PK function negatively^{43,44}, this could explain why also hereditary hemolytic anemias other than PKD have a secondarily impaired PK function.

Differences between PIEZO1 and KCNN4

In this study, we report an in-depth characterization of both PIEZO1-HX and KCNN4-HX RBCs. While both types of HX arise from an altered ion channel function resulting, subsequently, in inappropriate activation of the Gardos channel RBC properties differ substantially. We found PIEZO1-HX RBCs to be dehydrated as shown by an increase in the number of hyperchromic cells and O_{hyper} . In contrast, KCNN4-HX RBCs are less dehydrated, with a metabolic profile which is almost normal, and RBCs that are more deformable compared to PIEZO1-HX RBCs.

Although the two types of HX have chronic hemolysis, reticulocytosis and iron overload in common, the degree of anemia varies considerably, between KCNN4-HX and PIEZO1-HX, but also within the latter disorder.^{10,45} Another important difference between the two types of HX is the risk of post-splenectomy thrombosis. Several thromboembolic complications have been described in PIEZO1-HX patients after splenectomy^{10,12}, while no events have been reported in KCNN4-HX patients, but precaution should be taken as reports are anecdotal. The cause of occurrence of post-splenectomy thromboembolic complications is likely to be multifactorial and increased platelet aggregation, reticulocyte adhesion, high levels of circulating microparticles, and low nitric oxide levels have been suggested to play a role.¹⁰ Interestingly, we observed in our PIEZO1-HX patients cohort, that the 2 splenectomized patients, of whom 1 experienced thrombosis, displayed lowest O_{hyper} , RBC deformability, and partly highest hyperchromic cells. These findings imply that after removal of the spleen RBC dehydration further increases, resulting in less deformable RBCs that could occlude small vessels leading to thrombosis. In contrast, other hemolytic anemia's, such as South-East Asian Ovalocytosis, also present with strongly impaired RBC deformability

but generally do not present with hemolysis and anemia, suggesting that reduced deformability alone does not result in clearance by the spleen.⁴⁶ A recent study suggests that RBC dehydration promotes activation of certain adhesion molecules present on the RBC⁴⁷, which could also explain why splenectomy in healthy individuals gives rise to a modestly increased risk of thrombosis.

Limitations

A limitation of this study is the low samples size, in particular in the KCNN4-HX patient cohort. In the latter cohort we also limited ourselves to patients with KCNN4-HX variants affecting residues near the calmodulin binding site, that are the majority. However, a mutation falling in the region of the pore of the channel are dehydrated and would show a left shift in the osmotic gradient ektacytometry curve.⁴⁸ Another limitation is the heterogeneity of the PIEZO1-HX patients group with regard to splenectomy and phlebotomies, as both therapies are bound to influence the composition and density of the RBC population. However, phenotype varies considerably within individuals with a pathogenic *PIEZO1* mutation, which makes it also a strength that the analysis in this study was not limited to only one family or mutation.

Conclusion

Our results indicate that compromised PK function, possibly resulting from altered PIEZO1 function, could contribute to the pathophysiology of PIEZO1-HX by affecting RBC glycolysis and probably also other metabolic pathways. This is strengthened by the association of altered PK properties with the degree of RBC dehydration and reticulocytosis. In contrast to PIEZO1-HX patients, RBCs from patients with the most common form Gardos channelopathy have a less compromised PK function and are only slightly dehydrated which implies that (also) other pathways contribute to disease pathophysiology. We therefore, propose to regard PIEZO1 and KCNN4 as different disease entities and refrain from the terminology dehydrated stomatocytosis or hereditary xerocytosis. Our findings may enhance our understanding of both PIEZO1 channelopathy and Gardos channelopathy pathophysiology, and offer novel opportunities for therapeutic strategies.

References

- Zarychanski R, Schulz VP, Houston BL, et al. Mutations in the mechanotransduction protein PIEZO1 are associated with hereditary xerocytosis. *Blood*. 2012;120(9):1908-1915. doi:10.1182/blood-2012-04-422253
- Andolfo I, Alper SL, De Franceschi LD, et al. Multiple clinical forms of dehydrated hereditary stomatocytosis arise from mutations in PIEZO1. *Blood*. 2013;121(19):3925-3935. doi:10.1182/blood-2013-02-482489
- Glogowska E, Lezon-Geyda K, Maksimova Y, Schulz VP, Gallagher PG. Mutations in the Gardos channel (KCNN4) are associated with hereditary xerocytosis. *Blood*. 2015;126(11):1281-1284. doi:10.1182/blood-2015-07-657957
- Fermo E, Monedero-alonso D, Petkova-kirova P, et al. Gardos channelopathy : functional analysis of a novel KCNN4 variant. *Blood Adv*. 2020;4(24):6336-6341. doi:10.1182/bloodadvances.2020003285
- Fermo E, Bogdanova A, Petkova-Kirova P, et al. "Gardos Channelopathy": A variant of hereditary Stomatocytosis with complex molecular regulation. *Sci Rep*. 2017;7(1):1-13. doi:10.1038/s41598-017-01591-w
- Hertz L, Huisjes R, Llaudet-Planas E, et al. Is increased intracellular calcium in red blood cells a common component in the molecular mechanism causing anemia? *Front Physiol*. 2017;8(SEP). doi:10.3389/fphys.2017.00673
- Rapetti-Mauss R, Lacoste C, Picard V, et al. A mutation in the Gardos channel is associated with hereditary xerocytosis. *Blood*. 2015;126(11):1273-1280. doi:10.1182/blood-2015-04-642496
- Albuisson J, Murthy SE, Bandell M, et al. Dehydrated Hereditary Stomatocytosis linked to gain-of-function mutations in mechanically activated PIEZO1 ion channels. *Nat Commun*. 2013;4(3):1884. doi:10.1038/ncomms2899. Dehydrated
- Lew VL, Tiffert T. On the mechanism of human red blood cell longevity: Roles of calcium, the sodium pump, PIEZO1, and gardos channels. *Front Physiol*. 2017;8(DEC):1-7. doi:10.3389/fphys.2017.00977
- Picard V, Guitton C, Thuret I, et al. Clinical and biological features in PIEZO1-hereditary xerocytosis and gardos channelopathy: A retrospective series of 126 patients. *Haematologica*. 2019;104(8):1554-1564. doi:10.3324/haematol.2018.205328
- Iolascon A, Andolfo I, Barcellini W, et al. Recommendations regarding splenectomy in hereditary hemolytic anemias. *Haematologica*. 2017;102(8):1304-1313. doi:10.3324/haematol.2016.161166
- Stewart GW, Amess JAL, Eber SW, et al. Thrombo-embolic disease after splenectomy for hereditary stomatocytosis. *Br J Haematol*. 1996;93(2):303-310. doi:10.1046/j.1365-2141.1996.4881033.x
- Jais X, Till SJ, Cynober T, et al. An extreme consequence of splenectomy in dehydrated hereditary stomatocytosis: Gradual thrombo-embolic pulmonary hypertension and lung-heart transplantation. *Hemoglobin*. 2003;27(3):139-147. doi:10.1081/HEM-120023377
- Perel Y, Dhermy D, Carrere A, et al. Portal vein thrombosis after splenectomy for hereditary stomatocytosis in childhood. *Eur J Pediatr*. 1999;158(8):628-630. doi:10.1007/s004310051165
- Gallagher PG, Chang SH, Rettig MP, et al. Altered erythrocyte endothelial adherence and membrane phospholipid asymmetry in hereditary hydrocytosis. *Blood*. 2003;101(11):4625-4627. doi:10.1182/blood-2001-12-0329
- Smith BD, Segel GB. Abnormal erythrocyte endothelial adherence in hereditary stomatocytosis. *Blood*. 1997;89(9):3451-3456. doi:10.1182/blood.v89.9.3451
- DaCosta L, Suner L, Galimand J, et al. Diagnostic tool for red blood cell membrane disorders : Assessment of a new generation ektacytometer. *Blood Cells, Mol Dis*. 2016;56(1):9-22. doi:10.1016/j.bcmd.2015.09.001
- Rapetti-Mauss R, Soriani O, Vinti H, Badens C, Guizouarn H. Senicapoc: A potent candidate for the treatment of a subset of hereditary xerocytosis caused by mutations in the gardos channel. *Haematologica*. 2016;101(11):e431-e435. doi:10.3324/haematol.2016.149104
- Mentzer WC, Smith WB, Goldstone J, Shohet SB. Hereditary stomatocytosis: membrane and metabolism studies. *Blood*. 1975;46(5):659-669.

20. Kiger L, Oliveira L, Guitton C, et al. Piezo1-xerocytosis red cell metabolome shows impaired glycolysis and increased hemoglobin oxygen affinity. *Blood Adv.* 2021;5(1):84-88. doi:10.1182/bloodadvances.2020003028
21. Rab MAE, Bos J, van Oirschot BA, et al. Decreased activity and stability of pyruvate kinase in sickle cell disease: a novel target for therapy by mitapivat. *Blood.* 2021;blood.2020:doi: 10.1182/blood.2020008635. Online ahead of print. doi:10.1182/blood-2019-129996
22. Huisjes R, Solinge WW, Levin MD, Wijk R, Riedl JA. Digital microscopy as a screening tool for the diagnosis of hereditary hemolytic anemia. *Int J Lab Hematol.* 2017;40(2):159-168. doi:10.1111/ijlh.12758
23. Lazarova E, Gulbis B, Oirschot B Van, Van Wijk R. Next-generation osmotic gradient ektacytometry for the diagnosis of hereditary spherocytosis: Interlaboratory method validation and experience. *Clin Chem Lab Med.* 2017;55(3):394-402. doi:10.1515/cclm-2016-0290
24. Van Dooijeweert B, Broeks MH, Verhoeven-Duif NM, et al. Untargeted metabolic profiling in dried blood spots identifies disease fingerprint for pyruvate kinase deficiency. *Haematologica.* 2020;Online ahe. doi:10.3324/haematol.2020.266957
25. Haijes HA, Willemsen M, van der Ham M, et al. Direct infusion based metabolomics identifies metabolic disease in patients' dried blood spots and plasma. *Metabolites.* 2019;9(1). doi:10.3390/metabo9010012
26. Wishart DS. Metabolomics for investigating physiological and pathophysiological processes. *Physiol Rev.* 2019;99(4):1819-1875. doi:10.1152/physrev.00035.2018
27. Beutler E. *Red Cell Metabolism. A Manual of Biochemical Methods.*; 1980.
28. Beutler E, Blume K, Kaplan J, Lohr G, Ramot B, Valentine W. International Committee for Standardization in Haematology: Recommended Methods for Red-Cell Enzyme Analysis. *Br J Haematol.* 1977;35(August 1977):331-340.
29. Blume KG, Arnold H, Lohr GW, Beutler E. Additional diagnostic procedures for the detection of abnormal red cell pyruvate kinase. *Clin Chim Acta.* 1973;43(3):443-446. doi:10.1016/0009-8981(73)90487-7
30. Kung C, Hixon J, Kosinski PA, et al. AG-348 enhances pyruvate kinase activity in red blood cells from patients with pyruvate kinase deficiency. *Blood.* 2017;130(11):1347-1356. doi:10.1182/blood-2016-11-75325
31. Allen EL, Ulanet DB, Pirman D, et al. Differential Aspartate Usage Identifies a Subset of Cancer Cells Particularly Dependent on OGDH. *CellReports.* 2016;17(3):876-890. doi:10.1016/j.celrep.2016.09.052
32. Clasquin MF, Melamud E, Rabinowitz JD. LC-MS Data Processing with MAVEN: A Metabolomic Analysis and Visualization Engine. *Curr Protoc Bioinforma.* 2012;37(14). doi:10.1002/0471250953.bi1411s37.LC-MS
33. Kim H, Kosinski P, Kung C, Dang L, Chen Y, Yang H. A fit-for-purpose LC-MS/MS method for the simultaneous quantitation of ATP and 2,3-DPG in human K2EDTA whole blood. *J Chromatogr B.* 2017;1061-1062:89-96. doi:10.1016/j.jchromb.2017.07.010
34. Berrevoets MC, Bos J, Huisjes R, et al. Ektacytometry Analysis of Post-splenectomy Red Blood Cell Properties Identifies Cell Membrane Stability Test as a Novel Biomarker of Membrane Health in Hereditary Spherocytosis. *Front Physiol.* 2021;12(March):1-10. doi:10.3389/fphys.2021.641384
35. Moura PL, Hawley BR, Dobbe JGG, et al. PIEZO1 gain-of-function mutations delay reticulocyte maturation in hereditary xerocytosis. *Haematologica.* 2020;105(6):e268-2271.
36. Caulier A, Jankovsky N, Demont Y, et al. PIEZO1 activation delays erythroid differentiation of normal and hereditary xerocytosis-derived human progenitor cells. *Haematologica.* 2020;105(3):610-622. doi:10.3324/haematol.2019.218503
37. Bianchi P, Fermo E, Glader B, et al. Addressing the diagnostic gaps in pyruvate kinase deficiency: Consensus recommendations on the diagnosis of pyruvate kinase deficiency. *Am J Hematol.* 2019;94(1):149-161. doi:10.1002/ajh.25325
38. Knight T, Zaidi AU, Wu S, Gadgeel M, Buck S, Ravindranath Y. Mild erythrocytosis as a presenting manifestation of PIEZO1 associated erythrocyte volume disorders. *Pediatr Hematol Oncol.* 2019;36(5):317-326. doi:10.1080/08880018.2019.1637984

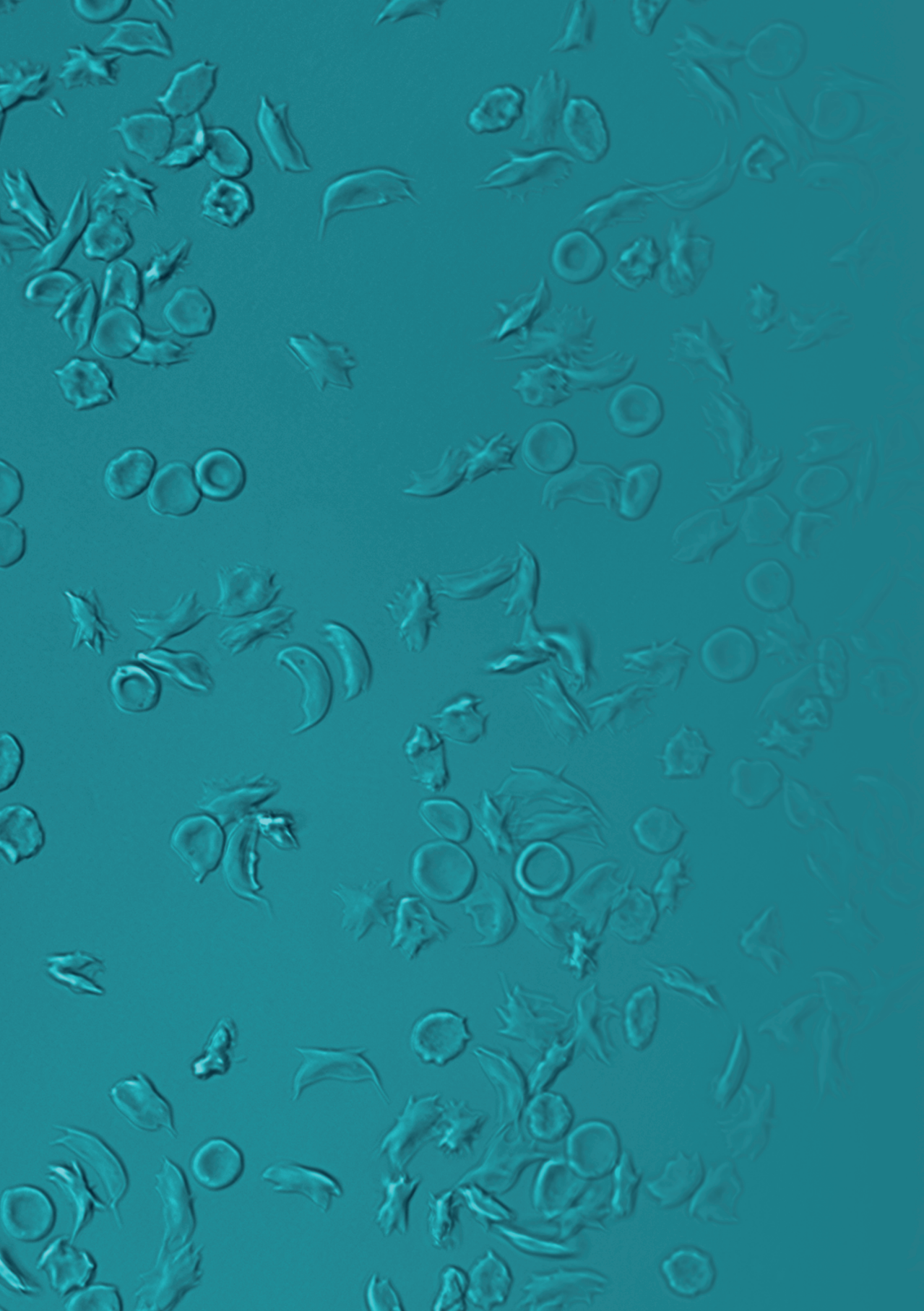
39. Filser M, Giansily-Blaizot M, Grenier M, et al. Increased incidence of germline PIEZO1 mutations in individuals with idiopathic erythrocytosis. *Blood*. Published online 2020. doi:10.1182/blood.2020008424
40. Lew VL, Etzion Z, Bookchin RM. Dehydration response of sickle cells to sickling-induced Ca⁺⁺ permeabilization. *Blood*. 2002;99(7):2578-2585. doi:10.1182/blood.V99.7.2578
41. Eaton JW, Skelton TD, Swofford HS, Kolpin CE, Jacob HS. Elevated erythrocyte calcium in sickle cell disease. *Nature*. 1973;246(5428):105-106. doi:10.1038/246105a0
42. George A, Pushkaran S, Konstantinidis DG, et al. Erythrocyte NADPH oxidase activity modulated by Rac GTPases, PKC, and plasma cytokines contributes to oxidative stress in sickle cell disease. *Blood*. 2013;121(11):2099-2107. doi:10.1182/blood-2012-07-441188
43. Van Berkel TJC, Koster JF, Staal GE. On the molecular basis of pyruvate kinase deficiency. I. Primary defect or consequence of increased glutathione disulfide concentration. *Biochim Biophys Acta*. 1973;321(2):496-502.
44. Anastasiou D, Pouligiannis G, Asara JM, et al. Inhibition of Pyruvate Kinase M2 by Reactive Oxygen Species Contributes to Cellular Antioxidant Responses. *Science (80-)*. 2011;334:1278-1283. doi:10.5061/dryad.bp23483h
45. Andolfo I, Russo R, Rosato BE, et al. Genotype-phenotype correlation and risk stratification in a cohort of 123 hereditary stomatocytosis patients. *Am J Hematol*. 2018;93(12):1509-1517. doi:10.1002/ajh.25276
46. Da Costa L, Galimand J, Fenneteau O, Mohandas N. Hereditary spherocytosis, elliptocytosis, and other red cell membrane disorders. *Blood Rev*. 2013;27(4):167-178. doi:10.1016/j.blre.2013.04.003
47. Klei TRL, Dalimot JJ, Beuger BM, et al. The Gardos effect drives erythrocyte senescence and leads to Lu / BCAM and CD44 adhesion molecule activation. *Blood Adv*. 2020;4(24). doi:10.1182/bloodadvances.2020003077
48. Rivera A, Vandorpe DH, Shmukler BE, et al. Erythrocyte ion content and dehydration modulate maximal gardos channel activity in KCNN4 V282M/+ hereditary xerocytosis red cells. *Am J Physiol - Cell Physiol*. 2019;317(2):C287-C302. doi:10.1152/ajpcell.00074.2019

Supplemental Table 1. Pyruvate and hexokinase activity are shown for ten PIEZO1 patients and three KCNN4 patients included in this study. Mean values (standard deviation) of nine healthy controls are shown.

Nr.	Sex	Gene affected	PK activity	HK activity
P1	M	PIEZO1	5.7	1.5
P2 [§]	F	PIEZO1	4.1	1.1
P3 [§]	M	PIEZO1	7.8	1.2
P4 [§]	M	PIEZO1	9.0	2.2
P5	M	PIEZO1	4.5	1.2
P6 [§]	F	PIEZO1	5.9	1.3
P7 [§]	F	PIEZO1	6.1	1.3
P8 [§]	F	PIEZO1	4.2	0.9
P9 [§]	F	PIEZO1	6.3	1.1
P10	M	PIEZO1	3.2	0.6
Nr.	Sex	Gene affected	PK activity	HK activity
P11*	F	KCNN4	7.1	1.2
P12*	M	KCNN4	7.9	1.3
P13	M	KCNN4	8.1	1.0
Contr.			6.8 (1.8)	0.8 (0.1)

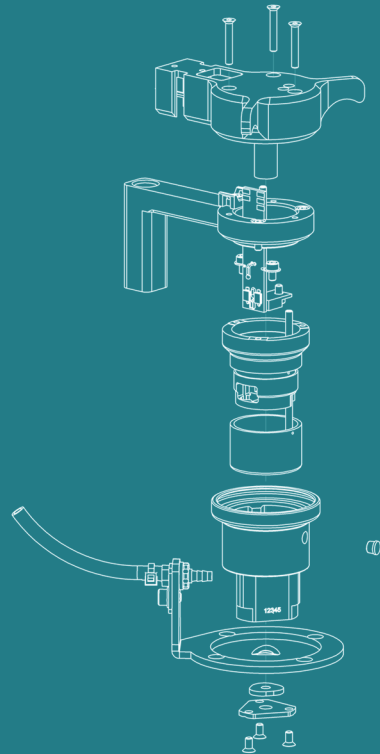
M, male. F, female. PK, pyruvate kinase; HK, hexokinase.

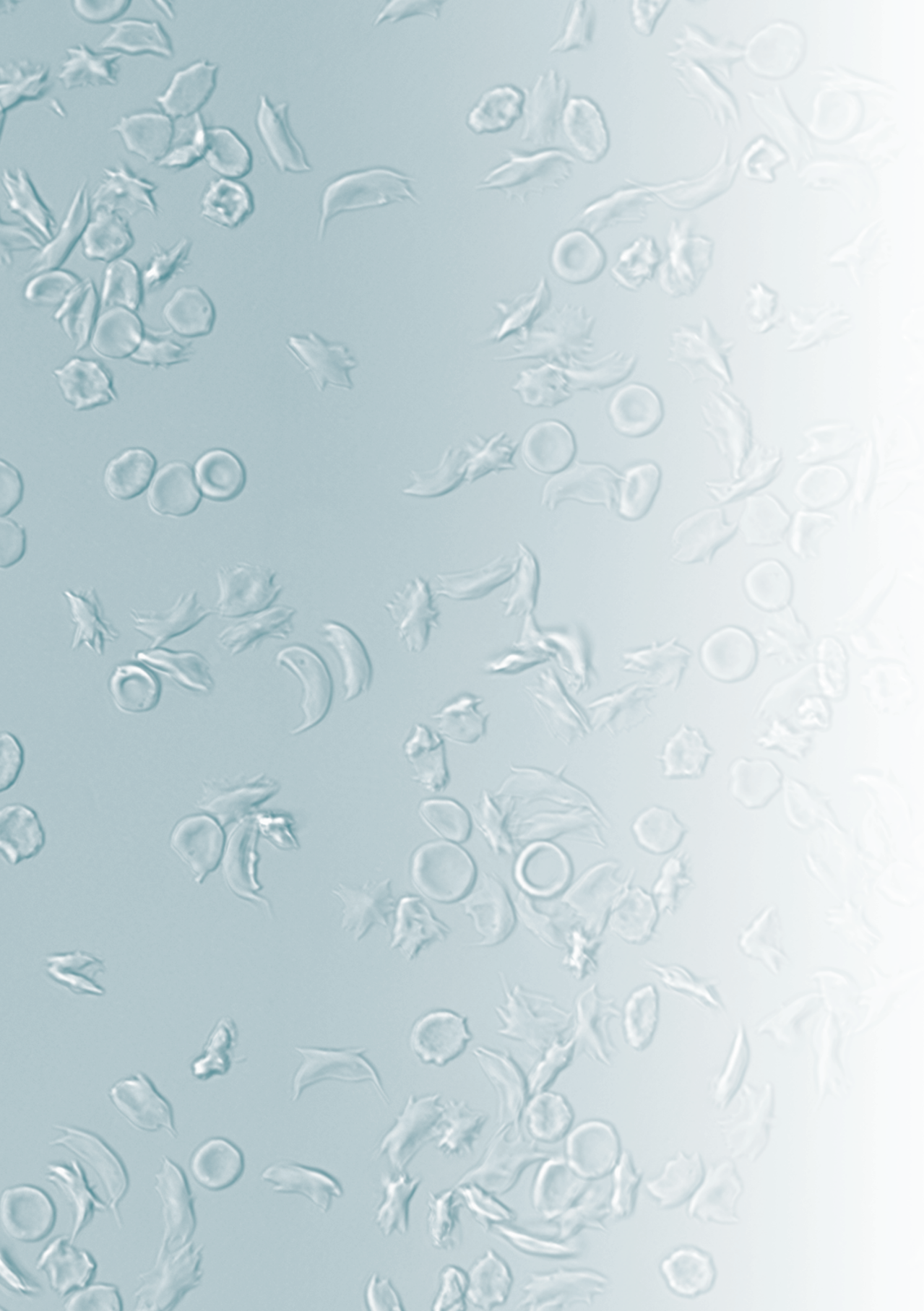
[§] Patients are from the same family, *Patients are from the same family



Part IV

Summary and general discussion





Chapter 13

Summary and general discussion

Summary

This thesis describes the exploration of novel biomarkers in relation to therapy or clinical severity in various forms of rare hereditary hemolytic anemia (HHA), such as sickle cell disease (SCD), pyruvate kinase deficiency (PKD), hereditary spherocytosis (HS) and hereditary xerocytosis (HX). A paramount example is the methodological validation and the start of clinical validation of biomarkers generated by a newly developed ektacytometry-based assay: oxygen gradient ektacytometry, a next generation sickling assay in SCD.

The development and analytical validation of oxygen gradient ektacytometry, a new application of the Laser optical rotational red cell analyzer (Lorrc) is elaborated in *Part I* of this thesis. In **Chapter 2** the oxygenscan module is introduced and its technical performance described in detail. In particular, the effects of factors that are known to influence red cell sickling, such as pH, temperature, levels of hemoglobin S (HbS) and 2,3-diphosphoglycerate (2,3-DPG) have been tested with oxygen gradient ektacytometry. In addition, for the first time, differences in sickling behavior between SCD genotypes are reported, including HbS trait. Oxygen gradient ektacytometry was also used to evaluate new therapies *in vitro*, such as voxelotor (GBT440) and 5-HMF (5-hydroxymethyl-2-furfural). More importantly, in this study we show that the oxygen gradient ektacytometry technique can detect the difference between RBCs from individuals with HbS trait (HbAS) and a mixture of HbSS and HbAA RBCs. This is of importance in light of allogeneic stem cell transplantation and the expanding gene therapeutic strategies that aim to induce either fetal hemoglobin (HbF) or HbS.

Chapter 3, a video article, provides the scientific community with a detailed protocol and knowledge to properly perform oxygen gradient ektacytometry measurements. This is highly important since this technique is sensitive to environmental factors such as temperature of the sample and the device, but also sample handling. Equally important factors, such as technical settings and storage conditions of the sample before it is measured are highlighted in **Chapter 4**. In this chapter the need for standardization of a fixed RBC count for every measurement is shown, which is very important next to sample handling and storage conditions to obtain reproducible measurements. In addition, this study shows that Point of Sickling (PoS), the pO_2 where RBC sickling is initiated is the least influenced by the factors described above, except for RBC count.

To successfully introduce and implement oxygen gradient ektacytometry into the field it is essential to combine precise standard operation procedures and standardization as described in the Chapters of *Part I*.

In *Part II* of this thesis oxygen gradient ektacytometry is further validated in patients with SCD in relation to clinical complications.

Chapter 5 describes the association of oxygen gradient ektacytometry-derived biomarkers PoS and Elmin with vaso-occlusive crises (VOC) in an adult and pediatric cohort of SCD patients. Moreover, the effect of hydroxyurea (HU) and blood transfusion on PoS and El_{min} was investigated in patients who started this standard of care therapy. Results showed that oxygen gradient ektacytometry-derived biomarkers are capable to detect the HU-induced changes in RBC properties, HbF levels and subsequently sickling behavior. In addition, the

effect of blood transfusion on sickling behavior is reported. Further clinical validation is described in **Chapter 6**, which confirms the previously found association of PoS with VOC but extends it to larger cohorts. More importantly the association with other complications such as acute chest syndrome (ACS) and cerebral infarction (stroke or silent cerebral infarcts) is reported. In patients with high PoS values the complication rate (i.e. the amount of different clinical complications within the individual) was significantly higher compared to individuals with low PoS values. Odds ratios for development of one of the major complications (ACS, VOC or cerebral infarction) was significantly increased with every 10 mmHg PoS increase in both adults and children with SCD, further supporting the association of this biomarker with clinical severity. In addition, the potency of blood viscosity as a biomarker was investigated and a significant OR for osteonecrosis was found in the pediatric cohort.

Apart from the first clinical validation that is reported in chapter 5 and 6, other applications of oxygen gradient ektactometry in SCD are described in *Part II* of this thesis. **Chapter 7**, describes a case of twins with SCD in which optimal hydroxyurea dosing was achieved with the use of oxygen gradient ektactometry; an unexpected worsening of PoS, El_{\min} and El_{\max} lead to evaluation of the HU dosage which appeared to be under dosed when corrected for body weight. The subsequent higher HU dose that was prescribed resulted in the improvement of oxygen gradient ektactometry-derived biomarkers. These findings highlight that oxygen gradient ektactometry provides the clinician with information on RBC characteristics and sickling propensity that help optimize hydroxyurea dosing to maximize clinical benefits.

In **Chapter 8**, a new therapeutic agent mitapivat, an allosteric PK activator, was tested *ex vivo* on RBCs from SCD patients using oxygen gradient ektactometry as a functional read out for efficacy. The secondary deficiency in PK and reduced stability of this enzyme in SCD represents a novel pathophysiological feature of SCD and is associated with elevated 2,3-DPG levels. Induction of PK-activity and restoration of stability by mitapivat leads to decreased levels of 2,3-DPG, decrease in p50 and, subsequently, a reduction in sickling as reflected by a reduction in PoS. Therefore, this small molecule mitapivat, which is currently in clinical trial for treatment of hereditary deficiency of PK, is a potential new therapy for SCD.

As part of an in-depth characterization of RBCs of sickle cell anemia (SCA) and HbSC patients, oxygen gradient ektactometry and other RBC characteristics and functional assays are evaluated in **Chapter 9**. RBCs of individuals with SCA are substantially different from HbSC RBCs when assessed with oxygen gradient ektactometry-derived biomarkers PoS, El_{\min} and, in particular, Recovery, the parameter that reflects unsickling during reoxygenation. While in the SCA cohort PoS is associated with several clinical complications, including ACS, cerebral infarction and VOC, this association is not found in the HbSC cohort. Blood viscosity however was found to be associated with occurrence in ACS in HbSC children, in contrast to SCA in which no significant OR for ACS was found. HbSC patients have a more dense or dehydrated RBC population which is more homogeneous compared to SCA. These findings have implications for the identification of biomarkers for SCA and HbSC, but also for therapy. As new therapeutic strategies for SCD, in particular SCA, are rapidly expanding, the question arises if those therapies are also applicable for individuals with HbSC.

Part III of this thesis describes other ektacytometry-based methods in hereditary hemolytic anemias such as PK deficiency (PKD), hereditary spherocytosis (HS) and hereditary xerocytosis (HX). In **Chapter 10** the effects of mitapivat are evaluated in an *ex vivo* study on RBCs from PKD patients with a broad range of mutations in the gene coding for red blood cell PK. RBCs from these patients were incubated with mitapivat and subsequently showed substantial improvement in PK activity and stability, which was accompanied by a rise in ATP. Osmotic gradient ektacytometry showed improvement in deformability in half of the PKD patients. These findings provide a rationale to further explore this therapeutic strategy and could be useful in understanding why some patients do not respond to this small molecule *in vivo*.

Chapter 11 shows the effects of splenectomy, an established treatment in HS, in a longitudinal study on RBC characteristics, density and deformability. In this study, RBC deformability is assessed with the Cell Membrane Stability Test (CMST), that measures deformability during an extensive period at high shear stress, thereby assessing the RBC's ability to shed membrane and resist shear stress. The CMST improved after splenectomy and the CMST-derived parameter ΔEI correlates with hyperchromic cells (%) and reticulocytes (%), indicating clinical benefit. Moreover, the CMST could discriminate between splenectomized and non-splenectomized HS patients in a cross sectional cohort study, which provides rationale to further explore its potential as a biomarker of membrane health in larger cohorts.

In **Chapter 12** RBCs of individuals with PIEZO1 or KCNN4 mutations, both causing hereditary xerocytosis, were investigated by means of osmotic gradient ektacytometry and CMST. To explore why the increased dehydration, as found by osmotic gradient ektacytometry, is a feature of PIEZO1-HX RBCs but not of KCNN4-HX RBCs, the metabolic profile was assessed. This shows a distinct pattern for PIEZO1-HX compared to KCNN4-HX. RBCs from patients with PIEZO1-HX have secondary PK deficiency and reduced enzyme stability which was more pronounced compared to KCNN4-HX individuals. In addition, PK protein and 2,3-DPG levels were lower in PIEZO1 patient RBCs which further highlights that the hemolytic anemia caused by KCNN4 mutations results from a different pathologic mechanism. Moreover, there was an association between degree of dehydration and degree of PK stability and activity, suggesting an interplay between PK dysfunction and RBC dehydration. Altogether these findings show that even though these two disorders both have stomatocytes on peripheral blood film, their pathophysiology is substantially different and therefore they should be considered as two distinct diseases, preferably designated PIEZO1 channelopathy and KCNN4 or Gardos channelopathy.

General discussion

Burden of disease in hereditary hemolytic anemia and sickle cell disease

Hereditary hemolytic anemias are red blood cell (RBC) disorders that can be classified in three main categories: RBC membrane defects (including hereditary spherocytosis), RBC enzyme defects (including pyruvate kinase deficiency) and disorders of hemoglobin (including sickle cell disease). Although HHA might be a rare disorder in The Netherlands, globally it is one of the top causes of years lived with disability by anemia.¹ Generally, patients present with fully compensated to severe anemia, with concomitant symptoms including fatigue, jaundice and reduced exercise tolerance. Complications that can occur are iron overload^{2,3}, gallstones, thrombosis⁴, and several other organs can be affected.⁵ However, the phenotype varies considerably between the different types of HHA and even within patients with the same RBC disorder. Moreover, sickle cell disease (SCD) has a distinct pathophysiology and generally a far more devastating clinical course compared to other types of HHA.

Sickle cell disease (SCD) is the major cause of anemia and accounts for the majority of years lost to disability by anemia in northern America and Western Europe.¹ Although this disease is classified as rare in the Netherlands, due to migration the incidence is rising throughout Europe. Globally, SCD accounts for 300,000 diagnosis made in infants each year, which is further increasing.⁶ While SCD originates from only one single mutation in the β -globin gene, patients present with a range of acute and chronic complications that can be severe or even fatal.⁷ Vaso-occlusive crisis (VOC), the hallmark complication of SCD, results from occlusion of blood vessels by poorly deformable sickled RBCs. The pathophysiology of VOC is highly complex with other factors next to RBC sickling that add to the development of a crisis.⁸ Hemolysis, increased red cell adhesion, endothelial dysfunction, inflammation, oxidative stress, and hemostatic activation, all contribute to the development of VOC, although their relative contribution remains subject to debate.⁸⁻¹⁰ The non-RBC factors are also found in other disease conditions, yet no other disease is associated with VOC, highlighting the key contribution of the sickled RBC to SCD pathophysiology.⁸

Biomarkers in sickle cell disease

SCD comprises several different genotypes, such as homozygous HbS (HbSS), compound heterozygous HbS and HbC (hemoglobin SC disease), compound heterozygous HbS and β -thalassemia (HbS/ β -thal), which contributes to the heterogeneity and variable severity of the disease⁶, and even individuals with the same genotype demonstrate variable clinical expression. Biomarkers that can assess or predict overall disease severity are lacking. Currently, parameters that are known modifiers of clinical severity are used, most commonly fetal hemoglobin levels or conventional laboratory parameters such as hemoglobin²⁴, mean corpuscular volume (MCV) and hemolysis parameters.¹⁶⁻¹⁸

However, several biomarkers have been proposed that assess specific complications, including RBC deformability at normoxic conditions which showed a correlation between an increase in RBC deformability and osteonecrosis¹¹ or painful sickle cell crises.^{12,13} In contrast to these findings low deformability correlated with high hemolytic rate and higher risk of complications such as leg ulcers¹⁴, and glomerulopathy.¹⁵

A combination of markers of hemolysis, lactate dehydrogenase (LDH), bilirubin and absolute reticulocyte count (ARC) (i.e. hemolytic index) are associated with complications attributed to hemolysis^{16–19} but not with VOC.¹⁹

The inflammatory biomarker high-sensitivity C-reactive protein (hs-CRP) was associated with the occurrence of VOC, in two studies.²⁰ TNF- α and IL-1 levels were significantly elevated in patients with frequent VOC with significant correlation with VOC frequency.²⁰ However, up till now no specific cytokine or immune cell type that is seen in patients with SCD holds the potential to serve as a biomarker for overall clinical severity in SCD. This is also due to the highly complex pathophysiology that involves activation of different immune pathways, as well as the short half-life of many inflammatory cytokines.²¹ Although there are several biomarkers that are associated with SCD-associated complications none of them have been further clinically validated and therefore it is difficult to assess their potential as biomarker for overall disease severity in SCD. This also applies for other innovative approaches that have been developed to characterize and quantify sickling behavior: none of these techniques however have been clinically validated in large patient cohorts.^{22,23}

In the ideal situation a single biomarker provides the clinician with information on clinical severity and response to a certain therapy. However, regarding the highly complex pathophysiology of SCD it seems reasonable to assume that several biomarkers are needed to reflect all aspects contributing to disease pathology.

New treatment strategies in sickle cell disease warrant new biomarkers such as PoS

Until recently hydroxyurea (HU) and blood transfusion have been the only therapy available for patients with SCD. This has been expanded recently to four Food and Drug Association-approved pharmacologic therapies for routine SCD care in the US, including HU.^{24–26} There are also several other agents currently in clinical trials on the North American continent and in Europe. Current targets of therapy are HbS polymerization, vaso-occlusion (i.e. inhibition of P-selectin and/or L-selectin), inflammation and genotype changing strategies.²⁷ Gene therapy approaches include gene addition using lentiviral vector-based strategies that aim to generate an anti-sickling β -globin variant, for instance T87Q^{28,29}, or aim to induce HbF production. Gene editing strategies include the clustered regularly interspaced short palindromic repeat (CRISPR)-associated nuclease Cas9 approach to disrupt the *BCL11A* gene (a major inhibitor of γ -globin gene expression) which induces HbF expression.^{30–32} The amount of HbF induction needed to be achieved by gene therapy to effect a cure is still a topic for discussion and in most clinical trials sickling behavior is not functionally assessed, as microscopy based sickling assays are static and do not report on patient specific sickling characteristics.³²

In allogeneic hematopoietic stem cell transplantation (HSCT) for SCD, HbAS or HbAA individuals, preferably related to the recipient, can serve as donors. Also here, efficacy of HSCT, or engraftment following transplant is generally limited to measurements of HbS levels and donor chimerism.³³

The best way to choose which drug to prescribe to which patient is a topic of intense discussion. Clinically relevant biomarkers, such as oxygen gradient ektacytometry, are needed for several indications: 1) to select the optimal therapy based on the patient's particular blood rheology, according to the principles of precision medicine, 2) to monitor efficacy in an objective, rapid manner rather than watching for clinical complications which can take years to emerge, and 3) to provide objective clinically relevant endpoints for clinical trials. 4) to compare gene therapy approaches head-to-head to be able to select optimal strategies.

As new treatment strategies are rapidly expanding, targeting mechanisms outside of fetal hemoglobin (HbF) induction, other clinically relevant biomarkers besides HbF are needed. PoS captures all characteristics of the RBC that determines sickling including HbF and MCV. More importantly, PoS is associated with clinical complications and treatment response which makes it a promising biomarker. However, there are limitations and the technique could be optimized further in order to fully exploit its potential as a marker of clinical severity. Limitations of this technique are that it measures passive deformation and the total RBC population at once which could hamper detection of modest improvements in sickling behavior and RBC properties of RBC subpopulations. Furthermore, the viscous solution (polyvinylpyrrolidone) that is mixed with the sample, has fixed characteristics, i.e. pH, osmolarity and viscosity, and such experimental conditions differ from physiological conditions. Ideally the measurement should be performed with a viscous solution that matches the characteristics of the patient's blood, in particular the osmolarity. The need for standardization that is described in **Chapter 3 and 4** highlights how delicate this technique is. Oxygen gradient ektacytometry can be further improved by standardization of software settings and standardization of hardware settings of the ektacytometer. More importantly, larger cohorts of individuals with SCD should be studied to validate oxygen gradient ektacytometry-derived biomarkers and assess specificity, sensitivity, positive predictive value and negative predictive value for specific clinical complications and overall disease severity. Longitudinal studies could provide evidence for a causal relation between chronic and acute complications and oxygen gradient ektacytometry-derived parameters. However, in particular for acute complications this seems challenging since prior studies have shown that during crises there is a bimodal evolution course. The first phase is characterized by the increase in pain which is accompanied by increase in dense RBCs and decreased deformability which can also be present 1-3 days before the onset of pain. During the second phase, when a decrease in pain and reduced number of dense cells is observed, RBC deformability is reported to be increased and even higher than values measured during steady state.¹² This indicates that the moment of measurement during this bimodal evolution, when patients present themselves at the ER, is crucial for interpretation of findings of longitudinal studies. Since the majority of patients don't visit the hospital just before a crises, but rather when the crisis has been going on for one or more days it seems reasonable to assume that findings will not be conclusive when measurements in steady state are compared to measurements obtained during a crisis.

The challenge with identifying and validating biomarkers in SCD is that they generally only assess one specific factor involved in the complex pathophysiology of sickle cell disease, which involves not only RBC sickling but also numerous other factors.⁸ Therefore other

possible biomarkers are also assessed and described in **Chapter 6** and **9**, including blood viscosity and dense red blood cells (DRBC). However, markers of inflammation^{20,21}, endothelial dysfunction³⁴ and adhesion to the endothelium should also be taken into account. In order to be able to accurately predict disease severity it seems obvious that biomarkers that reflect different aspects of SCD pathophysiology need to be combined. Not only biomarkers that reflect RBC function, hemostasis, inflammation, and oxidative stress are needed, also a patient's genetic make-up should be assessed to determine known disease modifiers such as the co-inheritance of alpha-thalassemia^{7,35}, but more importantly also unknown modifiers.³⁶ Due to the highly complex interplay between all factors that contribute to SCD pathophysiology the use of artificial intelligence is an exciting tool that might aid in prediction models. It would be worthwhile to develop an algorithm that would be able to identify overall or patient specific biomarkers that would predict complications. This could be realized by generating patient specific data on biomarkers at steady state, just before and during an acute event, in a longitudinal manner.

Especially for high risk and high cost curative therapies the identification of clinically relevant biomarkers is of importance. Current guidelines for allogeneic SCT suggest clinical follow-up measurements should include donor chimerism and HbS levels. Also, different gene therapy strategies induce different functional hemoglobins and a functional analysis of the resulting RBC population would be the best way to compare different strategies head to head. VOC is still the primary endpoint in ongoing gene therapy trials, however lack of VOC does not demonstrate a cure as organ damage may still be ongoing. Therefore, novel functional biomarkers like El_{min} and PoS could better assess the effectivity of these therapies in individual patients, indicating if the treatment was successful enough to prevent clinically relevant sickling.

In allogeneic SCT the appropriate amount of donor chimerism has been reported to be at least 20% to reverse the sickle phenotype, based on a study of three transplanted individuals.³⁷ However, donor chimerism and HbS levels do not capture clinically relevant sickling in the individual, because a mixture of 50% HbAA with 50% HbSS RBCs compared to 100% HbAS RBCs gives very different oxygen gradient ektacytometry-derived biomarkers results even though HbS levels are the same.³⁸ This is highlighted in Figure 4 of **Chapter 2**, where it is shown that comparable HbS levels in HbAS individuals or a mixture of HbAA and HbSS RBCs (resembling HbSS individuals on chronic transfusion therapy) generates substantially different PoS values, with the latter displaying PoS values that are also found among patients that experience clinical complications. As a result, a severely affected patient might need a higher percentage of chimerism and a lower HbS level to prevent clinically relevant sickling. Based on findings presented in this thesis functional analysis of sickling behavior by oxygen gradient ektacytometry should be implemented in clinical follow after allogeneic SCT to ensure that the individual donor chimerism is sufficient to reverse the SCD phenotype.³⁸

SCD has different genotypes, and as described in **Chapter 9**, HbSC disease has a distinct pathophysiology. It can be concluded that biomarkers that are associated with clinical complications in SCA are not associated with complications in HbSC disease. From the

economical perspective of pharmaceutical companies it is far more rewarding to develop new treatment strategies for SCA than for HbSC disease, even though the latter comprises around 25-30% of individuals with SCD, who are from African origin.³⁹ Clinical trials focusing on HbSC disease are scarce, and at best there is a small subpopulation of individuals with HbSC disease included in large SCD trials.¹⁹ For example, while the efficacy and safety of HU have been studied extensively in individuals with HbSS, only a few studies focused on HbSC disease⁴⁰, with the most prominent one being a retrospective cohort study with 133 individuals with HbSC that reported a substantial reduction in pain-related episodes.⁴¹ Our findings described in **Chapter 9** that blood viscosity can serve as a possible biomarker for acute chest syndrome indicate that therapeutic strategies that reduces blood viscosity might be beneficial specifically for the HbSC patient group. This is supported by prior studies that used phlebotomy to prevent acute events, which was successful in 71%.⁴² Other approaches that could reduce blood viscosity include iron depletion, thereby inducing iron deficiency, which decreases sickling tendency in SCD mice.⁴³ Recent studies show that the induction of iron depletion as potential therapy for SCA⁴⁴ could also be beneficial for HbSC.⁴⁵ Especially therapies that are registered for other indications or diseases are of interest since they might be much more easily accessible for patients.

Precision medicine/personalized treatment is warranted in SCD

We are in debt to our patients with SCD. If in other fields of hematology, such precision medicine is applied, and risk scores are easily adapted with new insights, we should do the same for patients with SCD. Recent studies show how SCD also affects brain tissue in a way that limits the opportunities for SCD patients; opportunities that are already low due to social-economic factors and racism.⁴⁶ Even though the first findings of SCD have been reported more than a century ago, until recently therapeutic options have been limited to blood transfusion and HU. This stagnation in the development of therapy is thought to be partly due to inadequate research funding as a result of racism.⁴⁶ For example, in case of cystic fibrosis, a congenital disease affecting only “white” individuals for which 7-10 times more funding per patient has been granted which resulted in 15 FDA approved therapies compared to only 4 for SCD in the US.⁴⁷

We need to treat SCD patients better, starting more early in life, before irreversible damage is done. Especially now that numerous new treatment strategies for SCD are developed it is important to personalize treatment for the individual patients benefit but also from an social-economical point of view.

The need for biomarkers in other types of HHA

Although the burden of disease for SCD is particularly high, other forms of HHA can also be quite invalidating, which is in the majority of patients a result of severe anemia and frequent blood transfusions. New therapies that are currently in clinical trial for PKD include mitapivat⁴⁸ that is discussed in **Chapter 10** and gene therapy.⁴⁹ The primary outcome parameter is transfusion need or hemoglobin level, the latter being an important and clinically relevant biomarker. However, a biomarker directly related to the pathophysiological mechanism causing the severe anemia in PKD is currently lacking. If such a biomarker were identified and could predict the efficacy of splenectomy, that would be worthwhile, also for other forms of chronic HHA due to enzyme deficiencies, or HS.

Biomarkers in HS are needed to assess the efficacy of (partial) splenectomy, for example when partial splenectomy is performed by embolization. It would also be beneficial to create a new clinical severity score as the one that is currently used in the clinic is not complete because functional analysis of HS RBCs are not included.⁵⁰ More importantly, such a score should not primarily include splenectomy since that is a consequence of the disease and not a pathophysiological sign, and subject to the physicians opinion. With an increasing number of available functional assays such as the CMST that is discussed in **Chapter 11** and **12** but also metabolomics analysis (*van Dooijeweert et al*, Hemasphere in revision), a more comprehensive severity score could be developed that would be a more accurate reflection of the pathophysiology. Furthermore next to rheological and routine laboratory parameters, it is of high importance to include clinical complaints such as fatigue, failure to thrive and exercise intolerance.

Hereditary xerocytosis is a red cell disorder that is characterized by the occurrence of stomatocytes on the peripheral blood film. There are different subtypes according to cellular hydration status, i.e. dehydrated stomatocytosis and overhydrated stomatocytosis, or according to the mutation found. As highlighted in **Chapter 12** of this thesis these 2 channelopathies only share the occurrence of stomatocytes, which also differs quite extensively between the two.⁵¹ Digital analysis of peripheral blood smears of patients with various types of HHA has shown that spherocytes, stomatocytes, and elliptocytes occur in several different types of HHAs and that they are not restricted to the disorder they were named after.⁵⁵ The limitation of morphology analysis is that it is 2 dimensional. Innovative 3D morphology analysis of RBCs is a promising tool which is further improved by machine learning algorithms (*Simionato et al*, PLOS Computational Biology, submitted; *Simionato et al*, submitted), thus potentially developing into a new biomarker.

Biomarkers of clinical severity in HX are lacking. However, RBC hydration markers differ significantly between the two channelopathies and might therefore be worthwhile to be investigated as potential biomarkers. Future studies should also include intracellular calcium measurements and its possible relation to altered PK function.

Red cell (de)hydration in SCD and other HHAs: a potential biomarker?

Maintenance of RBC hydration and volume is a dynamic process and several factors are involved including hemoglobin concentration, ion transport, membrane surface area, and the complex interaction between solute and conductance of the membrane for ions and cations.⁵² In this thesis several different assays have been used that reflect different aspects of RBC hydration. Especially the functional assays that are ektacytometry-based could be worthwhile to explore for their potential as a biomarker in HHA. Laboratory findings described in this thesis chapters are used to investigate RBC dehydration indifferent categories of HHA. Hemocytometry and RBC functional parameters results are listed in Table 1 and categorized according to the specific RBC disorder. Correlation analysis between RBC hydration biomarkers and the different RBC disorders showed associations of hemoglobin and reticulocyte count with various makers of hydration.

When we assessed the whole SCD cohort including HbSC and HbCC correlation analysis showed that PoS was associated with both Hb ($R = -0.566$, $p=0.001$) and reticulocytes ($R =$

0.650, $p < 0.0001$). Hypochromic cells also correlated with Hb ($R = -0.739$, $p < 0.0001$) and reticulocytes ($R = 0.599$, $p < 0.0001$). In addition, O_{hyper} also correlated to Hb ($R = -0.455$, $p = 0.013$) and reticulocytes ($R = 0.443$, $p = 0.016$). This indicates that RBCs of the more anemic SCA patients are more dehydrated, contain more hypochromic cells and are more prone to sickle at higher oxygen tensions. Interestingly, individuals with HbCC, the patient group with a mild disease burden and the least clinical complications of the three hemoglobinopathies have the most dehydrated RBCs and lowest RBC deformability, indicating that an additional trigger facilitates clearance of RBCs by the spleen.⁵³

In PKD there is a significant correlation with EI_{max} and hemoglobin ($R = 0.767$, $p = 0.001$) and inverse correlation with percentage reticulocytes ($R = -0.734$, $p = 0.003$) indicating that RBC deformability is lower when patients are more anemic. Opposite results were found for O_{hyper} that correlated inversely with Hb ($R = -0.587$, $p = 0.023$) and percentage reticulocytes ($R = 0.419$, $p = 0.120$), indicating that RBCs are more hydrated when patients are anemic which could be due to the high percentage of reticulocytes that is present in PKD patients. In the HS cohort micro DRBCs correlated inversely with Hb ($R = -0.705$, $p = 0.023$) and positively with reticulocytes ($R = 0.508$, $p = 0.039$) indicating that small sized dense RBCs are higher when patients are more anemic. DeltaEI (ΔEI) also correlated with reticulocytes ($R = 0.470$, $p = 0.036$), but not with Hb. In the group with a channelopathy none of the RBC hydration markers was associated with Hb. There was a correlation of reticulocytes with both ΔEI ($R = -0.586$, $p = 0.038$) and hyperchromic cells ($R = 0.556$, $p = 0.051$) indicating that with high reticulocyte percentages there was more capacity to shed membrane *in vitro* (during the CMST). The data of functional assays that reflect RBC hydration that are presented in Table 1 could represent attractive targets for future studies in the search for clinically relevant biomarkers. However, the data presented in Table 1 is based of small patient cohorts. Hence, larger studies are warranted to thoroughly assess the associations found so far. But, although sample size was small, these results raise the question whether findings are directly the result of reticulocytosis or that the whole RBC population is affected. Further analysis that include density separation experiments to fractionate the RBC population can shed light on this.

Personalized diagnostics in HHA

Identification, validation and eventually implementation in routine diagnostics of novel biomarkers are all equally important aspects and require a specialized (often academic) setting that includes collaboration between laboratory and clinical departments as well as between hospitals and research institutes. Clinically relevant biomarkers in HHA could further improve patient care by enabling precision medicine. More importantly, with the use of big data of RBC characteristics that have been gathered for the last decade from several centers over the world biomarkers could be identified, which results in a better understanding how different mutations relate to red cell characteristics and function. In this light artificial intelligence could be helpful in further unravelling which specific biomarker is the most relevant in the pathophysiology of specific HHAs. This subsequently would enable further analysis to improve severity scores, which likely will improve patient management and enable personalized integrative diagnostics and treatment.

Table 1. Laboratory parameters and functional assay-derived parameters that reflect RBC hydration in RBC disorders.

Type of defect	SCA	HbSC	HbCC	PIEZO1	KCNNA4	HS	PKD	HC
	Hb	Hb	Hb	channel	channel	membrane	enzyme	-
Hemocytometry parameters								
Hb (g/dL)	9.4 ± 1.2 (6.7–12.3)	12.1 ± 1.2 (10.7–14.1)	11.9 ± 2.2 (10.4–13.5)	14.0 ± 2.5 (9.8–17.7)	11.3 ± 1.4 (10.4–13.0)	12.3 ± 2.5 (9.8–17.7)	10.2 ± 2.0 (6.6–13.4)	14.2 ± 1.3 (11.9–17.2)
Reticulocytes (%)	8.5 ± 3.6 (4.0–16.9)	3.5 ± 2.6 (1.9–9.8)	3.0 ± 0.6 (2.6–3.5)	12.3 ± 5.2 (3.2–19.8)	8.1 ± 0.5 (7.8–8.6)	9.2 ± 5.8 (2.3–19.7)	36.2 ± 25.7 (5.0–85.0)	1.3 ± 0.4 (0.4–2.3)
MCV (fL)	90 ± 17 (69–125)	76 ± 14 (59–102)	72 ± 2 (71–73)	97 ± 8 (81 – 105)	95 ± 6 (89 – 101)	84 ± 7.2 (64 – 93)	113 ± 9 (98 – 124)	90 ± 7 (64 – 105)
MCHC (g/dL)	35.7 ± 1.8 (33.4–40.0)	35.6 ± 1.5 (33.7–38.3)	38.7 ± 1.8 (37.4–40.0)	36.5 ± 1.9 (32.9–38.8)	35.2 ± 1.4 (34.2–36.7)	36.4 ± 1.5 (34.0–39.5)	32.8 ± 1.3 (30.4–34.6)	33.9 ± 1.6 (30.6–37.1)
Hypochr. cells (%)	17.0 ± 10.8 (4.2–46.6)	3.6 ± 2.7 (0.5–9.1)	6.3 ± 0.6 (5.8–6.7)	2.7 ± 3.4 (0.0–11.5)	4.6 ± 1.1 (3.4 – 5.3)	6.3 ± 5.3 (0.9 – 15.7)	17.2 ± 14.2 (1.3–45.9)	8.4 ± 7.4 (0.6–29.4)
Hyperchr. cells (%)	2.4 ± 2.7 (0.0 – 12.5)	2.7 ± 5.3 (0.1 – 15.6)	3.4 ± 1.3 (2.6 – 4.3)	9.4 ± 6.0 (1.2–20.7)	2.7 ± 0.6 (2.0 – 3.1)	13.2 ± 9.2 (0.2–32.9)	0.2 ± 0.5 (0.0 – 1.5)	0.4 ± 0.7 (0.0 – 2.8)
normo DRBC (%)	4.0 ± 3.0 (0.5 – 10.1)	6.0 ± 2.9 (2.1 – 9.1)	22.8	6.4 ± 4.4 (2.4–15.3)	5.4 ± 3.3 (3.2 – 9.2)	15.4 ± 10.9 (1.7 – 36.1)	n/a	0.7 ± 0.6 (0.0 – 2.5)
micro DRBC (%)	1.1 ± 0.9 (0.1 – 2.8)	5.8 ± 5.4 (0.2 – 14.8)	9.7	0.3 ± 0.5 (0.0 – 1.6)	0.3 ± 0.2 (0.1 – 0.5)	2.3 ± 2.3 (0.2 – 6.7)	n/a	0.1 ± 0.2 (0.0 – 0.8)
Total DRBC (%)	5.2 ± 3.0 (1.2 – 11.2)	11.8 ± 6.6 (3.6 – 23.7)	32.5	6.7 ± 4.3 (2.4–15.4)	5.7 ± 3.5 (3.3– 9.7)	17.8 ± 12.1 (2.1 – 40.3)	n/a	0.8 ± 0.6 (0.2 – 2.5)
Functional RBC characteristics								
PoS (mmHg)	55.9 ± 8.7 (39.2 – 72.4)	44.7 ± 7.1 (37.1–55.3)	47.3 ± 0.7 (46.7–47.7)	n/a	n/a	n/a	n/a	-
El _{max} -Oxy(EI)	0.41 ± 0.08 (0.24 – 0.55)	0.41 ± 0.05 (0.30–0.48)	0.23 ± 0.0 (0.22–0.23)	n/a	n/a	n/a	n/a	0.60 ± 0.01 (0.59 – 0.61)
El _{min} (EI)	0.08 ± 0.05 (-0.01–0.19)	0.11 ± 0.06 (-0.01–0.20)	0.11 ± 0.02 (0.09–0.13)	n/a	n/a	n/a	n/a	0.60 ± 0.01 (0.57 – 0.61)

Table 1. Continued

Type of defect	SCA		HbSC		HbCC		PIEZO1		KCNN4		HS		PKD		HC		
	Hb	O _{min}	Hb	O _{hyper}	Hb	O _{hyper}	channel	channel	channel	channel	membrane	enzyme	enzyme	enzyme	enzyme	enzyme	
O _{min} (mOsm/kg)	107 ± 22 (90 - 194)	90 ± 4 (82 - 95)	96 ± 1 (95 - 97)	111 ± 15 (90 - 139)	144 ± 7 (137 - 151)	161 ± 9 (145 - 175)	148 ± 6 (141 - 156)	146 ± 8 (138 - 165)									
El _{max} -Osm (EI)	0.51 ± 0.05 (0.41 - 0.57)	0.54 ± 0.02 (0.51 - 0.57)	0.50 ± 0.01 (0.49 - 0.50)	0.58 ± 0.02 (0.55 - 0.60)	0.58 ± 0.02 (0.57 - 0.60)	0.54 ± 0.03 (0.48 - 0.58)	0.59 ± 0.02 (0.56 - 0.61)	0.60 ± 0.01 (0.60 - 0.61)									
O _{hyper} (mOsm/kg)	375 ± 18 (344 - 400)	337 ± 10 (319 - 345)	315 ± 3 (313 - 317)	370 ± 19 (336 - 407)	427 ± 3 (425 - 431)	425 ± 16 (397 - 446)	454 ± 23 (412 - 503)	457 ± 21 (459 - 501)									
ΔEI (EI)	-0.09 ± 0.05 (-0.18 - 0.0)	-0.11 ± 0.03 (-0.15 - -0.08)	-0.08 ± 0.01 (-0.09 - -0.08)	-0.15 ± 0.04 (-0.18 - -0.05)	-0.04 ± 0.02 (-0.06 - -0.03)	-0.02 ± 0.05 (0.05 - -0.13)	n/a	-0.13 ± 0.06 (-0.23 - 0.0)									
Clinical implications																	
Effect of splenectomy post-splenectomy	Yes*	Yes*	Yes*	No	unknown	unknown	Yes	Yes	Yes	Yes	Yes	Yes	Yes	Yes	Yes	Yes	Not applicable
Risk of thrombosis post-splenectomy	++	++	++	+++	unknown	unknown	++	++	++	++	++	++	++	++	++	++	+ (3-fold higher) ⁵⁴
Possible functional biomarkers	Pos El _{min}	Blood viscosity O _{hyper}	unknown	Hyperchromic Cells ΔEI	Hyperchromic Cells ΔEI	Hyperchromic Cells ΔEI	Hyperchromic Cells ΔEI	Hyperchromic Cells ΔEI	Hyperchromic Cells ΔEI	Hyperchromic Cells ΔEI	Hyperchromic Cells ΔEI	Hyperchromic Cells ΔEI	Hyperchromic Cells ΔEI	Hyperchromic Cells ΔEI	Hyperchromic Cells ΔEI	Hyperchromic Cells ΔEI	El _{max} O _{hyper}
Clinically assessed biomarker	Pos	Blood viscosity	-	-	-	-	-	-	-	-	-	-	-	-	-	-	Not applicable

The different patient groups include sickle cell anemia (SCA, n=22), Hemoglobin SC disease (HbCC, n=2), PIEZO1 channelopathy (n=10), KCNN4 channelopathy (n=3), hereditary spherocytosis (HS, n=20), pyruvate kinase deficiency (PKD, n=15) and healthy controls (HC, n=9). HbA, hereditary hemolytic anemia; Hb, hemoglobin; MCV, mean corpuscular volume; MCHC, mean corpuscular hemoglobin concentration; Hypochrom, hypochromic cells; Hyperchrom, hyperchromic cells; DRBCs, dense red blood cells; PoS, point of sickling; El_{max}, maximum elongation index, El_{min}, minimum elongation index; O_{min}, osmolarity when minimum EI is measured; O_{hyper}, osmolarity at which 50% of EImax is measured in the hypertonic range; n/a, not addressed.

*Indication for splenectomy is >2 acute splenic sequestration crises, massive splenomegaly or symptomatic hypersplenism⁵⁰

The interplay between RBC diagnostics, research and patient care: the need for centers of expertise

To accomplish timely and accurate diagnosis of HHA it is important to refer patients with unexplained anemia to established (inter) national centers of expertise. Centralization of healthcare for patients with HHA will improve patient care since hematologists working in the broad field of both benign and malignant hematology generally will not be up to date on current knowledge and developments such as organ damage⁵, or possible new therapies.⁵⁶⁻⁵⁸ More importantly, through centralization research will be facilitated, by means of pre-clinical studies, patient registries and eventually clinical trials, which subsequently, will improve patient care. Furthermore, research and diagnostic laboratories should work together with clinical departments to provide optimal care based on patients' needs. In order to achieve this, it is important to have physician scientists, who work both in clinic and in the laboratory, to connect these two different worlds. This will create synergy and will boost translational research since it will generate especially clinical relevant research but it will also enable rapid implementation of new prognostic or diagnostics tests. On the other side, the laboratory will pave the way for the patient clinic with pre-clinical studies on potential therapies, which further enables clinical trials. It is important that clinicians realize that laboratory experiments are often laborious and require a certain amount of preparation that highly exceeds the wrongfully assumption that, for instance, oxygen gradient ektacytometry, is merely a push on the button of the machine. Therefore, knowledge of the opportunities but also limitations of laboratory methods of the physician scientist will lead to more possibilities and eventually improve and complement clinical research. In this way a center of expertise with an outpatient clinic, integrated diagnostics and research can be built with all late breaking developments readily available for the patient.

To further strengthen such centers of expertise it is in particular for rare diseases such as HHA worthwhile to collaborate with other expertise centers all over the world and share findings and techniques. A great example is the ERN-EuroBloodNet, which is a European reference network for rare hematological diseases that brings clinicians and scientists together to enhance knowledge and facilitate patient registries and research in large consortia.

Closing remarks

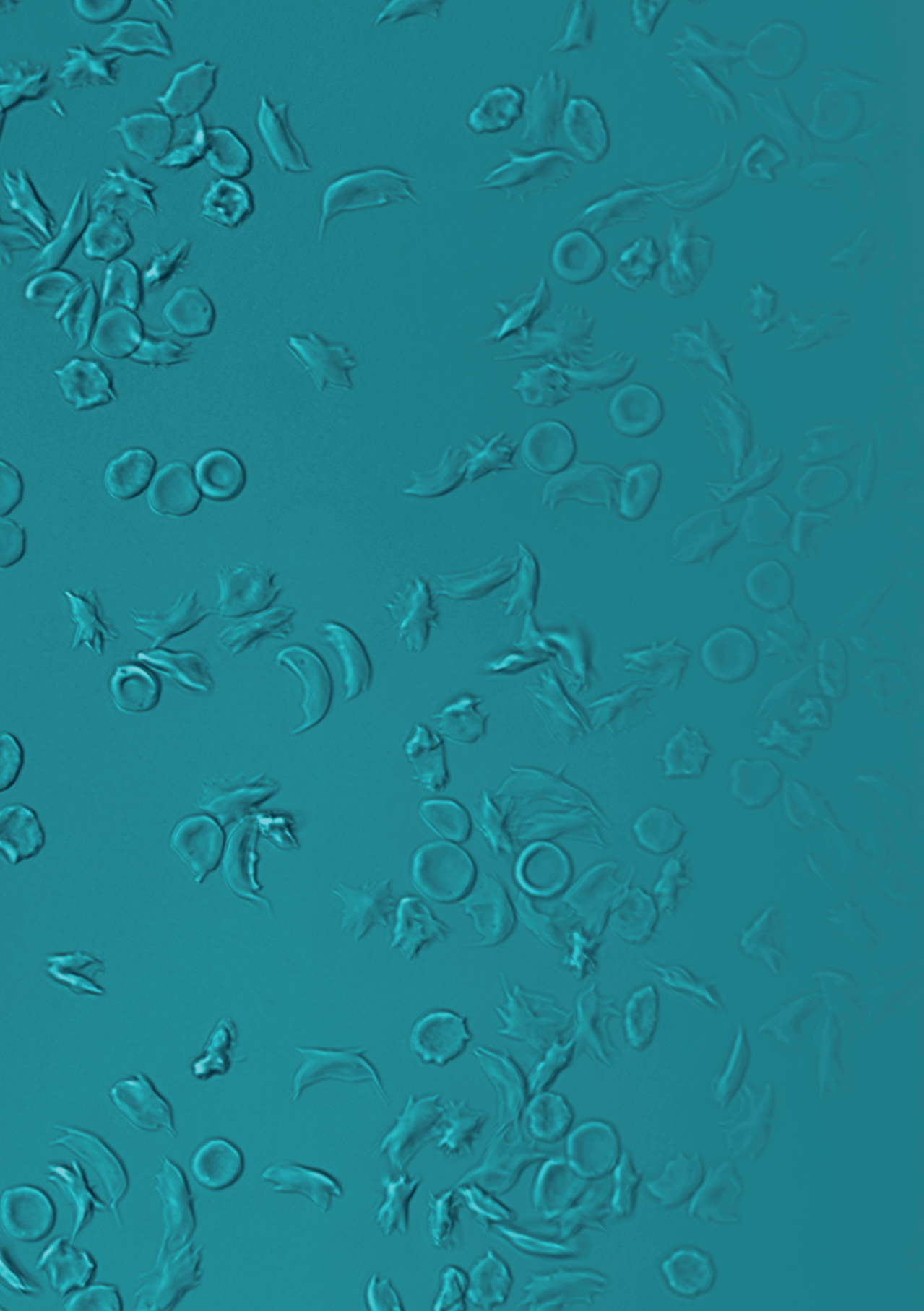
Novel biomarkers, such as the ones described in this thesis, that capture red cell function are necessary for diagnosis, management and treatment development in the field of HHA. Ideally these novel biomarkers are identified or developed in specialized expertise centers to enable clinical validation and implementation. It is time to reconsider disease categories and severity scores, as new understandings and innovative tools that measure red cell function are becoming increasingly important in red cell disorders. Assessing individual patients RBC characteristics in HHA, especially SCD, is needed, according to the principle of precision medicine, to improve patient care.

References

1. Kassebaum NJ, Jasrasaria R, Naghavi M, et al. A systematic analysis of global anemia burden from 1990 to 2010. *Blood J.* 2015;123(5):615-625.
2. van Straaten S, Biemond BJ, Kerkhoffs JL, Gitz-Francois J, van Wijk R, van Beers EJ. Iron overload in patients with rare hereditary hemolytic anemia: Evidence-based suggestion on whom and how to screen. *Am J Hematol.* 2018;93(11):E374-E376.
3. van Beers EJ, van Straaten S, Morton HD, et al. Prevalence and management of iron overload in pyruvate kinase deficiency: report from the Pyruvate Kinase Deficiency Natural History Study Pyruvate. *Haematologica.* 2019;104(e53).
4. Ataga KI. Hypercoagulability and thrombotic complications in hemolytic anemias. *Haematologica.* 2009;94(11):1481-1484. doi:10.3324/haematol.2009.013672
5. van Straaten S, Verhoeven J, Hagens S, et al. Organ involvement occurs in all forms of hereditary haemolytic anaemia. *Br J Haematol.* 2019;185(3):602-605.
6. Kato GJ, Piel FB, Reid CD, et al. Sickle cell disease. *Nat Rev Dis Prim.* 2018;4:1-22.
7. Piel, F.B., Steinberg, M.H., and Rees DC. Sickle Cell Disease. *N Engl J Med.* 2017;376(16):1561-1573.
8. Kalpatthi R, Novelli EM. Measuring success: Utility of biomarkers in sickle cell disease clinical trials and care. *Hematology.* 2018;2018(1):482-492. doi:10.1182/asheducation-2018.1.482
9. Liu Y, Zhong H, Bao W, et al. Patrolling monocytes scavenge endothelial-adherent sickle RBCs: A novel mechanism of inhibition of vaso-occlusion in SCD. *Blood.* 2019;134(7):579-590.
10. Manwani D, Frenette PS. Vaso-occlusion in sickle cell disease: pathophysiology and novel targeted therapies. *Blood.* 2013;122(24):3892-3898. doi:10.1182/asheducation-2013.1.362
11. Lemonne N, Lamarre Y, Romana M, Mukisi-mukaza, M; Hardy-Dessources, M.-D; Tarer, V; Mougenel, D; Waltz, Xavier; Tressieres, B; Lalanne-Mistrih, M.-L; Etienne-Julan, M; Connes P. Does increased red blood cell deformability raise the risk for osteonecrosis in sickle cell anemia? *Blood.* 2013;121(15):3054-3057.
12. Ballas, S K Larner, J Smith ED, Surrey S, Schwartz, E Rappaport EF. Rheologic predictors of the severity of the painful sickle cell crisis. *Blood.* 1988;72(4):1216-1223.
13. Lande WM, Andrews DL, Clark MR, et al. The Incidence of Painful Crisis in Homozygous Sickle Cell Disease: Correlation with Red Cell Deformability. *Blood.* 1988;72(6):2056-2059.
14. Connes P, Lamarre Y, Hardy-Dessources MD, et al. Decreased hematocrit-to-viscosity ratio and increased lactate dehydrogenase level in patients with sickle cell anemia and recurrent leg ulcers. *PLoS One.* 2013;8(11):6-10. doi:10.1371/journal.pone.0079680
15. Lamarre Y, Romana M, Lemonne N, et al. Alpha thalassemia protects sickle cell anemia patients from macro-albuminuria through its effects on red blood cell rheological properties. *Clin Hemorheol Microcirc.* 2014;57(1):63-72. doi:10.3233/CH-131772
16. Kato GJ, McGowan V, Machado RF, et al. Lactate dehydrogenase as a biomarker of hemolysis-associated nitric oxide resistance, priapism, leg ulceration, pulmonary hypertension, and death in patients with sickle cell disease. *Blood.* 2006;107(6):2279-2285. doi:10.1182/blood-2005-06-2373
17. Bernaudin F, Verlhac S, Chevret S, et al. G6PD deficiency, absence of α -thalassemia, and hemolytic rate at baseline are significant independent risk factors for abnormally high cerebral velocities in patients with sickle cell anemia. *Blood.* 2008;112(10):4314-4317.
18. Novelli EM, Hildesheim M, Rosano C, et al. Elevated pulse pressure is associated with hemolysis, proteinuria and chronic kidney disease in sickle cell disease. *PLoS One.* 2014;9(12):1-14. doi:10.1371/journal.pone.0114309
19. Ataga KI, Reid M, Ballas SK, et al. Improvements in haemolysis and indicators of erythrocyte survival do not correlate with acute vaso-occlusive crises in patients with sickle cell disease: A phase III randomized, placebo-controlled, double-blind study of the gardos channel blocker senicapoc. *Br J Haematol.* 2011;153(1):92-104.
20. Garadah TS, Jaradat AA, AlAlawi ME, Hassan AB, Sequeira RP. Pain frequency, severity and QT dispersion in adult patients with sickle cell anemia: Correlation with inflammatory markers. *J Blood Med.* 2016;7:255-261. doi:10.2147/JBM.S114585

21. Nader E, Romana M, Connes P. The Red Blood Cell—Inflammation Vicious Circle in Sickle Cell Disease. *Front Immunol.* 2020;11(March):1-11. doi:10.3389/fimmu.2020.00454
22. Li Q, Henry ER, Hofrichter J, et al. Kinetic assay shows that increasing red cell volume could be a treatment for sickle cell disease. *Proc Natl Acad Sci.* 2017;114(5):E689-E696.
23. van Beers EJ, Samsel L, Mendelsohn L, et al. Imaging flow cytometry for automated detection of hypoxia-induced erythrocyte shape change in sickle cell disease. *Am J Hematol.* 2014;89(6):598-603. doi:10.1002/ajh.23699
24. Vichinsky E, Hoppe CC, Ataga KI, et al. A Phase 3 randomized trial of voxelotor in sickle cell disease. *N Engl J Med.* 2019;381(6):509-519. doi:10.1056/NEJMoa1903212
25. Ataga KI, Kutlar A, Kanter J, et al. Crizanlizumab for the prevention of pain crises in sickle cell disease. *N Engl J Med.* 2017;376(5):429-439. doi:10.1056/NEJMoa1611770
26. Niihara Y, Miller ST, Kanter J, et al. A phase 3 trial of l-glutamine in sickle cell disease. *N Engl J Med.* 2018;379(3):226-235. doi:10.1056/NEJMoa1715971
27. Salinas Cisneros G, Thein SL. Recent Advances in the Treatment of Sickle Cell Disease. *Front Physiol.* 2020;11(May):1-15. doi:10.3389/fphys.2020.00435
28. Poletti V, Urbinati F, Charrier S, et al. Pre-clinical Development of a Lentiviral Vector Expressing the Anti-sickling β AS3 Globin for Gene Therapy for Sickle Cell Disease. *Mol Ther - Methods Clin Dev.* 2018;11(December):167-179. doi:10.1016/j.omtm.2018.10.014
29. Thompson AA, Walters MC, Mapara MY, et al. Resolution of Serious Vaso-Occlusive Pain Crises and Reduction in Patient-Reported Pain Intensity: Results from the Ongoing Phase 1/2 HGB-206 Group C Study of LentiGlobin for Sickle Cell Disease (bb1111) Gene Therapy. *Blood.* 2020;136(Supplement 1):16-17. doi:10.1182/blood-2020-134940
30. Masuda T, Wang X, Maeda M, et al. Gene regulation: Transcription factors LRF and BCL11A independently repress expression of fetal hemoglobin. *Science (80-).* 2016;351(6270):285-289. doi:10.1126/science.aad3312
31. Martyn GE, Wienert B, Yang L, et al. Natural regulatory mutations elevate the fetal globin gene via disruption of BCL11A or ZBTB7A binding. *Nat Genet.* 2018;50(4):498-503. doi:10.1038/s41588-018-0085-0
32. Antoniani C, Meneghini V, Lattanzi A, et al. Induction of fetal hemoglobin synthesis by CRISPR/Cas9-mediated editing of the human β -globin locus. *Blood.* 2018;131(17):1960-1973. doi:10.1182/blood-2017-10-811505
33. Stenger EO, Shenoy S, Krishnamurti L. How I treat sickle cell disease with hematopoietic cell transplantation. *Blood.* 2019;134(25):2249-2260. doi:10.1182/blood.2019000821
34. Smith TP, Schlenz AM, Schatz JC, Maitra R and, Sweitzer SM. Modulation of pain in pediatric sickle cell disease: understanding the balance between endothelin mediated vasoconstriction and apelin mediated vasodilation. *Blood Cells Mol Dis.* 2015;54(2):155-159.
35. Hofrichter J, Ross PD, Eaton WA. Kinetics and mechanism of deoxyhemoglobin S gelation: a new approach to understanding sickle cell disease. *Proc Natl Acad Sci U S A.* 1974;71(12):4864-4868. doi:10.1073/pnas.71.12.4864
36. Hamda C Ben, Sangeda R, Mwita L, et al. A common molecular signature of patients with sickle cell disease revealed by microarray meta-analysis and a genome-wide association study. *PLoS One.* 2018;13(7):1-21. doi:10.1371/journal.pone.0199461
37. Fitzhugh CD, Cordes S, Taylor T, et al. At least 20% donor myeloid chimerism is necessary to reverse the sickle phenotype after allogeneic HSCT. *Blood.* 2017;130(17):1946-1948. doi:10.1182/blood-2017-03-772392
38. John TD, Lu M, Kanne CK, et al. Rheological Assessments of Sickle Cell Patients Post Allogeneic Hematopoietic Cell Transplant. *Blood.* 2019;134(Supplement_1):996.
39. Rees DC, Williams TN, Gladwin MT. Sickle-cell disease. *Lancet.* 2010;376:2018-2031.
40. Nevitt S, Jones A, Howard J. Hydroxyurea (hydroxycarbamide) for sickle cell disease. *Cochrane Database Syst Rev.* 2017;4(4):CD002202.
41. Luchtman-Jones L, Pressel S, Hilliard L, et al. Effects of hydroxyurea treatment for patients with hemoglobin SC disease. *Am J Hematol.* 2016;91(2):238-242. doi:10.1002/ajh.24255
42. Lionnet, Francois; Hammoudi, Nadjib; Stankovic Stojanovic, Katja; Avellino, Virginie; Grateau, Gilles; Giro, Robert; Haymann J-P. Hemoglobin sickle cell disease complications : a clinical study of 179 cases. *Haematologica.* 2012;97(8):1136-1141.

43. Parrow NL, Violet P-C, Ajit George N, et al. Dietary Iron Restriction Improves Markers of Disease Severity in Murine Sickle Cell Anemia. *Blood*. Published online 2020.
44. Castro OL, Nouraei M, Luchtman-Jones L, et al. Lower Ferritin Concentrations Are Associated with Decreased Hemolysis in Sickle Cell Disease Children without Iron Overload. *Blood*. 2009;114(22):2571. doi:10.1182/blood.V114.22.2571.2571
45. Summirell CCG, Sheehan VA. Use of hydroxyurea and phlebotomy in pediatric patients with hemoglobin SC disease. *Exp Biol Med*. 2016;241(7):737-744. doi:10.1177/1535370216639737
46. Power-Hays A, McGann PT. When Actions Speak Louder Than Words — Racism and Sickle Cell Disease. *N Engl J Med*. 2020;383(20):1902-1903. doi:10.1056/nejmp2022125
47. Farooq F, Mogayzel PJ, Lanzkron S, Haywood C, Strouse JJ. Comparison of US Federal and Foundation Funding of Research for Sickle Cell Disease and Cystic Fibrosis and Factors Associated With Research Productivity. *JAMA Netw open*. 2020;3(3):e201737.
48. Grace RF, Rose C, Layton M, et al. Safety and Efficacy of Mitapivat in Pyruvate Kinase Deficiency. *N Engl J Med*. 2019;381(10):933-944. doi:10.1056/NEJMoa1902678
49. López Lorenzo JL, Navarro S, Shah AJ, et al. Lentiviral Mediated Gene Therapy for Pyruvate Kinase Deficiency: A Global Phase 1 Study for Adult and Pediatric Patients. *Blood*. 2020;136(Supplement 1):47. doi:10.1182/blood-2020-137246
50. Iolascon A, Andolfo I, Barcellini W, et al. Recommendations regarding splenectomy in hereditary hemolytic anemias. *Haematologica*. 2017;102(8):1304-1313.
51. Picard V, Guitton C, Thuret I, et al. Clinical and biological features in PIEZO1-hereditary xerocytosis and gardos channelopathy: A retrospective series of 126 patients. *Haematologica*. 2019;104(8):1554-1564. doi:10.3324/haematol.2018.205328
52. Brugnara C. Erythrocyte membrane transport physiology. *Curr Opin Hematol*. 1997;4(2):122-127.
53. Klei TRL, Dalimot JJ, Beuger BM, et al. The Gardos effect drives erythrocyte senescence and leads to Lu / BCAM and CD44 adhesion molecule activation. *Blood Adv*. 2020;4(24).
54. Thomsen RW, Schoonen WM, Farkas DK, Riis A, Fryzek JP, Sørensen HT. Risk of venous thromboembolism in splenectomized patients compared with the general population and appendectomized patients: A 10-year nationwide cohort study. *J Thromb Haemost*. 2010;8(6):1413-1416.
55. Huisjes R, Solinge WW, Levin MD, Wijk R, Riedl JA. Digital microscopy as a screening tool for the diagnosis of hereditary hemolytic anemia. *Int J Lab Hematol*. 2017;40(2):159-168.
56. Romero LO, Massey AE, Mata-Daboin AD, et al. Dietary fatty acids fine-tune Piezo1 mechanical response. *Nat Commun*. 2019;10(1):1-14. doi:10.1038/s41467-019-09055-7
57. Rapetti-Mauss R, Soriani O, Vinti H, Badens C, Guizouarn H. Senicapoc: A potent candidate for the treatment of a subset of hereditary xerocytosis caused by mutations in the gardos channel. *Haematologica*. 2016;101(11):e431-e435. doi:10.3324/haematol.2016.149104
58. Jensen RFG, Dziegiel MH, Rieneck K, Birgens H, Glenthøj A. Erythrocytapheresis as a novel treatment option for adult patients with pyruvate kinase deficiency. *Haematologica*. 2020;105(7):e373-e375.



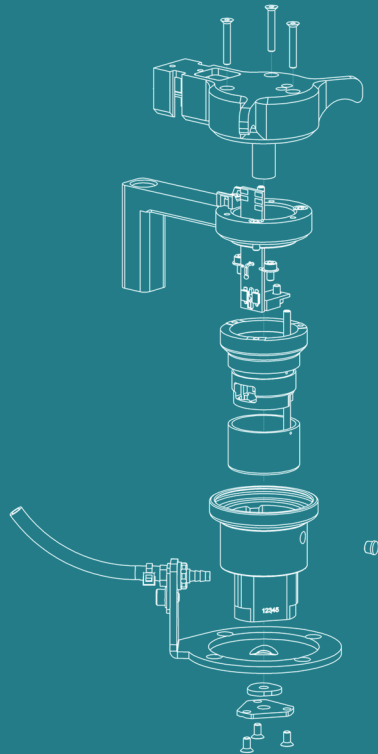
Appendices

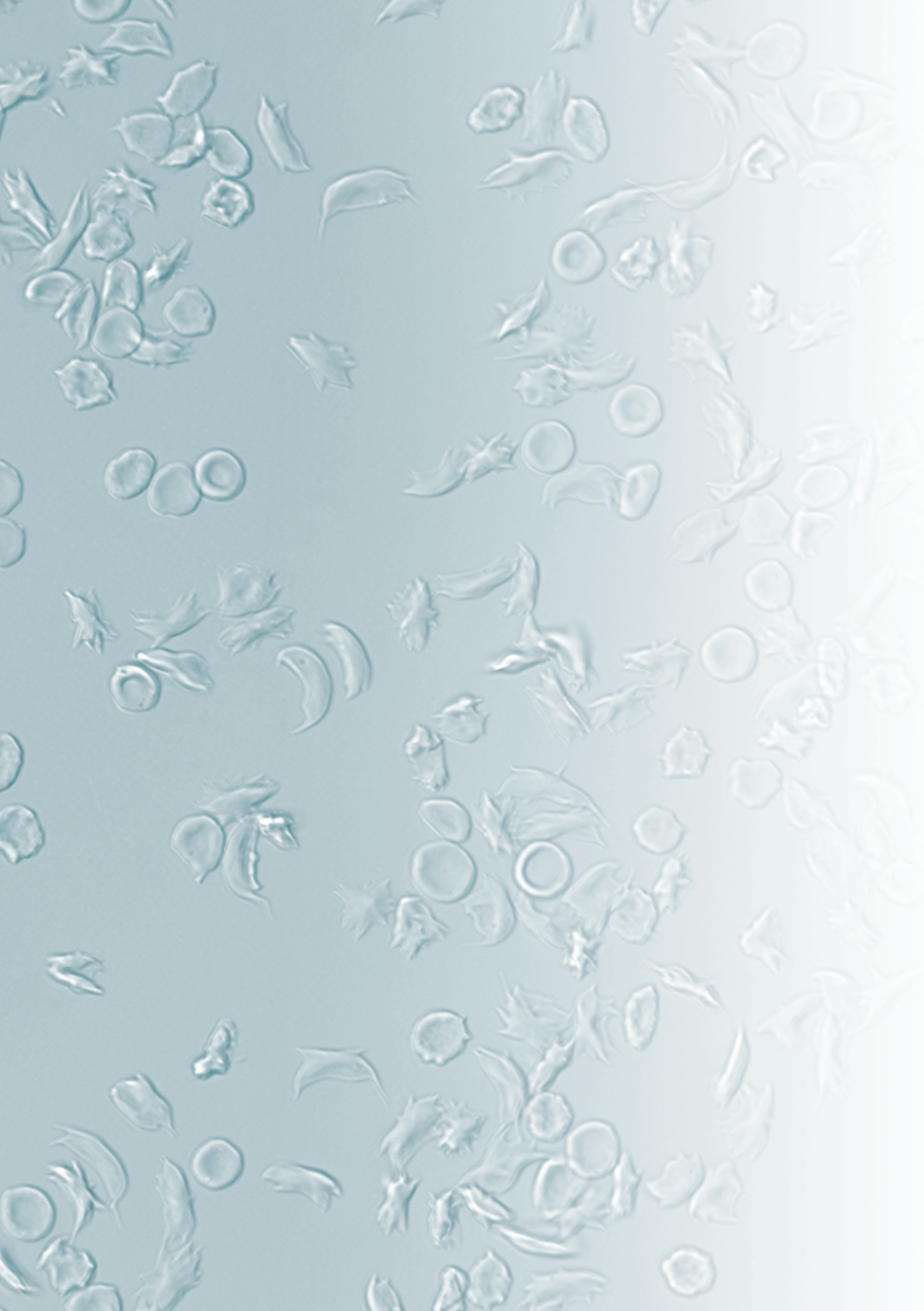
Nederlandse samenvatting (Dutch summary)

List of publications

Dankwoord (acknowledgements)

Curriculum Vitae





Nederlandse samenvatting (Dutch summary)

Dit proefschrift beschrijft hoe verschillende karakteristieken van de rode bloedcel kunnen worden gebruikt als marker van ziekte-ernst bij verschillende soorten erfelijke hemolytische anemie. De belangrijkste functie van de rode bloedcel is het transporteren van zuurstof vanuit de longen naar de verschillende weefsels in het lichaam. De vervormbaarheid van de rode bloedcel is hiervoor cruciaal aangezien de diameter van de kleinste bloedvaten kleiner is dan die van de rode bloedcel zelf. Vervormbaarheid van rode bloedcellen kan worden gemeten en gekwantificeerd door middel van ektacytometrie. Om te kunnen vervormen en zuurstof transport te bewerkstelligen is energie nodig. Voor energie is de rode bloedcel afhankelijk van de glycolyse, het metabole systeem waarin het enzym pyruvaatkinase een belangrijke rol speelt.

Pyruvaatkinase deficiëntie

Wanneer het enzym pyruvaatkinase niet goed werkt als gevolg van een mutatie in het gen dat codeert voor het pyruvaatkinase eiwit spreekt men van pyruvaatkinase-deficiëntie (PKD). Patiënten met PKD hebben voornamelijk klachten als gevolg van bloedarmoede die zodanig ernstig kan zijn dat frequente bloedtransfusies noodzakelijk zijn. Behoudens deze bloedtransfusies en andere ondersteunende maatregelen, is er op dit moment geen voor de patiënt beschikbare behandeling die deze aandoening geneest. Wel wordt er in klinische studies gekeken naar mogelijke nieuwe behandelingen zoals gentherapie en medicijnen die het enzym pyruvaatkinase activeren.

Sikkelcelziekte

Sikkelcelziekte is een andere, relatief veel voorkomende ernstige erfelijke aandoening van de rode bloedcel. Een enkele puntmutatie in het gen dat codeert voor bèta-globine zorgt ervoor dat patiënten een afwijkend hemoglobine maken (HbS). Deze vorm van hemoglobine heeft de karakteristieke eigenschap dat het onoplosbaar wordt bij lage zuurstofspanning, waardoor rode bloedcellen gaan 'sikkelen' en slecht vervormbaar worden. Hierdoor treedt onder andere intravasale hemolyse op en kunnen bloedvaten acuut verstopt raken, hetgeen zorgt voor pijnlijke crisis. Naast deze pijnlijke crisis die ontstaat door occlusie van bloedvaten in de botten, kan dit ook optreden in de longen, wat resulteert in het potentieel fatale 'acute chest syndroom', of in de hersenen waardoor een herseninfarct ontstaat. Andere orgaansystemen zoals nieren, ogen, de milt en lever kunnen eveneens zijn aangedaan. Er zijn in Nederland 2 geregistreerde behandelingen voor sikkelcelziekte: bloedtransfusie en hydroxyurea, een medicijn dat het sikkelen vermindert en inflammatie lijkt te doen afnemen. In de Verenigde Staten zijn inmiddels 2 nieuwe medicijnen beschikbaar naast hydroxyurea en bloedtransfusie. Er zijn echter vele nieuwe behandelstrategieën in ontwikkeling voor deze ernstige aandoening.

Erfelijke sferocytose

Erfelijke sferocytose kenmerkt zich ook door een hemolytische bloedarmoede. Bij deze aandoening wordt dit veroorzaakt door een mutatie in het gen dat codeert voor een van de eiwitten die het membraan van de rode bloedcel stabiliseren. Mutaties in deze

membraaneiwitten resulteren in membraaninstabiliteit, hetgeen leidt tot de vorming van bolvormige en daardoor slecht vervormbare rode bloedcellen ('sferocyten'), die ook als zodanig met behulp van de microscoop te herkennen zijn.

Een belangrijke behandeling van erfelijke sferocytose is het verwijderen van de milt. In de milt worden verouderde rode bloedcellen afgebroken, en bij sferocytose is dit proces versneld vanwege de afwijkende vervormbaarheid en vorm van de rode bloedcel.

Erfelijke xerocytose

Deze erfelijke rode bloedcel aandoening wordt gekenmerkt door gedehydrateerde rode bloedcellen als gevolg van een mutatie in de genen die de vochtbalans van de rode cel controleren. De meest voorkomende mutaties betreffen mutaties in de 2 genen (*PIEZO1* en *KCNN4*) die coderen voor kanalen die zich in het membraan van de rode bloedcel bevinden. De vervormbaarheid van deze rode bloedcellen die ernstig gedehydrateerd (uitgedroogd) zijn is afgenomen waardoor ze ook sneller worden afgebroken in de milt. Om dit verlies aan rode bloedcellen te compenseren worden vanuit het beenmerg veel nieuwe rode bloedcellen gemaakt en zijn er veel jonge rode bloedcellen (reticulocyten) in het bloed aanwezig. Patiënten met erfelijke xerocytose kunnen zich presenteren met bloedarmoede, echter vaak komt deze aandoening aan het licht vanwege de vaak voorkomende ijzerstapeling. Behandeling voor deze aandoening is beperkt tot bloedtransfusie indien er sprake is van ernstige anemie en aderlaten om ijzerstapeling te voorkomen.

In dit proefschrift wordt de vervormbaarheid van de rode bloedcel als mogelijke marker voor ziekte ernst en respons op therapie bij bovenstaande aandoeningen beschreven. Ook wordt gekeken naar de activiteit en stabiliteit van het enzym pyruvaatkinase bij bovengenoemde rode bloedcelaandoeningen.

In *Deel 1* van dit proefschrift wordt de techniek en eerste validatie van zuurstofgradiënt ektacytometrie (oxygenscan) beschreven. Zuurstofgradiënt ektacytometrie meet de vervormbaarheid van rode bloedcellen tijdens afnemende zuurstofspanning. In tegenstelling tot rode bloedcellen van gezonde mensen zullen rode bloedcellen van mensen met sikkelcelziekte bij verlaging van de zuurstofspanning hun vervormbaarheid verliezen, oftewel sikkelen, als gevolg van het afwijkende hemoglobine S. De precieze zuurstofspanning waarop de rode bloedcellen gaan sikkelen ('Point of Sickling', PoS) kan nu voor het eerst gemeten en heel precies gekwantificeerd worden met zuurstofgradiënt-ektacytometrie. Hoe deze test precies werkt wordt uitgelegd in **hoofdstuk 2**.

Daarnaast wordt het effect van pH, temperatuur, percentage afwijkend hemoglobine S, 2,3-DPG (een glycolytisch tussenproduct), en osmolariteit op de parameters van zuurstofgradiënt-ektacytometrie, zoals het Punt van sikkelen, onderzocht. **Hoofdstuk 3** is naast een geschreven artikel ook een video artikel waarin heel precies wordt beschreven en gevisualiseerd hoe de test uitgevoerd moet worden. In **hoofdstuk 4** wordt aan de hand van een aantal voorbeelden beschreven hoe belangrijk het is om goed te standaardiseren. Aangezien zuurstofgradiënt-ektacytometrie een gevoelige techniek is, kan het standaardiseren, bijvoorbeeld dat er altijd dezelfde hoeveelheid rode bloedcellen worden gebruikt, bijdragen aan beter reproduceerbare en daardoor meer betrouwbare metingen.

In *Deel II* wordt zuurstofgradiënt-ektacytometrie verder gevalideerd in relatie tot complicaties van patiënten met sikkelcelziekte. Daarnaast wordt de nieuwe techniek als uitkomstmaat gebruikt bij het testen van bestaande en nieuwe therapieën.

Hoofdstuk 5 beschrijft hoe parameters zoals PoS geassocieerd is met het optreden van een crise in het verleden. Daarnaast blijkt dat de PoS en de andere parameters goed het effect van bestaande behandelingen als hydroxyurea en bloedtransfusie op de rode bloedcellen kan laten zien en op die manier goed de effectiviteit van therapie kan meten. In **hoofdstuk 6** wordt de techniek verder klinisch gevalideerd door onderzoek in grotere cohorten van zowel kinderen als volwassenen met sikkelcelziekte. Belangrijke uitkomsten zijn dat er een associatie is tussen een hoger Punt van sikkelen, dus een hogere zuurstofspanning waarbij de rode bloedcellen gaan sikkelen, en in het verleden opgetreden ernstige complicaties zoals een herseninfarct, acute chest syndroom en pijnlijke crise. Dit geeft aan dat de PoS is geassocieerd met ziekte-ernst.

Hoofdstuk 7 beschrijft een casus van een tweeling met sikkelcelziekte waarbij zuurstofgradiënt-ektacytometrie metingen zijn gedaan vlak voor en tijdens behandeling met hydroxyurea. Met behulp van de zuurstofgradiënt-ektacytometrie werd snel duidelijk dat een niet optimale dosis hydroxyurea werd gegeven aan de kinderen. Dit kwam doordat de zuurstofscan in bij beide kinderen drastisch was verslechterd ondanks goede inname van het medicijn, wat tot gevolg had dat de dosering werd opgehoogd nadat bleek dat de kinderen flink in gewicht waren toegenomen. Dit is een voorbeeld hoe de zuurstofscan kan helpen om de optimale dosering van hydroxyurea te bepalen.

In **hoofdstuk 8** wordt een tot dusverre onbegrepen metabole afwijking in rode bloedcellen van patiënten met sikkelcelziekte beschreven, namelijk een verhoging van de hoeveelheid 2,3-DPG. Deze verhoging van 2,3-DPG lijkt het gevolg te zijn van een tekort aan pyruvaatkinase activiteit. De verhoogde hoeveelheid 2,3-DPG is ongunstig omdat daardoor de zuurstofaffiniteit van hemoglobine wordt verlaagd, hetgeen het sikkelen bevordert. Deze studie laat zien dat het pyruvaatkinase van patiënten met sikkelcelziekte kan worden geactiveerd met behulp van een kleine moleculaire activator: mitapivat. Ex vivo behandeling van de rode bloedcellen van patiënten met sikkelcelziekte met deze activator verhoogt de pyruvaatkinase-activiteit, verlaagt de hoeveelheid 2,3-DPG, verhoogt de zuurstofaffiniteit van hemoglobine, en vermindert daarmee uiteindelijk het sikkelen van rode bloedcellen, gemeten met zuurstof-gradiënt ektacytometrie.

In **hoofdstuk 9** worden de verschillen tussen 2 subtypes van sikkelcelziekte op het gebied van verschillende soorten ektacytometrie, inclusief zuurstofgradiënt-ektacytometrie, naast andere laboratoriumtesten zoals viscositeit van het bloed beschreven. In de meest voorkomende vorm van sikkelcelziekte, HbSS oftewel homozygote sikkelcelziekte, is de PoS een belangrijke marker van ziekte-ernst. Echter bij een samengesteld heterozygote vorm van sikkelcelziekte, waarbij het hemoglobine SC wordt gemaakt, is juist de viscositeit van het bloed een belangrijke marker van ziekte-ernst. Verschillen betreft rode bloedcel karakteristieken tussen HbSS en HbSC zijn belangrijk aangezien dit implicaties kan hebben voor de behandeling.

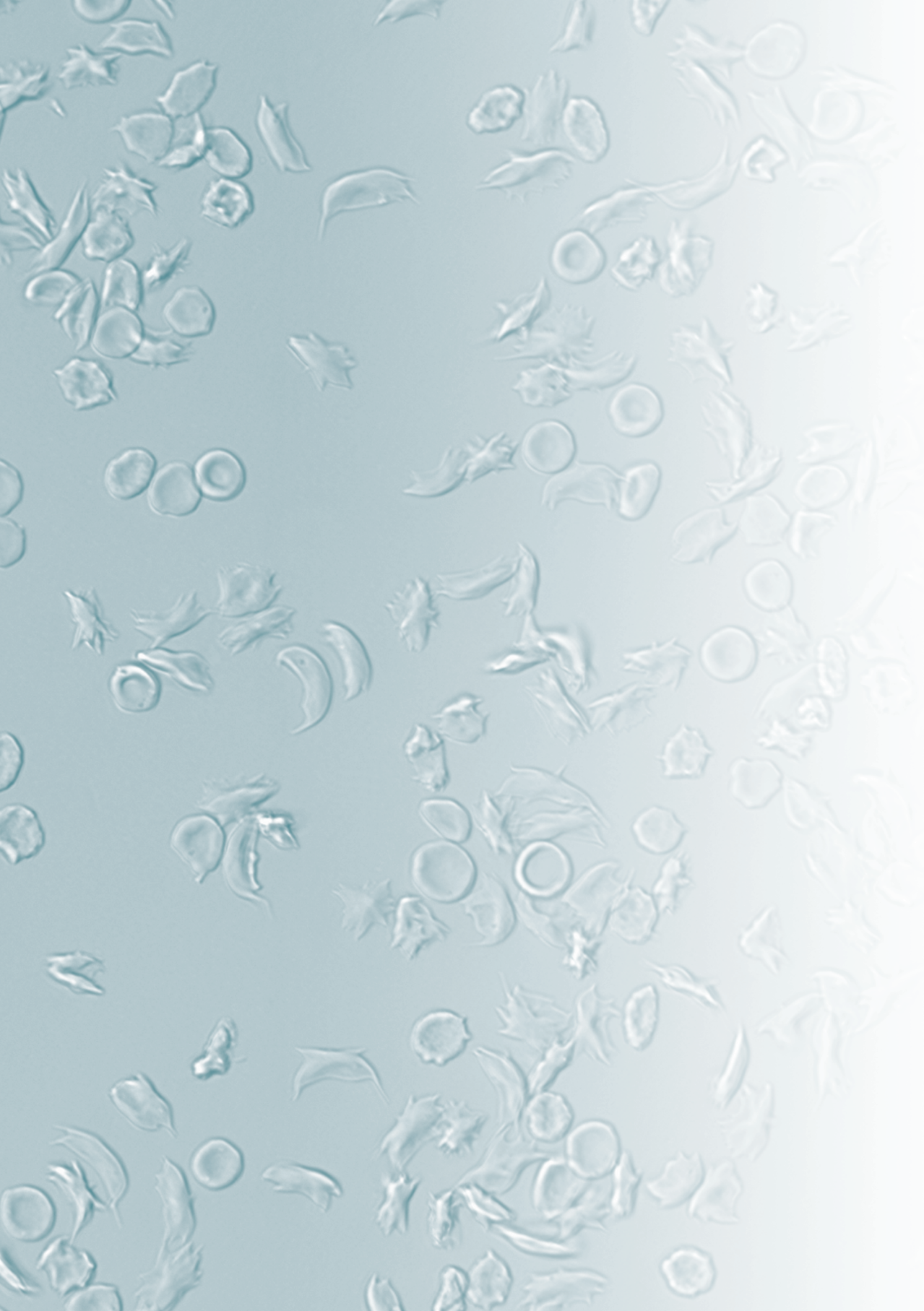
In *Deel III* worden andere toepassingen van ektacytometrie beschreven, en de relatie van vervormbaarheid tot de activiteit en stabiliteit van het enzym pyruvaatkinase.

Hoofdstuk 10 beschrijft de verschillende karakteristieken van het enzym pyruvaatkinase bij patiënten met PKD. Ex vivo behandeling rode bloedcellen van deze patiëntengroep met mitapivat resulteert in een toename aan activiteit en stabiliteit van pyruvaatkinase. Deze bevindingen geven aan dat mitapivat potentie heeft als behandeling van PKD.

In **hoofdstuk 11** wordt met de nieuw ontwikkelde cel membraan stabiliteit test (CMST) onderzocht wat het effect is van miltectomie bij erfelijke sferocytose. De CMST is een ektacytometrie test waarbij de stabiliteit van het celmembraan in kaart wordt gebracht. In dit hoofdstuk wordt beschreven dat de stabiliteit van het rode celmembraan is verbeterd na miltectomie en dat het gedrag van de rode bloedcellen tijdens de CMST meer lijkt op dat van gezonde rode bloedcellen.

Hoofdstuk 12 laat de verschillen zien tussen de 2 soorten erfelijke xerocytose (PIEZO1 en KCNN4). Naast verschillen in vervormbaarheid van de rode bloedcellen, gemeten met ektacytometrie, is er ook sprake van een verschil in activiteit en stabiliteit van het enzym pyruvaatkinase. Een belangrijk aspect van met name de PIEZO1 vorm van xerocytose is dat de dehydratie geassocieerd lijkt te zijn met de afname van activiteit en stabiliteit van pyruvaatkinase.

De bevindingen die in dit proefschrift zijn beschreven laten zien dat ektacytometrie, en in het bijzonder zuurstofgradiënt-ektacytometrie, potentie heeft als marker van effectiviteit van therapie en mogelijk ook ziekte-ernst in sikkelcelziekte. Biomarkers die rode bloed cel karakteristieken weergeven zijn belangrijk in de diagnose, behandeling en prognose van zeldzame erfelijke anemieën. Deze markers bieden de mogelijkheid om een behandeling op maat te kunnen geven aan patiënten met een erfelijke rode bloedcel aandoening.



LIST OF PUBLICATIONS

This thesis

Rab M.A.E., Kanne C.K, Boisson C, Bos J, van Oirschot B.A, Houwing M.E, Renoux C, Bartels M, Nur E, Cnossen M.H, Joly P, Fort R, Connes P, van Wijk R, Sheehan V.A, and van Beers E.J. *Oxygen gradient ektacytometry-derived biomarkers are associated with the occurrence of cerebral infarction, acute chest syndrome and vaso-occlusive crisis in sickle cell disease.* (Submitted)

Houwing, M.E., Bos, J., Teuben, S.A.M.C., Schutgens, R.E.G., van Wijk, R., van Beers, E.J., Cnossen, M.H., and Rab, M.A.E. *Use of the oxygen gradient ektacytometry in the titration of hydroxyurea dosing in children with sickle cell disease.* (Submitted)

Rab M.A.E., Bos J, van Oirschot B.A, van Straaten S, Kosinski P.A, Chubukov V, Kim H, Mangus H, Schutgens R.E.G, Pasterkamp G, Dang L, Kung C, van Beers E.J, van Wijk R. *Decreased activity and stability of pyruvate kinase in sickle cell disease: a novel target for therapy by mitapivat.* **Blood** 2021 May 27;137(21):2997-3001

Berrevoets M.B, Bos J, Huisjes R, Merckx T.H, van Solinge W.W, Riedl J, van Herwaarden M.Y.A, van Beers E.J, Bartels M, van Wijk R, and Rab M.A.E. *Ektacytometry analysis of post-splenectomy red blood cell properties identifies Cell membrane Stability Test as a novel biomarker of membrane health in hereditary spherocytosis.* **Frontiers in Physiology** 2021 Mar 25;12:641384

Rab M.A.E., Kanne C.K, Bos J, Boisson C, Houwing M.E, Gerritsma J, Teske E, Renoux C, Riedl J, Schutgens R.E.G, Bartels M, Nur E, Joly P, Fort R, Cnossen M.H, van Wijk R, Connes P, van Beers E.J, and Sheehan V.A. *Oxygen gradient ektacytometry derived-biomarkers are associated with vaso-occlusive crises and correlate with treatment response in sickle cell disease.* **American Journal of Hematology** 2021 Jan;96(1):E29-E32

Rab M.A.E., van Oirschot B.A, Kosinski P.A Hixon J, Johnson K., Chubukov V, Dang L, Pasterkamp G, van Straaten, S, van Solinge, W.W, van Beers, E.J, Kung, C, van Wijk, R. *AG-348 (Mitapivat), an allosteric activator of red cell pyruvate kinase, increases enzymatic activity, protein stability and ATP levels over a broad range of PKLR genotypes.* **Haematologica** 2021 Jan 1;106(1):238-249

Rab M.A.E., Kanne C.K, Boisson C, Boisson, C, van Oirschot, B.A, Nader E, Renoux, C, Joly P, Fort R, van Beers, E.J, Sheehan V.A, van Wijk, R, Connes, P. *Methodological aspects of the oxygenscan in sickle cell disease: a need for standardization.* **American Journal of Hematology** 2020 Jan;95(1):E5-E8.

Rab M.A.E., van Oirschot, B.A, Bos J Kanne C.K, Sheehan V.A, van Beers E.J, van Wijk R. *Characterization of sickling during controlled automated deoxygenation with oxygen gradient ektacytometry: the oxygenscan.* **J. Vis. Exp.** 2019; nov 5; (153)

Rab M.A.E. van Oirschot, B.A, Bos J, Merckx T.H, van Wesel A.C.W, Abdulmalik O, Safo M.K, Versluijs A.B, Houwing M.E, Cnossen M.H, Riedl J, Schutgens R.E.G, Pasterkamp G, Bartels M, van Beers E.J, van Wijk R. *Rapid and reproducible characterization of sickling during automated deoxygenation in sickle cell disease patients.* **American Journal of Hematology** 2019; May;94(5):575-584

Other publications

van Dooijeweert B, Broeks M.H, Verhoeven-Duif N.M, van Solinge W.W, van Beers E.J, Rab M.A.E, Nieuwenhuis E.E.S, Jans J.J.M, Bartels M, van Wijk R. *Metabolic fingerprint in hereditary spherocytosis correlates with red blood cell characteristics and clinical severity* **Hemasphere**. 2021 Jun 12;5(7):e591.

Boisson C, Rab M.A.E, Nader E, Renoux C, Kanne C, Bos J, van Oirschot B.A, Joly P, Fort R, Gauthier A, Stauffer E, Poutrel S, Kebaili K, Cannas G., Garnier N, Renard C, Hequet O, Hot A, Bertrand Y, van Wijk R, Sheehan V.A, van Beers E.J, and Connes P. *Effects of genotypes, treatment and acute complications in sickle cell disease on oxygenscan parameters.* **Cells** 2021 Apr 5;10(4):811

Cloos A-S, Hussen-Daenen L.G.M, Maja M, Stommen A, Vanderroost J, van der Smissen P, Rab M, Westerink J, Mignolet E, Larondelle Y, Terrasi R, Muccioli G, Dumitru A, Alsteens D, van Wijk R, Tyteca D. *Acantocytes in hypobetalipoproteinemia exhibit impaired cytoskeletal and membrane biophysical properties and results from maturation defect – a case study.* **Frontiers in Physiology** 2021 Feb 23;12:638027

Aglialoro F, Abay A, Yagci N, Rab M.A.E, Kaestner L, van Wijk R, von Lindern M, and van den Akker E. *Mechanical stress mediated Ca²⁺ induced signal transduction in erythroblasts modulates erythropoiesis.* **International Journal of Molecular Sciences** 2021 Jan 19;22(2):955

Boisson C, Rab M.A.E, Nader E, Renoux C, van Oirschot B.A, Joly P, Fort R, Stauffer E, van Beers E.J, Sheehan V.A, van Wijk R, and Connes, P. *Methodological aspects of oxygen gradient ektacytometry in sickle cell disease: effects of sample storage on outcome parameters in distinct patient subgroups.* **Clinical Hemorheology and Microcirculation**. 2021;77(4):391-394

Van Dijk M.J, Rab M.A.E, van Wijk R, Schols S.E.M, Biemond B.J, Rijneveld A.W, Nur E, Kerkhoffs J.L, van Beers, E.J. *Pyruvaatkinase-activatie door mitapivat (AG-348) in sikkelcelziekte: de ESTIMATE-studie.* **Nederlands Tijdschrift voor Hematologie** 2020 17: 310-312

Moura P.L, Dobbe J.G.G, Streekstra G.J, Rab M.A.E, Veldthuis M, Fermo E, van Wijk R, van Zwieten R, Bianchi P, Toye A.M, Satchwell T.J. *Rapid diagnosis of hereditary haemolytic anaemias using automated rheoscopy and supervised machine learning.* **British Journal Haematology** 2020 Aug;190(4):e250-e255

Lu M, Rab M.A.E., Shevkopyas S.S, Sheehan, V.A. *Blood rheology biomarkers in sickle cell disease*. **Exp Biol Med (Maywood)** 2020 Jan;245(2):155-165

Moura P.L, Hawley B.R, Dobbe J.G.G, Streekstra G.J, Rab M.A.E., Bianchi P, van Wijk R, Toyé A.M, Satchwell T.J. *PIEZO1 gain-of-function mutations delay reticulocyte maturation in hereditary xerocytosis*. **Haematologica** 2020 Jun;105(6):e268-e271.

Huisjes R, Makhro A, Llaudet-Planas E, Hertz L, Petkova-Kirova P, Verhagen L.P, Pignatelli S, Rab M.A.E., Schiffelers R.M, Seiler E, van Solinge W.W, Vives Corróns J.L, Mañú-Pereira M, Kaestner L, Bogdanova A, van Wijk R. *Density, heterogeneity and deformability of red cells as markers of clinical severity in hereditary spherocytosis*. **Haematologica** 2020 Jan 31;105(2):338-347

Rab M.A.E., Meerveld-Eggink A, van Velzen-Blad H, van Loon D, Rijkers G.T. and de Weerdt O. *Persistent changes in circulating white blood cells after splenectomy*. **International Journal of Hematology** 2018;107(2):157-165

Textbook chapters

Rab M.A.E. and van Wijk, R. *Enzymes of the red blood cell*. In: **Tietz Textbook of Laboratory Medicine**. 7th edition, edited by Rifai N, Chiu R.W.K., Young I., Burnham C.D., and Wittwer C.T. (in press, publication date February 2022)

Rab M.A.E. and Rijkers, G.T. *Antibody response to pneumococcal polysaccharide vaccination in patients treated with biologicals*. In book: **Pneumococcal Conjugate Vaccines**. 2012. DOI.10.2217/ebo.12.6

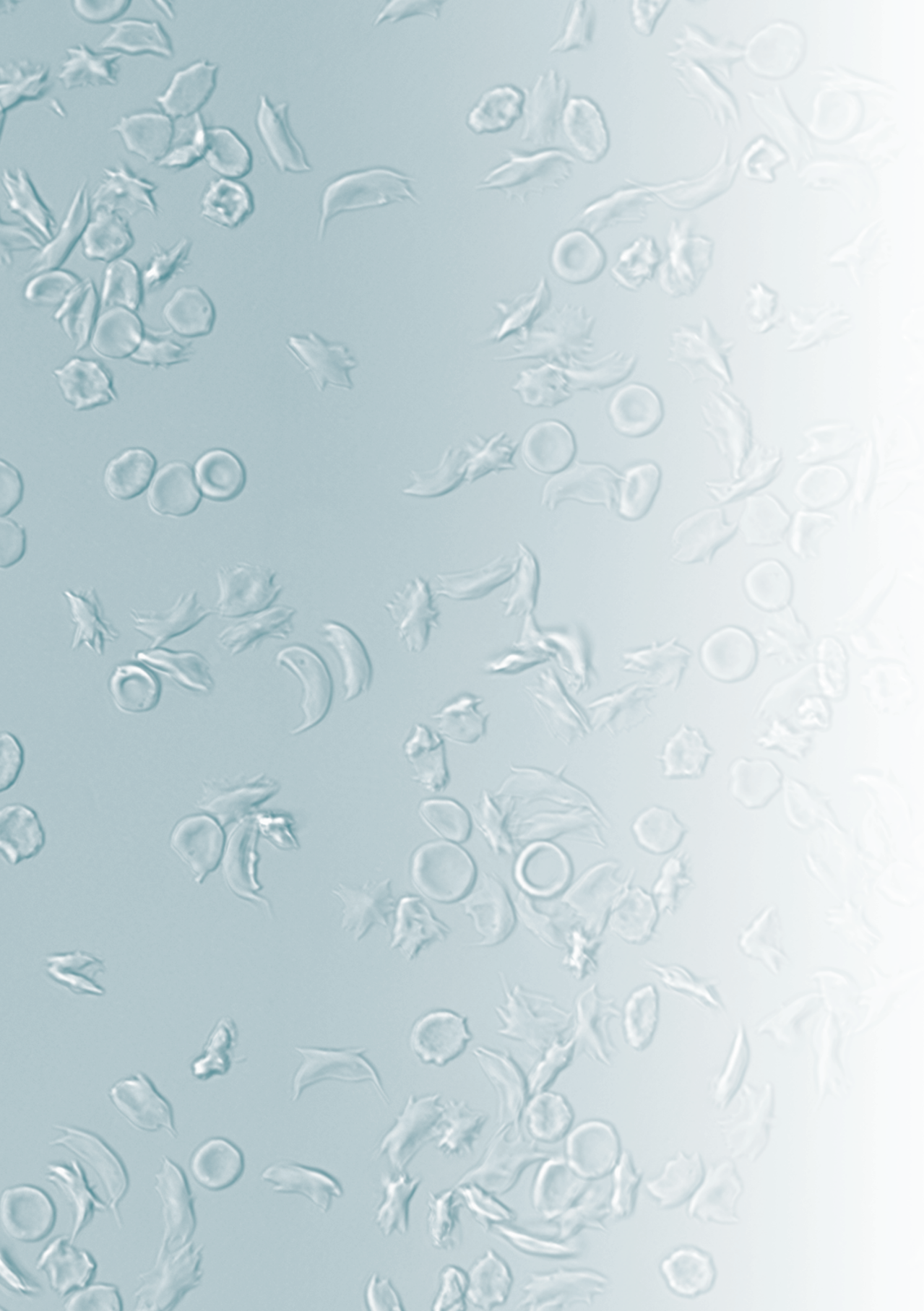
Awards

- 2020 **ASH Abstract Achievement Award**, 62th ASH Annual Meeting and Exposition, virtual edition.
- 2019 **ASH Abstract Achievement Award**, 61th ASH Annual Meeting and Exposition in Orlando, Florida, USA.
- 2019 **EHA Travel grant**, EHA-SWG Scientific Meeting on Red Cell and Iron Metabolism Defects: From basic science to clinical case application. Madrid, Spain.
- 2019 **EHA Travel grant**, 24th Congress of the European Hematology Association, Amsterdam, The Netherlands
- 2019 **Trainee Travel Award**, ISLH, 32th International Symposium on Technical Innovations in Laboratory Hematology in Vancouver, Canada
- 2018 **ASH Abstract Achievement Award**, 60th ASH Annual Meeting and Exposition in San Diego, California, USA.
- 2018 **EHA Travel grant**, 23rd Congress of the European Hematology Association, Stockholm, Sweden

Oral & Poster presentations

- 2020 **Poster presentation**, 62th ASH Annual Meeting and Exposition (virtual): “Oxygen gradient ektacytometry-derived biomarkers are associated with the occurrence of cerebral infarction, acute chest syndrome and vaso-occlusive crisis in sickle cell disease”.
- 2020 **Poster presentation**, 62th ASH Annual Meeting and Exposition (virtual): “Secondary Deficiency of Pyruvate Kinase and Altered Red Cell Metabolism in Hereditary Xerocytosis Caused By PIEZO1 and KCNN4 Defects”.
- 2020 **Oral presentation**, Annual Sickle Cell Disease and Thalassemia conference (ASCAT), virtual: “Oxygen gradient ektacytometry-derived biomarkers are associated with the occurrence of cerebral infarction, acute chest syndrome and vaso-occlusive crisis in sickle cell disease”.
- 2020 **Oral presentation**, 23rd European Red Cell Society Meeting, virtual meeting: “Decreased activity and stability of red cell pyruvate kinase in sickle cell disease: a potential target for therapy by AG-348 (Mitapivat), an allosteric activator of pyruvate kinase”.
- 2020 **Poster presentation**, 25th Congress of the European Hematology Association, virtual meeting. “Secondary Deficiency of Pyruvate Kinase and Altered Red Cell Metabolism in Hereditary Xerocytosis Caused By PIEZO1 and KCNN4 Defects”.
- 2020 **Oral presentation**, 14th Dutch Hematology Congress, Papendal, The Netherlands: “The Oxygenscan Provides Clinically Relevant Biomarkers for Treatment Efficacy That Are Associated with Frequency of Vaso-Occlusive Crisis in Sickle Cell Disease”.
- 2020 **Oral presentation**, 14th Dutch Hematology Congress, Papendal, The Netherlands: “Decreased Activity and Stability of Pyruvate Kinase in Hereditary Hemolytic Anemia: A Potential Target for Therapy By AG-348 (Mitapivat), an Allosteric Activator of Red Blood Cell Pyruvate Kinase”.
- 2019 **Poster presentation**, 61th ASH Annual Meeting and Exposition in Orlando, Florida, USA: “The Oxygenscan Provides Clinically Relevant Biomarkers for Treatment Efficacy That Are Associated with Frequency of Vaso-Occlusive Crisis in Sickle Cell Disease”.
- 2019 **Poster presentation**, 61th ASH Annual Meeting and Exposition in Orlando, Florida, USA: “Decreased Activity and Stability of Pyruvate Kinase in Hereditary Hemolytic Anemia: A Potential Target for Therapy By AG-348 (Mitapivat), an Allosteric Activator of Red Blood Cell Pyruvate Kinase”.
- 2019 **Oral presentation**, EHA-SWG Scientific Meeting on Red Cell and Iron Metabolism Defects, Madrid, Spain: “Co-inheritance of hereditary spherocytosis aggravates sickling in a patient with hemoglobin S trait”.
- 2019 **Oral presentation**, EHA-SWG Scientific Meeting on Red Cell and Iron Metabolism Defects, Madrid, Spain: “Characterization of red blood cell functional properties in a patient with sitosterolemia due to homozygosity for the c.361C>T p.(Arg121*) nonsense mutation in ABCG8”.
- 2019 **Poster presentation**, 24th Congress of the European Hematology Association, Amsterdam, The Netherlands: “Decreased activity and stability of pyruvate kinase in sickle cell disease and thalassemia: a potential target for therapy”

- 2019 **Poster presentation.** 24th Congress of the European Hematology Association, Amsterdam, The Netherlands: "The oxygenscan: a comprehensible functional red blood cell test to monitor treatment efficacy in patients with sickle cell disease"
- 2019 **Poster presentation.** 32nd International Symposium on Technical Innovations in Laboratory Hematology in Vancouver, Canada: "The oxygenscan: rapid and reproducible characterization of sickling during automated deoxygenation in sickle cell disease patients".
- 2019 **Oral presentation.** 22nd European Red Cell Society Meeting, Ascona, Switzerland: "Rapid and reproducible characterization of sickling during automated deoxygenation in sickle cell disease patients"
- 2019 **Oral presentation.** 13th Dutch Hematology Congress, Papendal, The Netherlands: "The Oxygenscan: a test for patient specific biomarkers in sickle cell anemia"
- 2018 **Poster presentation.** 60th ASH Annual Meeting and Exposition in San Diego, California, USA: "The Oxygenscan: a rapid and reproducible test to determine patient-specific, clinically relevant biomarkers of disease severity in sickle cell anemia"
- 2018 **Oral presentation.** Joint Conference of Three Societies of Biorheology, Krakow, Poland: "The Oxygenscan: continuous measurement of red blood cell deformability with oxygen gradient ektacytometry to monitor disease severity and treatment effect in sickle cell disease"
- 2018 **Poster presentation.** 23rd Congress of the European Hematology Association, Stockholm, Sweden: "The Oxygenscan: continuous measurement and quantification of sickling during de- and reoxygenation to monitor disease severity and treatment effect in sickle cell disease"
- 2017 **Poster presentation.** 21st European Red Cell Society Meeting, Heidelberg, Germany: "Cell Membrane Stability Test in Hereditary Spherocytosis"



ACKNOWLEDGEMENTS (DANKWOORD)

Last but not least: het dankwoord. Met het schrijven van het meest gelezen hoofdstuk van een proefschrift realiseerde ik me dat er heel veel mensen direct of indirect hebben bijgedragen, waarbij de patiënten de belangrijkste zijn. Vaak kwamen die speciaal voor de in het proefschrift beschreven studies naar het ziekenhuis: bedankt!

Mijn grootste dank gaat uit naar mijn directe begeleiders die het mogelijk hebben gemaakt voor mij om dit project te kunnen doen: **Richard**, zonder jou was dit proefschrift er niet geweest. Hoewel mijn project wat traag op gang kwam bleef jij altijd positief. Van jou kreeg ik de ruimte en steun om het onderzoek rondom de oxygenscan verder uit te bouwen. Vooral de laatste jaren hebben we wat af gespard over toekomstige projecten, dat maakte het erg leuk en zo kwamen we op de beste ideeën. Mooi hoe je tijdens drukke experimenten (waar bijna de hele Rode Cel groep aan meedeed) nooit te beroerd was om te helpen. Dank voor je vertrouwen, en de gezelligheid tijdens congressen. Ik zie uit naar de toekomst op 't lab en bij de diagnostiek.

Ward, jouw bevoegenheid en enthousiasme werkt erg stimulerend. Jouw klinische blik op de projecten is van grote waarde geweest afgelopen jaren. Daarnaast heb jij belangrijke connecties gelegd en regelde je 'even' wat nieuwe potentiële medicijnen om uit te testen met de oxygenscan. Mede door jou is SCORE opgericht wat heel waardevol is voor de zorg voor patiënten met sikkelcelziekte en wetenschappelijk onderzoek in deze groep.

Gerard, mijn promotor, die aan de wieg stond van de samenwerking met RR Mechatronics, dank voor je input. Jij ziet als geen ander de kansen en mogelijkheden voor interessante samenwerkingen met het bedrijfsleven en hebt me het belang laten zien om onze expertise op het gebied van de oxygenscan al in een vroeg stadium te delen met andere labs.

Roger, al voordat jij mijn promotor werd wist je me al te helpen door de juiste vragen te stellen wat me deed realiseren dat ik labonderzoek wilde gaan doen. Veel dank hiervoor. Nadien heb je me goed kunnen bijstaan met je kritische blik en input op de statistiek van mijn artikelen, zonder jou was ik lost in statistics.

Wouter, als afdelingshoofd overzag jij mijn werkzaamheden van een afstandje en hoewel je niet direct betrokken was, kon ik altijd bij jou terecht. Dank voor je goede adviezen en je steun!

Vivien, I am grateful of how we collaborated last couple of years, it has been rewarding. Thank you for your support and your hospitality in Houston where I visited your lab and we started our collaboration. What you have accomplished has been inspiring for me (and most likely others too). I look forward to working with you in the future.

Git, mijn paranimf, wat hebben we samen wat afgedacht en gespard over de oxygenscan. Jouw input was onmisbaar, maar bovenal was het ook leuk om samen te brainstormen over aanpassingen en verbeteringen, met daarbij soms verhitte discussies en het heeft ons

beiden ook slapeloze nachten bezorgd. Ik ben je erg dankbaar voor je kritische blik, je kennis over menige techniek of assay, je support en je altijd aanwezige bereidheid om mee te denken als ik weer eens een (te ambitieus) experiment had bedacht. En wat is het toch altijd weer heerlijk en inspirerend om bij jou thuis door jullie prachtige bos te mogen wandelen, dank voor de gastvrijheid!

Jennifer, eerst als student bij mij op het lab aan de slag en nadien als analist. Je hebt een grote bijdrage geleverd aan dit proefschrift en wat ben je een goede aanwinst voor ons team. Jouw geordendheid heeft mij enigszins in het gareel gehouden om het lab er niet ook zo uit te laten zien als mijn bureau. Ik ben heel erg blij dat je nu vast bij de groep hoort, welverdiend! En we moeten nu echt een keer gaan softballen.

Dan de Jannen/mannen van RR Mechatronics, om te beginnen met **Jan de Zoeten**, met jou is het nooit saai, of je nu de ober van het restaurant op de kast probeer te jagen met confronterende vegetarische uitspraken of weer een 'wild' idee oppert wat vaag nog iets met de Lorrca te maken heeft. Dank voor je ideeën en bereidheid om op de onhandigste momenten naar het UMCU te komen om de Lorrca te repareren of ons telefonisch te begeleiden hoe het moederboard te vervangen. **Jan Buis**, dank dat je met ons het avontuur bent aan gegaan en nog steeds aangaat. **Sisto**, jouw bijdrage is essentieel geweest. Dank voor je vertrouwen in onze suggesties en observaties en volledige commitment aan het project. Ik denk met veel plezier terug aan onze trip naar Lyon. Ik ben blij dat we de samenwerking voortzetten met de verdere validatiestudies en hopelijk op korte termijn Shearox!

Elaine, jij mag ook niet ontbreken, als een van de weinig vrouwen tussen de techneuten heb je goed je 'mannetje' weten te staan.

Celeste, you have been great to work with at Vivien's lab, your work on the Lorrca on the other side of the ocean has been valuable. Thank you for your efforts!

Philippe, it has been nice and fun to work with you on the Eurostars project. Thank you for your support. **Camille**, thank you for your efforts to incorporate the different measurement protocols.

Marije, als kinderhematoloog en lid van de RBC onderzoeksgroep hebben we fijn samen gewerkt. Het was erg gezellig in Ascona tijdens de ERCS en in Madrid. Dank voor je bijdrage en het meedenken bij mijn projecten.

Tesy, vanaf het begin van het Lorrca project was jij erbij en samen hebben we de eerste jaren geploeterd om de oxygenscan en andere assays aan de praat te krijgen, dank voor je inzet!

Mitchel, als student tijdens de corona periode waren er weinig mogelijkheden om zelf metingen te doen op het lab, maar jij wist data van 2 projecten zorgvuldig en onverstoordbaar te analyseren wat o.a. leidde tot een mooie publicatie.

Dear **Penelope, Charles, and Lenny** from Agios. It has been very nice to collaborate with you. Your desire to unravel the function of pyruvate kinase is inspiring. Thank you for your support and hopefully we can meet at ASH in person again.

Judith, dank voor je bijdrage aan de metabolomics data! En leuk dat je mijn buurtgenoot bent.

Leden van de staf van het CDL, om te beginnen **Ray**, knap hoe je de research afdeling leidt met een vrolijke noot, en daarnaast vind ik het helemaal mooi om je in het lab nog even wat liposomen in elkaar te zien draaien. **Imo**, ondanks dat ons waterstofperoxide project met varkensbloed geen artikel heeft opgeleverd, was het wel een leuke studie, dank voor je bijdrage en support als hoofd van Arcadia! Leden van het MT, **Karen, Dörte, Jan, Ray, Imo** en Wouter, dank voor jullie steun, en dank dat jullie mij de kans geven om het rode bloedcel onderzoek en de diagnostiek de komende jaren verder te gaan vormgeven. Klinisch chemici, **Albert, Wouter TG, Hans, Eef, Maarten, Ruben**, af en toe kruisen onze wegen en zijn jullie altijd bereid om mee te denken, dank daarvoor! Met nog in het bijzonder dank voor Albert, die me gered heeft in Vancouver toen ik zonder geld bij het hotel stond omdat ik de pincode van mijn credit card niet meer wist.

Analisten van de Speciele hematologie, dank dat jullie geregeld wat samples meenamen in jullie analyses. **Medewerkers van het routine Centraal Diagnostisch Lab**, dank dat jullie altijd bereid waren om een uitstrijkje van ons mee te nemen in het kleuren, of later om Sapphire's te meten.

Joukje, jij regelt het wel en wee van de afdeling met zo'n efficiëntie en doelgerichtheid, respect! Ook dank aan **Carin, Sonja** en **Ineke**.

Leden van het **SCORE consortium**, het is erg inspirerend om de meetings bij te wonen, heel mooi om alle initiatieven te zien vanuit de verschillende centra. In het bijzonder **Maite**, mede dankzij jou hebben we zoveel patiënten kunnen includeren in de Sicklecelscreen studie. Het was altijd gezellig om even langs te komen in EMC om samples te halen, en ik vind het inspirerend hoe jij je hebt ingezet voor de kinderen met sikkelcelziekte. **Marjon**, jij was bereid om onze onderzoeken te combineren waardoor de Sicklecelscreen echt van de grond kwam. Jouw betrokkenheid bij de patiëntengroep en je inzet om SCORE op te zetten vind ik bewonderenswaardig. Mede door jou voelde ik me erg welkom bij SCORE. **Erfan**, dank ook voor jouw inzet om patiënten te includeren en je waardevolle input op de artikelen die daaruit zijn voortgekomen. Maar ook **Bart, Anita, Ineke, Edith, Jorn**, dank voor jullie hulp.

Dank ook aan de collega's van de Van Creveldkliniek. **Els**, die ook patiënten heeft geïncludeerd voor mijn studies en de verpleegkundigen **Karen, Michelle, Simone** en **Hanny**, die altijd bereid waren me te helpen wanneer het bloedprikken niet lukte. De VCK-artsen: **Karin, Kathelijn, Idske, Paul, Monique, Lize** en mede-puppies (met wie ik op de dinsdag op de VCK zat: **Maaïke, Merel** en **Piet** (al was je geen puppie)), het was leuk om ook wat van de

klinische kant van de VCK te mogen zien. En de promovendi van nu, **Anne, Wobke, Marieke, Olav, Isolde, Maria, Eline, Johan** en **Floor**, succes met (het afronden van) jullie PhD.

Marieke, Alies, Anouk en **Marleen** van de dagbehandeling, dank voor jullie flexibiliteit en medewerking als ik weer eens een patiënt wilde includeren. En de chocolade die ik regelmatig van jullie toegestopt kreeg, merci.

Bedankt ook **Martin** en **Erik**, dat we bij jullie van de faculteit Diergeneeskunde onze Dense Cell metingen kunnen doen.

En ook niet onbelangrijk, al die fijne en gezellige collega's.
Om te beginnen die van de RBC onderzoeksgroep:

Stéphanie, het eerste gedeelte van mijn PhD kenmerkte zich door capu's met jou en epic tripjes naar congressen waarbij San Diego, Stockholm en Madrid toch wel by far het gaafst waren, mede dankzij jouw immer succesvolle inspanningen om een toplocatie te vinden om te overnachten. Wat een tijden waren dat! Succes met je verdere opleiding tot kinderarts en je kersverse gezin.

Birgit, mede wintersport liefhebber, wat kan jij goed skiën en wat tof dat we met het lab naar Winterberg zijn geweest, zonder jou was dat nooit van de grond gekomen. Gezellig om in mijn laatste jaar van m'n PhD nog even samen naar de ASH te zijn geweest. Maar damn corona, dat hadden veel meer congressen moeten zijn. Heel gaaf en verdiend dat je die plek voor de kindergeneeskunde hebt gekregen! Succes!

Myrthe, mooi hoe jij als mede AIOS Interne zo'n mooie klinische studie doet naar het effect van een nieuw medicijn en dan ook al het labwerk zelf doet. Zie je wel, dokters kunnen ook pipetteren :-). Het is altijd gezellig om experimenten te doen als jij er ook bent. En knap hoe jij betrokken bent bij zowel het lab als de VCK.

Annet, jij floreert met het moleculaire werk en weet alles van iedereen op het lab. Tijdens het stapelen van de percoll lagen hebben we heerlijk kunnen kletsen over alles en nog wat en heb je me 'even' bijgespijkerd over de ins en outs van het lab.

Andere leden van de RBC onderzoeksgroep, **Simon**, het was fijn om jou erbij te hebben, met je enorme loyaliteit, je efforts om de journalclub op te zetten, succes met de volgende stap. **Annelies**, knap hoe jij verschillende onderwerpen van rode bloedcel ziekten zo snel kan transformeren naar een artikel. Succes met het afronden van je PhD. **Jonathan**, onze nieuwe aanwinst, heel tof dat je bij ons je PhD komt doen en ik blij dat ik je co-promotor ben.

En dan al m'n roomies:

Roomies van G02.632, als was het heel kort: **Anil, Jessica** en **Mirjam**, het was gezellig. **Zonne**, als vast lid bij de coffee corner rond 10u (inmiddels bij G02.631) was het fijn om successen en frustraties te kunnen delen. Succes met je verdere opleiding tot reumatoloog.

Rick, wat was het gezellig op G02.631, met elke ochtend het foute uur van Q-music en jouw blokkenschema's aan de muur. Met je aanstekelijke grijns zorgde je voor veel vrolijkheid op de kamer. **Martijn** (Tinus), ik ken weinig PhDs die zoveel hebben gepipetteerd. Respect hoe jij je erdoorheen hebt geslagen. Dank voor het ouwehoeren en natuurlijk samen klagen tijdens een kopje koffie. Zonder jouw nespresso-apparaat was Minke's coffee corner er nooit geweest. Succes met het afronden van je PhD en je nieuwe baan. **Dan**, you have done crazy experiments, with working hours that have been even more crazy, but your perseverance ultimately led to very nice results. It was very nice chatting with you, thanks for the 'gezelligheid'. Good luck with finishing your PhD and your new job just across the street. **Susan**, al was het maar kort dat we roomies zijn geweest, het was vaak hilarisch, en gelukkig zijn we het erover eens dat vouwwagens awesome zijn (vooral de Holtkampers).

Roomies van G02.629: aan mij de eer om met de 3 Veni-winnaars **Steven, Olivier** en **Sander** op de kamer te hebben gezeten, al was het maar kort, ik vond het gezellig. **Arjan** (altijd gezellig om onze kinderen bij het UMC zwembad op te halen), **Judith, Marian**, en **Maria-Laura**, hoewel we niet heel lang 'joy hebben geshared', het was een welkome afwisseling met klinische werkzaamheden om even bij jullie op de kamer te zijn.

En dan mijn allernieuwste roomies op G02.629: **Chantal** en **Demian**, leuk om tijdens de laatste fase met jullie een kamer te delen, zo leer ik ook wat over Nike en Pokémon kaarten. Succes met het afronden van jullie PhDs.

Analisten van het lab: **Arjan, Noortje, Simone, Silvie, Jerney, Cor** en **Arnold**, jullie zijn de vaste kern van het lab, zorgen voor continuïteit en bovenal dat alles op het lab reilt en zeilt. Dank daarvoor.

En dan de andere PhD's: **Marc** (golden boy, kijk jou het allemaal goed regelen), **Tessa, Minka, Pol, Rowan, Hinde, Diego, Omnia, Wariya**, heel veel succes met jullie PhDs, het komt allemaal goed!

Pieter, als vroegere kamergenoot van Richard heb je heb je veel van de ups-and-downs van ons onderzoek mee gekregen. Knap hoe jij de ene na de andere beurs binnen sleept. **Hester**, jij werd als kamergenoot ook vaak ongewild deelgenoot van de Lorrca experimenten. Inspirerend hoe jij het vrouwen hart op de kaart gezet hebt, en daarmee ook de noodzaak om te kijken naar 'gender differences' in de gehele wetenschap. Nog gefeliciteerd met het professorschap! **Coen**, jouw betrokkenheid bij je mensen en aanwezigheid op het lab werkt zijn vruchten af. Bij de lunch had je altijd zeer entertainende verhalen en altijd werd er wel een 'papertje' gesubmit. **Rolf** (eigenlijk van de VCK), het was leuk om samen in de labuitjes-commissie te hebben gezeten, dank voor de gesprekken bij de koffieautomaat.

Astrid en **Cheryl** van 'Koffie a.k.a. Intervisie' (vooral het eerste), het was erg fijn om als AIOS Interne tegelijkertijd een PhD project te starten in het UMC. As, heel leuk om samen met jou de laatste loodjes van onze promoties te regelen.

Mijn begeleiders van mijn vorige onderzoek in het Sint Antonius Ziekenhuis: als we toen

geweten hadden dat vaccinatie onderzoek zo hip zou zijn anno 2021 zouden we er nooit mee gestopt zijn. **Ger**, dank voor je inzet, commitment en je indrukwekkende kennis over de immunologie. **Heleen**, dank dat je me zo hebt bijgestaan bij het schrijven van mijn 1^e artikel, daar heb ik heel veel aan gehad. **Okke**, jij zag iets wat ik nog niet zag, maar later door jou wel realiseerde, dank voor je geloof in mij!

Simone, mijn mentor, op het juiste moment stelde jij de juiste vragen en gaf je me goed advies, daarvoor ben ik je heel erg dankbaar. **Tom**, als opleider was je erg goed voor ons, arts-assistenten in het Sint Antonius Ziekenhuis, en via jou ben ik in het RBC onderzoek terecht gekomen.

Hematologen van het Sint Antonius Ziekenhuis, **Maaïke, Harry, Gerda, Josephine**, (en **Okke**) door jullie is mijn liefde voor de hematologie verder gegroeid, dank voor de fijne en leerzame tijd die ik heb gehad bij jullie op de afdeling en dagbehandeling.

En dan ook de opleiders in het UMC **Karin** en **Jan Jelrik**: Ook al zat ik een verdieping hoger in het lab gedurende 4 jaar, ik kon altijd bij jullie terecht. Dank voor je steun Karin! Opleiders van de hematologie, **Anna** en **Reinier**, het is heel leuk om bij jullie de differentiatie te mogen doen, dank voor de goede sfeer en opleidingsklimaat. Reinier, dank voor het advies dat je gaf al voor je mijn opleider was.

Hematologen, mede-fellows, PA-ers, verpleegkundigen en andere medewerkers van de hematologie van het UMCU, bedankt voor het warme welkom bij jullie.

Dank **Summies**, voor het aanwakkeren van mijn innerlijke drive om mij tot het uiterste te laten gaan om de nerd-award te veroveren.

Matties van de Vrije School. Vijftien jaar bij elkaar in de klas zitten schept een band. Al zien we elkaar niet vaak, vanaf minuut 1 is het weer als vanouds. **Eef**, met veel plezier denk ik terug aan onze eindeloze baksessies (met Haarlemmer bruin), wie had gedacht dat we alle 2 met een vrouw zouden thuis komen. Wij kunnen alles bespreken en er gelijk ook grappen over maken. **Lisa**, al vanaf jongs af aan fietsten we samen naar school, door jou kwam ik nog enigszins op tijd. Nu we beiden 3 kinderen verder zijn is het heerlijk om met jou de hele avond te kunnen tafelen en alles te kunnen delen, dank daarvoor. **Iv**, heel fijn om met jou in het bubbelbad te zitten en te filosoferen over het leven. **Jann**, ik ben blij dat we elkaar niet uit het oog zijn verloren, hopelijk gaan we snel weer een keer zeilen.

Lieve **Vera**, de vele etentjes (meestal kaasfondue) zijn waardevol geweest. Jij zag als eerste hoe blij ik was in het lab, als ik erover vertelde. Ook al zien we elkaar de laatste tijd weinig, ik wil je danken voor je wijsheid de afgelopen jaren.

WISE (**Annelies, Ruth, Saskia en Suzanne**) bestaand uit leukste roeiers van Dames 2003. Voor mensen die geselecteerd waren o.b.v. ons 'enorme' talent om te roeien, is het toch een gezellige boel geweest in de boot en de jaren daarna, op de racefiets of met een jengelende peuter aan ons been in de speeltuin. Ons recente weekend was een groot feest. Ik hoop dat we elkaar blijven zien ondanks dat we inmiddels over het hele land verspreid zijn.

En ook van de roeivereniging, **Kevin** en **Roel**, van de power of 3, tijd voor een borrel! Of gewoon weer een tripje naar Madrid. **Robin** en **Antoin**, als coaches hebben we mooie tijden beleefd. Tijd om die reünie maar te gaan regelen.

Dames van veterinnen B van HC Kromme Rijn, wat fijn dat jullie me als hockey naïef persoon hebben geadopteerd. Op het veld was een van de weinige momenten dat ik even niet aan het onderzoek dacht, en de gezelligheid nadien droeg daar ook aan bij.

Lieve buren, wat is het toch heerlijk wonen in onze Oranjebuurt. **Mer & Kim**, wat fijn dat ik gebruik mocht maken van jullie 'mansion' op Texel, waar ik heel wat schrijfwerk heb kunnen doen. Maar bovenal dank voor de gezellige borrels en BBQ's, en het opvangen van onze kinderen tijdens de lockdown. Daarvoor wil ik **Boukje** en **Saaske** ook bedanken, en natuurlijk voor de gezelligheid de afgelopen jaren. En dan wil ik ook **Trui** noemen die altijd geïnteresseerd is in mijn onderzoek en of ik het nog wel red. Ik heb veel respect voor hoe jij in het leven staat en daardoor een belangrijk deel uit maakt van onze straat. **Henkt**, met jou kon ik goed praten over het onderzoek gezien jouw ervaring als professor en carrière bij diergeneeskunde. Het leven is niet eerlijk, wat had ik je er graag bij gehad bij mijn verdediging.

Lieve **Clazien** en **Herman**, altijd geïnteresseerd in mijn onderzoek, en of ik al eindelijk klaar was, jullie leefden met me mee. Dank voor jullie bereidheid om op stel en sprong naar ons te komen als er weer een kind ziek was of als ik weer eens een extra experiment in het lab moest doen. De kinderen genieten van de tijd met opa & oma tijdens de woensdagmiddagen en de leuke uitstapjes tijdens de vakanties.

Suus, mijn andere paranimf, ik ben blij dat je naast me staat bij mijn verdediging. Als je omslaat met de dubbeltwee bij -1°C kan je niet anders dan goede vrienden worden. Na dat jaar roeien, en die 2 topjaren als coach van de 1^e jaars 8+, hebben we ook menig rondje gefietst op de racer. Heel fijn dat je net als ik nabij Utrecht bent gaan wonen en ook op de Uithof werkt, dan lukt het toch nog ondanks drukke agenda's/kinderen om af en toe koffie te drinken. Met jou kan ik alles bespreken of dat nu tijdens koffie, racefietsen of in de kroeg (moeten we echt weer doen nu het weer mag) is.

Laurens, ik ken je al vanaf dat we gezellig samen op het boxkleed lagen. Toen was je al deel van onze familie en dat is niet veranderd. Wij hebben aan een half woord genoeg. **Marieke**, jouw tomeloze interesse en vermogen om voor iedereen in de bres te springen vind ik bewonderenswaardig! Het is altijd heerlijk geweest om met de kinderen bij jullie te zijn of dat nu met Oud & Nieuw, op vakantie of gewoon bij jullie of bij ons thuis is. Dank voor wat jullie aan ons hebben gegeven, het grootste goed! En wat een heerlijke extra familie met ook **Jasper**, **Carlijn**, **Jasmijn** en **Camiel**.

Lieve **Sies**, als mijn favoriete tante heb je vroeger al goed gescoord met de pannenkoekenboot en apenheul. Afgelopen jaren ben jij onderdeel van ons gezin geworden en ook nu zien de kinderen je als hun eigen tante.

Jel, lieve broer, het toevoegen van jou als 1 van mijn 'emergency' contacten bij mijn Garmin zegt genoeg denk ik. Bij jou voel ik me veilig, en ik ken maar weinig mensen die zo relaxed zijn en zoveel rust uitstralen als jij. Als oom Jelmer doe je het ook erg goed! En **Lisa**, de taalkundige van onze familie en degene die mijn broer zo blij maakt; wat fijn dat jij mijn schoonzus bent.

Wietst, mijn lieve zus, er zijn al teveel mijlpalen geweest waar je niet bij was, dus deze kan er ook wel bij. En hoewel het ok is, blijft het stom dat je er niet meer bent. Jij had dit heel gaaf gevonden en without question was je mijn paranimf geweest. Ik mis je!

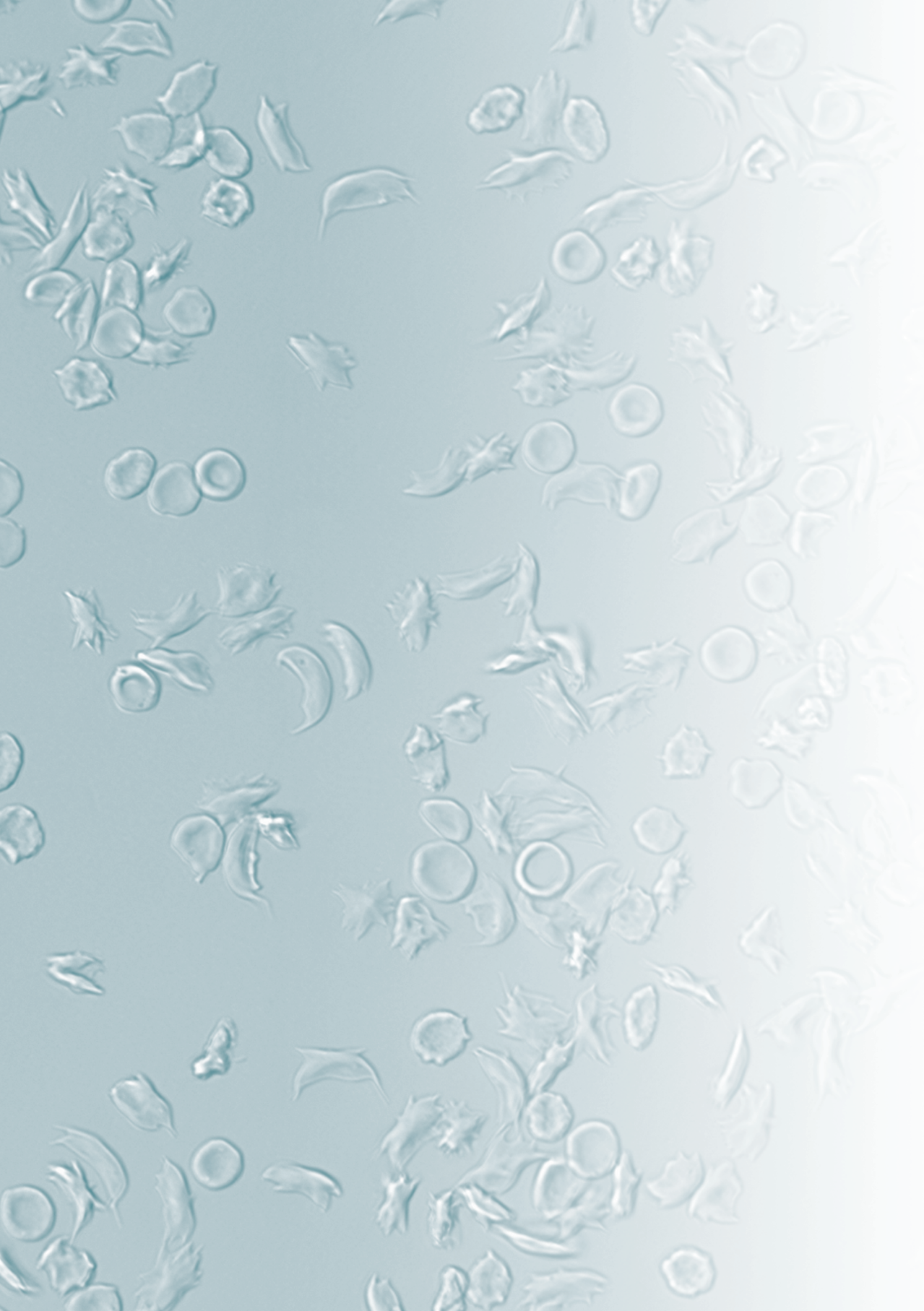
Lieve **Pap**, dit proefschrift is ook een beetje voor jou. Je had me graag naar de TU zien gaan, maar hebt me volledig gesteund in mijn keuze voor geneeskunde. Zoals je ziet heb ik toch wel wat liefde voor de techniek geërfd van je, en blijk ik eigenlijk best technisch te zijn.

Mam, dank voor je interesse voor werkelijk elk aspect in mijn leven en je bereidheid om te komen oppassen.

Tijdens mijn jeugd en studententijd heb ik me bij jullie altijd vrij gevoeld in mijn keuzes, en nu ik zelf kinderen heb weet ik dat dat best lastig kan zijn. Ik ben trots op hoe jullie de draad weer hebben opgepakt na het overlijden van Wiets. Dank voor de opa en oma die jullie zijn voor de kids, maar bovenal heel veel dank voor jullie onvoorwaardelijke liefde, steun en vertrouwen in mij.

Lieve **Julia**, **Sterre** en **Boaz**, wat zijn jullie heerlijke kinderen en wat groeien jullie snel op. Het is elke dag fijn om thuis te komen bij jullie en met zoveel blijdschap onthaald te worden. Het is bij tijden best pittig en druk geweest, maar vooral door jullie heb ik dat allemaal kunnen doorstaan. Wat houd ik immens veel van jullie.

Lieve **Lau**, jij hebt me zowel mentaal als praktisch gezien bijgestaan afgelopen jaren. Altijd bereid om mee te denken, weer eens een presentatie aan te horen (pfff, weer die Elmax), en vooral door me de ruimte te geven om toch nog even een experiment s' avonds of in het weekend te doen. Doordat jij zo heerlijk efficiënt bent regel je alles thuis vlekkeloos en geef je mij daardoor veel mogelijkheden. Dank voor je steun en begrip afgelopen jaren, zonder jou was dit nooit gelukt. Met jou aan mijn zijde lukt alles. Ik hou van je!



CURRICULUM VITAE

Minke Ariena Elisabeth Rab was born in The Hague in 1982 where she obtained her VWO degree at The Vrije School. In Utrecht she studied biomedical sciences for three years followed by the Selective Utrecht Medical Masters (SUMMA) program at the University Medical Center Utrecht (UMCU). After graduating as a medical doctor and master of science she started working as a junior doctor not in training at the St. Antonius Hospital. In 2012 she started her residency Internal medicine at the St. Antonius Hospital. In 2015 she started her PhD-project at the Central Diagnostic Laboratory-Research and Van Creveldkliniek under supervision of dr. Richard van Wijk, dr. Eduard van Beers, prof. Dr. Gerard Pasterkamp and prof. dr. Roger Schutgens. During her PhD she played a major role in the development of the oxygenscan, a novel ektacytometry-based technique, and its clinical validation in the field of sickle cell disease. She (co)-authored eight publications in peer reviewed journals on this single topic and is recognized as a world-leading expert on this technique. She is currently involved in several international collaborations, has presented her work at several national and international conferences and won several international awards for her scientific work. In addition, she is a co-applicant of five awarded international grant applications from both the pharmaceutical industry and EU programs.

In February 2021 she started her fellowship hematology at the UMC Utrecht. She combines this with a position at the Central Diagnostic Laboratory-Research of the UMC Utrecht where she continues her research career in combination with a position in the diagnostic lab where she is involved in the laboratory diagnosis of rare red blood cell disorders.

